Volume 70
Number 6, 1998

International Journal of QUANTUM CHEMISTRY

Editor-in-Chief
PER-OLOV LÖWDIN

Editors
ERKKI BRÄNDAS
YNGVE ÖHRN

Associate Editors
OSVALDO GOSCINSKI
STEN LUNELL
JOHN R. SABIN
MICHAEL C. ZERNER

Assistant Editor
LEIF ERIKSSON

Proceedings of the
International Symposium on the
Application of Fundamental Theory to

Problems of Biology and Pharmacology

Held at the Ponce de Leon Resort,
St. Augustine, Florida,
February 21–27, 1998

Editor-in-Chief: Per-Olov Löwdin
Special Editors: Yngve Öhrn
John R. Sabin
Michael C. Zerner

A Wiley-Interscience Publication
John Wiley & Sons, Inc.
Visit Wiley Journals Online
www.interscience.wiley.com

ISSN 0020-7608

International Journal of

Quantum Chemistry

Editor-in-Chief

Per-Olov Löwdin
University of Florida at Gainesville, USA
Uppsala University, Sweden

Editors

Erkki Brändas
Uppsala University, Sweden

Yngve Öhrn
University of Florida at Gainesville, USA

Associate Editors

Osvaldo Goscinski
Uppsala University, Sweden

Sten Lunell
Uppsala University, Sweden

John R. Sabin
University of Florida at Gainesville, USA

Michael C. Zerner
University of Florida at Gainesville, USA

Assistant Editor

Leif Eriksson
Uppsala University, Sweden

Honorary Editors

Gerhard Herzberg
National Research Council,
Ottawa, Ontario, Canada

Jerome Karle
Naval Research Laboratory at
Washington, DC, USA

Rudy Marcus
California Institute of Technology at
Pasadena, USA

Editorial Board

Jiri Čížek
University of Waterloo, Ontario, Canada

Enrico Clementi
Université Louis Pasteur, Strasbourg, France

Raymond Daudel
Académie Européene de Arts, des Sciences
et des Lettres, Paris, France

Ernest Davidson
Indiana University at Bloomington, USA

George G. Hall
University of Nottingham, UK

Laurens Jansen
Kusnacht, Switzerland

Norman H. March
University of Oxford, UK

Roy McWeeny
Università di Pisa, Italy

Saburo Nagakura
Graduate University for Advanced Studies,
Yokohama, Japan

Kimio Ohno
Hokkaido Information University, Japan

Josef Paldus
University of Waterloo, Ontario, Canada

Robert G. Parr
University of North Carolina at Chapel Hill, USA

Ruben Pauncz
Technion, Haifa, Israel

John A. Pople
Northwestern University at Evanston, Illinois, USA

Alberte Pullman
Institut de Biologie Physico-Chimique,
Paris, France

Paul von Ragué Schleyer
Universität Erlangen-Nürnberg,
Erlangen, Germany

Harrison Shull
Naval Postgraduate School,
Monterey, California, USA

Tang Au-Chin
Jilin University, Changchun, China

Rudolf Zahradník
Czech Academy of Sciences,
Prague, Czech Republic

Advisory Editorial Board

Teijo Åberg
Helsinki University of Technology, Espoo,
Finland

Axel D. Becke
Queen's University, Kingston, Ontario, Canada

Gian Luigi Bendazzoli
Università di Bologna, Italy

Jerzy Cioslowski
The Florida State University at Tallahassee, USA

Timothy Clark
Universität Erlangen-Nürnberg, Germany

Mireille Defranceschi
DPEL/SERGD/LMVT,
Fontenay Aux Roses, France

Karl F. Freed
The University of Chicago, Illinois, USA

Odd Gropen
University of Tromsø, Norway

Trygve Helgaker
University of Oslo, Norway

Ming-Bao Huang
Academia Sinica,
Beijing, People's Republic of China

Hiroshi Kashiwagi
Kyushu Institute of Technology, Fukuoka, Japan

Eugene S. Kryachko
Academy of Sciences of Ukraine, Kiev, Ukraine

Sven Larsson
Chalmers University of Technology,
Gothenburg, Sweden

Lucas Lathouwers
Universitair Centrum (RUCA), Antwerp, Belgium

Shyi-Long Lee
National Chung Chang University,
Taiwan, Republic of China

Josef Michl
University of Colorado at Boulder, USA

Nimrod Moiseyev
Israel Institute of Technology, Israel

John D. Morgan III
University of Delaware at Newark, USA

Cleanthes A. Nicolaides
National Hellenic Research Foundation, Greece

J. Vincent Ortiz
Kansas State University at Manhattan, USA

Lars Pettersson
University of Stockholm, Sweden

Leon Phillips
University of Canterbury,
Christchurch, New Zealand

Martin Quack
ETH Zürich, Switzerland

Leo Radom
Australian National University, Australia

William Reinhardt
University of Washington at Seattle, USA

Sten Rettrup
H. C. Ørsted Institut, Copenhagen, Denmark

C. Magnus L. Rittby
Texas Christian University at Fort Worth, USA

Michael Robb
King's College, London, UK

Mary Beth Ruskai
University of Massachusetts at Lowell, USA

Harold Scheraga
Cornell University at Ithaca, New York, USA

Vipin Srivastava
University of Hyderabad, India

Nicolai F. Stepanov
Moscow State University, Russia

Jiazong Sun
Jilin University, Changchun,
People's Republic of China

Donald G. Truhlar
University of Minnesota at Minneapolis, USA

Peter Wolynes
University of Illinois at Urbana, USA

Robert E. Wyatt
The University of Texas at Austin, USA

Editorial Production, John Wiley: Sheila Kaminsky

REPORT DOCUMENTATION PAGE

Form Approved
OMB No. 0704-0188

Public reporting burden for this collection of information is estimated to average 1 hour per response, including the time for reviewing instructions, searching existing data sources, gathering and maintaining the data needed, and completing and reviewing the collection of information. Send comments regarding this burden estimate or any other aspect of this collection of information, including suggestions for reducing this burden to Washington Headquarters Services, Directorate for Information Operations and Reports, 1215 Jefferson Davis Highway, Suite 1204, Arlington, VA 22202-4302, and to the Office of Management and Budget, Paperwork Reduction Project (0704-0188), Washington, DC 20503.

1. AGENCY USE ONLY *(Leave blank)*	2. REPORT DATE 3/23/99	3. REPORT TYPE AND DATES COVERED FINAL 10/1/97 - 9/30/98

4. TITLE AND SUBTITLE

PARTIAL SUPPORT OF 1998 SANIBEL SYMPOSIUM

5. FUNDING NUMBERS

G
N00014-98-1-0215

6. AUTHOR(S)

YNGVE ÖHRN

7. PERFORMING ORGANIZATION NAMES(S) AND ADDRESS(ES)

UNIVERSITY OF FLORIDA
QUANTUM THEORY PROJECT
PO BOX 118435
GAINESVILLE, FL 32611-8435

8. PERFORMING ORGANIZATION REPORT NUMBER

1

9. SPONSORING / MONITORING AGENCY NAMES(S) AND ADDRESS(ES)

OFFICE OF NAVAL RESEARCH
CHEMISTRY DIVISION CODE 313
800 NORTH QUINCY STREET
ARLINGTON, VA22217-5000

10. SPONSORING / MONITORING AGENCY REPORT NUMBER

TECHNICAL REPORT 1

11. SUPPLEMENTARY NOTES

a. DISTRIBUTION / AVAILABILITY STATEMENT

APPROVED FOR PUBLIC RELEASE AND SALE

12. DISTRIBUTION CODE

UNLIMITED

13. ABSTRACT *(Maximum 200 words)*

PROCEEDINGS OF THE 1998 SANIBEL SYMPOSIUM

14. SUBJECT TERMS

15. NUMBER OF PAGES

16. PRICE CODE

17. SECURITY CLASSIFICATION OF REPORT	18. SECURITY CLASSIFICATION OF THIS PAGE	19. SECURITY CLASSIFICATION OF ABSTRACT	20. LIMITATION OF ABSTRACT
UNCLASSIFIED	UNCLASSIFIED	UNCLASSIFIED	UL

International Journal of QUANTUM CHEMISTRY
Quantum Biology Symposium No. 25

Proceedings of the International Symposium on the Application of Fundamental Theory to Problems of Biology and Pharmacology

Held at Ponce de Leon Resort, St. Augustine, Florida,
February 21–27, 1998

Editor-in-Chief: Per-Olov Löwdin
Special Editors: Yngve Öhrn, John R. Sabin, and
Michael C. Zerner

DTIC QUALITY INSPECTED 4

an Interscience® Publication
published by JOHN WILEY & SONS

19990329 040

DISTRIBUTION STATEMENT A
Approved for Public Release
Distribution Unlimited

DISTRIBUTION STATEMENT A
Approved for Public Release
Distribution Unlimited

The *International Journal of Quantum Chemistry* (ISSN 0020-7608) is published semimonthly with one extra issue in January, March, May, July, August, and November by John Wiley & Sons, Inc., 605 Third Avenue, New York, New York 10158.

Copyright © 1998 John Wiley & Sons, Inc. All rights reserved. No part of this publication may be reproduced in any form or by any means, except as permitted under section 107 or 108 of the 1976 United States Copyright Act, without either the prior written permission of the publisher, or authorization through the Copyright Clearance Center, 222 Rosewood Drive, Danvers, MA 01923, (508) 750-8400, fax (508) 750-4470. Periodicals postage paid at New York, NY, and at additional mailing offices.

The code and the copyright notice appearing at the bottom of the first page of an article in this journal indicate the copyright owner's consent that copies of the article may be made for personal or internal use, or for the personal or internal use of specific clients, on the condition that the copier pay for copying beyond that permitted by Sections 107 or 108 of the US Copyright Law.

This consent does not extend to the other kinds of copying, such as copying for general distribution, for advertising or promotional purposes, for creating new collective work, or for resale. Such permission requests and other permission inquiries should be addressed to the Permissions Dept.

Subscription price (Volumes 66–70, 1998): $4,439.00 in the US, $4,739.00 in Canada and Mexico, $4,964.00 outside North America. All subscriptions outside US will be sent by air. Personal rate (available only if there is an institutional subscription): $195.00 in North America, $375.00 outside North America. Subscriptions at the personal rate are available only to individuals. Payment must be made in US dollars drawn on a US bank. Claims for undelivered copies will be accepted only after the following issue has been received. Please enclose a copy of the mailing label. Missing copies will be supplied when losses have been sustained in transit and where reserve stock permits.

Please allow four weeks for processing a change of address. For subscription inquiries, please call (212) 850-6645; e-mail: SUBINFO@Wiley.com.

Postmaster: Send address changes to *International Journal of Quantum Chemistry*, Caroline Rothaug, Director, Subscription Fulfillment and Distribution, Subscription Department, John Wiley & Sons, Inc., 605 Third Avenue, New York, NY 10158.

Advertising Sales: Inquiries concerning advertising should be forwarded to Advertising Sales Manager, Advertising Sales, John Wiley & Sons, Inc., 605 Third Avenue, New York, NY 10158; (212) 850-8832. Advertising Sales, European Contacts: Bob Kern or Nicky Douglas, John Wiley & Sons, Ltd., Baffins Lane, Chichester, West Sussex PO19 1UD, England. Tel.: 44 1243 770 350/367; Fax: 44 1243 770 432; e-mail: adsales@wiley.co.uk.

Reprints: Reprint sales and Inquiries should be directed to the customer service department, John Wiley & Sons, Inc. 605 Third Ave., New York, NY 10158. Tel: 212-850-8776.

Manuscripts should be submitted in triplicate and accompanied by an executed Copyright Transfer Form to the Editorial Office, *International Journal of Quantum Chemistry*, Quantum Chemistry Group, Uppsala University, Box 518, S-75120, Uppsala, Sweden. Authors may also submit manuscripts to the Editorial Office, *International Journal of Quantum Chemistry*, Quantum Theory Project, 2301 NP Building #92, P.O. Box 118435, Museum Road and North South Drive, University of Florida, Gainesville, Florida 32611-8435. **Information for Contributors** appears in the first and last issue of each volume. **All other correspondence** should be addressed to the *International Journal of Quantum Chemistry*, Publisher, Interscience Division, Professional, Reference, and Trade Group, John Wiley & Sons, Inc., 605 Third Avenue, New York, NewYork 10158, U.S.A. The contents of this journal are indexed or abstracted in *Chemical Abstracts, Chemical Titles, Chemical Database, Current Contents/Physical, Chemical, and Earth Sciences, Research Alert (ISI), Science Citation Index (ISI)*, and *SCISEARCH Database (ISI)*.

This paper meets the requirements of ANSI/NISO Z39. 48–1992 (Permanence of Paper). ♾

International Journal of

Quantum Chemistry

Volume 70
Number 6, December 20, 1998

Contents

Introduction
N. Y. Öhrn, J. R. Sabin, and M. C. Zerner **1099**

List of Participants **1101**

On the Origin of the Lack of Anticonvulsant Activity of Some Valpromide Derivatives
S. M. Tasso, L. Bruno-Blanch, and G. L. Estiú **1127**

Molecular Surface Electrostatic Potentials of Anticonvulsant Drugs
J. S. Murray, F. Abu-Awwad, P. Politzer, L. C. Wilson, A. S. Troupin, and R. E. Wall **1137**

Phytochrome Structure: A New Methodological Approach
C. R. W. Guimarães, J. Delphino da Motta Neto, and R. Bicca de Alencastro **1145**

Studies on the Hydrogenation Steps of the Nitrogen Molecule at the *Azotobacter vinelandii* Nitrogenase Site
K. K. Stavrev and M. C. Zerner **1159**

RHF Conformational Analysis of the Auxin Phytohormones *n*-Ethyl–Indole-3-Acetic Acid ($n = 4, 5, 6$)
M. Ramek and S. Tomić **1169**

pK_a of Cytosine on the Third Strand of Triplex DNA: Preliminary Poisson–Boltzmann Calculations
G. R. Pack, L. Wong, and G. Lamm **1177**

(continued)

Visit Wiley Journals Online
WILEY InterScience®
www.interscience.wiley.com

Volume 70, Number 6 was mailed the week of November 16, 1998.

Parametric Transform and Moment Indices in the Molecular Dynamics of *n*-Alkanes
S. P. Molnar and J. W. King **1185**

Theoretical Approach to the Pharmacophoric Pattern of $\mathrm{GABA_B}$ Analogs
M. L. Lorenzini, L. Bruno-Blanch, and G. L. Estiú **1195**

Optimal Molecular Connectivity Descriptors for Nitrogen-Containing Molecules
M. Randić, and J. Cz. Dobrowolski **1209**

Volume Title Page **1217**

Author Index **1219**

Subject Index **1225**

Volume Table of Contents .... **I**

Published Symposia .... **XII**

Introduction

The 38th Annual Sanibel Symposium, organized by the faculty and staff of the Quantum Theory Project of the University of Florida, was held on February 21–27, 1998. This year, the Ponce de Leon Conference Center in St. Augustine, Florida, was the site of the gathering of more than 300 scientists.

The symposium followed the established format with plenary and poster sessions. A compact 7-day integrated program of quantum biology, quantum chemistry, and condensed matter physics was presented. The topics of the sessions covered by these proceedings included Spectroscopy of Base Pairs, Quantum/Classical Molecular Mechanics, Simulations of Biological Systems, Metals in Biology, and Linear Scaling.

The articles were subjected to the ordinary refereeing procedures of the *International Journal of Quantum Chemistry*. The articles presented in the sessions on quantum chemistry, condensed matter physics, and associated poster sessions are published in a separate issue of the *International Journal of Quantum Chemistry*.

The organizers acknowledge the following sponsors for their support of the 1998 Sanibel Symposium:

- Army Research Office through Grant #DAAG55-98-1-117. "The views, opinions, and/or findings contained in this report are those of the author(s) and should not be construed as an official Department of the Army position, policy, or decision, unless so designated by other documentation."
- The Office of Naval Research through Grant #N00014-98-1-0215. "This work relates to Department of the Navy Grant #N00014-98-1-0215 issued by the Office of Naval Research. The United States Government has the royalty-free license throughout the world in all copyrightable material contained herein."
- IBM Corporation
- HyperCube, Inc.
- Q-Chem, Inc
- The University of Florida

Very special thanks go to the staff of the Quantum Theory Project of the University of Florida for handling the numerous administrative, clerical, and practical details. The organizers are proud to recognize the contributions of Mrs. Judy Parker, Ms. Coralu Clements, Ms. Sandra Weakland, Dr. Greg Pearl, and Mr. Cristián Cárdenas. All the graduate students of the Quantum Theory Project who served as "gofers" are gratefully recognized for their contributions to the 1998 Sanibel Symposium.

N. Y. Öhrn
J. R. Sabin
M. C. Zerner

International Journal of Quantum Chemistry, Vol. 70, 1099 (1998)
© 1998 John Wiley & Sons, Inc.
CCC 0020-7608 / 98 / 0601099-01

List of Participants

Albert, Katrin
University of Florida
Quantum Theory Project
P.O. Box 118435
Gainesville, FL 32611-8435
USA
Phone: 352-392-1597
Fax: 352-392-8722
albert@qtp.ufl.edu

Arteca, Gustavo A.
Laurentian University
Departments of Chemistry and Biochemistry
Ramsey Lake Road
Sudbury, Ontario P3E 2C6
Canada
Phone: 705-675-1151
Fax: 705-675-4844
gustavo@nickel.laurentian.ca

Baeck, Kyoung-Koo
Kang-Nung University
Department of Chemistry
Ji-Byun-Dong, 123
Kang-Won-Do 210-702
South Korea
Phone: 82-391-640-2307
Fax: 82-391-647-1183
baeck@chem.kangnung.ac.kr

Bartlett, Rodney J.
University of Florida
Quantum Theory Project
P.O. Box 118435
Gainesville, FL 32611-8435
USA
Phone: 352-392-1597
Fax: 352-392-8722
bartlett@qtp.ufl.edu

Bernhardsson, Anders
Lund University
Theoretical Chemistry
Box 124
Lund 221 00
Sweden
Phone: 46-46-2220384
Fax: 46-46-2224543
anders.bernhardsson@teokem.lu.se

Beveridge, David
Wesleyan University
Department of Chemistry
Hall-Atwater Laboratories
Middletown, CT 06457
USA
Phone: 860-685-2575
Fax: 860-685-2211
dbeveridge@wesleyan.edu

Bicca de Alencastro, Ricardo
Universidade Federal de Rio de Janeiro
Inst. de Quimica
Bloco A-CT Sala 622, Cidade Univ.
Rio de Janeiro RJ 21949-900
Brazil
Phone: 55-021-590-3544
Fax: 55-021-2904746
bicca@iq.ufrj.br

Billing, Gert D.
University of Copenhagen
H.C. Ørsted Institute
Department of Chemistry
Copenhagen
Denmark
Phone: 453-532-0252
Fax: 453-532-0259
gdb@moldyn.ki.ku.dk

International Journal of Quantum Chemistry, Vol. 70, 1101–1125 (1998)
© 1998 John Wiley & Sons, Inc.
CCC 0020-7608 / 98 / 0601101-25

LIST OF PARTICIPANTS

Bishop, David M.
University of Ottawa
Department of Chemistry
10 Marie Curie
Ottawa, Ontario K1M 0Z3
Canada
Phone: 613-562-5181
Fax: 613-562-5170
dbishop@science.uottawa.ca

Boettger, Jonathan C.
Los Alamos National Laboratory
Group T-1
MS B221
Los Alamos, NM 87545
USA
Phone: 505-667-7483
Fax: 505-665-5757
jn@lanl.gov

Bögel, Horst
University of Halle
Inst Phys. Chem. (Merseburg)
Geusaerstr.
Halle D-06099
Germany
Phone: 49-3461-46-2127
Fax: 49-3461-46-2381
boegel@chemie.uni-halle.de

Boone, Amy
University of Florida
Department of Chemistry
P.O. Box 117200
Gainesville, FL 32611-7200
USA
Phone: 352-392-0541
Fax: 352-392-0872
boone@chem.ufl.edu

Boudreaux, Edward A.
University of New Orleans
Department of Chemistry
Lake Front
New Orleans, LA 70148
USA
Phone: 504-286-6311
Fax: 504-286-6860

Bouferguene, Ahmed
Florida A & M University
Department of Physics
205 Jones Hall
Tallahassee, FL 32307
USA
Phone: 850-599-3470
Fax: 850-599-3577
boufer@cennas.nhmfl.gov

Brändas, Erkki J.
Uppsala University
Department of Quantum Chemistry
P.O. Box 518
Uppsala S-75120
Sweden
Phone: 46-18-4713263
Fax: 46-18-502402
erkki@kvac.uu.se

Broo, Anders
Chalmers University of Technology
Physical Chemistry
Kernivagen 3
Göteborg 41296
Sweden
Phone: 46-31-772-3051
Fax: 46-31-772-3858
broo@phc.chalmers.se

Brown, Richard E.
Michigan Technological University
Chemistry Department
Houghton, MI 49931
USA
Phone: 906-487-2383
Fax: 906-487-2061
rebrown@MTU.edu

Bunge, Carlos F.
Universidade Nacional Autonoma de Mexico
Institute of Physics
AP 20-364
Mexico City DF 01000
Mexico
Phone: 525-622-5014
Fax: 525-622-5015
bunge@fenix.ifisicacu.unam.mx

Burke, Kieron
Rutgers University
Department of Chemistry
1019 West High St.
Kadoon Heights, NJ 08035
USA
Phone: 609-225-6156
Fax: 609-225-6506
kieron@crab.rutgers.edu

Butler, Leslie G.
Louisiana State University
Department of Chemistry
1126 Beakenham Dr.
Baton Rouge, LA 70808
USA
Phone: 504-769-9751
Fax: 504-388-3458
les.butler@chemgate.chem.lsu.edu

Calderone, Anna
Facultes Universitaires Notre Dame de la Paix
Physics Department
rue de Bruxelles
Namur 5000
Belgium
Phone: 32-81-724705
Fax: 32-81-724707
anna.calderone@scf.fundp.ac.be

Canuto, Sylvio
Universidade de São Paulo
Instituto de Fisica
CPX 66318
São Paulo 05389-970
Brazil
Phone: 55-11-818-6983
Fax: 55-11-818-6831
canuto@if.usp.br

Cao, Jianshu
University of California, San Diego
Department of Chemistry
9500 Gilman Dr. 0339
La Jolla, CA 92093
USA
Phone: 619-534-0290
Fax: 619-534-7654
jcao@ucsd.edu

Càrdenas-Lailhacar, Cristiàn
University of Florida
Quantum Theory Project
P.O. Box 118435
Gainesville, FL 32611-8440
USA
Phone: 352-392-6713
Fax: 352-392-8722
cardenas@qtp.ufl.edu

Casida, Mark
Universite de Montreal
Department of Chemistry
C.P. 6128, Succ Centre-ville
Montreal, Quebec H3C 3J7
Canada
Phone: 514-343-6111 x-3901
Fax: 514-343-2458
casida@chimie.umontreal.ca

Castillo, Sidonio
Universidad Autonoma Metropolitana-Azcapotzalco
Ciencias Basicas
Av San Pablo #180
Mexico DF 02200
Mexico
Phone: 52-5-724-4218
Fax: 52-5-723-5940
sca@hp9000a1.uam.mx

Castro, Eduardo A.
Universidad Nacional de La Plata
Facultad de Ciencias Exactus
Calles 47 y 115, C.C. 962
La Plata 1900
Argentina
Phone: 54-1-21-214037
Fax: 54-1-21-259485
castro@nahuel.biol.unlp.edu.ar

Challacombe, Matt
Los Alamos National Laboratory
Group T-12
MS B268
Los Alamos, NM 87545
USA
Phone: 505-665-5905
Fax: 505-665-3909
mchalla@lanl.gov

LIST OF PARTICIPANTS

Champagne, Benoît
FUNDP
CTA Lab
Rue de Bruxelles 61
Namur B-5000
Belgium
Phone: 32-81-724557
Fax: 32-81-724530
benoit.champagne@fundp.ac.be

Chatfield, David
Florida International University
Department of Chemistry
Miami, FL 33199
USA
Phone: 305-348-3977
Fax: 305-348-3772
chatfiel@fiu.edu

Cheng, Hai-Ping
University of Florida
Quantum Theory Project
P.O. Box 118435
Gainesville, FL 32611-8435
USA
Phone: 352-392-1597
Fax: 352-392-8722
cheng@qtp.ufl.edu

Chou, Mei-Yin
Georgia Institute of Technology
Department of Physics
Atlanta, GA 30332
USA
Phone: 404-894-4688
Fax: 404-894-9958
meiyin.chou@physics.gatech.edu

Chu, San-Yan
National Tsing Hua University, Taiwan
Department of Chemistry
Hsinchu, Taiwan 30043
Republic of China
Phone: 866-35-721634
Fax: 886-35-711082
sychu@chem.nthu.edu.tw

Chun, Paul
University of Florida
Department of Biochemistry & Molecular Biology
Box 100245
Gainesville, FL 32610-0245
USA
Phone: 352-392-3356
Fax: 352-392-2953
pwchun@pine.circa.ufl.edu

Clark, Tim
University Erlangen-Nurnberg
CCC
Naegelshachstr. 25
Erlangen D-91052
Germany
Phone: 49-9131-852948
Fax: 49-9131-856565
clark@organik.uni-erlangen.de

Coffin, James
IBM, Computational Chemistry
Computational Chemistry
8632 Forest Glenn
Irving, TX 75063
USA
Phone: 972-432-9701
Fax: 800-706-6351 Pager
jmcoffi@us.ibm.com

Colgate, Sam
University of Florida
Department of Chemistry
P.O. Box 117200
Gainesville, FL 32611-7200
USA
Phone: 352-392-5876
Fax: 352-392-0872
colgate@physical4.chem.ufl.edu

Cooper, David L.
University of Liverpool
Department of Chemistry
P.O. Box 147
Liverpool L69 7ZD
UK
Phone: 44-151-794-3532
Fax: 44-151-794-3588
dlc@liv.ac.uk

Cory, Marshall
University of Florida
Quantum Theory Project
P.O. Box 118435
Gainesville, FL 32611-8435
USA
Phone: 352-392-1597
Fax: 352-392-8722
cory@qtp.ufl.edu

Coutinho, Kaline
Universidade de Mogi das Cruzes
Cx.P. 411
Mogi das Cruzes SP 08701-970
Brazil
kaline@onsager.if.usp.br

Coutinho-Neto, Mauricio
University of Florida
Quantum Theory Project
P.O. Box 118435
Gainesville, FL 32611-8435
USA
Phone: 352-392-7184
Fax: 352-392-8722
coutinho@qtp.ufl.edu

Crawford, T. Daniel
University of Georgia
Department of Chemistry
Center for Computational Quantum Chemistry
Athens, GA 30602
USA
Phone: 706-542-7738
Fax: 706-542-0406
crawdad@otanes.ccqc.uga.edu

Cuan, Angeles
Instituto Mexicano del Pertoleo
Gerencia de Catalizadores
Eje Central Lazaro Cardenas 152
Gustavo A. Madero DF 07730
Mexico
Phone: 52-5-567-2927
Fax: 52-5-567-2927
angeles@briseida.ind.imp.mx

Da Costa, Herbert
University of Florida
Quantum Theory Project
P.O. Box 118435
Gainesville, FL 32611-8435
USA
Phone: 352-392-3010
Fax: 352-392-8722
dacosta@qtp.ufl.edu

Dalskov, Erik K.
University of Lund
Theoretical Chemistry—Chemical Center
P.O. Box 124
Lund S-221 00
Sweden
Phone: 46-46-222-4915
Fax: 46-46-222-4543
teoekd@garm.teokem.lu.se

Das, Guru P.
Wright Laboratory
MLBP
654, Area B
Wright Patterson AFB, OH 45433
USA
Phone: 937-429-2307
Fax: 937-255-9147
dasgp@picard.ml.wpafb.af.mil

Davidson, Ernest
Indiana University
Department of Chemistry
Bloomington, IN 47405
USA
Phone: 812-855-6013
Fax: 812-855-8300
davidson@indiana.edu

De Kee, Dan
University of Florida
Quantum Theory Project
P.O. Box 118435
Gainesville, FL 32611-8435
USA
Phone: 352-392-9306
Fax: 352-392-8722
dekee@qtp.ufl.edu

Del Bene, Janet E.
Youngstown State University
Department of Chemistry
One University Plaza
Youngstown, OH 44555
USA
Phone: 330-742-3466
Fax: 330-742-1579
fro42008@ysub.ysu.edu

Deleuze, Michael S.D.
Limburgs Universitqire Centrum
SBG
Gebow D
Diepenbeek B-3590
Belgium
Phone: 32-11-26-83-03
Fax: 32-11-26-83-01
deleuze@luc.ac.be

Deumens, Erik
University of Florida
Quantum Theory Project
P.O. Box 118435
Gainesville, FL 32611-8435
USA
Phone: 352-392-1597
Fax: 352-392-8722
deumens@qtp.ufl.edu

Dobrowolski, Jan Cz.
Drug Institute
Lab. Theor. Meth. and Calc.
30/34 Chelmska Street
Warsaw 00-725
Poland
Phone: 48-22-412940
Fax: 48-22-410652
janek@urania.il.waw.pl

Dombroski, Jeremy P.
Q-Chem, Inc.
Four Triangle Drive, Suite 160
Export, PA 15632-9255
USA
Phone: 412-325-9969
Fax: 412-325-2062
jack@q-chem.com

Ehara, Masahiro
Kyoto University
Synthetic Chemistry and Biological Chemistry
Sakyo-ku
Kyoto 606-01
Japan
Phone: 81-75-753-5660
Fax: 81-75-753-5910
ehara@sbchem.kyoto-u.ac.jp

Enevoldsen, Thomas
Odense University
Department of Chemistry
Campusvej 55
Odense M DK-5230
Denmark
Phone: 45-6557-2568
tec@dou.dk

Estiu, Guillermina L.
Universidad Nacional de La Plata
Dept. Quimica
Calle 47 Y 115 CC962
La Plata, Buenos Aires 1900
Argentina
Phone: 54-21-210784 EX 41
Fax: 54-21-259485
estiu@nahuel.biol.unlp.edu.ar

Fazzio, Adelberto
University of San Paulo
Materials Science
CP 66318
Sao Paulo SP 05315-570
Brazil
Phone: 55-11-818-6983
Fax: 55-11-818-6831
fazzio@if.usp.br

Feller, David F.
Battelle PNNL
K1-96
Richland, WA 99352
USA
Phone: 509-375-2617
Fax: 509-375-6631
d3el02@emsl.pnl.gov

Ferris, Kim F.
National Laboratory Pacific Northwest
Environmental & Energy Science
P.O. Box 999, MS-K2-44
Richland, WA 99352
USA
Phone: 509-375-3754
Fax: 509-375-2186
kim@darter.pnl.gov

Fischer, Sighart
Technische Universität München
Theoretische Physik T 38
James-Franck-Str. 12
Garching B München 85747
Germany
Phone: 49-089-289-12393
Fax: 49-089-289-12444
fischer@venus.t30.physik.tu-muenchen.de

Flamant, Isabelle
Universitaires Notre-Dame de la Paix
Lab de Chimie Theorique Appliquee FUNDP
Rue de Bruxelles 61
Namur 5000
Belgium
Phone: 32-81-724530
Fax: 32-81-724530
isabelle.flamant@fundp.ac.be

Flock, Michaela
University of Leuven
Department of Chemistry
Celestynenlaan 200F
Heverlee-Leuven B-3000
Belgium
Phone: 32-16-327-984
Fax: 32-16-32-7992
michaela@hartree.quantchem.kuleuven.ac.be

Folland, Nathan O.
Kansas State University
Physics Department
Cardwell Hall
Manhattan, KS 66506-2601
USA
Phone: 785-532-1615
Fax: 785-841-3038
nof@ksu.edu

Fuks, David
Ben-Gurion University of the Negev
Materials Eng. Department
P.O. Box 653
Beer-Sheva 84105
Israel
Phone: 972-7-6461460
Fax: 972-7-6472946
fuks@bgumail.bgu.ac.il

Gill, Peter
University of Cambridge
Department of Chemistry
Cambridge CB2 1EW
UK
Phone: 44-1223-336-344
Fax: 44-1223-336-362
pmg@euler.ch.cam.ac.uk

Giribet, Claudia G.
University of Buenos Aires
Physics
Ciudad Universitaria-Pab. 1
Buenos Aires 1428
Argentina
Phone: 54-1-788-9101
Fax: 54-1-782-7647
giribet@df.uba.ar

Goldman, Barbara M.
John Wiley & Sons, Inc.
605 Third Avenue
New York, NY 10158-0012
Phone: 212-850-6007
Fax: 212-850-6264
bgoldman@wiley.com

Goodman, Lionel
Rutgers, The State University of New Jersey
Department of Chemistry
P.O. Box 939
Piscataway, NJ 08854
USA
Phone: 908-445-2603
Fax: 908-445-5312
goodman@rutchem.rutgers.edu

Gubanov, Vladimir
San Jose State University
Physics Department
One Washington Square
San Jose, CA 95192-0106
USA
Phone: 408/924-5249
Fax: 408/924-4815
vgubanov@msn.com

Hagmann, Mark J.
Florida International University
Department of Electrical &
Computer Engineering
Miami, FL 33199
USA
Phone: 305-348-3017
Fax: 305-348-3707
hagmann@eng.flu.edu

Hall, Michael B.
Texas A & M University
Chemistry Department
Mailstop 3255
College Station, TX 77843-3255
USA
Phone: 409-845-1843
Fax: 409-845-4719
hall@chemux.tamu.edu

Handy, Nicholas C.
University of Cambridge
Department of Chemistry
Lensfield Road
Cambridge CB2 1EW
UK
Phone: 44-1223-336373
Fax: 44-1223-336362
nch1@cam.ac.uk

Harris, Frank E.
University of Utah
Department of Chemistry
Salt Lake City, UT 84112
USA
Phone: 801-581-8445
Fax: 801-581-8433
harris@dirac.chem.utah.edu

Havel, Timothy F.
Harvard Medical School
Department of BCMP
240 Longwood Avenue
Boston, MA 02115
USA
Phone: 617-432-3242
Fax: 617-738-0516
havel@menelaus.med.harvard.edu

Hedström, Magnus
University of Florida
Quantum Theory Project
P.O. Box 118435
Gainesville, FL 32611-8435
USA
Phone: 352-392-6973
Fax: 352-392-8722
hedstrom@qtp.ufl.edu

Herman, Michael
Tulane University
Chemistry Department
New Orleans, LA 70118
USA
Phone: 504-862-3582
Fax: 504-865-5596

Hess, Bernd A.
Inst fuer Physikalische and Theoretische Chemie
Theoretical Chemistry
Wegelerstrasse 12
Bonn 53115
Germany
Phone: 49-228-732920
Fax: 49-228-739064
hess@uni-bonn.de

Hill, Susan E.
Pacific Northwest National Lab
EMSL
MS D1-96
Richland, WA 99352
USA
Phone: 509-375-6370
Fax: 509-375-6631
sehill@boys.pnl.gov

Hillebrand, Claudia
University of Florida
Quantum Theory Project
P.O. Box 118435
Gainesville, FL 32611
USA
Phone: 352/392-1597
Fax: 352/392-8722
hildebrand@qtp.ufl.edu

Hirata, So
The Graduate University for Advanced Studies and
School of Mathematical & Physical Science
Myodaiji
Okazaki Aichi 444
Japan
Phone: 81-564-55-7261
Fax: 81-564-53-4660
soh@ims.ac.jp

Hobza, Pavel
J. Heyrovsky Institute of Physical Chemistry
Dolejskova 3
Prague 8 18223
Czech Republic
Phone: 420 2 66052056
Fax: 420 2 8582307
hobza@indy.jh-inst.cas.cz

Hogreve, H. J.
CNRS
Centre de Physique Theorique
Luminy, Case 907
Marseille Cedex 9 F-13288
France
Phone:
Fax: 33-491-269553
hogreve@cpt.univ-mrs.fr

Hu, Zhenming
Kyoto University, Graduate School of Engineering
Dept. of Synth. Chemistry and Biological Chemistry
Kyoto-606-01
Sakyo-Ku, Kyoto 606-01
Japan
Phone: 81-75-753-5659
Fax: 81-75-753-5910
hu@quantl.synchem.kyoto-u.ac.jp

Ishikawa, Yasuyuki
University of Puerto Rico
Chemistry Department
P.O. Box 23346
San Juan, Puerto Rico 00931-3346
Phone: 787-764-0000 EST 7399
Fax: 787-751-0625
ishikawa@rrpac.upr.clu.edu

Itskowitz, Peter
University of North Carolina
Department of Physics and Astronomy
CB #3255
Chapel Hill, NC 27599
USA
Phone: 919-962-0165
Fax: 919-962-0480
itskowit@physics.unc.edu

Ivanov, Stanislav
University of Florida
Quantum Theory Project
P.O. Box 118435
Gainesville, FL 32611-8435
USA
Phone: 352-392-6973
Fax: 352-392-8722
ivanov@qtp.ufl.edu

Jamorski, Christine
University of Florida
Quantum Theory Project
P.O. Box 118435
Gainesville, FL 32611-8435
USA
Phone: 352-392-6711
Fax: 352-392-8722
jamorski@qtp.ufl.edu

Jauregui-Renaud, Rocio
Universidad Nacional Autonoma de Mexico
Instituto de Fisica
Apdo Postal 20-364
Mexico DF 01000
Mexico
Phone: 525-622-5014
Fax: 525-622-5015
rocio@fenix.ifisicacu.unam.mx

Johnson, Walter R.
Notre Dame University
Department of Physics
334 Nieuwland Science Bldg.
Notre Dame, IN 46556
USA
Phone: 219-631-6651
Fax: 219-631-5952
WRJ@atomic3.phys.ND.edu

Jubert, Alicia H.
Universidad Nacional de La Plata
Facultad de Ciencias Exactas
CC 962
La Plata, Buenos Aires 1900
Argentina
Phone: 54-1-214037
Fax: 54-1-259485
jubert@nahuel.biol.unlp.edu.ar

Karassev, Valentin
Instituto Venezolano de Investigaciones Cientificas
Centro de Quimica
Aptso. 21827
Caracas 1020-A
Venezuela
Phone: 58-2-504-13-57
Fax: 58-2-504-13-50
vkarasev@maria.ivic.ve

Karle, Jerome
Naval Research Laboratory
Laboratory for the Structure of Matter
Code 6030 Naval Research Laboratory
Washington, DC 20375-5341
USA
Phone: 202-767-2665
Fax: 202-767-0953
williams@herker.nrl.navy.mil

Karna, Shashi
U.S. Air Force Phillips Laboratory, VTM
Space Mission Technologies Div
3550 Aberdeen Ave SE
Kirtland AFB, NM 87117-5776
USA
Phone: 505-853-3158
Fax: 505-846-2290
karnas@plk.af.mil

Kaschner, Roland
Forschungszentrum Jülich
IFF
Jülich D-52425
Germany
Phone: 49-2461-612859
Fax: 49-2461-612850
r.kaschner@fz-juelich.de

Kasha, Michael
Florida State University
Institute of Molecular Biophysics
452 Molecular Biophysics
Tallahassee, FL 32306
USA
Phone: 850-644-6452
Fax: 850-561-1406
kasha@sb.fsu.edu

Kedziora, Gary S.
Northwestern University
Chemistry
2145 Sheridan Avenue
Evanston, IL 60208-3113
USA
Phone: 847-467-4857
Fax: 847-491-7713
kedziora@chem.nwu.edu

Keshari, Vijaya
University of Puerto Rico
Department of Chemistry
Avenida R Barcelo
Cayey, Puerto Rico 00736
USA
Phone: 787-738-0702
Fax: 787-738-6962
shlok@mailexcite.com

King, James W.
Foundation for Chemistry
P.O. Box 116
Balsam, NC 28707-0116
USA
Phone: 704-452-7570
Fax: 704-452-5432
jwking@sprynet.com

King, Rollin A.
University of Georgia
Center for Computational Quantum Chemistry
Chemistry Building
Athens, GA 30602
USA
Phone: 706-542-7738
Fax: 706-542-0406
rking@tigranes.ccqc

King-Smith, Dominic
Molecular Simulations, Inc.
9685 Scranton Road
San Diego, CA 92121-3752
USA
Phone: 619-458-9990
dks@msi.com

Kirchner, Eric
Harvard-Smithsonian Center for Astrophysics
60 Garden Street
Cambridge, MA 02138
USA
Phone: 617-495-7237

Kirtman, Bernard
University of California, Santa Barbara
Department of Chemistry
Santa Barbara, CA 93106
USA
Phone: 805-893-2217
Fax: 805-893-4120
kirtman@chem.ucsb.edu

Klessinger, Martin
Universität Münster
Organisch-Chemisches Institut
Corrensstr. 40
Muenster D-48149
Germany
Phone: 49-251-8333-241
Fax: 49-251-8339-772
klessim@uni-muenster.de

Korkin, Anatoli
Motorola, Inc.
SPS
2200 W. Broadway, MD M350
Mesa, AR 85202
USA
Phone: 602-655-3171
Fax: 602-655-2285
korkin@act.sps.mot.com

Krause, Jeffrey L.
University of Florida
Quantum Theory Project
P.O. Box 118435
Gainesville, FL 32611-8435
USA
Phone: 352/392-1597
Fax: 352/392-8722
krause@qtp.edu

Krauss, Morris
National Institute of Science Technology
Center for Advanced Research Biotechnology
9600 Gudelsky Drive
Rockville, MD 20850
USA
Phone: 301-738-6242
Fax: 301-738-6255
krauss@ibm9.carb.nist.gov

Kryachko, Eugene
The John Hopkins University
Department of Chemistry
3400 N. Charles Street
Baltimore, MD 21218
USA
Phone: 410-546-7462
Fax: 410-546-8420
eugene@jhunix.hcf.jhu.edu

Krylov, Anna
University of California, Berkeley
Department of Chemistry
308
Berkeley, CA 94720
USA
Phone: 510-643-2935
Fax: 510-643-1255
anna@elba.cchem.berkeley.edu

Kubli-Garfias, Carlos
National Autonomous University of Mexico
Lab of Hormonal Chemistry
Apartado Postal 70-469
Mexico City 04511
Mexico
Phone: 525-6-223815
Fax: 525-5-500048
kubli@servidor.unam.mx

Kumar, Anil
Florida A & M University
Department of Physics
Tallahassee, FL 32307
USA
Phone: 850-599-3470
Fax: 850-599-3577

Ladik, Janos
Universität Erlangen-Nürnberg
Inst. of Theoretical Chemistry
Egerlandstrasse 3
Erlangen D-97058
Germany
Phone: 49-9131-857766
Fax: 49-9131-857736
ladik@pctc.chemie.uni-erlangen.de

Laidig, William D.
Procter & Gamble Co.
Miami Valley Laboratories
P.O. Box 538707
Cincinnati, OH 45253-8707
USA
Phone: 513-627-2857
Fax: 513-627-1233
laidig@pg.com

LIST OF PARTICIPANTS

Lanig, Harald
Computer-Chemie-Centrum
Naegelsbachstrasse 25
Erlangen D-91052
Germany
Phone: 49-9131-852948
Fax: 49-9131-856565
clark@organik.uni-erlangen.de

Lazzeretti, Paolo
University of Modena
Departimento di Chimica
Via Campi 183
Modena 41100
Italy
Phone: 39-59-378450
Fax: 39-59-373543
lazzeret@c220.unimo.it

Lee, Michael S.
University of California, Berkeley
Department of Chemistry
Head-Gordon Group, 31 Lewis
Berkeley, CA 94720
USA
Phone: 510-848-5296
Fax:
lee@bastille.cchem.berkeley.edu

Leininger, Matt L.
University of Georgia
Center for Computational Chemistry
Chemistry Building
Athens, GA 30602
USA
Phone: 706-542-7738
Fax: 706-542-0406
mlleinin@harpagos.ccqc.uga.edu

Lengsfield, Byron H.
IBM Almaden Research Center
650 Harry Road
San Jose, CA 95120
USA
Phone: 408-927-2032
Fax:
bbyron@almaden.ibm.com

Leszczynski, Jerzy
Jackson State University
Department of Chemistry
17910
Jackson, MS 39217
USA
Phone: 601-973-3482
Fax: 601-973-3674
jerzy@tiger.jsums.edu

Levy, Ronald
Rutgers University
Department of Chemistry
P.O. Box 939
Piscataway, NJ 08855-0939
USA
Phone: 732-445-3947
Fax: 732-445-5958
ronlevy@lutece.rutgers.edu

Light, John C.
University of Chicago
Department of Chemistry
5735 S. Ellis Avenue
Chicago, IL 60637
USA
Phone: 773-702-7197
Fax: 773-702-8314
light@pclight.uchicago.edu

Loew, Gilda
Molecular Research Institute
845 Page Mill Road
Palo Alto, CA 94304
USA
Phone: 650-424-9924
Fax: 650-424-9501
loew@montara.molres.org

Lohr, Lawrence
University of Michigan
Department of Chemistry
Ann Arbor, MI 48109-1055
USA
Phone: 313-764-3148
Fax: 313-647-4865
llohr@emich.edu

Lopez-Boada, Roberto
Florida State University
Department of Chemistry
Tallahassee, FL 32306-3006
USA
Phone: 850-644-3810
Fax: 850-644-8281
rboada@dirac.fsu.edu

Lotrich, Victor F.
University of Delaware
Department of Physics
Sharp Lab
Newark, DE 19716
USA
Phone: 302-831-3512
Fax: 302-831-1637
lotrich@udel.edu

Löwdin, Per-Olov
University of Florida
Quantum Theory Project
P.O. Box 118435
Gainesville, FL 32611-8435
USA
Phone: 352-392-1597
Fax: 352-392-8722
lowdin@kvac.uu.se

Luna-Garcia, Hector
Universidad Autonoma Metropolitana-Azcapotzalco
Ciencias Basicas
Av San Pablo 180
Mexico City DF 02200
Mexico
Phone: 915-724-4218
lghm@hp9000al.uam.mx

Magers, David H.
Mississippi College
Department of Chemistry
Box 4065
Clinton, MS 39058
USA
Phone: 617-495-4767
magers@mc.edu

Makri, Nancy
University of Illinois
Department of Chemistry
505 South Mathews Avenue
Urbana, IL 61801
USA
Phone: 217-333-6589
Fax: 217-244-0789
nancy@makri.scs.uiuc.edu

March, Norman
Oxford University
6 Northcroft Road
Egham, Surrey TW20 ODU
UK

Martens, Craig C.
University of California, Irvine
Department of Chemistry
Irvine, CA 92697-2025
USA
Phone: 714-824-8768
Fax: 714-824-8571
cmartens@uci.edu

Martin, Charles H.
University of Florida
Quantum Theory Project
P.O. Box 118435
Gainesville, FL 32611-8435
USA
Phone: 352-392-6711
Fax: 352-392-8722
martin@qtp.ufl.edu

Massa, Lou
City University of New York
Chemistry
695 Park Avenue
New York, NY 10021
USA
Phone: 212-772-5330
Fax: 212-772-5332
massa@mvaxgr.hunter.cuny.edu

Mayer, Istvan
Chemical Research Center Hungarian Academy
Institute for Chemistry
P.O. Box 17
Budapest H-1525
Hungary
Phone: 361-325-7900 ext. 295
Fax: 36-1-325-7554/325-7750
mayer@cric.chemres.hu

Mazziotti, David A.
Harvard University
Department of Chemistry
12 Oxford St.
Cambridge, MA 02138
USA
Phone: 617-547-1974
Fax: 617-495-1792
damazz@fas.harvard.edu

McGlynn, Sean P.
Louisiana State University
Department of Chemistry
329 Choppin
Baton Rouge, LA 70803
USA
Phone: 504-769-0021
Fax: 504-388-3458
sean.mcglynn@chemgate.chem.lsu.edu

Micha, David A.
University of Florida
Quantum Theory Project
P.O. Box 118435
Gainesville, FL 32611-8435
USA
Phone: 352-392-1597
Fax: 352/392-8722
micha@qtp.ufl.edu

Miller, William H.
University of California, Berkeley
Department of Chemistry
Berkeley, CA 94707
USA
Phone: 510-642-0653
Fax: 510-642-6262
miller@neon.cchem.berkeley.edu

Mogensen, Benny
University of Florida
Quantum Theory Project
P.O. Box 118435
Gainesville, FL 32611-8435
USA
Phone: 352/392-8113
Fax: 352/392-8722
benny@qtp.ufl.edu

Monkhorst, Hendrik J.
University of Florida
Quantum Theory Project
P.O. Box 118435
Gainesville, FL 32611-8435
USA
Phone: 352-392-1597
Fax: 352-392-8722
monkhors@qtp.ufl.edu

Mora-Delgado, Marco Antonio
Universidad Autonoma Metropolitana-Iztapalapa
Dpto de Quimica
Av Michoacan y La Purisima, Col Vicentina
Iztapalapa DFCP 09340
Mexico
Phone: 52-5-724-4675
Fax: 52-5-724-4666
mam@xanum.uam.mx

Morales, Jorge A.
University of Florida
Quantum Theory Project
P.O. Box 118435
Gainesville, FL 32611-8435
USA
Phone: 352-392-7184
Fax: 352-392-8722
morales@qtp.ufl.edu

Morgan III, John D.
University of Delaware
Department of Physics
Newark, DE 19716
USA
Phone: 302-831-2661
Fax: 302-831-1637
32399@udel.edu

Morita, Akihiro
Kyoto University
Department of Chemistry
Kitashirakawa, Sakyo-Ku
Kyoto 606
Japan
Phone: 81-75-753-4005
Fax: 81-75-753-4000
morita@kuchem.kyoto-u.ac.jp

Mosley, David H.
University of Namur
Lab. de CTA
Rue de Bruxelles 61
Namur B-5000
Belgium
Phone: 32-81-72-4554
Fax: 32-81-72-4567
david.mosley@fundp.ac.be

Motta, Carlos Augusto M.
Facultes Universitaires de Namur
Department of Organic Chemistry
Centro De Tec, Bloco A, Sala 609A, Cidade Uni. 68563
Rio De Janeiro 21947-900
Brazil
Phone: 55-021-590-3544
Fax: 55-021-290-4746
guto@pc140.iq.ufrj.br

Mukamel, Shaul
University of Rochester
Department of Chemistry
Hutchison Hall, 500 Wilson Blvd. P.O. RC Box 270216
Rochester, NY 14627-0216
USA
Phone: 716/275-3080
Fax: 716-473-6889
mukamel@chem.rochester.edu

Nagao, Hidemi
Institute of Molecular Science
Myodaiji
Okasaki, Aichi 444
Japan
Phone: 81-6-850-5405
Fax: 81-6-850-5550
nagao@chem.sci.osaka-u.ac.jp

Nagel, Bengt
Royal Institute of Technology
Theoretical Physics
Stockholm S-100 44
Sweden
Phone: 46-8-790168
Fax: 46-8-10 48 79
nagel@theophys.kth.se

Nagy, Ágnes
Kossuth Lajos University
Institute of Theoretical Physics
P.O. Box 5
Debrecen H-4010
Hungary
Phone: 36-52-417266
Fax: 36-52-431722-1291
nalev@tigris.klte.hu

Nakano, Haruyuki
University of Tokyo
Department of Applied Chemistry
7-3-1 Hongo, Bunkyo-ku
Tokyo 113
Japan
Phone: 81-3-5802-3757
Fax: 81-3-5802-3757
nakano@qcl.t.u-tokyo.ac.jp

Nakayama, Akira
University of Tokyo
Department of Chem. System Eng.
7-3-1 Hongo
Bunkyo-ku, Tokyo 113
Japan
Phone: 81-3-3812-2111 x7286
Fax: 81-3-3818-5643
nakayama@tcl.t.u-tokyo.ac.jp

Nicholas, John B.
PNNL
EMSL
1502 SE Oxford
Richland, WA 99352
USA
Phone: 509-375-6559
Fax: 509-375-6631
jb-nicholas@pnl.gov

Nicholson, Donald M.
Oak Ridge National Laboratory
Building 4500-S
Oak Ridge, TN 37831-6114
USA
Phone: 423-574-5873
Fax: 423-574-7659
nicholsondm@ornl.gov

Nooijen, Marcel
Princeton University
Department of Chemistry
Frick Lab #123B
Princeton, NJ 08540
USA
Phone: 609-258-3168
Fax: 609-258-6746
nooijen@princeton.edu

Öhrn, Yngve
University of Florida
Quantum Theory Project
P.O. Box 118435
Gainesville, FL 32611-8435
USA
Phone: 352-392-1597
Fax: 352-392-8722
ohrn@qtp.ufl.edu

Ohta, Koji
Osaka National Research Institute, AIST, MITI
Department of Optical Materials
1-8-31 Midorigaoka
Ikeda, Osaka 563-8577
Japan
Phone: 81-627-51-9523
Fax: 81-627-51-9628
ohta@onri.go.jp

Olsen, Jeppe
University of Lund
Theoretical Chemistry Dept.
P.O. Box 124
Lund 22100
Sweden
Phone: 46-46-222-8240
Fax: 46-46-222-4543
teojeo@garm.teokem.lu.se

Ortiz, Vincent
Kansas State University
Department of Chemistry
Manhattan, KS 66506
USA
Phone: 913-532-6665
Fax: 913-532-6666
ortiz@ksu.edu

Ostlund, Neil S.
Hypercube, Inc.
2135 NW 15th Ave
Gainesville, FL 32605
USA
Phone: 352-378-9776
Fax: 352-392-8722
ostlund@hyper.com

Ozment Payne, Judy
Penn State University
Division of Science and Engineering
1600 Woodland Road
Abington, PA 19001
USA
Phone: 215-881-7471
Fax: 215-881-7623
o96@psu.edu

Paikeday, Joseph M.
Southeast Missouri State University
Department of Physics
One University Plaza MS 6600
Cape Girardeau, MO 63701-4799
USA
Phone: 573-651-2393
Fax: 573-651-2223
c314scp@semovm.semo.edu

Pandey, Ravindra
Michigan Technological University
Physics Department
1400 Townsend Drive
Houghton, MI 49931
USA
Phone: 906-487-2831
Fax: 906-487-2933
pandey@mtu.edu

Pearl, Greg Martin
University of Florida
Quantum Theory Project
P.O. Box 118435
Gainesville, FL 32611-8435
USA
Phone: 352-392-6713
Fax: 352-392-8722
pearl@qtp.ufl.edu

Perera, Ajith
University of Florida
Quantum Theory Project
P.O. Box 118435
Gainesville, FL 32611-8435
USA
Phone: 352-392-6973
Fax: 352-392-8722
perera@qtp.ufl.edu

Perpete, Eric A.
Facultes Universitaires de Namur
C.T.A.
Rue de Bruxelles, 61
Namur 5000
Belgium
Phone: 32-81-724557
Fax: 32-81-729530
eperpete@messiaen.scf.fundp.ac

Person, Willis
University of Florida
Department of Chemistry
P.O. Box 117200
Gainesville, FL 32611-7200
USA
Phone: 352-392-0528
Fax: 352-392-0872
person@pine.circa.ufl.edu

Persson, Petter
Uppsala University
Department of Quantum Chemistry
Box 518
S-751 20 Uppsala
Sweden
Phone: 46-18-4713579
Fax: 46-18-502402
petter@kvac.uu.se

Piecuch, Piotr
University of Florida
Department of Chemistry
P.O. Box 118435
Gainesville, FL 32611-8435
USA
Phone: 352-392-9227
Fax: 352-392-8722
piecuch@qtp.ufl.edu

Politzer, Peter
University of New Orleans
Chemistry Department
Lakefront Campus
New Orleans, LA 70148-2820
USA
Phone: 504/286-6850
Fax: 504/286-6860
papcm@uno.edu

Pople, John
Northwestern University
Department of Chemistry
2145 N. Sheridan Road
Evanston, IL 60208-3113
USA
Phone: 847-491-3403
Fax: 847-491-7713
pople@lithium.chem.nwu.edu

Porter, Leonard E.
Washington State University
Radiation Safety Office
Nuclear Radiation Center
Pullman, WA 99164-1302
USA
Phone: 509-335-7057
Fax: 509-335-1615
porterl@mail.wsu.edu

Poulain, Enrique
Instituto Technologico de Tlalnepantla
Division de Estudios de Posgrado
Apdo Postal 750
Tlalnepantla de Baz DF 54070
Mexico
Phone: 52-5-390-0310
Fax: 52-5-565-3910
sca@hp9000a1.uam.mx

Priyadarshy, Satyam
University of Pittsburgh
Department of Chemistry
219 Parkman Avenue
Pittsburgh, PA 15260
USA
Phone: 412-624-8200
Fax: 412-624-8552
satyam@vms.cis.pitt.edu

Probst, Michael
Innsbruck University
Department of Inorganic Chemistry
Innrain 520
Innsbruck A-6020
Austria
Phone: 43-512-5075153
Fax: 43-512-5072934
michael.probst@uibk.ac.at

Purvis, George D.
Oxford Molecular
P.O. Box 4003
Beaverton, OR 97076
USA
Phone: 503-526-5006
Fax: 503-526-5099
gpurvis@oxmol.com

Pyykkö, Pekka
University of Helsinki
Department of Chemistry
P.O. Box 55
Helsinki FIN-00014
Finland
Phone: 358-9-191-40171
Fax: 358-9-191-40169
pekka.pyykko@helsinki.fi

Quintao, Andrea D.
Universidade Federal de Minas Gerias
Dept. of Fisica
Av. Antoio Carlos 6627, Pampulha
Belo Horizonte Minas Gerais 30123-970
Brazil
Phone: 55-031-4995633
Fax: 55-031-499-5600
aquintao@fisica.ufmg.br

Ramek, Michael
Technical University of Graz
Physics & Theoretical Chemistry
Brockmanngasse 27
Graz A-8010
Austria
Phone: 43-316-873-8227
Fax: 43-316-873-8720
ramek@ptc.tu-graz.ac.at

Randic, Milan
Drake University
Department of Math & Computer Science
Des Moines, IA 50311
USA
Phone: 515-271-2163
Fax: 515-271-2055

Rassolov, Vitaly A.
Northwestern University
Department of Chemistry
2145 Sheridan Road
Evanston, IL 60208-3113
USA
Phone: 847-491-3423
Fax: 847-491-7713
rassolov@chem.nwu.edu

Ratner, Mark A.
Northwestern University
Chemistry Department
2145 Sheridan Rd
Evanston, IL 60208-3113
USA
Phone: 847-491-5652
Fax: 847-491-7713
ratner@chem.nwu.edu

Récamier, Jose
Universidad Nacional Autonoma de Mexico
Lab Cuernavaca
Apdo Postal 48-3
Cuernavaca Morelos 62251
Mexico
Phone: 52-5-622-7763
Fax: 52-73-173077
pepe@ce.itisicam.unam.mx

Reyes, Andres
University of Florida
Quantum Theory Project
P.O. Box 118435
Gainesville, FL 32611-8435
USA
Phone: 352-392-3010
Fax: 352-392-8722
reyes@qtp.ufl.edu

Ritchie, Adam B.
Lawrence Livermore National Lab.
Livermore, CA 94550
USA
Phone: 510-423-9180
Fax: 510-422-5102
ritchie1@llnl.gov

Roos, Bjorn
University of Lund
Theoretical Chemistry Department
P.O. Box 124
Lund S-221 00
Sweden
Phone: 46-46-2228251
Fax: 46-46-2224543
teobor@garm.teokem.lu.se

Ruiz de Azua, Martin C.
Universidad de Buenos Aires
Dpto. de Fisica
Cdad Universitaria, Pab. 1
Buenos Aires 1428
Argentina
Phone: 54-1-782-1007
Fax: 54-1-782-7647
azua@df.uba.ar

Rychlewski, Jacek
A. Mickiewicz University
Department of Chemistry
Grunwaldzka 6
Poznan 60-780
Poland
Phone: 48-61-8699181 X-275
Fax: 48-61-8658008
rycmlew@man.poznan.pl

Sabin, John R.
University of Florida
Quantum Theory Project
P.O. Box 118435
Gainesville, FL 32611-8435
USA
Phone: 352-392-1597
Fax: 352-392-8722
sabin@qtp.ufl.edu

Sadeghi, Raymond
University of Florida
Quantum Theory Project
P.O. Box 118435
Gainesville, FL 32611-8435
USA
Phone: 352-392-6973
Fax: 352-392-8722
rsadeghi@qtp.ufl.edu

Saha, B. C.
Florida A & M University
Department of Physics
112A Jones Hall
Tallahassee, FL 32307
USA
Phone: 850-599-3470
Fax: 850-599-3577
saha@cennas.nhmfl.gov

Sahni, Viraht
Brooklyn College of CUNY
Department of Physics
2900 Bedford Avenue
Brooklyn, NY 11210-2889
USA
Phone: 718-951-5785
Fax: 718-951-4407
vvvbc@cunyvm.cuny.edu

Santana, Pedro
University of Florida
Quantum Theory Project
P.O. Box 118435
Gainesville, FL 32611-8435
USA
Phone: 352-392-1597
Fax: 352-392-8722
santana@qtp.ufl.edu

Santilli, Ruggero M.
Institute for Basic Research
Box 1577
Palm Harbor, FL 34682
USA
Phone: 813-934-9593
Fax: 813-934-9275
ibr@gte.net

Satoh, Katsuhiko
Institute of Molecular Science
Theoretical Studies
Okazaki 444-8585
Japan
Phone: 81-564-55-7308
Fax: 81-564-53-4660
ksatoh@ims.ac.jp

Saue, Trond
Universite Paul Sabatier
IRSAMC-LPQ
118 Route de Narbonne
Toulouse 31400
France
Phone: 33-516556948
Fax: 33-561556065
tsaue@irsamc1.ups-t1se.fr

Schmelcher, Peter
University of Heidelburg
Theoretical Chemistry Department
Im Neuenheimer Feld 253
Heidelberg D-69120
Germany
Phone: 49-6221-545208
Fax: 49-6221-545221
peter@tc.pci.uni-heidelberg.de

Schmidt, Peter
Office of Naval Research
Chemistry Division
800 North Quincy Street Code 1113
Arlington, VA 22217-5000
USA
Phone: 703-696-4362
schmidt@onrhq.onr.navy.mil

Schmiedekamp, Lumelle A.
Penn State University
Physics Department
1600 Woodland Road
Abington, PA 19001
USA
Phone: 215-881-7572
Fax: 215-881-7623
ams@psu.edu

Schuch, Dieter
JW Goethe-Universität
Inst. fur Theoretische Physik
Robert-Mayer-Str. 8-10
Frankfurt D-60054
Germany
Phone: 49-69-319523
Fax: 49-69-3088997
schuch@th.physik.uni-frankfurt.de

Schwegler, Eric
Minnesota Supercomputer Institute
1200 Washington Avenue South
Minneapolis, MN 55415
USA
Phone: 612-626-0763
Fax: 612-624-8861
schwegle@chem.umn.edu

Seel, Max
Michigan Technological University
Physics Department
1400 Townsend Drive
Houghton, MI 49931-1295
USA
Phone: 906-487-2156
Fax: 906-487-3347
seel@mtu.edu

Sekusak, Sanja
Rugjer Boskovic Institute
Department of Chemistry
Bijenicka 54
Zagreb
Croatia
Phone: 385-1-4561-089
Fax: 385-1-4680-084
sanja@indigo.irb.hr

Serrano, Lourdes M.
Lake Forest College
Department of Chemistry
Box 1122 555 N. Sheridan Road
Lake Forest, IL 60045
USA
Phone: 847-735-5867
Fax: 847-735-6194
serralm@student.lfc.edu

Seybold, Paul
Wright State University
Department of Chemistry
Dayton, OH 04535
USA
Phone: 937-775-2407
Fax: 937-775-2717
pseybold@wright.edu

Sherrill, David C.
University of California, Berkeley
Department of Chemistry
Box 308
Berkeley, CA 94720-1460
USA
Phone: 510-643-2935
Fax: 510-643-1255
sherrill@alum.mit.edu

Shields, George
Lake Forest College
Department of Chemistry
555 N. Sheridan Road
Lake Forest, IL 60045
USA
Phone: 708/735-5092
Fax: 708/735-6291
gshields@ifmail.lfc.edu

Shigeta, Yasuteru
Osaka University
Department of Chemistry
Machikane ya ma Machi
Toyonaka 560
Japan
Phone: 81-06-850-5405
Fax: 81-06-850-5550
shigeta@chem.sci.osaka-u.ac.jp

Shillady, Donald D.
Virginia Commonwealth University
Department of Chemistry
1001 W. Main Street, Kapp Hall
Richmond, VA 23284-8599
USA
Phone: 804-367-1298
Fax: 804-828-8599
dshillad@saturn.vcv.edu

Smeyers, Yves G.
Superior Council for Scientific Investigations
Institute of Matter Structure
Calle Serrano No 123
Madrid E-28006
Spain
Phone: 34-1-5855404
Fax: 34-1-5642431
emsmeyers@roca.csic.es

Smith, Vedene H.
Queen's University
Department of Chemistry
Kingston, Ontario K7L 3N6
Canada
Phone: 613-545-2650
Fax: 613-545-6669
vhsmith@chem.queens.ca

Soscun, Humberto
Universidad de Zulia
Fac. of Sciences, Dept. de Quimica
Grano de Oro, Mod. 2
Maracaibo Zulia AP 526,
Venezuela
Phone: 58-61-317902
Fax: 58-61-311348
humberto@sinamaica.ciens.luz.ve

Squire, Richard H.
Marshall University
Department of Chemistry
901 W. DuPont Avenue
Belle, WV 25015
USA
Phone: 304-357-1292
Fax: 304-357-1230
richard.h.squire@USA.dupont.com

Stanton, Christopher
University of Florida
Department of Physics
P.O. Box 118440
Gainesville, FL 32611-8440
USA
Phone: 352-392-8753
Fax:

Stavrev, Krassimir K.
Hypercube, Inc.
1115 NW 4th Street
Gainesville, FL 32601
USA
Phone: 352-371-7744
Fax: 352-371-3662
stavrev@hyper.com

Stevens, Walter J.
National Institute of Standards and Technology
Computational Chemistry
Building 221, Room A111
Gaithersburg, MD 20899
USA
Phone: 301-975-5968
Fax: 301-869-4020
walter.stevens@nist.gov

Sun, Jun-Qiang
University of Florida
Quantum Theory Project
P.O. Box 118435
Gainesville, FL 32611-8435
USA
Phone: 352-392-6715
Fax: 352-392-8722
sun@qtp.ufl.edu

Surjan, Peter R.
Eötvös University
Theoretical Chemistry
P.O. Box 32
Budapest 1518
Hungary
Phone: 36-1-209-0555-1632
Fax: 36-1-209-0602
surjan@para.chem.elte.hu

Talham, Dan
University of Florida
Department of Chemistry
P.O. Box 117200
Gainesville, FL 32611-7200
USA
Phone: 352-392-9016
Fax: 352-392-3255
talham@chem.ufl.edu

Talman, James
University of Western Ontario
Department of Applied Mathematics
WSC 173
London, Ontario N6A 5B7
Canada
Phone: 519-679-2111 EXT 8800
Fax: 519-661-3523
jdt@apmaths.uwo.ca

Tamm, Toomas
University of Helsinki
Department of Chemistry
P.O. Box 55
Helsinki FIN-00014
Finland
Phone: 358-9-191-40174
Fax: 358-9-191-40169
toomas@chem.helsinki.fi

Thakkar, Ajit J.
University of New Brunswick
Chemistry Department
Bag Service #45222
Fredericton NB E3B 6E2
Canada
Phone: 506-453-4629
Fax: 506-453-4981
ajit@unb.ca

Thorndyke, Brian
University of Florida
Quantum Theory Project
P.O. Box 118435
Gainesville, FL 32611-8435
USA
Phone: 352-392-6365
Fax: 352-392-8722
thorndyke@qtp.ufl.edu

Tobita, Motoi
University of Florida
Quantum Theory Project
P.O. Box 118435
Gainesville, FL 32611-8435
USA
Phone: 352-392-6365
Fax: 352-392-8722
tobita@qtp.ufl.edu

Törring, Jens T.
J. W. Goethe-Universitaet
Chemistry
Marie Curie Street, 11
Frankfurt am Main D-60439
Germany
Phone: 49-69-798-29786
Fax: 49-69-798-29404
toerring@chemie.uni-frankfurt.de

Tozer, David J.
University of Cambridge
Department of Chemistry
LCI, Bat. 420
Cambridge CB2 1EW
UK

Trickey, Samuel B.
University of Florida
Quantum Theory Project
P.O. Box 118435
Gainesville, FL 32611-8435
USA
Phone: 352-392-1597
Fax: 352-392-8722
trickey@qtp.ufl.edu

Trindle, Carl
University of Virginia
Chemistry Department
McCormick Road
Charlottesville, VA 22903
USA
Phone: 804-924-3168
Fax: 804-924-3710
cot@virginia.edu

Truhlar, Donald
University of Minnesota
Chemistry Department
207 Pleasant Street, S.E.
Minneapolis, MN 55455-0431
USA
Phone: 612-624-7555
Fax: 612-626-7541
truhlar@umn.edu

Tschumper, Gregory S.
University of Georgia
Center for Computational Quantum Chemistry
Chemistry Annex, Room 515
Athens, GA 30602-2556
USA
Phone: 706-542-7373
Fax: 706-542-0406
tschumpr@xerxes.ccqc.uga.edu

Tsurusawa, Takeshi
Institute for Molecular Science
Theoretical Studies
Myodaiji-Cho, Okazaki
Okazaki Achi 444-8585
Japan
Phone: 81-564-55-7308
Fax: 81-564-53-4660
ztakeshi@ims.ac.jp

Turner, Rebecca B.
Lake Forest College
Department of Chemistry
LFC Box 1188, 555 N. Sheridan Road
Lake Forest, IL 60045
USA
Phone: 847-735-5374
Fax: 847-735-6194
turnerb@student.lfc.edu

Ugalde, Jesus M.
Euskal Herriko Unibertsitatea
Kimika Fakultatea
P.K. 1072
Donostia 20080
Spain
Phone: 34-43-216-600
Fax: 34-43-212236
ugalde@sq.ehu.es

Vanderbilt, David
Rutgers University
Department of Physics and Astronomy
61 Robert Rd.
Princeton, NJ 08540
USA
Phone: 732-445-2514
Fax: 732-445-4400
dhv@physics.rutgers.edu

Vercauteren, Daniel
University of Namur
Chemistry Department
Rue de Bruxelles, 61
Namur B-5000
Belgium
Phone: 32-81-724534
Fax: 32-81-724530
daniel.vercauteren@sef.fundp.ac.bf

Vergenz, Robert
University of North Florida
Department of Natural Sciences
3456 St. Johns Bluff Road S.
Jacksonville, FL 32225-2645
USA
Phone: 904-721-1934

Vigneron, Jean-Pol
Universitaires Notre-Dame de la Paix
Department of Physics
Rue de Bruxelles 61
Namur 5000
Belgium
Phone: 32-81-724711
Fax: 32-81-724707
jean-pol.vigneron@scf.fundp.ac.be

Vilkas, Jonas M.
University of Puerto Rico
Department of Chemistry
P.O. Box 23346
San Juan, Puerto Rico 00931-3346
Phone: 787-764-0000 x-5908
Fax: 787-756-7717
vilkas@pauli.uprr.pr

Wagner-Brown, Katrina B.
Conceptual Mindworks
4318 Woodcock Dr. #210
San Antonio, TX 78228
USA
Phone: 210-536-4822
Fax: 210-536-2952
wagner@delta.broks.ad.mil

Warshel, Arieh
University of Southern California
Chemistry Department
1008 Westholme Ave.
Los Angeles, CA 90024
USA
Phone: 213-740-4114
Fax: 213-740-2701

Watts, John
University of Florida
Quantum Theory Project
P.O. Box 118435
Gainesville, FL 32611-8435
USA
Phone: 352-392-1597
Fax: 352-392-8722
watts@qtp.ufl.edu

Weatherford, Charles A.
Florida A & M University
Department of Physics
205 Jones Hall
Tallahassee, FL 32307
USA
Phone: 850-599-3470
Fax: 850-599-3577
weatherf@cennas.nhmfl.gov

Weiner, Brian
Pennsylvania State University
Department of Physics
College Place
Dubois, PA 15801
USA
Phone: 814-375-4700
Fax: 814-375-4784
bqw@psu.edu

Wenzel, Wolfgang
Dortmund University
Theoretical Physics
Otto-Hahn-Str 4
Dortmund D-44221
Germany
Phone: 49-251-755-3551
Fax: 49-251-755-3551
wenzel@wap.physik.uni-dortmund.de

Wilson, Kenneth
University of Florida
Quantum Theory Project
P.O. Box 118435
Gainesville, FL 32611-8435
USA
Phone: 352-392-6365
Fax: 352-392-8722
wilson@qtp.ufl.edu

Xantheas, Sotiris S.
Pacific Northwest National Lab
Environmental Molecular Sciences Lab
902 Batelle Blvd., MS K1-96
Richland, WA 99352
USA
Phone: 509-375-6878
Fax: 509-375-6631
ss_xantheas@pnl.edu

Yamada, Satoru
Osaka University
Department of Chemistry
Machikaneyama-cho 1-1
Toyonaka 560
Japan
Phone: 81-6-850-5405
Fax: 81-6-850-5550
yamada@chem.sci.osaka-u.ac.jp

Yau, Anthony
University of Florida
Quantum Theory Project
P.O. Box 118435
Gainesville, FL 32611-8435
USA
Phone: 352-392-6365
Fax: 352-392-8722
yau@qtp.ufl.edu

Yeager, Danny L.
Texas A & M University
Chemistry Department
MS-3255
College Station, TX 77843-3255
USA
Phone: 409-845-3436
Fax: 409-845-4719
yeager@chemvx.tamu.edu

Yi, Zhigang
University of Florida
Quantum Theory Project
P.O. Box 118435
Gainesville, FL 32611-8435
USA
Phone: 352/392-3010
Fax: 352/392-8722
yi@qtp.ufl.edu

Yoshioka, Yasunori
Osaka University
Department of Chemistry
Toyonaka, Osaka 560
Japan
Phone: 81-6-850-5406
Fax: 81-6-850-5550
yyoshi@chem.sci.osaka-u.ac.jp

Zakrzewski, Vyacheslav
Kansas State University
Department of Chemistry
111 Willard Hall
Manhattan, KS 66506-3701
USA
Phone: 785-532-6072
Fax: 913-532-6666
vgz@ksu.edu

Zerner, Michael C.
University of Florida
Quantum Theory Project
P.O. Box 118435
Gainesville, FL 32611-8435
USA
Phone: 352-392-1597
Fax: 352-392-8722
zerner@qtp.ufl.edu

Zeroka, Daniel
Lehigh University
Chemistry Department
Bldg. E5554, SCBRD-RTE, ERDEC
Aberdeen Proving Ground, MD 21010-5423
USA
Phone: 410-671-4825
Fax: 410-671-1120
dz00@lehigh.edu

Zhu, Chaoyuan
Institute for Molecular Science
Division of Theoretical Studies
Myodaiji Okazaki 444
Japan
Phone: 81-564-55-7309
Fax: 81-564-53-4660
zhu@ims.ac.jp

On the Origin of the Lack of Anticonvulsant Activity of Some Valpromide Derivatives

S. M. TASSO,[1] L. BRUNO-BLANCH,[1] G. L. ESTIÚ[2]

[1]*Química Medicinal, Facultad de Ciencias Exactas, Universidad Nacional de La Plata. C.C. 243-1900-La Plata, Argentina*

[2]*CEQUINOR, Departamento de Química, Facultad de Ciencias Exactas, Universidad Nacional de La Plata. C.C. 962-1900-La Plata, Argentina*

Received 25 February 1998; revised 8 June 1998; accepted 11 June 1998

ABSTRACT: Two closely related N-substituted valpromide derivatives: N-valproyl glycinamide and N-valproyl glycine are comparatively analyzed, the first of which is antiepileptic active whereas the second is not. The study is based on a conformational analysis using an AM1 Hamiltonian that not only search for the lower energy structures of each derivative but also for the energy involved in their mutual interconversion. Open structures have been compared with cyclic ones, the latter including those stabilized by either inter or intra molecular hydrogen bonds (dimers and monomers, respectively). H-bond formation has been also evaluated by means of ab initio G94(6–31 + G(d,p)) calculations for a smaller system (N-formylglycine/glycinamide) modeling both vacuum and solvent conditions. The conformational and electronic characteristics of the open and cyclic monomers, as well as of the dimer N-valproyl glycinamide and N-valproyl glycine structures are discussed. On the basis of the results of their comparative analysis, we have redefined the pharmacophore previously proposed for N-substituted valpromides [Tasso, Bruno-Blanch, Estiu, Int. J. Quant. Chem. **65**(6), 1107 (1997)], relaxing some of the associated requirements. The corrected model requires one carbon atom or any bioisosteric substituent in an anticlinal conformation relative to the aminic nitrogen of the amide moiety, in addition to one hydrogen atom that should be antiperiplanar to the carbonyl oxygen. This model offers an explanation to the different response of N-valproyl glycinamide and N-valproyl glycine against convulsion, which is based on conformational restrictions. © 1998 John Wiley & Sons, Inc. Int J Quant Chem 70: 1127–1136, 1998

Key words: pharmacophoric pattern; antiepileptic activity; conformational analysis; N-valproyl glycine; N-valproyl glycinamide, valpromide

Correspondence to: L. Bruno-Blanch. Contract grant sponsors: CONICET; Universidad Nacional de La Plata; Cooperativa Farmacéutica de Quilmes (COFARQUIL); Laboratorios Bagó; Colegio de Farmacéuticos de la Provincia de Buenos Aires, Argentina.

International Journal of Quantum Chemistry, Vol. 70, 1127–1136 (1998)
© 1998 John Wiley & Sons, Inc.
CCC 0020-7608 / 98 / 061127-10

Introduction

γ-amino butyric acid (GABA) and glycine are among the most important inhibitory neurotransmitters, which play an important role in the control of neuronal activity in the mammalian central nervous system (CNS) and are thus related to convulsion and epilepsy [1–8]. Consequently, a tendency has developed to incorporate GABA and glycine derivatives into the newest antiepileptic agents, like gabapentin [9], milacemide [10], and N-benzyloxycarbonylglycine [11] among others.

The traditional therapy, on the other hand, includes valproic acid (vpa) as one of the four major antiepileptic drugs [12–14], whose main advantage is related to its wide spectrum of antiepileptic activity [12]. One of its main disadvantages, teratogenicity, has been assigned, on the basis of structure–teratogenicity relationships, to the carboxylic moiety, a fact that has deviated the research effort to the study of the derivatives of its primary amide, valpromide (vpd) [15]. Vpd was found to be more potent than vpa and less teratogenic [16, 17]. However, the importance of vpd over vpa in humans has no clinical implications, as vpd serves as a prodrug of vpa in humans [18]. Therefore, research in this line is presently related to the development of stable vpd analogs that will not undergo biotransformation to the corresponding acid [19–22].

Following an ongoing research centered on vpa, vpd, and their derivatives [19, 23], in this study we focus our interest on two glycine-containing compounds: N-valproyl glycine (glyvpd) and N-valproyl glycinamide (glydvpd).

N-valproyl glycine, a minor metabolite of vpa in rats [24], has not shown qualitative antiepileptic activity in mice [20]. N-valproyl glycinamide is a more recently tested compound, more effective than vpa [20]. Recent pharmacokinetic studies have concluded that, in dogs, none of the investigated compounds serve as a prodrug or a chemical delivery system for vpa and glycine. Among them, N-valproyl glycinamide shows a better pharmacokinetic profile, a fact capable of explaining its larger antiepileptic activity [20].

A previous structure–activity relationship (SAR) analysis of several N-substituted derivatives of vpd [19] has allowed us to identify a pharmacophoric pattern that has to be complied in order for the compounds to be active. The pharmacophore, shown in Figure 1, was mainly related to the anticlinal orientation of the amide function relative to the hydrocarbon chains of the valproyl moiety. Its definition involved both the nuclear coordinates and the local charges on the atomic centers. Because valproyl glycine and valproyl glycinamide are also N-substituted valpromides, we have extended the conformational analysis to these molecules in order to discern whether their stable conformations comply or not with the definition of the pharmacophore. Moreover, from their comparison, our goal is to find out whether their different response against convulsion can be explained on a structural basis, a fact that would reinforce the concepts derived from the study of their pharmacokinetic properties [20].

On the basis of the knowledge that N-acetyl glycine stabilizes as a dimer structure through intermolecular hydrogen bonds [25], the stability of monomers and dimers of glyvpd and glydvpd has been compared within the conformational study. Cyclic monomers, stabilized through intramolecular H bonds have been also included in the comparative analysis. However, the strength of the H bonds, and the consequent stabilization of the previously described structures, is largely de-

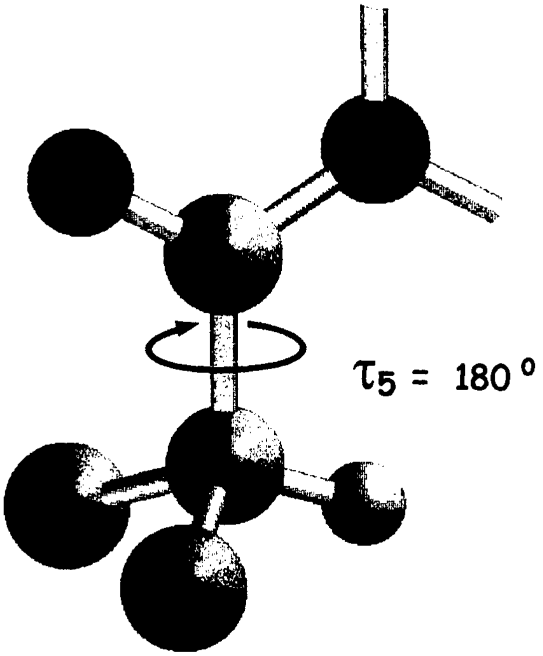

FIGURE 1. Pharmacophore proposed for N-substituted valpromides. τ_5 is defined in Figure 4. Blue, nitrogen; red, oxygen; light blue, carbon; gray, hydrogen; yellow, alkyl or aryl substituents.

termined by the dielectric constant of the media. In this framework, because no information about the valpromide receptor is presently accessible, no inference can be made about the polarity of the environment in the interaction site. In order to gain insight in the influence of the media on the biological response, calculations in vacuum and for the solvent simulated by water as a continuum have been used to approach low and high polarity media, respectively, and have been evaluated in a comparative manner.

Outline of the Calculation Procedure

A conformational analysis has been performed in order to discern whether the pharmacophore, shown in Figure 1, is defined in the conformation of minimum energy of glyvpd (Fig. 2) and/or glydvpd (Fig.3). Because the size of the molecules is not compatible with good-quality ab initio calculations, an AM1 model Hamiltonian [26] (MOPAC 7.0 package [27]) has been chosen for the conformational search in vacuum, which implies the comparison of open and cyclic structures. The choice of AM1 among the available semiempirical methodologies has been largely justified in Refs. [12, 28].

For the open monomers, the structures associated with the initial guesses for a gradient-driven full-geometry optimization were generated by means of modifications of the torsional angles τ_5–τ_8 (Fig. 4) and of those defined in the hydrocarbon chain (τ_1–τ_4). These, and the other geometry parameters were completely relaxed during the optimizations. In this framework, the conformational search has been performed as follows:

1. The τ_5 value was modified in 90° steps from 0° to 270° for both glyvpd and glydvpd. Intermediate values were not considered because all the optimizations starting from the above-mentioned ones converged to values close to either $\tau_5 = 0°$ or $\tau_5 = 180°$.
2. For each of the τ_5 values, τ_6 has been varied in 90° steps. In a similar fashion to that described for τ_5 two minima were found, associated, respectively, with the orientation of the hydrogen atom toward O_9 (Fig. 4) or opposite to it. The first one is the most stable because it minimizes steric repulsion.
3. As the next step of the optimization, modifications of τ_7 in 60° and τ_8 in 90° steps have been performed for each pair of τ_5, τ_6 values.
4. It is well known that the "all trans" conformation is the most stable for the hydrocarbon chain. A thorough discussion of this subject can be found in Ref. [23]. This conformation has been confirmed, however, for the different derivatives, by means of distortions of the τ_1–τ_4 angles in 60° and 90° from their

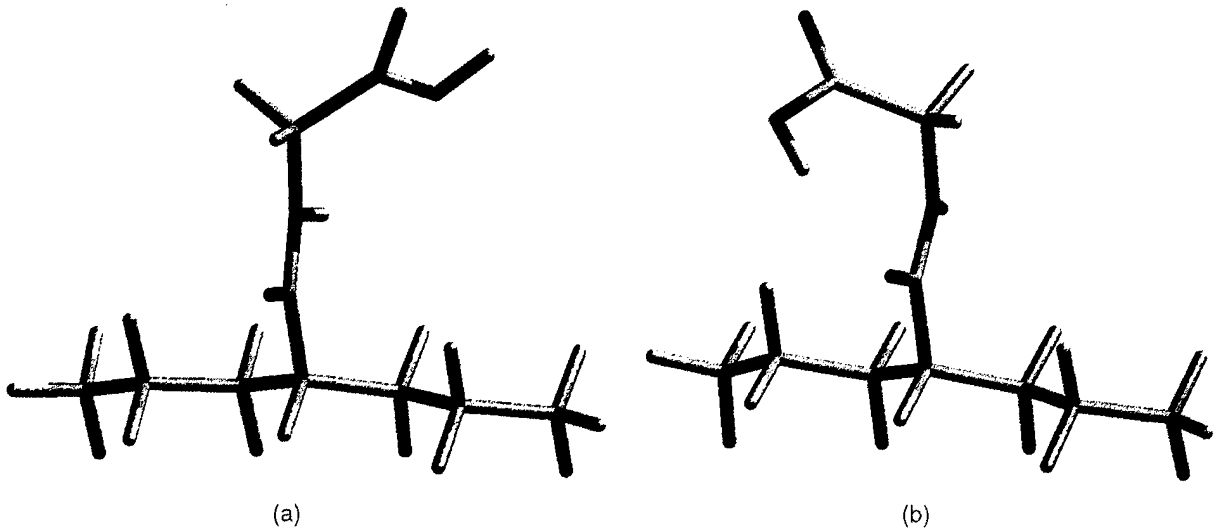

FIGURE 2. Most stable conformations of glyvpd. (a) Open monomer. (b) Cyclic monomer.

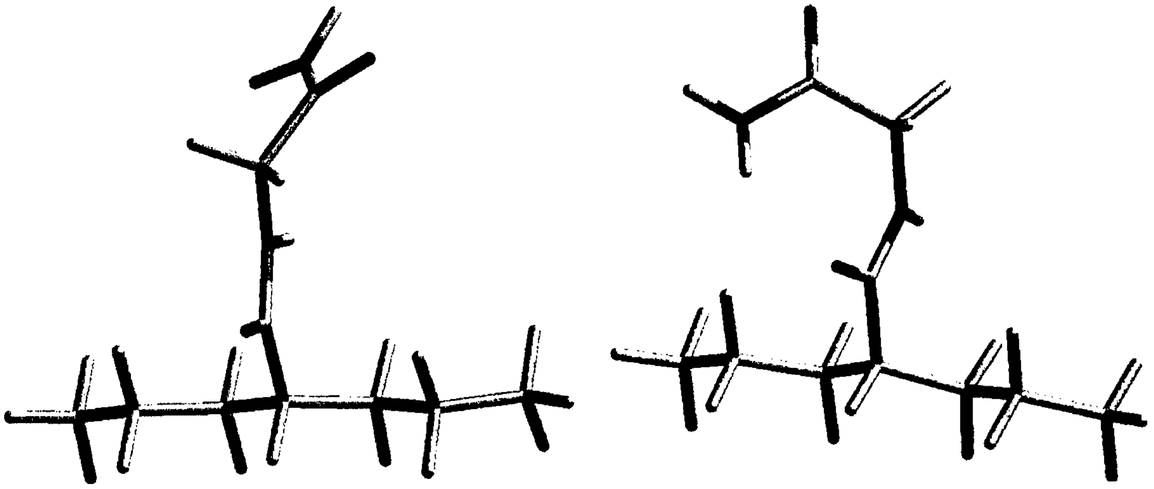
(a) (b)

FIGURE 3. Most stable conformations of glydvpd. (a) Open monomer. (b) Cyclic monomer.

starting 180°, followed by full optimization of the resulting structure.

The initial structures for the cyclic monomers have been built by means of the definition of the appropriate combination of the τ_6–τ_8 torsional angle values that lead to the stabilization of an intramolecular H bond between the carboxylic oxygen of the valproyl moiety and the H atom of the hydroxy or amide group of the gly or glyd moieties, respectively.

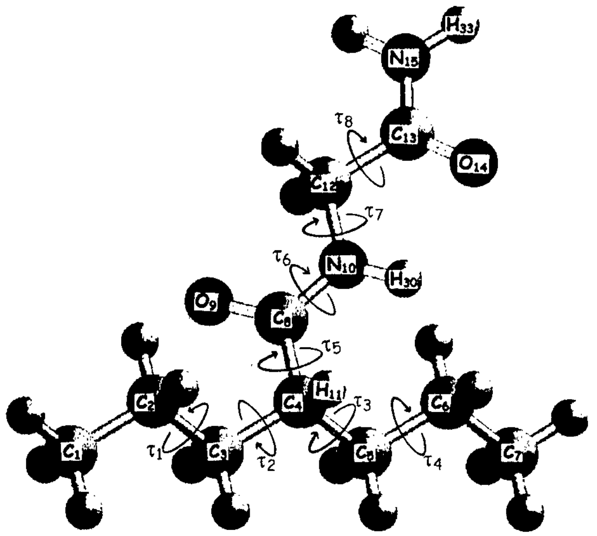

FIGURE 4. Atom numbering and torsional angles in the glydvpd molecule. N_{15} is replaced by O_{15} in glyvpd. $\tau_1 = C_1C_2C_3C_4$, $\tau_2 = C_2C_3C_4C_5$, $\tau_3 = C_3C_4C_5C_6$, $\tau_4 = C_4C_5C_6C_7$, $\tau_5 = O_9C_8C_4H_{11}$, $\tau_6 = O_9C_8N_{10}C_{12}$, $\tau_7 = C_8N_{10}C_{12}C_{13}$, $\tau_8 = N_{10}C_{12}C_{13}N_{15}$

Cyclic and open monomers have been used to build the dimers (Figs. 5 and 6), which comprise H-bond formation between the carbonyl oxygen and the amine nitrogen of the glycine moiety (O_{14}—N_{10}). Syn- and antiperiplanar conformations of the monomers, comprising both open and cyclic units, have been used to build the starting structures. Their stability has been compared after a full geometry relaxation.

For both the cyclic and open monomers, as well as for the dimeric structures, AM1 calculations have been also used to evaluate the torsional barrier around the CC bond associated with τ_5. The keyword PRECISE has been always used throughout the calculations.

The difficulties associated with the accurate quantum chemical description of the interactions involved in H bonds are well documented [29–31]. It is well known that the results of their semiempirical evaluation have to be considered with caution. In order to confirm the conclusions from them derived, ab initio G-94(HF/6-31 + G(d, p) calculations [32] have been performed for molecules that, being smaller than glyvpd and glydvpd, retain the local characteristics in the moieties involved in the H bonds: N-formyl glycine and N-formyl glycinamide. The stability of cyclic

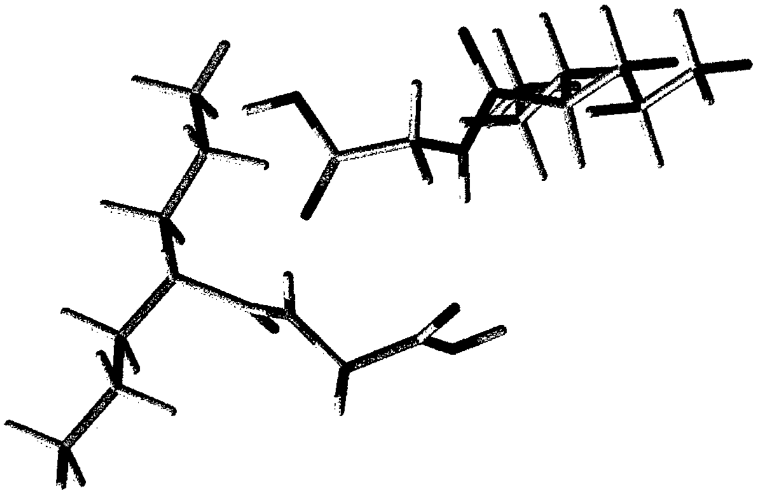

FIGURE 5. Most stable conformation of dimeric glyvpd.

and open monomers, as well as dimer structures, has been compared for these molecules, at this level of theory, for both vacuum and solvent simulated conditions. The solvent to be approached, physiological media, is mainly defined by water. It has been modeled, thus, by water as a continuum within an Onsager approach [33].

Electronic descriptors have been derived from a Mulliken population analysis [34] performed at the AM1 level. In spite of the lack of precision of this analysis for absolute calculations, their results are widely accepted in this field for the study of the trends in their variation on well-defined atomic centers that follow structural modifications performed to a parent structure [35, 36].

Results and Discussion

GLYVPD AND GLYDVPD MONOMERS

In agreement with the results of our previous calculations for a set of N-substituted vpd [19], two minima result from the AM1 geometry optimization procedure, which are related to values of τ_5 close to 0° and 180°, respectively, and define

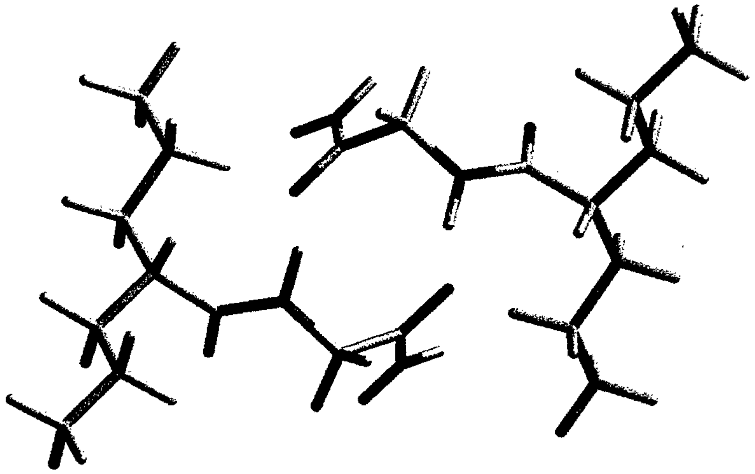

FIGURE 6. Most stable conformation of dimeric glydvpd.

synperiplanar and antiperiplanar O_9 to H_{11} conformations (Fig. 4). According to the results shown in Tables I and II, the synperiplanar conformation is preferred by both glyvpd and glydvpd. The previous discussion is valid for open and cyclic monomers. Although only the antiperiplanar conformation has been found to be associated with the antiepileptic activity [19], the energy difference between both orientations within a given cyclization pattern is close to 1 kcal/mol (Tables I and II), showing that both conformers can coexist in equilibrium. Moreover, the calculated energy barrier for their mutual interconversion (close to 2.6 kcal/mol) demonstrates that the active conformation can be easily attained, at a low energy cost, in the receptor site.

Whereas the cyclic conformation is more stable for the amide at the semiempirical AM1 level, the open structure is preferred for the acid (Tables I and II). Cyclization does not imply, however, that the structure become rigid, and the torsional freedom around the C_4C_8 bond does not depend on the internal array of the glycine moiety. The results of the ab initio calculations for the isolated molecules (Tables III and IV) are in close agreement with the semiempirical ones, stabilizing in a larger extent the cyclic structure for the N-formyl glycinamide. When the physiological media is modeled by water as a continuum, the energy difference between open and cyclic structures remains almost unchanged, showing that the possibility of cyclization, which may influence the interaction at the receptor site, is not dependent on the nature of the environmental solvent.

It can be concluded, from the comparison of the energies associated with the different stable monomeric conformations of glyvpd and glydvpd, that the structural requirements imposed by the pharmacophoric pattern previously defined [19] can be easily attained by both molecules at a very low energy cost, because of their rotational freedom around τ_5. No difference between them, capable of justifying their different response against convulsion, can be derived from the study of the isolated units.

GLYVPD AND GLYDVPD DIMERS

According to the semiempirical calculations, dimeric conformations are more stable than the monomeric ones (Tables I and II). Whereas the coordination of open units leads to more stable structures than the cyclic ones for glyvpd, implying an energy gain close to 6 kcal/mol, the coordi-

TABLE I
Stable Conformers of N-valproyl-glycine derived from the AM1 conformational analysis.[a]

	Conformer	d O—H$_{\text{intra}}$	d O—H$_{\text{inter}}$	τ_5	τ_6	τ_7	τ_8	ΔE
Monomers	1-syn	> 5.0		5.8	9.0	113.6	22.8	0.0
	2-anti	> 5.0		166.7	13.0	100.0	6.7	0.4
	3-syn	> 5.0		0.4	−166.2	91.7	56.4	3.5
	4-anti	> 5.0		168.6	−174.6	98.3	50.2	2.9
	5-syn	2.2		−2.6	0.1	81.3	−69.5	3.0
	6-anti	2.1		164.0	−3.0	80.9	−70.3	4.0
Dimers	7-syn-syn	> 5.0	2.2	1.7	−2.1	150.1	−162.5	−5.9[b]
		> 5.0	2.2	4.0	−0.3	145.5	−148.8	
	8-anti-anti	> 5.0	2.1	−173.5	6.8	115.1	−164.3	−6.2[b]
		> 5.0	2.1	−177.8	5.9	120.5	−162.1	
	9-syn-syn	2.1	2.1	10.1	−4.7	80.6	−113.5	−3.3[b]
		2.1	2.1	13.1	−2.1	80.6	−112.8	
	10-anti-anti	2.1	2.1	−175.7	−2.2	77.6	−114.6	−1.4[b]
		2.1	2.1	179.8	−2.8	79.4	−113.2	

[a] d O—H$_{\text{intra}}$ = distance (Å) between O_9 and H_{33} of the same molecule.
d O—H$_{\text{inter}}$ = distance (Å) between O_{14} and H_{30} of different monomers.
τ_5 = dihedral angle defined by $O_9C_8C_4H_{11}$ atoms.
τ_6 = dihedral angle defined by $O_9C_8N_{10}C_{12}$ atoms.
τ_7 = dihedral angle defined by $C_8N_{10}C_{12}C_{13}$ atoms.
τ_8 = dihedral angle defined by $N_{10}C_{12}C_{13}O_{15}$ atoms.
ΔE = energy difference (kcal) relative to the most stable conformer [$\Delta E = E - E_{(1\text{-syn})}$].
[b] = energy difference (kcal) relative to twice the energy of the most stable conformer [$\Delta E = E - 2 \times E_{(1\text{-syn})}$].

TABLE II

Stable Conformers of N-valproyl-glycinamide derived from the AM1 conformational analysis.[a]

	Conformer	d O—H$_{intra}$	d O—H$_{intra}$	τ_5	τ_6	τ_7	τ_8	ΔE
Monomers	1-syn	2.2		−2.7	−2.6	−80.7	53.3	0.0
	2-anti	2.2		159.3	0.2	80.7	−63.0	0.9
	3-syn	> 3.7		3.3	8.3	143.6	58.6	4.4
	4-anti	> 3.7		166.3	168.8	91.1	−4.4	4.8
	5-syn	> 3.7		2.2	−170.3	90.9	35.7	5.9
	6-anti	> 3.7		−169.3	9.1	122.4	55.6	5.3
Dimers	7-syn-syn	2.2	2.1	5.6	0.0	81.0	−107.6	−10.1[b]
		2.2	2.1	2.0	4.6	77.8	−111.0	
	8-anti-anti	2.2	2.1	174.2	3.1	79.2	−104.6	−7.8[b]
		2.2	2.1	174.3	1.8	79.5	−106.9	
	9-anti-anti	4.3	2.2	−171.4	5.3	111.1	−146.7	−1.8[b]
		4.3	2.1	−171.5	6.2	109.9	−148.2	

[a] d O—H$_{intra}$ = distance (Å) between O_9 and H_{33} of the same molecule.
d O—H$_{inter}$ = distance (Å) between O_{14} and H_{30} of different molecules.
τ_5 = dihedral angle defined by $O_9C_8C_4H_{11}$ atoms.
τ_6 = dihedral angle defined by $O_9C_8N_{10}C_{12}$ atoms.
τ_7 = dihedral angle defined by $C_8N_{10}C_{12}C_{13}$ atoms.
τ_8 = dihedral angle defined by $N_{10}C_{12}C_{13}N_{15}$ atoms.
ΔE = energy difference (kcal) relative to the most stable conformer [$\Delta E = E - E_{(1\text{-syn})}$].
[b] = energy difference (kcal) relative to twice the energy of the most stable conformer [$\Delta E = E - 2 \times E_{(1\text{-syn})}$].

nation of cyclic glydvpd units stabilizes the dimers in almost 10 kcal/mol more than that of open ones. For both molecules, syn- and antiperiplanar conformations of the monomers lead to structures of similar energies after dimerization.

The coordination of antiperiplanar conformations retains, in the dimer, the molecular portion that defines the pharmacophore (Figs. 5 and 6). On the other hand, the energy difference between the anti-anti and syn-syn conformers is as small as the energy difference between the anti and syn conformations of the monomers (Tables I and II). This fact demonstrates that anti-anti, anti-syn, and syn-syn dimers can be formed, and in the first two cases result, according to our structural model for the pharmacophore, in biologically active structures for both glyvpd and glydvpd.

The N-substituted carboxamide portion of dimeric glyvpd and glydvpd bears a disubstitution on the nitrogen atom (Figs. 5 and 6), and, regarding its conformation, complies with the requirements imposed by the pharmacophore when the anti-anti and the anti-syn dimers are considered for both molecules. However, recent pharma-

TABLE III

Most relevant ab initio calculated structural data of the stable conformers of N-formyl-glycine.[a]

	Conformer	d O—H$_{intra}$	τ_6	τ_7	τ_8	ΔE
In vacuo	1	5.4	−176.0	106.5	35.3	0.0
	2	2.0	−6.0	79.0	−60.5	0.2
In solvent	1	6.1	−171.3	82.5	172.7	0.0
	2	1.8	−13.1	75.4	−52.9	0.3

[a] d O—H$_{intra}$ = distance (Å) between O_9 and H_{33}.
τ_6 = dihedral angle defined by $O_9C_8N_{10}C_{12}$ atoms.
τ_7 = dihedral angle defined by $C_8N_{10}C_{12}C_{13}$ atoms.
τ_8 = dihedral angle defined by $N_{10}C_{12}C_{13}O_{15}$ atoms.
ΔE = energy difference (kcal) relative to the most stable conformer [$\Delta E = E - E_{(1)}$].

TABLE IV

Most relevant ab initio calculated structural data for the stable conformers of N-formyl-glycinamide.[a]

	Conformer	d O—H$_{intra}$	τ_6	τ_7	τ_8	ΔE
In vacuo	1	2.2	2.8	−85.3	66.6	0.0
	2	3.8	−173.7	−112.6	8.8	2.4
In solvent	1	2.1	7.7	−82.9	48.9	0.0
	2	3.8	−174.7	−94.6	−9.7	4.0

[a] d O—H$_{intra}$ = distance (Å) between O_9 and H_{33}.
τ_6 = dihedral angle defined by $O_9C_8N_{10}C_{12}$ atoms.
τ_7 = dihedral angle defined by $C_8N_{10}C_{12}C_{13}$ atoms.
τ_8 = dihedral angle defined by $N_{10}C_{12}C_{13}N_{15}$ atoms.
ΔE = energy difference (kcal) relative to the most stable conformer [$\Delta E = E - E_{(1)}$].

cological tests performed in our laboratory have demonstrated that disubstitution on the nitrogen, when it implies voluminous groups, larger that ethyl, leads to inactive structures, even when the conformational requirements imposed by the pharmacophore are satisfied. This effect, which is presently under investigation, seems to be associated with a steric hindrance to approach the receptor site.

Both glycine (glycinamide) and monomeric glyvpd (glydvpd), which are the N-substituents in the dimers, are large enough to block, in some way, the activity. However, there is another —NH_2 group in the glycinamide moiety of glydvpd (Fig. 6). Its orientation is fixed in glydvpd by dimerization, synclinal to one hydrogen on the C atom adjacent to the one to which it is bonded. This H atom is antiperiplanar, thus, to the oxygen, and satisfies, in this way, the geometric requirements defined by the pharmacophore (Fig. 1). When electronic descriptors are considered, the electronic distribution of this group also matches the one calculated for the group shown in Figure 1 (Table V). This group can be considered, thus, responsible for the pharmacophoric activity. Provided that this group can approach the receptor site, the energy involved in the interaction will be large enough to break the H bond that may hinder the availability of the carbonyl oxygen. The comparison of this group with the one shown in Figure 1 shows that the similarities between them apply to the H atom but not to the other substituents of the tertiary carbon atom (C_{12}). Whereas, in agreement with our model, the H atom is opposite to the carbonyl oxygen, the other substituents are not carbon atoms, but one nitrogen and one hydrogen. This evidence can lead to two different conclusions:

1. We can redefine our pharmacophore relaxing the requirement of having two carbon-containing groups bonded to the sp^3 carbon atom of Figure 1. The corrected model requires one carbon atom or any bioisosteric substitution* in an anticlinal conformation relative to the aminic nitrogen of the amide moiety, in addition to the hydrogen atom that is antiperiplanar to the carbonyl oxygen. No requirements are posed on the nature of the third substituent of the carbon atom.
2. We can reconsider the new group to which the activity is assigned. It becomes evident that the portion involved resembles more closely glycinamide than vpd. On this basis, and with the knowledge that glycine is also an inhibitory neurotransmitter, we can associate the antiepileptic activity of glydvpd with its glycinamide moiety. A question is now open of whether the activity of glydvpd is originated in the binding of either the vpd or the glyd moieties to their specific receptor sites.

We strongly support the first conclusion because the second one does not explain, again, the lack of activity of glyvpd, which should also be capable of reaching the glycinergic receptors.

We can accept, on this basis, that a second pharmacophoric group in the glydvpd molecule, which is lacking in glyvpd, is responsible for its antiepileptic activity. This explanation does not have to disregard the pharmacokinetic evidence,

---

* NH substitutes bioisosterically a C atom [37].

TABLE V

AM1 calculated charges on the atoms that define both pharmacophoric groups.[a]

Conformer	$q\ O_8$	$q\ O_9$	$q\ N_{10}$	$q\ C_{13}$	$q\ O_{14}$	$q\ N_{15}$
Pharmacophore	+0.30	−0.38	−0.37	+0.30	−0.38	−0.37
glyvpd: 2-anti	+0.30	−0.35	−0.35	—	—	—
glydvpd: 2-anti	+0.31	−0.39	−0.37	+0.27	−0.38	−0.43
glyvpd: 10-anti-anti	+0.31	−0.37	−0.38	—	—	—
	+0.31	−0.37	−0.38	—	—	—
glydvpd: 11-anti-anti	+0.31	−0.40	−0.37	+0.28	−0.43	−0.42
	+0.31	−0.40	−0.37	+0.28	−0.43	−0.42

[a] In the glyvpd molecule the second group is lacking.

which shows a large retention time (half-life) of glydvpd in the body, in dogs [20], a fact that improves the possibility of interaction of the drug before elimination. Both interpretations, pharmacokinetical and structural, refer to different steps of the interaction: transport inside the body and interaction at the receptor site, respectively. Even if a lower concentration of glyvpd can reach the receptor site, it will not show antiepileptic activity according to the results of the conformational analysis and the structural pattern here proposed.

CONCLUSIONS

We have performed a conformational analysis of glyvpd and glydvpd at a semiempirical AM1 level, considering H-bond formation in the stabilization of monomer and dimer structures. The results related to H-bond formation have been confirmed by ab initio G94(6−31 + G(d,p)) calculations for a smaller system (N-formylglycine/glycinamide), for both the isolated molecules and solvent simulated conditions.

Both methodologies give similar results, stabilizing the dimers over the monomers, and favoring the cyclic monomers over the open ones for glydvpd. In relation to the different response of glyvpd and glydvpd against convulsion, we conclude that no justification can be given on the basis of the structural data of the monomers. Both of them, either as cyclic or as open units, satisfy the requirements imposed by the pharmacophore that we have previously proposed [19].

Dimerization leads to disubstitution of the aminic nitrogen of vpd, a fact that, depending on the size of the substituents, has been found to block the anticonvulsant activity.

We associate the antiepileptic activity of glydvpd to the —NH_2 group of the glyd moiety which, while not present in glyvpd, defines, with the adjacent groups, a similar pattern to the one shown in Figure 1. On the basis of their differences we have redefined our pharmacophore. The corrected model requires one carbon atom or any bioisosteric substituent in an anticlinal conformation relative to the aminic nitrogen of the amide moiety, in addition to one hydrogen atom that should be antiperiplanar to the carbonyl oxygen. No additional requirement concerning the third substituent of the sp^3 carbon atom of Figure 1 is included in the definition of the pharmacophore.

ACKNOWLEDGMENTS

G. L. Estiú is a member of the Consejo Nacional de Investigaciones Científicas y Técnicas de la República Argentina (CONICET), and L. E. Bruno-Blanch of the Facultad de Ciencias Exactas, Universidad Nacional de La Plata. One of us (S.M.T.) acknowledges Laboratorios Bagó (Argentina) for a research fellowship.

This work was supported in part through grants from CONICET, Universidad Nacional de La Plata, Cooperativa Farmacéutica de Quilmes (COFARQUIL), Laboratorios Bagó, and Colegio de Farmacéuticos de la Provincia de Buenos Aires, Argentina.

We gratefully acknowledge the use of the computer facilities of the Cátedra de Química Cuántica, Facultad de Química, Universidad de la República Oriental del Uruguay.

References

1. W. Sieghart, Pharmacol. Rev. **47**(2), 181 (1995).
2. N. G. Bowery, Ann. Rev. Pharmacol. Toxicol. **33**, 109 (1993).
3. M. H. Aprison, E. Galvez-Ruano, and K. B. Lipkowitz, J. Neurosci. Res. **43**, 127 (1996).
4. M. H. Aprison, E. Galvez-Ruano, D. H. Robertson, and K. B. Lipkowitz, J. Neurosci. Res. **43**, 372 (1996).
5. R. W. Chapman, J. A. Hey, C. A. Rizzo, and D. C. Bolser, Trends Pharmacol. Sci. **14**, 26 (1993).
6. H. Bittiger, W. Froestl, S. J. Mickel, and H. R. Olpe, Trends Pharmacol. Sci. **14**, 391 (1993).
7. G. Satzinger, Arzneim.-Forsch./Drug Res. **44(I)**, 261 (1994).
8. B. Frolund, U. Kristiansen, L. Brehm, A. B. Hansen, P. Krogsgaard-Larsen, and E. Falch, J. Med. Chem. **38**, 3287 (1995).
9. D. Chadwick, Ed., *New Trends in Epilepsy Management: The Role of Gabapentin* (Royal Society of Medicine Services Ltd., London, 1993).
10. J. Roba, R. Cavalier, A. Cordi, H. Gorrisen, M. Herin, P. Janssens de Varebeke, C. Onkelinx, M. Remacle, and W. van Dorssen, in *New Anticonvulsant Drug*, B. S. Meldrum and R. J. Porter, Eds. (John Libby, London, 1986).
11. D. M. Lambert, J. H. Poupaert, J. M. Maloteaux, and P. Dumont, Neuropharmacol. Neurotoxicol. **5**, 777 (1994).
12. D. Chadwick, Epilepsia **35** (Suppl. 4), S3 (1994).
13. M. Bialer, A. Haj-Yehia, K. Badir, and S. Hadad, Pharm. World Sci. **16**(1), 2 (1994).
14. (a) E. A. Swinyard, J. H. Woodhead, H. Steve White, and M. R. Franklin, in *Antiepileptic Drugs*, R. Levy, R. Mattson, B. Meldrum, J. K. Penry, and F. E. Dreyfuss, Eds. (Raven, New York, 1989), Chapter 5. (b) R. H. Levy and D. D. Shen, in *Antiepileptic Drugs*, 3rd ed., R. Levy, R. Mattson, B. Meldrum, J. K. Penry, and F. E. Dreifuss, Eds. (Raven, New York, 1989), Chapter 41.

15. H. Nau and G. Hendrickx, Atlas Sci. Pharmacol., 52 (1987).
16. A. Haj-Yehia and M. Bialer, J. Pharm. Sci. **79**(8), 719 (1990).
17. W. Loscher and H. Nau, Neuropharmacology **24**, 427 (1985).
18. M. Bialer, A. Rubinstein, J. Dubrovsky, Y. Raz, and O. Abramsky, Int. J. Pharm. **23**, 25 (1985).
19. S. M. Tasso, L. Bruno-Blanch, and G. L. Estiú, Int. J. Quant. Chem. **65**(6), 1107 (1997).
20. S. Hadad and M. Bialer, Pharm. Res. **12**, 905 (1995).
21. M. Bialer, S. Hadad, B. Kadry, A. Abdul-Hai, A. Haj-Yehia, J. Sterling, Y. Herzig, and B. Yagen, Pharm. Res. **13**, 284 (1996).
22. A. Haj-Yehia, S. Hadad, and M. Bialer, Pharm. Res. **9**, 1058 (1992).
23. G. L. Estiú and L. Bruno-Blanch, Int. J. Quant. Chem.-Quantum Biol. Symp. **22**, 39 (1995).
24. R. G. Granneman, S.-I. Wang, J. M. Machinist, and J. W. Kesterson, Xinobiotica **14**, 375 (1984).
25. L. B Clark, J. Am. Chem. Soc. **117**, 7974 (1995).
26. J. J. P. Stewart, in *Reviews in Computational Chemistry*, Vol. 1, K. B. Lipkowitz, and D. B. Boyd, Eds. (VCH, New York, 1990).
27. J. J. P. Stewart, Mopac, version 7.0, F. J. Seiler Research Laboratory. United States Air Force Academy, CO 80840, 1994.
28. G. L. Estiú, J. Mol. Structure (THEOCHEM), **401** 157 (1997).
29. J. Gao, in Reviews in Computational Chemistry, Vol. 7, K. B. Lipkowitz and D. B. Boyd, Eds., (VCH, New York, 1996).
30. A. St-Amant, in *Reviews in Computational Chemistry*, Vol 7, K. B. Lipkowitz and D. B. Boyd, Eds. (VCH, New York, 1996).
31. E. Davidson, in *Reviews in Computational Chemistry*, Vol. 2, K. B. Lipkowitz and D. B. Boyd, Eds. (VCH, New York, 1991).
32. M. J. Frisch, G. W. Trucks, H. B. Schlegel, P. M. W. Gill, B. G. Johnson, M. A. Robb, J. R. Cheeseman, T. Keith, G. A. Petersson, J. A. Montgomery, K. Raghavachari, M. A. Al-Laham, V. G. Zakrzewski, J. V. Ortiz, J. B. Foresman, C. Y. Peng, P. Y. Ayala, W. Chen, M. W. Wong, J. L. Andres, E. S. Replogle, R. Gomperts, R. L. Martin, D. J. Fox, J. S. Binkley, D. J. Defrees, J. Baker, J. J. P. Stewart, M. Head-Gordon, C. Gonzalez, and J. A. Pople, Gaussian, (4, Revision B.3), Gaussian, Inc., Pittsburgh, 1995.
33. L. Onsager, Electric Moments of Molecules in Liquids, **58**, 1486 (1936).
34. R. S. Mülliken, J. Chem. Phys. **36**, 3428 (1962).
35. A. E. Reed, R. B. Weinstock, and F. Weinhold, J. Chem. Phys. **83**, 735 (1985). J. P. Foster and F. Weinhold, J. Am. Chem. Soc. **102**, 7211 (1980).
36. L. E. Chirlian and M. M. Francl, J. Comput. Chem. **8**, 894 (1987).
37. G. Patani and E. LaVoie, Chem. Rev. **96**, 3147 (1996).

Molecular Surface Electrostatic Potentials of Anticonvulsant Drugs

JANE S. MURRAY,[1] FAKHER ABU-AWWAD,[1] PETER POLITZER,[1] LESLIE C. WILSON,[2] ALLAN S. TROUPIN,[2] RYAN E. WALL[2]
[1]*Department of Chemistry, University of New Orleans, New Orleans, Louisiana 70148*
[2]*Department of Chemistry, Loyola University, New Orleans, Louisiana 70118*

Received 24 February 1998; accepted 21 May 1998

ABSTRACT: The computed molecular surface electrostatic potentials of a group of anticonvulsants of various chemical types were investigated with the objective of identifying common features that may be related to their activities. The calculations were carried out with the density functional B3P86/6-31G* procedure, using HF/STO-3G*-optimized geometries. Analysis of several statistically based properties of the surface potentials indicates that the negative regions are of primary importance and that an optimum intermediate level of local polarity, or internal charge separation, is required.

© 1998 John Wiley & Sons, Inc. Int J Quant Chem 70: 1137–1143, 1998

Introduction

Anticonvulsant or antiepileptic drugs are compounds that are found clinically to help control epileptic seizures [1–3]. They cover a range of chemical categories, which act upon different types of convulsive disorders. For example, certain barbiturates and hydantoins are effective against grand mal and psychomotor epilepsy, while some succinimides are used against petit mal epilepsy. The mechanisms of action of these and other anticonvulsants are not fully understood; one explanation for their selectivity is that they interact, initially or finally, with different receptors.

The interaction of a molecule with a receptor is an example of a "recognition" process, in which the receptor recognizes that the molecule has certain key features that will promote their interaction. This occurs before any processes of bond breaking or bond making take place. Such key features have often been identified through the analysis of the electrostatic potential $V(\mathbf{r})$ that is created in the space surrounding a molecule by its nuclei and electrons. It is through this potential that a molecule interacts with other systems in its vicinity. The affinity of a particular molecule for a specific receptor has been shown in a number of cases to depend upon the degree to which the electrostatic potential of the former possesses certain characteristics that have been established as being necessary for effectively interacting with that receptor [4–11].

Our objective in this work was to use the molecular electrostatic potential $V(\mathbf{r})$ as a tool for comparing and analyzing a large group of anticonvul-

Correspondence to: P. Politzer.

© 1998 John Wiley & Sons, Inc.

sant drugs of various chemical types. **1–6** are derivatives of the five-membered hydantoin ring. **7–9** are barbiturates, related to the six-membered heterocycle barbituric acid; **10** is obtained from **7** by the reduction of one carbonyl group. **11–13** are carbamazepine and two of its derivatives, respectively. **14** is an acetyl urea, phenacemide. **15–17** are derivatives of the five-membered heterocycle succinimide, and **18–21** are an assortment of other types. A striking feature of most of these 21 molecules is the prevalence of ureide and amide linkages, usually in cyclic form. All of them except **5** and **6** exhibit anticonvulsant activity, to varying degrees [1–3]. Some also have rather severe side effects, including skin rashes, fever, and dizziness, and in the case of phenacemide (**14**), bone marrow depression and hepatocellular damage [1].

Our approach was to analyze the electrostatic potentials on the molecular surfaces of **1–21**, both qualitatively in terms of relative patterns of positive and negative regions and quantitatively using a number of statistically derived descriptors. We have sought to identify features of the surface electrostatic potentials that may be related to anticonvulsant activity.

Methods

The electrostatic potentials on the molecular surfaces of **1–21** were computed with the density functional B3P86/6-31G* procedure, using structures optimized at the HF/STO-3G* level and the Gaussian 94 code [12]:

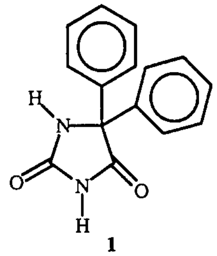
1

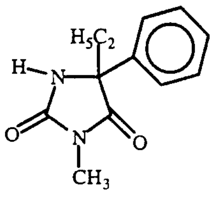
2

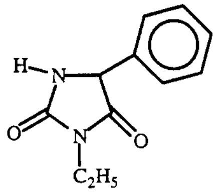
3

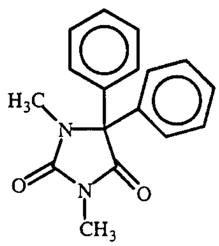
4

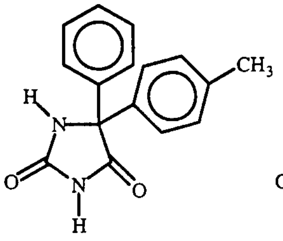
5

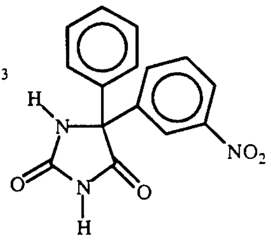
6

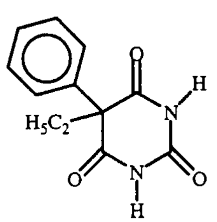
7

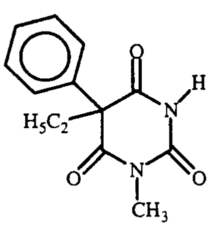
8

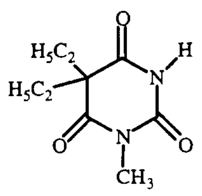
9

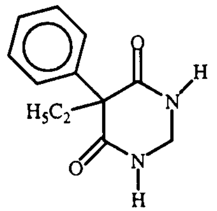
10

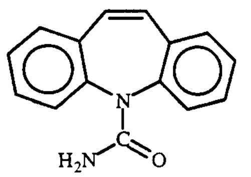
11

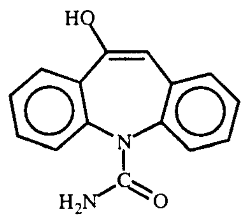
12

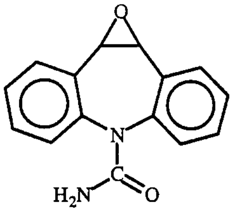
13

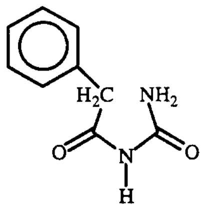
14

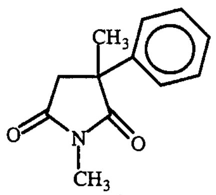
15

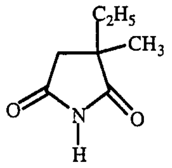
16

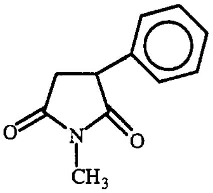
17

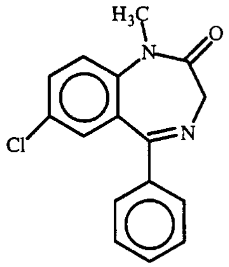
18

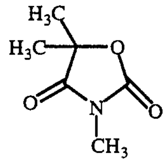
19

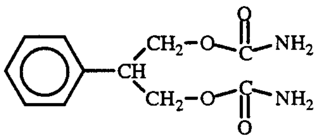
20

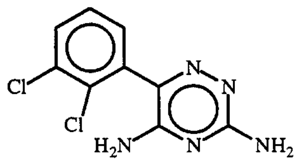
21

Following Bader et al. [13], the surfaces were taken to be the 0.001 au contour of the molecular electronic density, $\rho(\mathbf{r})$.

The electrostatic potential $V(\mathbf{r})$ created in the space surrounding a molecule by its nuclei and electrons is given rigorously by Eq. (1):

$$V(\mathbf{r}) = \sum_A \frac{Z_A}{|\mathbf{R}_A - \mathbf{r}|} - \int \frac{\rho(\mathbf{r}')d\mathbf{r}'}{|\mathbf{r}' - \mathbf{r}|}. \qquad (1)$$

Z_A is the charge on nucleus A, located at $\mathbf{R}_A$. The sign of $V(\mathbf{r})$ at any point $\mathbf{r}$ is the net result of the positive and negative contributions of the nuclei and electrons. Sites reactive toward electrophiles can be identified and ranked by means of the locations and magnitudes of the most negative potentials, either on the molecular surface ($V_{S,min}$) or in three dimensions (V_{min}), while the most positive surface potentials ($V_{S,max}$) play an analogous role for nucleophilic attack [14–17].

To extract additional information from the electrostatic potential on the molecular surface, we have introduced several statistical quantities that reflect its detailed pattern and physically meaningful features [18–21]. These quantities (Π, σ_{tot}^2, and ν) are given by Eqs. (2)–(4), which involve summations over a grid of points covering the entire surface:

$$\Pi = \frac{1}{n} \sum_{i=1}^{n} |V(\mathbf{r}_i) - \overline{V}_S| \qquad (2)$$

$$\sigma_{tot}^2 = \sigma_+^2 + \sigma_-^2 = \frac{1}{m} \sum_{i=1}^{m} \left[V^+(\mathbf{r}_i) - \overline{V}_S^+\right]^2 + \frac{1}{n} \sum_{j=1}^{n} \left[V^-(\mathbf{r}_j) - \overline{V}_S^-\right]^2 \qquad (3)$$

$\overline{V}_S$ is the average potential: $\overline{V}_S = \frac{1}{n}\Sigma_{i=1}^{n} V(\mathbf{r}_i)$. $V^+(\mathbf{r}_i)$ and $V^-(\mathbf{r}_j)$ are the positive and negative values of $V(\mathbf{r})$ on the surface, and $\overline{V}_S^+$ and $\overline{V}_S^-$ are the averages: $\overline{V}_S^+ = \frac{1}{m}\Sigma_{i=1}^{m} V^+(\mathbf{r}_i)$ and $\overline{V}_S^- = \frac{1}{n}\Sigma_{j=1}^{n} V^-(\mathbf{r}_j)$.

$$\nu = \frac{\sigma_+^2 \sigma_-^2}{\left[\sigma_{tot}^2\right]^2} \qquad (14)$$

Π is the average deviation of the potential on the surface; it is interpreted as a measure of the local polarity, or internal charge separation, that is present even in molecules with zero dipole moments, such as BF_3 and *para*-dinitrobenzene [18,19,21]. σ_{tot}^2 is the sum of the variances of the positive and negative surface potentials, σ_+^2 and σ_-^2, respectively. The variance is a measure of the spread, or range, of a collection of values, and by definition emphasizes the extremes. σ_+^2, σ_-^2, and σ_{tot}^2 are viewed as indicating the net positive, negative, and total electrostatic interaction tendencies of a molecule. The effectiveness of σ_{tot}^2 can be increased in some instances by combining it with an index of "electrostatic balance." This refers to the degree of similarity between σ_+^2 and σ_-^2, which indicates the extent to which the molecule can interact through both its positive and its negative surface regions. The quantity ν is a measure of this similarity; as σ_+^2 and σ_-^2 approach each other in magnitude, whether they be large or small, ν approaches an upper limit of 0.250. The product $\nu\sigma_{tot}^2$ is an important term in representing properties such as boiling points, critical temperatures, and heats of vaporization and sublimation, in which the molecules are interacting with others of the same kind [18,19,21].

Results

Examples of the molecular surface electrostatic potentials of **1**–**21** are shown in Figures 1–3, for phenytoin (**1**), phenobarbital (**7**), and carbamazepine (**11**). In general, the most positive potentials (red regions) are associated with amine, amide, or hydroxyl hydrogens; the most negative (pink regions) are due to carbonyl oxygens and/or nitrogen lone pairs. As seen in Figures 1–3, the local maxima and minima are generally in close proximity, on protruding portions or ends of

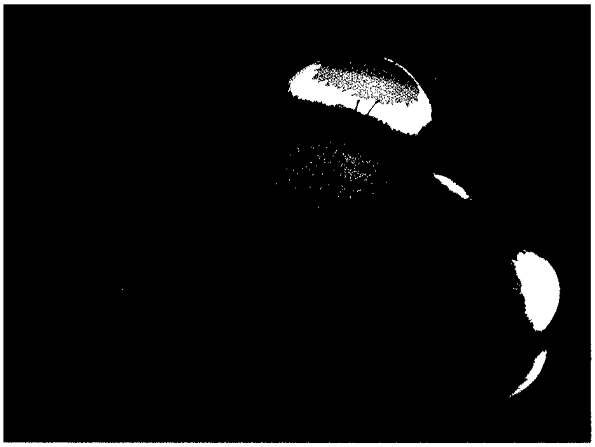

FIGURE 1. Calculated electrostatic potential on the molecular surface of phenytoin (**1**). Potential ranges, in kcal / mol: (red) more positive than 30; (yellow) between 15 and 30; (green) between 0 and 15; (blue) between −15 and 0; (pink) more negative than −15.

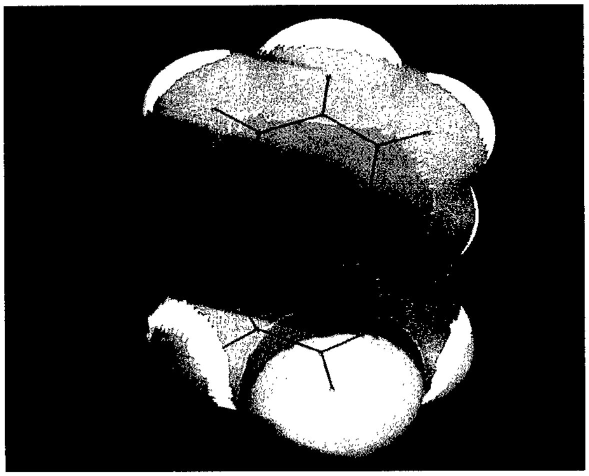

FIGURE 2. Calculated electrostatic potential on the molecular surface of phenobarbital (**7**). Potential ranges, in kcal / mol: (red) more positive than 30; (yellow) between 15 and 30; (green) between 0 and 15; (blue) between −15 and 0; (pink) more negative than −15.

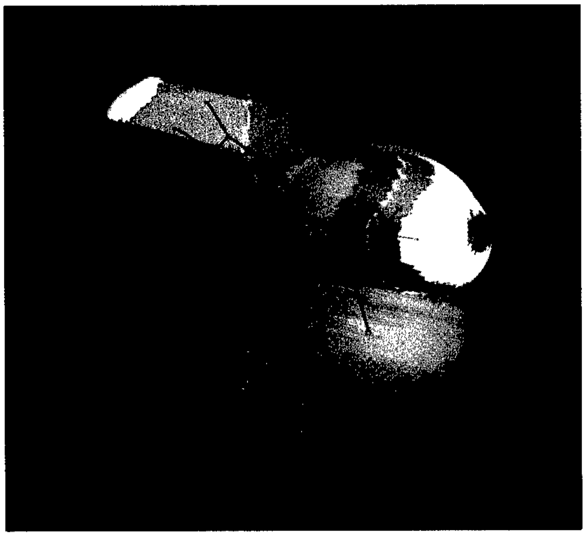

FIGURE 3. Calculated electrostatic potential on the molecular surface of carbamazepine (**11**). Potential ranges, in kcal / mol: (red) more positive than 30; (yellow) between 15 and 30; (green) between 0 and 15; (blue) between −15 and 0; (pink) more negative than −15.

TABLE I
Calculated molecular surface properties.

Molecule	Surface area (Å²)	Π	σ_+^2	σ_-^2	σ_{tot}^2	ν	$V_{S,max}$	$V_{S,min}$
		(kcal / mol)	(kcal / mol)²				(kcal / mol)	
Hydantoins								
Phenytoin (**1**)	270.0	11.72	69.6	95.5	165.1	0.244	47.4	−34.1
Mephenytoin (**2**)	249.9	11.41	43.8	93.8	137.5	0.217	43.3	−33.9
Ethotoin (**3**)	240.3	11.64	43.6	120.4	164.0	0.195	38.6	−34.4
N,*N*′-Dimethylphenytoin (**4**)	301.4	10.26	18.3	105.6	123.9	0.126	17.5	−34.4
p-Methylphenytoin (**5**)	290.7	11.19	62.9	99.0	161.9	0.238	46.7	−34.7
m-Nitrophenytoin (*6*)	297.1	13.84	92.6	86.2	178.9	0.249	50.7	−31.7
Barbiturates								
Phenobarbital (**7**)	244.7	11.03	86.7	74.2	161.0	0.248	44.7	−28.6
Mephobarbital (**8**)	262.8	10.00	50.2	75.9	126.1	0.240	43.6	−28.4
Metharbital (**9**)	221.4	10.79	43.3	80.9	124.2	0.227	43.1	−28.2
Desoxybarbiturate								
Primidone (**10**)	237.7	12.77	120.7	102.9	223.7	0.248	43.7	−35.4
Carbamazepines								
Carbamazepine (**11**)	259.6	11.44	44.4	105.0	149.4	0.209	33.3	−42.2
1-Hydroxycarbamazepine (**12**)	267.0	12.36	97.6	97.4	195.0	0.250	54.3	−42.3
Epoxycarbamazepine (**13**)	262.1	11.87	55.3	110.7	166.0	0.222	35.8	−38.5
Acetyl urea								
Phenacemide (**14**)	215.5	14.38	113.4	116.9	230.4	0.250	47.4	−40.2
Succinimides								
Methsuximide (**15**)	236.7	10.79	22.1	88.1	110.3	0.160	21.1	−32.9
Ethosuximide (**16**)	179.3	12.78	46.2	97.6	143.8	0.218	43.6	−33.3
Phensuximide (**17**)	225.3	12.66	27.5	116.5	144.0	0.155	23.0	−36.3
Others								
Diazepam (**18**)	298.5	10.08	36.3	88.2	124.6	0.206	26.9	−35.9
Trimethadione (**19**)	177.2	13.52	17.4	90.2	107.6	0.136	20.5	−35.7
Felbatol (**20**)	259.9	13.71	108.4	111.2	219.6	0.250	46.4	−39.2
Lamotrigine (**21**)	249.6	12.53	99.4	94.5	193.9	0.250	38.5	−38.7

the molecules. The computed surface properties of **1**–**21**, including their areas, are presented in Table I.

Discussion

Table I contains at least three representatives of each of four chemical categories, plus six molecules of various other types. While the near-ubiquity of ureide and amide linkages is a common element, there are also substantial differences. There is a considerable range of sizes, the surface areas being between 177 and 301 Å². The molecules contain one to three rings, sometimes fused, which may be five-, six- or seven-membered, saturated or unsaturated. While a heterocyclic ring appears to be a key structural constituent in many instances, this is not the case in **14** and **20**.

The positive regions of the surface electrostatic potentials of these molecules provide further contrasts. As mentioned above, the strongest positive potentials, with $V_{S,max}$ between 33 and 54 kcal/mol, are produced by amine, amide, or hydroxyl hydrogens. However, there are no such hydrogens in **4**, **15**, and **17**–**19**, and their $V_{S,max}$ are, consequently, much weaker, between 17 and 27 kcal/mol. These five molecules also have among the lowest σ_+^2 and ν values, indicating that the positive regions on their surfaces are relatively weak.

On the other hand, the negative surface regions, while less extensive in area, are much more uniform in strength. The $V_{S,min}$ are all within a relatively narrow range, -28 to -42 kcal/mol, as are the σ_-^2, 74 to 120 (kcal/mole)^2. [In contrast, the σ_+^2 are between 17 and 121 (kcal/mol)^2.] It seems reasonable to infer that it is the negative potentials that are of primary importance in anticonvulsant activity.

A particularly striking point of similarity among the molecules in Table I is the local polarity, Π. In earlier work [18,19,22], encompassing well over 100 molecules, mostly organic, we found Π to vary between 2 and 24 kcal/mol; most often, however, it is less than 10 kcal/mol. What is notable in Table I is that 17 of the 21 Π values are between 10 and 13 kcal/mol and the largest overall is 14.38 kcal/mol. Thus, the internal charge separations in these molecules are quite significant, but are rather strictly circumscribed in magnitude. This suggests a need for a substantial but not excessive degree of hydrophilic character.

It is interesting to note that the surface electrostatic potentials of the inactive molecules, **5** and **6**, do not differ dramatically from those of the others. Their lack of anticonvulsant activity may reflect an interplay of several factors. For example, **5** and **6** are among the largest molecules in Table I; only two others are slightly larger. Thus, steric effects could be involved. **5** and **6** also have among the highest $V_{S,max}$ values; this increases the possibility of a nonproductive interaction with some negative site. The inactivities of **5** and **6** might be the results of several such contributing factors.

Summary

Our investigation of the molecular surface electrostatic potentials of anticonvulsants of different chemical types has identified two common features that may be related to their activities:

(a) Surface regions of relatively strong negative potentials. This suggests that the interactions with the receptor(s) involve positive sites on the latter, which may, for instance, be acting as hydrogen-bond donors.

(b) Local polarities within a rather narrow range of intermediate values. This may reflect a need for an optimum balance between hydrophilicity and hydrophobicity, such that the molecules be able to pass through the cell membrane but not enter into interactions that prevent them from reaching the appropriate receptor(s).

References

1. A. Goth, *Medical Pharmacology*, 6th ed. (C. V. Mosby, St. Louis, MO, 1972).
2. K. W. Leal and A. S. Troupin, *Clin. Chem.* **23**, 1964 (1977).
3. D. B. Smith and J. DeToledo, in *Diagnosis and Management of Seizure Disorders*, R. P. Lesser, Ed. (Demos, New York, 1991), Chap. 4.
4. G. Loew and D. S. Berkowitz, *J. Med. Chem.* **18**, 656 (1975).
5. C. Petrongolo and J. Tomasi, Int. J. Quantum Chem., Quantum Biol. Symp. **2**, 181 (1975).
6. R. Osman, H. Weinstein, and S. Topiol, Ann. N.Y. Acad. Sci **367**, 356 (1981).
7. H. Weinstein, R. Osman, J. P. Green, and S. Topiol, in *Chemical Applications of Atomic and Molecular Electrostatic Potentials*, P. Politzer and D. G. Truhlar, Eds. (Plenum Press, New York, 1981), p. 309.
8. M. Martin, F. Sanz, M. Campillo, L. Pardo, J. Perez, and J. Turmo, Int. J. Quantum Chem. **23**, 1627 (1983).
9. C. Thomson and R. Brandt, Int. J. Quantum Chem., Quantum Biol. Symp. **10**, 357 (1983).
10. P. Politzer, P. R. Laurence, and K. Jayasuriya, Env. Health Persp. **61**, 191 (1985).
11. P. Politzer and J. S. Murray, in *Theoretical Biochemistry and Molecular Biophysics: A Comprehensive Survey*, Vol. 2, D. L. Beveridge and R. Lavery, Eds. (Adenine Press, Schenectady, NY, 1991), Chap. 13.
12. M. J. Frisch, G. W. Trucks, H. B. Schlegel, P. M. W. Gill, B. G. Johnson, M. A. Robb, J. R. Cheeseman, T. A. Keith, G. A. Petersson, J. A. Montgomery, K. Raghavachari, M. A. Al-Laham, V. G. Zakrezewski, J. V. Ortiz, J. B. Foresman, J. Cioslowski, B. B. Stefanov, A. Nanayakkara, M. Challacombe, C. Y. Peng, P. Y. Ayala, W. Chen, M. W. Wong, J. L. Andres, E. S. Replogle, R. Gomperts, R. L. Martin, D. J. Fox, J. S. Binkley, D. J. Defrees, J. Baker, J. P. Stewart, M. Head-Gordon, C. Gonzalez, and J. A. Pople, *Gaussian* 94 (Gaussian, Inc., Pittsburgh, PA, 1995).
13. R. F. W. Bader, M. T. Carroll, J. R. Cheeseman, and C. Chang, J. Am. Chem. Soc. **109**, 7968 (1987).
14. E. Scrocco and J. Tomasi, in *Topics in Current Chemistry*, Vol. 42 (Springer-Verlag, Berlin, 1973), p. 95.
15. P. Politzer and K. C. Daiker, in *The Force Concept in Chemistry*, B. M. Deb, Ed. (Van Nostrand Reinhold, New York, 1981), Chap. 6.
16. P. Politzer and J. S. Murray, in *Reviews in Computational*

Chemistry, Vol. 2, K. B. Lipkowitz and D. B. Boyd, Eds. (VCH, New York, 1991), Chap. 7.

17. G. Náray-Szabó and G. G. Ferenczy, Chem. Rev. **95**, 829 (1995).
18. J. S. Murray, T. Brinck, P. Lane, K. Paulsen, and P. Politzer, J. Mol. Struct. (Theochem) **307**, 55 (1994).
19. J. S. Murray and P. Politzer, in *Quantitative Treatments of Solute/Solvent Interactions*, J. S. Murray and P. Politzer, Eds. (Elsevier, Amsterdam, 1994), Chap. 8.
20. T. Brinck, J. S. Murray, and P. Politzer, Mol. Phys. **76**, 609 (1992).
21. J. S. Murray and P. Politzer, J. Mol. Struct. (Theochem) **425**, 107 (1998).
22. J. S. Murray, P. Lane, and P. Politzer, Mol. Phys. **93**, 187 (1998).

Phytochrome Structure: A New Methodological Approach

CRISTIANO RUCH WERNECK GUIMARÃES,
JOAQUIM DELPHINO DA MOTTA NETO,
RICARDO BICCA DE ALENCASTRO
Physical Organic Chemistry Group, Departamento de Química Orgânica, Instituto de Química da UFRJ, Cidade Universitária, CT, Bloco A, lab. 609, Rio de Janeiro, RJ 21949-900, Brasil

Received 21 February 1998; accepted 7 May 1998

ABSTRACT: Higher plants use the protein phytochrome as a photosensor. In physiological temperatures phytochrome exists in two forms: Pr and Pfr. The chromophore of phytochrome is an open-chain tetrapyrrole. On the pathway from Pr to Pfr four intermediates (Lumi-R, Meta-Ra, Meta-Rb, and Meta-Rc) can be distinguished, while only two (Lumi-F and Meta-F) can be seen on the way back from Pfr to Pr. We have used the x-ray structure of the C-Phycocyanin protein *Fremyella diplosiphon* bacteria as a template to build a model (~ 200 atoms) that includes only the chromophore and five amino acids of the phytochrome (Arg316–Cys321–His322–Leu323–Gln324) around it. Using the existing experimental evidences, we have proposed a three-dimensional (3D) structure for Pr, Pfr, and intermediates and a mechanism for the photoisomerization as well. Structures were fully optimized using AM1 (Unichem package on a Cray J90-NACAD). Using the INDO/S method of Zerner and co-workers, we calculated the absorption spectra of the model compounds and compared them with the experimental data. The oscillator strength ratio is an indicator of the chomophore conformation in biliproteins. The calculated spectra reproduces well the spectra of the phytochrome (Pr, Pfr, and intermediates) except for the lower energy band. This result is attributed to the small number of amino acids in the models. The calculated ratios ($f_{\mathrm{VIS}}/f_{\mathrm{UV}} - f_{\mathrm{osc}}$ of visible band over f_{osc} of UV band and $f_2/f_1 - f_{\mathrm{osc}}$ of second absorption band over f_{osc} of first absorption band) for the models match very well the experimental ratios obtained for the phytochrome (Pr, Pfr, and intermediates). This supports the proposed mechanism for the photoisomerization process. © 1998 John Wiley & Sons, Inc. Int J Quant Chem 70: 1145–1157, 1998

Key words: phytochrome, absorption spectra; semiempirical

Correspondence to: R. B. de Alencastro.

Contract grant sponsors: CNPq-Brazil; Núcleo de Atendimento em Computação de Alto Desempenho (NACAD-COPPE-UFRJ).

International Journal of Quantum Chemistry, Vol. 70, 1145–1157 (1998)
© 1998 John Wiley & Sons, Inc.
CCC 0020-7608 / 98 / 061145-13

Introduction

Organisms can use light in two ways: either to use its energy to keep its cells functioning or to translate optical signals into some kind of biological response. Among the latter, there are the so-called visual pigments, rhodopsins in vertebrates and phytochrome in higher plants. Most biological photosensors are photochromic, i.e., after the initial photochemical event (a photochemical reaction in a generally very complex biochemical cycle), the system is restored to its initial, "ready" state [1] (for recent reviews on light signal transduction in plants, see [2–4]). Higher plants use only visible light for photosynthesis, but they respond to a much wider range of the electromagnetic spectrum, including the ultraviolet (UV) and the near-infrared (or far-red) light. Moreover, because higher plants have developed a very sophisticated sensory apparatus, they are able to identify the direction and the intensity of the incoming light [3]. The very diverse biological responses to the radiation are called photomorphogenesis.

The red/near-infrared region of the spectrum is recognized by photoreceptors known as phytochromes. Up to now, five phytochrome genes have been cloned in *Arabidopsis thaliana*, which correspond to five different proteins (phyA to phyE) [4, 5]. These different phytochrome molecules have specialized photosensory functions [6–8]. In this study, we will be referring to phytochrome A, the most studied phytochrome. All phytochrome molecules have the same basic structure: they are biliproteins with a molecular weight of 124–129 kDa (1100–1170 residues) and a single chromophore bound to a cysteine residue in the ~ 70-kDa N-terminal [9]. Phytochrome molecules exist as a dimer, with dimerization occurring through the C-terminal region [10]. The chromophore of phytochrome is a phycobilin, an open-chain tetrapyrrole [11]. In physiological temperatures, phytochrome exists in two forms: a red-absorbing inactive form (Pr, 660 nm) and a far-red-absorbing active form (Pfr, 730 nm). Saturation of the environment with 730-nm light induces a shift in the equilibrium between the two forms toward 99% of the Pr form, whereas saturation with 660-nm light shifts the equilibrium to 88% of the Pfr form, thus, triggering a physiological response [11].

The primary photochemical event is a double isomerization at the methine bridge between the pyrrole rings C and D (Fig. 1) [11]. However, Z–E isomerization of the chromophore requires some space in the protein pocket for rings C and D. Minimum space would be required for a corotation of the single bonds between C and D rings (*syn–anti*) [12]. Furthermore, there are contradictory results between Fourier transform infrared (FTIR) and Raman resonance methods related to the protonation state of the pyrrole nitrogen of ring B (Fig. 1). The FTIR method shows that both Pr and Pfr forms are protonated, whereas the Raman resonance (RR) spectrum shows a protonated Pr chomophore and a deprotonated Pfr chromophore [12].

Since it was first discovered by Borthwick, Hendricks, and their co-workers in the 1950s [13], phytochrome has been studied by many spectroscopy methods, including time-resolved absorp-

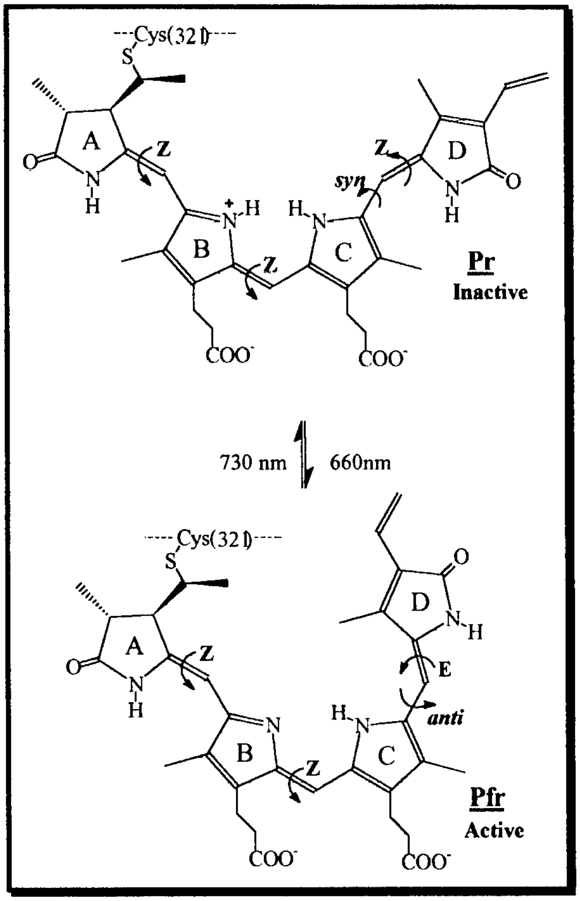

FIGURE 1. Proposed structure of the phytochrome chromophore in the native protein (Pr and Pfr forms) [11].

tion (TROD) [14], fluorescence [15], circular dichroism [16], FTIR [17], FT–RR spectroscopy [18], low-temperature spectroscopy [19], nanosecond laser flash photolysis [20], and femtosecond T-resolved spectroscopy [21]; on the other hand, up to now no X-ray cristallographic structure of phytochrome has been obtained. Both the primary structure and some aspects of the secondary structure of phytochrome from several different vegetals have been determined [22], but because phytochrome exists in very low concentrations in plants, the preparation of single crystals for X-ray analysis remains elusive.

From the theoretical point of view, a few attempts to study this problem have been made. In 1993, Smit and co-workers made a force field vibrational analysis of the chromophore using biliverdin dimethyl esters as model compounds [23]. Also in 1993, Scharnagl and co-workers studied the chromophore using molecular dynamics and INDO-S [24] and electrostatic calculations [25] to develop a model of the phycoerythrocyanin chromophore (from phycobiliproteins obtained from bacteria for which some X-ray structures had been previously obtained). More recently, using semiempirical and ab initio techniques, Korkin and co-workers calculated some neutral and protonated pyrromethenes of biological interest [26].

Based on the X-ray structure of C-Phycocyanin protein from *Fremyella diplosiphon* [27], Parker and co-workers [28] modeled the phytochrome chromophore binding pocket. They changed 20 residues around the chromophore binding site of C-Phycocyanin to the corresponding residues of *Avena* phytochrome A and minimized the model using sophisticated matching procedures, which included AM1 geometry optimization of the chromophore moiety.

Relaxation products observed in the conversion Pr-Pfr or Pfr-Pr with different absorption spectra are described as intermediates. From Pr to Pfr, at least four intermediates can be distinguished, while at least two can be seen from Pfr to Pr. Figure 2 shows schematically the phytochrome cycle, including the distinct intermediates as detected by time-resolved and low-temperature absorption spectroscopy [11].

Method and Computational Details

Due the small amount of the protein in the plant tissue, the three-dimensional (3D) structure of the phytochrome is unknown. We used the X-ray structure of the C-Phycocyanin protein of *F. diplosiphon* bacteria [27] as a template. Then, we built a reduced model including only the chromophore and five residues around it. Our aim was to evaluate the configurational and conformational changes that occur on the chromophore during photoisomerization. We also decided to examine the protonation state of the intermediates and of the Pfr form (Fig. 2) [12].

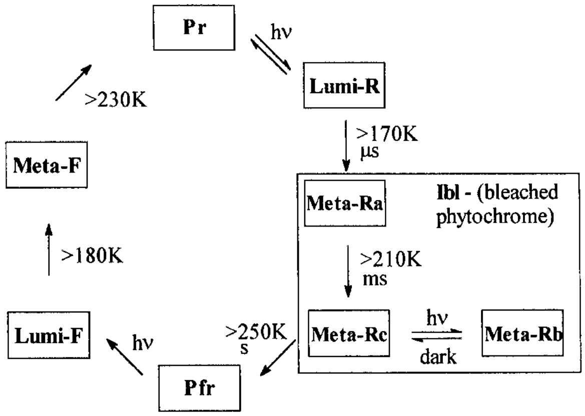

FIGURE 2. Schematic diagram of the photoconversion of the two phytochrome forms. Temperatures given are the minimum values for the individual relaxation steps; the times indicate the order of magnitude of the relaxation process at room temperature [11].

The C-Phycocyanin protein coordinates of *F. diplosiphon* were obtained from the Protein Data Bank. The model geometries (Pr, Pfr, and intermediates, ~ 200 atoms) were fully optimized using AM1 [29, 30] with keywords GNORM = 1.0, PRECISE, within the MOPAC program version 7.0 on a workstation IBM RISC/6000 and the UNICHEM package on a Cray J90 (NACAD-COPPE-UFRJ).

Absorption spectra were calculated using the INDO/S method of Zerner and co-workers [31, 32]. Solvent effects were included using a self-consistent reaction field (SCRF) routine, with dielectric constant $\varepsilon = 78.54$ (the chromophore selected is near the surface of the protein).

Results and Discussion

The central point of this work is an analysis of the electronic absorption spectra of *Avena* phytochrome A (Pr and Pfr forms) and the photoproducts observed during conversion between these forms [11]. As the spectra of tetrapyrroles is known to be sensitive to conformation, we thought it worthwhile to try to use the experimental spectra to model the unknown conformations. The key to this is the empirical evidence that the ratio of the oscillator strength of the visible band to the UV (Soret) band is an indicator of the conformation of the tetrapyrrole chromophore [33, 34]. The five amino acids used served two purposes: to mimic the peptide chain of the protein near the chromophore and to provide the interactions (protonation or otherwise) needed to stabilize the different conformations which correspond to the different intermediates. Therefore, the first step was to develop an operational model of the phytochrome molecule.

MODEL CONSTRUCTION

In the absence of an X-ray crystal structure of phytochrome, among other structures of analogue chromophores available from PDB (Protein Data Bank), we selected to use C-Phycocyanin of *F. diplosiphon* as a template. The C-Phycocyanin protein has three chromophores very similar to the phytochrome's chromophore (the only difference being in the D ring: the C-Phycocyanin chromophore has an ethyl group bound in the D ring instead of a vinyl group). Due to its high homology and because the amino acids close to the chromophore play the same role as in phytochrome [12], we have selected the β unit (β-CPC1) chromophore (Fig. 3).

We started building our model with the fragment W–Cys84–Leu85–Arg86–Asp87 (W, the tetrapyrrole chromophore, is in the Z,Z,Z *syn* conformation). In doing this, we took into consideration that the chromophore of phytochrome is similarly linked to Cys321 and that it has the same conformation. We then included Arg79 as a counterion to the propanoate side chains of rings B and C of the tetrapyrrole. A very important point is that full optimization of the model did not significantly change the conformation of the tetrapyrrole in relation to the X-ray structure. The root mean square (RMS) of superimposed structures was 1.4 Å for the C-Phycocyanin optimized model against the C-Phycocyanin crystal: 172 atoms superimposed, H excluded [Fig. 4(a)]. This suggests that the five selected amino acids are sufficient to represent the main interactions between the chromophore and the protein.

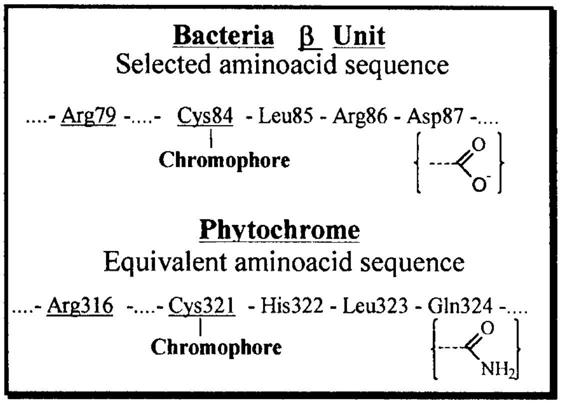
Bacteria β Unit
Selected aminoacid sequence
....- Arg79 -....- Cys84 - Leu85 - Arg86 - Asp87 -....
Chromophore
O
O⁻
Phytochrome
Equivalent aminoacid sequence
....- Arg316 -....- Cys321 - His322 - Leu323 - Gln324 -....
Chromophore
O
NH₂

FIGURE 3. Comparison of the selected amino acid sequence in the bacteria β-subunit and the equivalent amino acid sequence in the phytochrome.

The next step was to model the phytochrome chromophore. To do this, we used as a template the AM1 optimized structure of the C-Phycocyanin model described above. We kept the coordinates of the backbone atoms of the peptide chain and of the chromophore and changed its ethyl group for a vinyl group. Next, we made the following substitutions: Cys84 is renamed Cys321, Leu85 → His322, Arg86 → Leu323, and Asp87 → Gln324. We conserved the Arg79 fragment coordinates and renamed it Arg316. The new model was fully optimized at the AM1 level. It is important to notice that this procedure did not significantly change the conformation of the tetrapyrrole chromophore. The RMS of superimposed structures was 1.3 Å for the phytochrome-optimized model against the C-Phycocyanin crystal: 150 atoms superimposed; H excluded; superimposition backbone only, except for the Arg and Cys, which are conserved in both structures [Fig. 4(b)]. As mentioned above, we took this as a confirmation that the five selected amino acids in the C-Phycocyanin protein play the same role as the equivalent amino acids in phytochrome.

Asp87 is supposed to balance the positive charge of the protonated chromophore in the C-Phycocyanin protein. However, no aspartate is found in the corresponding position of the phytochrome sequence. As the phytochrome is believed to be protonated, at least in the Pr form [18], the positive charge must be balanced by an aspartate or glutamate further away from the chromophore [12]. If this is the case, then the conformational changes that occur during later stages of the phototransformation could remove the negative charge from near the chromophore, and hence lead to deprotonation.

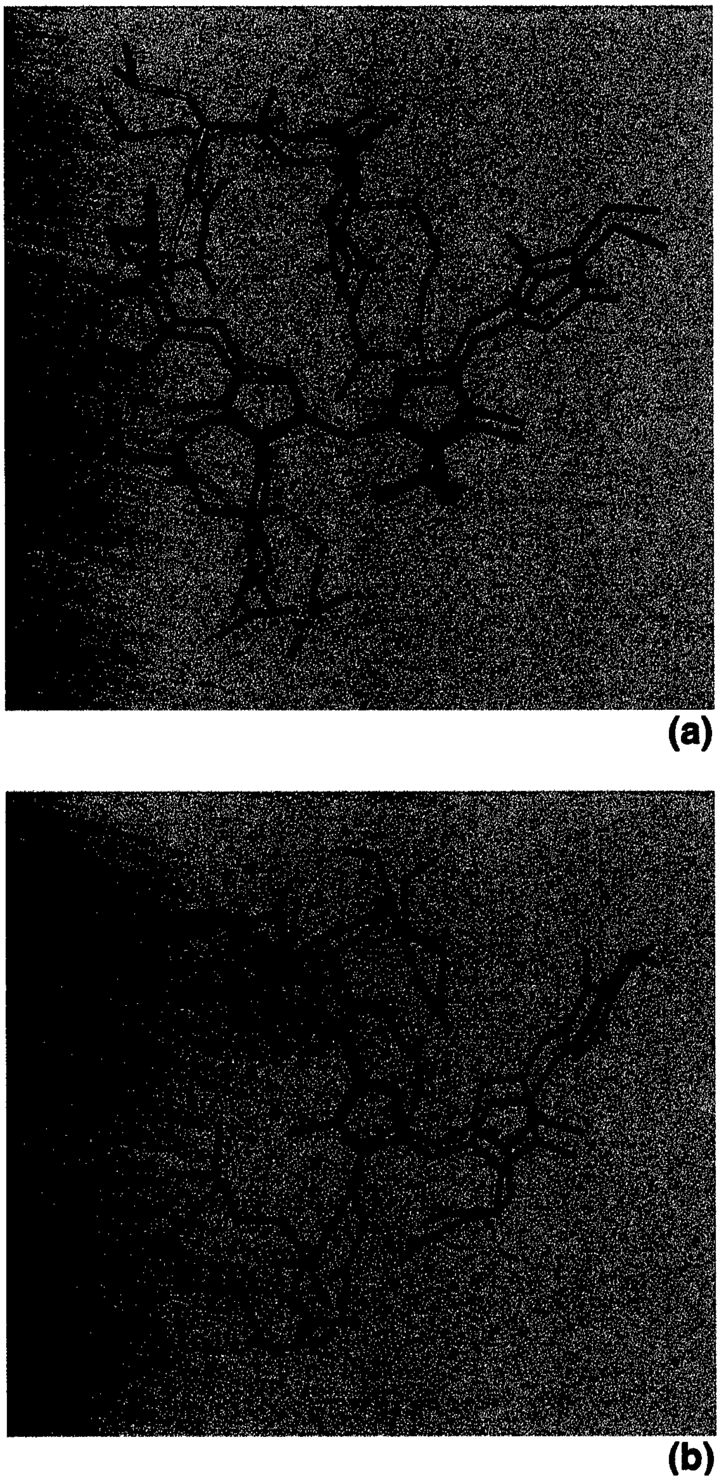

FIGURE 4. (a) Superimposed structures of the C-Phycocyanin-optimized model (green) against the C-Phycocyanin crystal (gray). (b) Superimposed structures of the phytochrome-optimized model (green) against the C-Phycocyanin crystal (gray).

A POSSIBLE MECHANISM FOR THE PHOTOCHEMICAL CYCLE

Nuclear magnetic resonance (NMR) and RR studies have shown that the Pfr form has ZZE *anti* configuration and is deprotonated [11]. Besides, these techniques have shown that the first intermediate (Lumi-R) on the pathway Pr → Pfr has a ZZE *anti* configuration and that there are modifications on the hydrogen bonding network involving interactions of the N–H groups of rings B and C with the protein environment [18]. Therefore, the first photochemical event would be the ZZZ *syn*–ZZE *anti* isomerization. Raman resonance studies have also shown that the primary photochemical event on the pathway Pfr → Pr is the double-bond reisomerization at the methine bridge C–D, i.e., the reversal of the photoreaction of Pr [18]. So, the first intermediate (Lumi-F) on the pathway Pfr → Pr has ZZZ *syn* isomerism. Another RR study has shown that the proton release on the pathway Pr → Pfr occurs between the Lumi-R intermediate and Meta-Ra intermediate [35].

Based on such experimental evidences and on the schematic photochemical cycle, first proposed by Eilfeld and Rüdiger [36], we propose a possible mechanism for intermediate conversion. We, then, proceed to model this mechanism.

The sequence starts with the protonated phytochrome in its Pr form, which has ZZZ *syn* configuration [18]. Its positive charge is balanced by either an aspartate or glutamate ion hydrogen bonded to the N^+–H group of ring B and N–H group of ring C. The primary photochemical event is the absorption of red light (~ 660 nm) leading to ZZZ *syn* → ZZE *anti* isomerization (Fig. 5). Steric hindrance between ring D and the negative amino acid residue disrupts the hydrogen bond (HB) network by moving the amino acid farther. To counterbalance the positive charge, the carbonyl group of Gln324 approaches and restores the HB network, thus forming the first intermediate (Lumi-R). Proton transfer from the N^+–H group of ring B to the carbonyl oxygen of Gln324 (N---H + O=C) generates the second intermediate (Meta-Ra). A subsequent proton transfer to the negative amino acid displaced in the first step generates the Meta-Rc intermediate. We believe that the major differences between Meta-Rc, Meta-Rb, and Pfr are conformational because in all three intermediates the chromophore is deprotonated, with Pfr as the most stable of the three.

The other leg of the cycle starts with the Pfr form. Under far-red light (730 nm) ZZE *anti* → ZZZ *syn* isomerization occurs. Steric hindrance from ring D is released and the neutral amino acid generated in the forward leg can reprotonate the nitrogen atom of ring B. The main differences between the intermediate Lumi-F and Meta-F are probably the conformation of the tetrapyrrole chromophore and the position of the neutral amino acid. In the case of Lumi-F and Meta-F, the amino acid is probably neutral and hydrogen bonded to the nitrogen atom of ring B, at least in the Meta-F intermediate (—O—H---N). As the temperature increases to 230 K (Fig. 2), the structure relaxes and complete proton transfer occurs (—O^----H—$^+$N), closing the cycle (Fig. 5).

MODELED INTERMEDIATES

Having thus rationalized the chemical transformations which occur upon photoisomerization, in order to establish the feasibility of our proposal, we proceeded to calculate the pertinent structures at the AM1 level. To simplify, we used an acetate as a probe instead of an aspartate or a glutamate. We started with our model of the Pr conformation, and after full optimization of the most stable conformation, we obtained the acetate anion hydrogen bonded to the chromophore. Next, we calculated a structure forcing ZZZ *syn* → ZZE *anti* isomerization and took the acetate group away from the chromophore. After full optimization, we obtained a structure in which the carbonyl oxygen of Gln324 replaced the acetate group as hydrogen bond acceptor, as expected for the Lumi-R intermediate. We transferred the proton from the chromophore (protonated nitrogen of ring B) to the carbonyl oxygen of Gln324 and fully optimized this intermediate (Meta-Ra). We saw then that there were no relevant hydrogen bonds in the model. The next step was to force proton transfer from Gln324 to the acetate probe. The fully optimized structure corresponds well to the expected structure for the Meta-Rc intermediate. The nitrogen of ring C, the acetic acid probe, and the carbonyl oxygen of Gln324 are hydrogen bonded. In order to build a putative Meta-Rb structure and restore the Pfr model, conformational changes and hydrogen bonds on the Meta-Rc model were necessary. To construct a model of Lumi-F from Pfr, we had to force the isomerization ZZE *anti* → ZZZ *syn* and to approach the protonated acetic acid to the nitrogen of ring B. After full optimization, we obtained

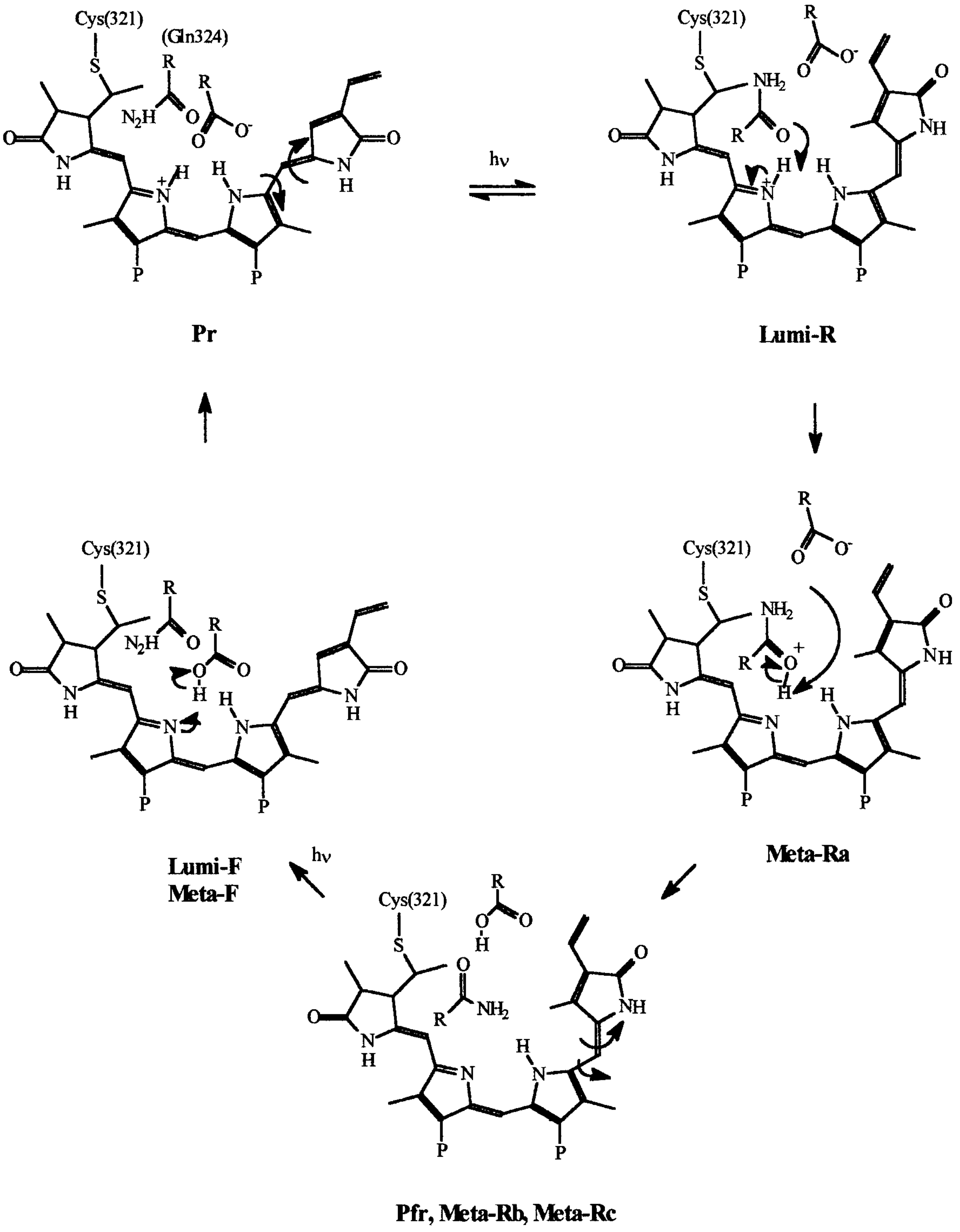
Cys(321)
(Gln324)
S
R
N₂H
O
O⁻
N
H
hν
Pr
Lumi-R
Meta-Ra
Lumi-F
Meta-F
Pfr, Meta-Rb, Meta-Rc
NH₂
NH
P

FIGURE 5. Proposed mechanism for the phytochrome intermediates (P = $CH_2CH_2COO^-$).

a stable structure that we assigned to Lumi-F. In this intermediate the hydroxyl oxygen of acetic acid is hydrogen bonded to the N-H group of ring C (N—H---O—H). To build the Meta-F model, we had to force a hydrogen bond between the hydroxyl group of the acetic acid and the nitrogen of ring B. After full optimization, the carbonyl oxygen of the probe was hydrogen bonded to the N-H group of ring C (C=O---H—N), and the hydroxyl group of the probe was hydrogen bonded

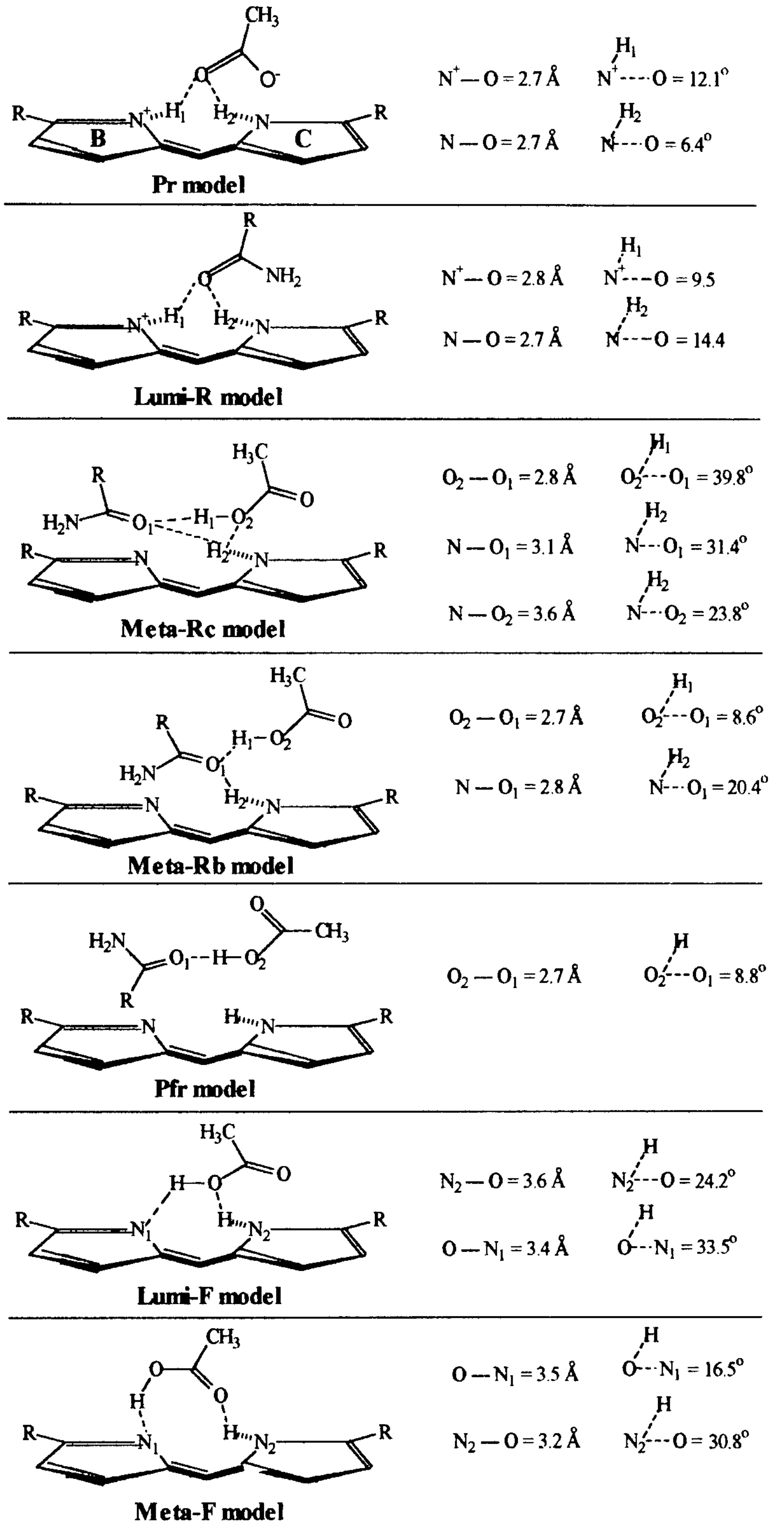
Pr model
N⁺—O = 2.7 Å
N—O = 2.7 Å
N⁺---O = 12.1°
N---O = 6.4°
Lumi-R model
N⁺—O = 2.8 Å
N—O = 2.7 Å
N⁺---O = 9.5
N---O = 14.4
Meta-Rc model
O2—O1 = 2.8 Å
N—O1 = 3.1 Å
N—O2 = 3.6 Å
O2---O1 = 39.8°
N---O1 = 31.4°
N---O2 = 23.8°
Meta-Rb model
O2—O1 = 2.7 Å
N—O1 = 2.8 Å
O2---O1 = 8.6°
N---O1 = 20.4°
Pfr model
O2—O1 = 2.7 Å
O2---O1 = 8.8°
Lumi-F model
N2—O = 3.6 Å
O—N1 = 3.4 Å
N2---O = 24.2°
O---N1 = 33.5°
Meta-F model
O—N1 = 3.5 Å
N2—O = 3.2 Å
O---N1 = 16.5°
N2---O = 30.8°

FIGURE 6. Relevant hydrogen bonds of the fully optimized Pr, Pfr, and intermediate models.

to the nitrogen of ring B (N---H—O). Complete proton transfer from Meta-F restored the original Pr model, thus closing the cycle. Figure 6 shows the relevant hydrogen-bonding network of the intermediates. Figures 7–10 show the fully optimized AM1 3D structures of Pr, Pfr, and intermediates.

Table I shows the principal dihedral angles of the fully optimized phytochrome and intermediates forms and also of the C-Phycocyanin protein X-ray structure. These results show that the fully optimized ZZZ *syn* models (Pr, Lumi-F, and Meta-F model) have almost the same C-Phycocyanin X-ray structure conformation. This again suggests that the amino acid sequence in the C-Phycocyanin protein plays the same role as the equivalent amino acid sequence in the phytochrome. Moreover, because of the *syn–anti* conformational change, the

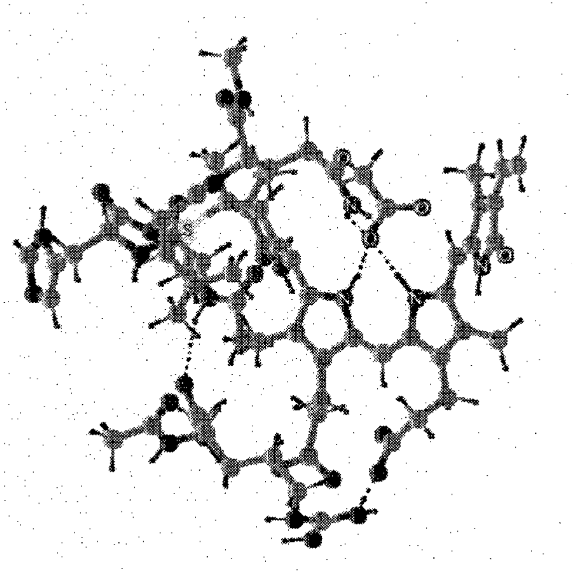

Pr model

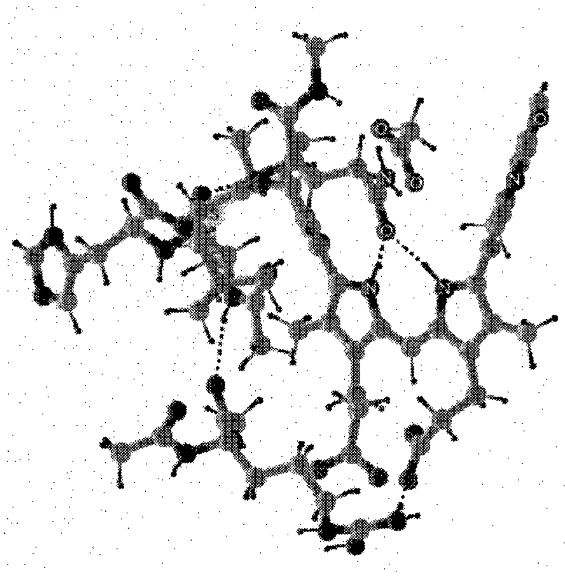

Lumi-R model

FIGURE 7. Fully AM1 optimized 3D structures of Pr and Lumi-R.

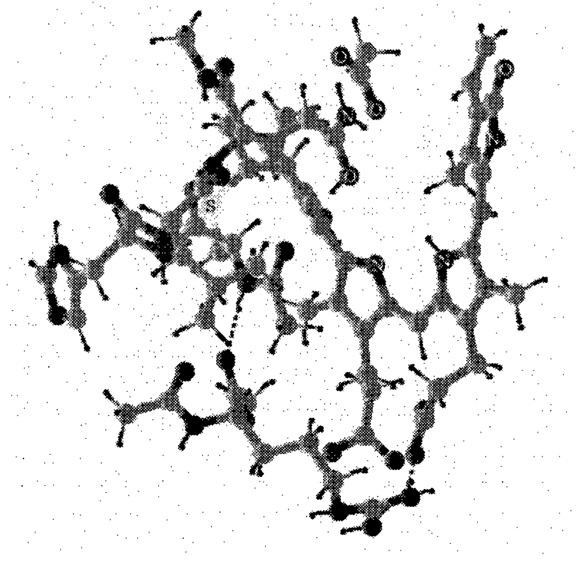

Meta-Ra model

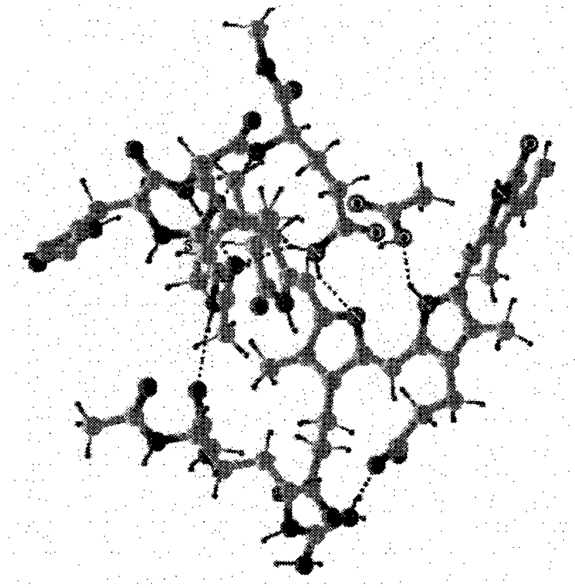

Meta-Rc model

FIGURE 8. Fully AM1 optimized 3D structures of Meta-Ra and Meta-Rc.

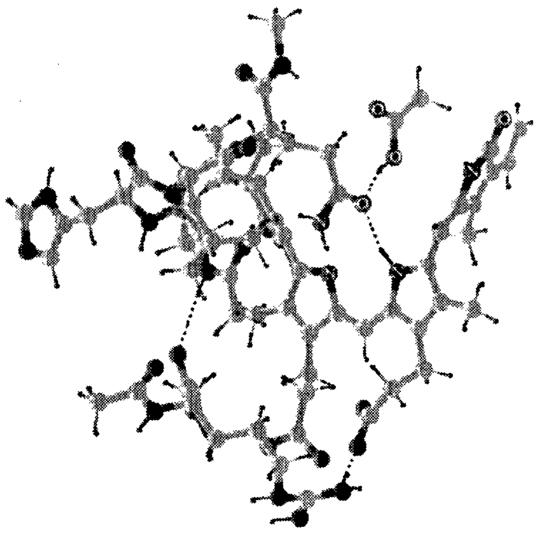

Meta-Rb model

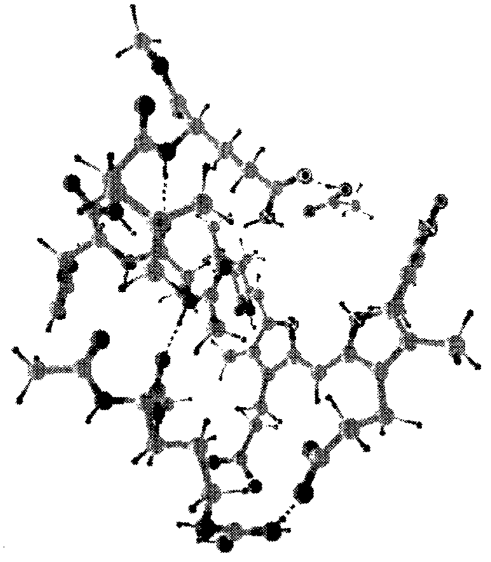

Pfr model

FIGURE 9. Fully AM1 optimized 3D structures of Meta-Rb and Pfr.

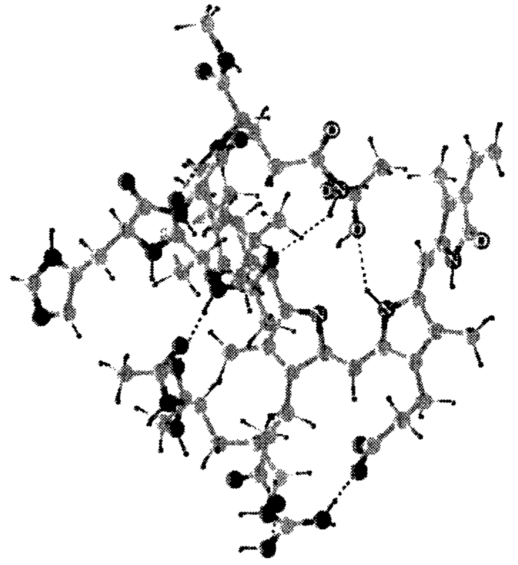

Lumi-F model

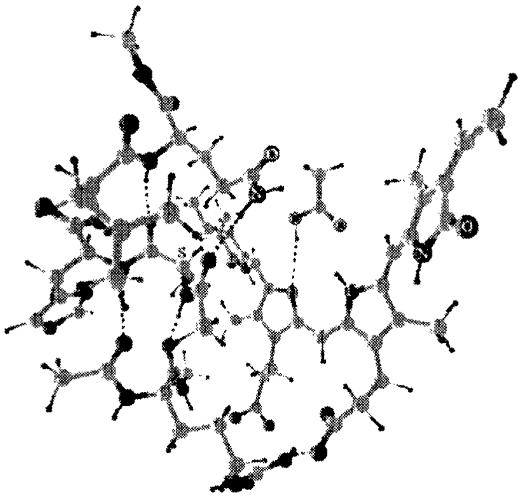

Meta-F model

FIGURE 10. Fully AM1 optimized 3D structures of Lumi-F and Meta-F.

only difference between the ZZZ *syn* and ZZE *anti* configuration (Lumi-R, Meta-Ra, Meta-Rb, Meta-Rc, and Pfr model) in the phytochrome models besides the double-bond dihedral angle (Z–E isomerization) is the γ dihedral angle.

ELECTRONIC SPECTRA

To further support our proposal, we calculated the electronic spectra of the above phytochrome models and compared them with the experimental (UV-Vis) spectra of Pr, Lumi-R, Meta-Ra, Meta-Rb, Meta-Rc, Pfr, Lumi-F, and Meta-F [11]. Here, it is important to calculate the position of the absorption bands, but it is more important to obtain the oscillator strength ratio of the visible to the UV (Soret) bands and the oscillator strength ratio of the second absorption band to the first absorption band. These ratios are considered indicators of the conformation of the tetrapyrrole rings in bilipro-

TABLE I

Conformation of proposed models.

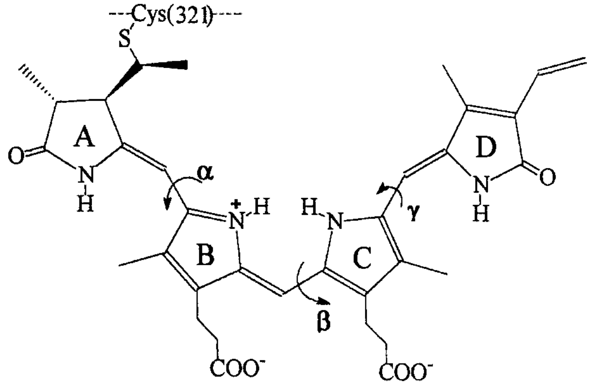

STRUCTURE	α(°)	β(°)	γ(°)
Crystal structure (bacteria)	158.0	0.5	143.0
Pr model	129.2	−1.0	145.0
Lumi-R model	130.5	−1.7	−59.2
Meta-Ra model	132.7	−10.8	−25.3
Meta-Rb model	130.6	−3.0	−74.6
Meta-Rc model	139.9	−3.5	−66.5
Pfr model	141.2	−6.5	−60.9
Lumi-F model	140.1	3.1	143.4
Meta-F model	140.4	−5.2	134.7

teins and in the free chromophores. When the chromophore conformation is extended, the $f_{\mathrm{VIS}}/f_{\mathrm{UV}}$ ratio is over 3.0; when it is semicyclic or semihelical, the $f_{\mathrm{VIS}}/f_{\mathrm{UV}}$ ratio is between 0.8 and 2.0; when it is cyclic or cyclohelical, the $f_{\mathrm{VIS}}/f_{\mathrm{UV}}$ ratio is ~ 0.4; and, finally, when the chromophore conformation is cyclic, the $f_{\mathrm{VIS}}/f_{\mathrm{UV}}$ ratio is ~ 0.15 [28].

Table II shows the calculated absorption spectra of the phytochrome models (Pr, Pfr, and intermediates). Calculations show three systems of peaks of mainly π character, which correspond to the experimental spectrum of phytochrome obtained by Thümmler and Rüdiger [11]. The two band systems of higher energy are in very good agreement with the observed spectra. The low energy band, however, shows only poor agreement. This might be due to the size of the model we have chosen since only five amino acid residues would hardly account for all field effects found in the chromoprotein. There is experimental evidence supporting this latter hypothesis [34, 37–39].

As stated above, the oscillator strength ratio is considered an indicator of the chromophore conformation in biliproteins [28]. Here, we used the experimental oscillator strength ratio of the second absorption band over the first absorption band

TABLE II

Comparison of spectroscopic data (UV–Vis) with the calculated spectra of the proposed models.

Form	$\nu(1)$ (cm^{-1})	$\nu(2)$ (cm^{-1})	$\nu(3)$ (cm^{-1})
Pr[a]	14,992	26,315	35,714
Pr model	19,607	28,653	37,453
Lumi-R[a]	14,430	26,041	n.a.
Lumi-R model	20,408	27,472	36,101
Meta-Ra[a]	15,082	25,906	n.a.
Meta-Ra model	20,202	28,011	34,013
Meta-Rb[a]	15,037	26,315	n.a.
Meta-Rb model	21,459	26,041	35,087
Meta-Rc[a]	13,793	25,839	n.a.
Meta-Rc model	20,618	25,252	34,482
Pfr[a]	13,495	24,813	35,714
Pfr model	20,894	26,659	34,746
Lumi-F[a]	14,858	25,773	n.a.
Lumi-F model	21,141	27,700	38,610
Meta-F[a]	15,151	26,246	n.a.
Meta-F model	21,052	26,954	34,364

[a] Experimental spectra [11]: (1), first absorption band; (2), second absorption band; (3), third absorption band.

TABLE III

Comparison of experimental and calculated oscillator strength ratio.[a]

Form	f_2/f_1	f_{VIS}/f_{UV}
Pr	1.10	1.36
Pr model	0.70	1.25
Lumi-R	0.86 (0.73)	n.a.
Lumi-R model	0.83	n.c.
Meta-Ra	1.37 (1.24)	n.a.
Meta-Ra model	1.01	n.c.
Meta-Rb	2.29 (2.16)	n.a.
Meta-Rb model	2.93	n.c.
Meta-Rc	1.45 (1.32)	n.a.
Meta-Rc model	1.73	n.c.
Pfr	1.10 (0.97)	0.88
Pfr model	1.70	0.72
Lumi-F	1.02 (0.89)	n.a.
Lumi-F model	0.78	n.c.
Meta-F	1.15 (1.02)	n.a.
Meta-F model	0.72	n.c.

[a] f_{VIS}/f_{UV}–$f_1/(f_2+f_3)$. The values in parenthesis excluded 0.13, the contribution of the equilibrium Pr–Pfr.

(f_2/f_1) [11] and the experimental oscillator strength ratio of the visible band (first absorption band, f_1) over the UV band (second absorption band, f_2, plus third absorption band, f_3) (f_{VIS}/f_{UV}) [28]. Saturation with 660-nm light shifts the equilibrium to the 88% Pfr form [1]. As a result, we discounted this contribution from the intermediates f_2/f_1 ratio and from the Pfr f_2/f_1 ratio. The f_{VIS}/f_{UV} ratio of Pfr was obtained excluding the Pr contribution [28]. Therefore, we concluded that the oscillator strength ratios calculated for the phytochrome models (Pr, Pfr, and intermediates) are in good agreement with the experimental results (Table III).

Concluding Remarks

Except for the lower energy band, the calculated spectra reproduce well the spectra of the phytochrome (Pr, Pfr, and intermediates). This result is attributed to the small number of amino acids included in the models (five amino acids + chromophore).

The calculated ratios (f_{VIS}/f_{UV} and f_2/f_1) for the models match very well the experimental ratios obtained for the phytochrome (Pr, Pfr, and intermediates). This supports the proposed mechanism for the photoisomerization process.

ACKNOWLEDGMENTS

This research has received partial financial support from CNPq-Brazil. We are indebted to the Núcleo de Atendimento em Computação de Alto Desempenho (NACAD-COPPE-UFRJ) for the grant of computational time on its Cray J90. The authors also thank Michael C. Zerner for the use of the computational facilities at the Quantum Theory Project (Florida).

References

1. S. E. Braslavsky, in *Studies in Organic Chemistry, Vol. 40, Photochromism: Molecules and Systems*, H. Dürr and H. Bouas-Laurent, Eds. (Elsevier, Amsterdam, 1990), Chapter 19, pp. 738–755.
2. T. W. Mcnellis and X.-W. Deng, Plant Cell **7**, 1749 (1995).
3. J. M. Staub and X.-W. Deng, Photochem. Photobiol. **64**(6), 897 (1996).
4. P. H. Quail, M. T. Boylan, B. M. Parks, T. W. Short, Y. Xu, and D. Wagner, Science **268**, 675 (1995).
5. A. G. von Armin and X.-W Deng, Annu. Rev. Plant Physiol. Plant Molec. Biol. **47**, 215 (1996).
6. A. C. McCormac, D. Wagner, M. T. Boylan, P. H. Quail, H. Smith, and G. C. Whitelam, Plant J. **4**, 19 (1993).
7. G. C. Whitelam and N. P. Harberd, Plant Cell Environ. **17**, 615 (1994).
8. H. Smith, Annu. Rev. Plant. Physiol. Plant. Molec. Biol. **167**, 330 (1995)
9. P. H. Quail, Annu. Rev. Genet. **25**, 389 (1991).
10. M. D. Edgerton and A. M. Jones, Biochemistry **32**, 8239 (1993).
11. W. Rüdiger and F. Thümmler, Angew. Chem. Int. Ed. **30**, 1216 (1991).
12. W. Rüdiger, Photochem. Photobiol. **56** (5), 803 (1992).
13. H. A. Borthwick, S. B. Hendricks, M. W. Parker, E. H. Toole, and V. K. Toole, Proc. Natl. Acad. Sci. USA **38**, 662 (1952).
14. E. Chen, V. N. Lapko, J. W. Lewis, P.-S. Song, and D. S. Kliger, Biochemistry **35**, 843 (1996).
15. L. Li, J. T. Murphy, and J. C. Lagarias, Biochemistry **34**, 7923 (1995).
16. S. C. Björling, C.-F. Zhang, D. L. Farrens, P.-S. Song, and D. S. Kliger, J. Am. Chem. Soc. **114**, 4581 (1992).
17. H. Foerstendorf, E. Mummert, E. Schäfer, H. Scheer, and F. Siebert, Biochemistry **35**, 1079 (1996).
18. J. Matysik, P. Hildebrandt, W. Schlamann, S. E. Braslavsky, and K. Schaffner, Biochemistry **34**, 10497 (1995).
19. S. Iwakami, N. Yoshizawa, H. Hamaguchi, Y. Inoue, and K. Manabe, J. Photochem. Photobiol. B: Biology **33**, 239 (1996).
20. P. Schmidt, U. H. Westphal, K. Worm, S. E. Braslavsky, W. Gärtner, and K. Schaffner, J. Photochem. Photobiol. B: Biology **34**, 73 (1996).
21. R. Buchler, G. Hermann, D. V. Lap, and S. Rentsch, Chem. Phys. Lett. **233**(5–6), 514 (1995).
22. S. Tokutomi, T. Sugimoto, and M. Mimuro, Photochem. Photobiol. **56**(4), 542 (1992).

23. K. Smit, J. Matysik P. Hildebrandt, and F. Mark, J. Phys. Chem. **97**, 11887 (1993).
24. C. Scharnagl and S. F. Fischer, Photochem. Photobiol. **57**(1), 63 (1993).
25. C. Scharnagl, C. Cometta-Morini, and S. F. Fischer, Int. J. Quant. Chem.: Quant. Biol. Symp. **20**, 199 (1993).
26. A. Korkin, F. Mark, K. Schaffner, L. Gorb, and J. Leszczynski, J. Mol. Structure (Theochem) **388**, 121 (1996).
27. M. Duerring, G. B. Schmidt, and R. Huber, J. Mol. Biol. **211**, 633 (1991).
28. W. Parker, P. Goebel, C. R. Ross, II, P.-S. Song, and J. J. Stezowski, Bioconjugate Chem. **5**, 21 (1994).
29. M. J. S. Dewar, E. G. Zoebisch, E. F. Healy, and J. J. P. Stewart, J. Am. Chem. Soc. **107**(13), 3902 (1985).
30. M. J. S. Dewar and E. G. Zoebisch, J. Mol. Structure (Theochem) **180**, 1 (1988).
31. J. Ridley and M. C. Zerner, Theor. Chim. Acta **32**, 111 (1973).
32. M. C. Zerner, G. H. Loew, R. F. Kirchner, and U. T. Mueller-Westerhoff, J. Am. Chem. Soc. **102**(2), 589 (1980).
33. P.-S. Song, Q. Chae, and J. G. Gardner, Biochim Biophys. Acta **576**, 479 (1979).
34. F. Thümmler and W. Rüdiger, Tetrahedron **39**(11), 1943 (1983).
35. Y. Mizutani, S. Tokutomi, and T. Kitagawa, Biochemistry **33**, 153 (1994).
36. P. Eilfeld and W. Rüdiger, Z. Naturforsch. **40C**, 109 (1985).
37. B. W. Rospendowski, D. L. Farrens, T. M. Cotton, and P.-S. Song, FEBS Lett. **258**, 1 (1989).
38. D. L. Farrens, M.-M. Cordonnier, L. H. Pratt, and P.-S. Song, Photochem. Photobiol. **56**(5), 725 (1992).
39. E. Chen, W. Parker, J. W. Lewis, P.-S. Song, and D. S. Kliger, J. Am. Chem. Soc. **115**, 9854 (1993).

Studies on the Hydrogenation Steps of the Nitrogen Molecule at the *Azotobacter vinelandii* Nitrogenase Site

KRASSIMIR K. STAVREV,[1,2] **MICHAEL C. ZERNER**[3]
[1] *Hypercube, Inc., 1115 NW 4th Street, Gainesville, Florida 32601*
[2] *College of Medicine, University of Florida, Gainesville, FL 32610-0177*
[3] *Quantum Theory Project, University of Florida, Gainesville, Florida 32611-8435*

Received 9 March 1998; accepted 30 April 1998

ABSTRACT: We follow the initial activation of the nitrogen molecule at the FeMo cofactor of nitrogenase and subsequently model the hydrogenation of N_2 up to the fourth protonation step using the intermediate neglect of differential overlap quantum-chemical model. The results obtained favor a reaction mechanism going through hydrazido intermediates on the 4-Fe surfaces, externally to the FeMo cofactor. Calculations using density functional theory on smaller model systems also support the suggested mechanism over other possible schemes that involve early release of the first molecule of ammonia as a product of the enzymatic reaction. We also demonstrate that dielectric stabilization due to the protein around the cofactor could lower markedly the barrier for the product release as an ammonium ion. © 1998 John Wiley & Sons, Inc. Int J Quant Chem 70: 1159–1168, 1998

Key words: nitrogenase; nitrogen fixation; INDO; DFT, PM3tm

INTRODUCTION

The mechanisms of biological nitrogen fixation (nif) have been a challenge for scientists for over a hundred years, following the discovery of the bacterial process by Hellriegel and Willfart in 1886 [1]. Much of the interest in this area stems from the important role that nitrogen compounds play in biology and commerce and that no industrial process exists that competes well with nature. The interest in this area has increased dramatically in the last several years after the solution of the X-ray structure of the enzyme nitrogenase (N_2ase) at near-atomic resolution for different nif-type bacteria [2–4]. Various types of nitrogenases (FeMo, FeV, and Fe only) have been reported exhibiting similar chemistry [3]. Among other similarities, the

Correspondence to: K. K. Stavrev.
Contract grant sponsor: Office of Naval Research.
Contract grant sponsor: National Science Foundation.
Contract grant number: CHE-9312651.
Contract grant sponsor: SUR grant from IBM.

© 1998 John Wiley & Sons, Inc.
CCC 0020-7608 / 98 / 061159-10

presence of a six-atom prism built of coordinationally unsaturated Fe atoms at the center of the metal cofactor has been the primary target of theoretical speculation on the possible mechanism that involves the interaction of the substrate(s)—N_2 and a number of other small molecules—with the metal cluster [2–4]. Several theoretical models were examined and reviewed critically in the literature in the last few years [5–18].

In previous works [8, 9] we have proposed and examined a theoretical model for the active site of *Azotobacter vinelandii* FeMo cofactor based on the experimental structure by Rees et al. [2], spectroscopic evidence for the ground electronic state of the cluster and the intermediate neglect of the differential overlap (INDO) as a theoretical method [8]. We have shown that the initial activation of the N_2 molecule inside the cofactor is favored [8] and the access of the substrate to the cluster interior can be further facilitated by the electron addition to the cofactor prior or during the enzymatic reaction [9, 10]. We have compared two possible models for the active site having 39 and 41 open-shell electrons and have shown that these two models produce very similar results [8, 9]. The spin distributions within the native, reduced, and oxidized forms of the FeMo cofactor were also examined using the projected unrestricted Hartree–Fock (PUHF) methodology [9] implemented recently in the ZINDO program [11] and have reproduced to a good extent the available experimental data, pointing to a significant delocalization of the electron density over the metal open shells (*d*-orbitals), and the existence of two distinct groups of unpaired spin on the Fe atoms coupled anti-ferromagnetically through the three μ-sulfur bridges [9].

In this work we examine further the above theoretical model [8] in attempts to provide information on the reaction intermediates that can possibly form during the hydrogenation of the activated N_2 molecule. As in our previous work we use the INDO model in the restricted open-shell Hartree–Fock (ROHF) approximation and the model structure discussed in detail earlier [8]. Density functional theory (DFT), employing the Becke–Lee–Yang–Parr (BLYP) functional [12] and a double-zeta basis set (DZVP) with polarization including the Turbomole program [13], supplement parts of this work, especially in the cases where a preference is given to a particular intermediate over other possible structures.

Results and Discussion

Several nif reaction schemes have been proposed and discussed in the literature [4]. Among them, the reaction model by Thorneley and Lowe [14] has been well established based on kinetic studies of the reaction. This model suggests the early release of the first ammonia molecule as a most probable event in the course of the nif reaction. Other schemes have also been studied by Coucouvanis and co-workers [15] on the basis of model Mo/Fe/S compounds showing a particular reactivity with hydrazine and leading to its reduction to ammonia in which the heteroatom (Mo or V) plays an important role. As N_2H_4 is on the nitrogen fixation reaction path [16], it could be that the biological process may turn to the formation of hydrazine (fully or only partly) during the reaction. Studies on model nif-Fe/S complexes done by Sellmann and Sutter [17] also point strongly to such a possibility. In addition, chemical quenching of the bacterial nif reaction does, indeed, show the presence of hydrazine [14]; however, the observed N_2H_4 can also be formed from $N—NH_2$ or $N{\equiv}NH$ intermediates when a strong acid or base is used to halt the nif reaction and intercept the intermediates. Other types of nitrogenase, such as the FeV type with a similar structure [3], also produce N_2H_4 as a regular product of the bacterial nif reaction.

In any case, the reaction mechanism is presently unclear.

Figure 1 shows the catalytic cycle of the N_2 fixation process the way we model it through single H steps. It starts and ends with the bare model cofactor and involves, as a first step, the incorporation of the N_2 molecule in the cluster interior where it forms multiple Fe—N bonds with the six irons of the central prism, as shown in Figure 2. The number of metal–nitrogen bonds, however, may vary given the substrate mobility and the dynamics of the system due to vibrations or electron transfer to the active site which we studied in some detail [8, 9]. Spatial limitations, however, do not allow the cluster at its present structure to accommodate any of the intermediates, and we find further stages of the hydrogenation process to occur outside the cofactor, predominantly on the 4-Fe face described by Dance [6]. Besides the largest contact area provided by this

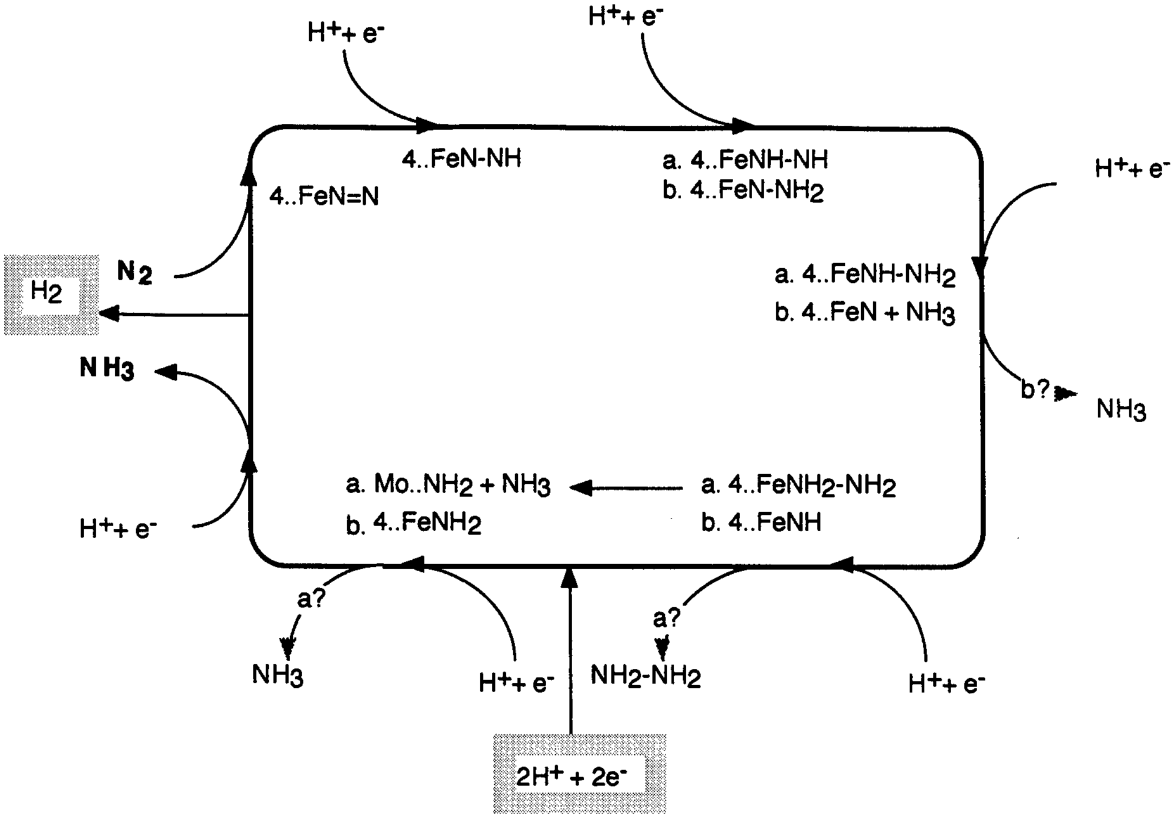
H⁺+ e⁻
H⁺+ e⁻
4..FeN-NH
a. 4..FeNH-NH
b. 4..FeN-NH2
H⁺+ e⁻
4..FeN=N
H2
N2
a. 4..FeNH-NH2
b. 4..FeN + NH3
NH3
b?
NH3
a. Mo..NH2 + NH3
b. 4..FeNH2
a. 4..FeNH2-NH2
b. 4..FeNH
H⁺+ e⁻
a?
NH3
H⁺+ e⁻
a?
NH2-NH2
H⁺+ e⁻
2H⁺ + 2e⁻

FIGURE 1. A schematic for the reaction $N_2 + 8H^+ + 8e^- \rightarrow 2NH_3 + H_2$ catalyzed by the enzyme nitrogenase. In the present modeling, the evolution of H_2 has not been examined. It is tempting to speculate, however, that these added protons that eventually evolve as H_2 are used to free the Mo binding site for hydrazine migration.

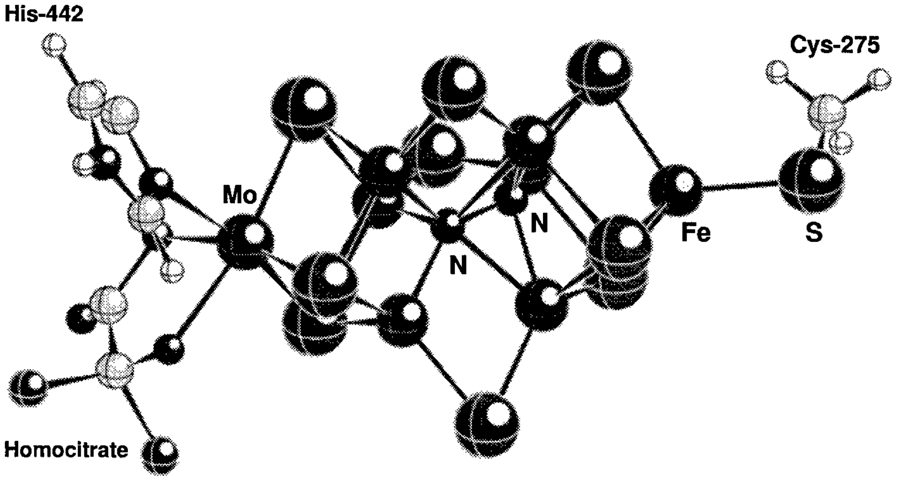
His-442
Cys-275
Mo
N
N
Fe
S
Homocitrate

FIGURE 2. The FeMo cofactor and the nitrogen molecule attached to it, see Refs. [2, 8].

4-Fe site (compared to the other two 4-Fe faces), it is also less crowded by the protein environment (nearest residue Arg-359) as seen from the experimental structure [2] and discussed widely in the literature [4, 5]. The protein and the cluster dynamics may, however, modify the picture significantly and allow for intermediates located on the two other alternative 4-Fe places that are available in the cluster.

Figure 3 shows the minimized positioning of the first N—NH intermediate on the FeMo cofactor surface. The structure has been obtained after the addition of an electron to the initially activated cofactor–N_2 system and subsequent protonation of the N_2 molecule. Although we find occasionally a small difference between the structures obtained after the addition of an H atom to the model system and that obtained via three-step hydrogenation (electron addition, relaxation, and protonation), we prefer the latter type of modeling, as it seems more natural and is supported by experimental findings implying similar sequence of events in Fe/S systems [18]. As in our previous work [8], we allowed for a complete freedom of movement of the substrate around the cofactor and we used the configuration-averaged Hartree–Fock methodology in its ROHF form to obtain the pure spin states [19]. The geometry optimizations and the relative energies that follow from them were calculated using the default set of geometric parameters in ZINDO, while the reported electronic properties are obtained using the spectroscopic model (INDO/S) on the relaxed structures. We have applied this approach successfully in a number of studies [20].

The calculated geometric and electronic properties (distances, atomic charges, bond indices) for the intermediates that we calculate in this work are summarized in Table I. As seen in this table, the charge on the nitrogen atoms remains negative and declines during the hydrogenation, due to the charge transfer from the metal *d*-orbitals into the π^* orbitals on the N_2 system. The hydrogenation has a relatively small effect on the N—N bond,

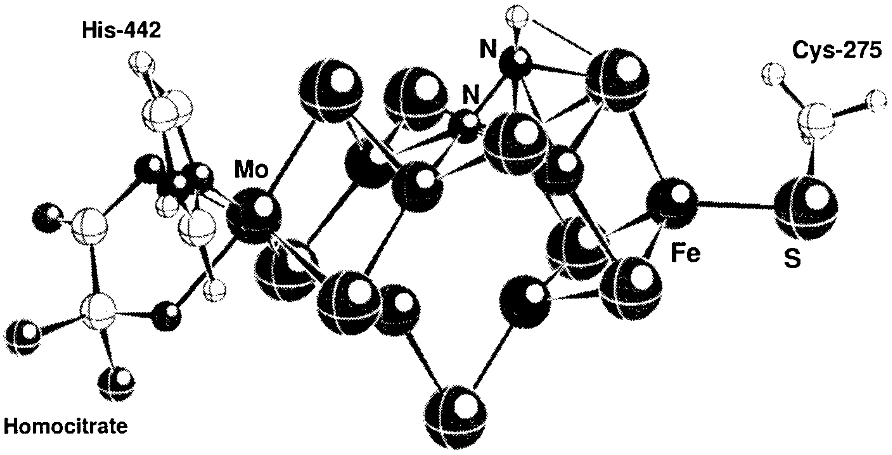

FIGURE 3. The most favored position of the N_2H_1 intermediate on the 4-Fe face of the obtained after energy minimization of the substrate.

TABLE I

Calculated N–N bond lengths (Å), Mulliken charges on the two nitrogen atoms, q(N), and the N–N Wiberg bond index (b.i.) between the N atoms for the reaction intermediates obtained after a geometry optimization.

System	R_{NN}	$q(N_1)$	$q(N_2)$	N—N b.i.
FeMo + N_2H_0	1.263	−0.486	−0.385	0.999
FeMo + N_2H_1	1.367	−0.544	−0.216	0.947
FeMo + N_2H_2	1.364	−0.407	−0.176	0.951
FeMo + N_2H_3	1.371	−0.281	−0.149	0.969
FeMo + N_2H_4	1.370	−0.298	0.048	0.952

however, as judged from the equilibrium N—N distances and bond indices shown in Table I. This is not unexpected as the final intermediate examined in this work, hydrazine, is a stable compound with a relatively long N—N bond (1.47 Å). The intermediate obtained on the surface of the cofactor has a shorter N—N bond (1.37 Å), most probably due to specific bonding to the metal surface.

As further seen from Figures 3–6, the N_2H_x intermediates tend to form stable configurations on the same 4-Fe face of the FeMo cofactor, and, most importantly, symmetrically hydrogenate the N—N molecule over other possibilities that involve sequential attachment of the H atoms to preferentially one N atom. This is a very important observation which, if proven true, may speak in favor of a dominant path for the nif reaction going through hydrazido intermediates rather than releasing the first ammonia at the third protonation step. This problem has been given some attention in the literature using model systems [22], and there are indications that the addition of three protons may lead to the formation of NH-NH_2 intermediates rather than N-NH_3. Our calculations, summarized in Figure 7, support this idea, showing increasingly higher energy differences between the N_2H_x isomers with the increase of x. Large barriers are expected to exist for the release of the first ammonia at the third and even fourth protonation steps, typically over 200 kcal/mol. Although seemingly high (ZINDO is known to overbind, often by a factor of 2–3) the calculated energy differences clearly indicate that hydrazine should be formed, provided the cluster and the protein relaxation effects are assumed to be small. The latter effects are difficult to estimate because the size of the system makes optimizing all structures completely a task almost impossible, even for a semiempirical method such as ZINDO. We have tried, however, at least to verify the energy differences between the N_2H_2 isomers using more reliable theories on smaller model systems. Table II, for example, shows the contribution to the total energy difference between the two N_2H_2 isomers, which comes from the intermediate alone. The calculations, done at various levels of theory, show that the NH-NH has a considerably lower energy ground state as that of the the N-H_2 analog and that the metal system in fact contributes to decreasing this difference to approximately −20 kcal/mol; see Figure 7. The same observation holds obviously for the N_2H_3 intermediates where the energy difference is even larger, −90 kcal/mol, in favor of the NH-NH_2 form (Fig. 7). The consistency of the results we obtained using the much faster ZINDO model and the more accurate DFT-ACM (B3LYP) and ab initio MP2 models (Table II) gives us some confidence in proceding with the former.

We have tried to further verify at least the trend for the above-mentioned energetics using DFT similar to that explored by others [23], the BLYP functional and the DZVP basis set. We used a bimetallic Fe cluster (Fig. 8) to model part of the 3-coordinated Fe site and the preferential attachment of the N_2H_x intermediates to it. The calculations have been done using the Turbomole DFT program [13]. Full geometry optimizations were

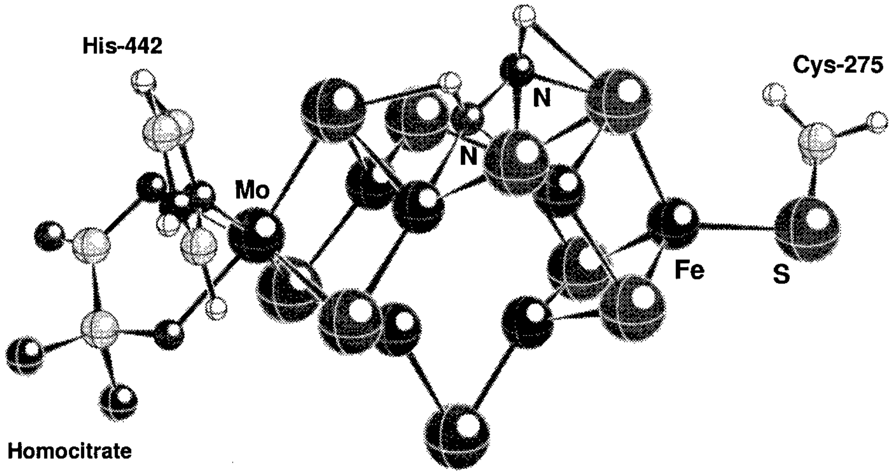

FIGURE 4. The most favored position of the N_2H_2 intermediate on the 4-Fe face of the obtained after energy minimization of the substrate.

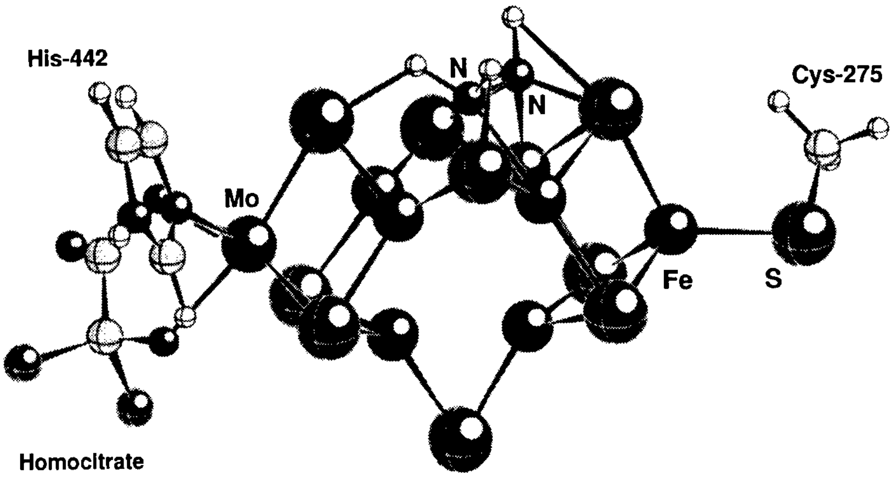

FIGURE 5. The most favored position of the N_2H_3 intermediate on the 4-Fe face of the obtained after energy minimization of the substrate.

done to include the effects of the Fe–S–Fe relaxation. The results obtained confirm the ZINDO observations qualitatively, though the energy differences are much smaller than those obtained from the semiempirical calculation: −6.1 kcal/mol for the N_2H_2 isomers and −4.6 kcal/mol in the case of N_2H_3 intermediates from the DFT calculations, compared to −39.7 and −56.2 kcal/mol, respectively, for the ZINDO calculations. Poor DFT energy convergence in the case of N_2H_4 intermediates did not allow an estimation of the differences between them. The ZINDO results give a preference for the NH_2–NH_2 over NH–NH_3 by −93 kcal/mol on the 2-Fe model system. Comparing the DFT and the ZINDO results on this metal–substrate model, we observe a significant difference, 7 to 9 times for the first two couples of isomers above, between the calculated energy differences (in absolute value) obtained using ZINDO for the same DFT optimized structures based on the 2-Fe model calculations. It is difficult to say whether these differences, in the scale of the energetics, stem from overbinding in INDO, or underbinding in DFT, or both. Perhaps more elaborate approaches can reveal the origin of this effect, but as far as the trend is concerned, both methods

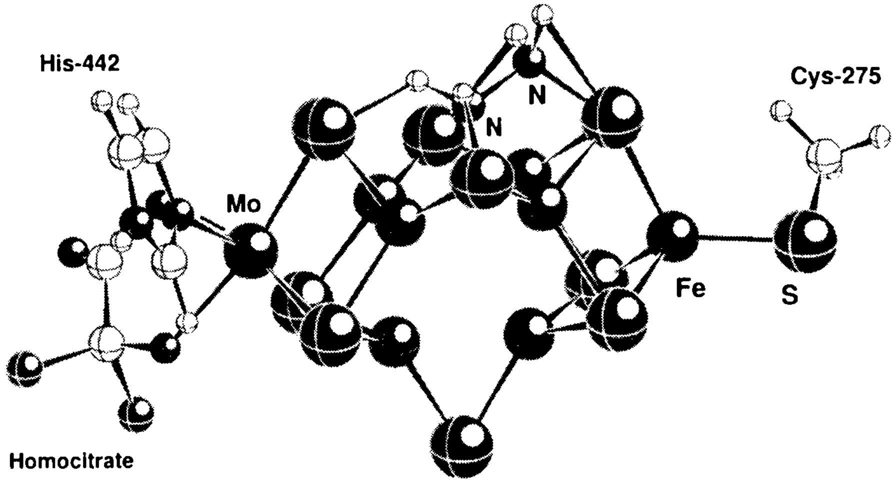

FIGURE 6. The most favored position of the N_2H_4 (hydrazine) intermediate on the 4-Fe face of the obtained after energy minimization of the substrate.

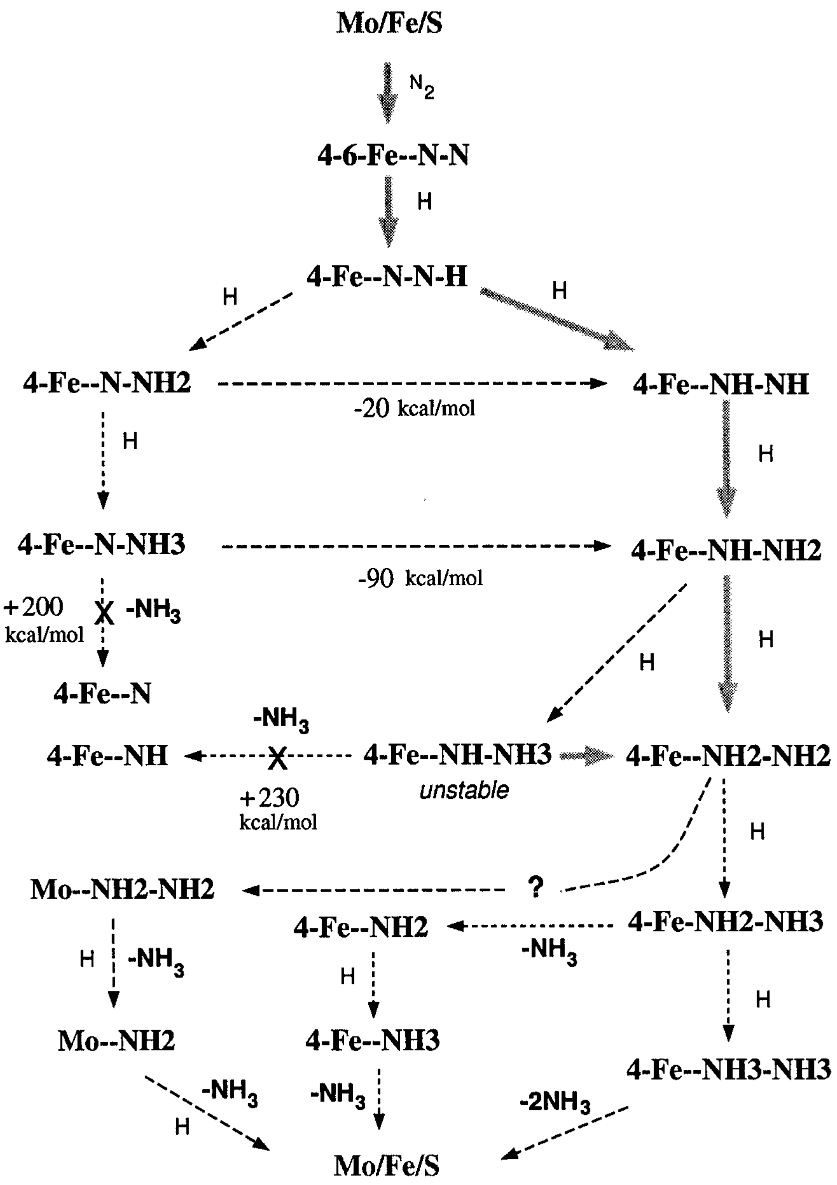
Mo/Fe/S
N2
4-6-Fe--N-N
H
4-Fe--N-N-H
H
H
4-Fe--N-NH2
-20 kcal/mol
4-Fe--NH-NH
H
H
4-Fe--N-NH3
-90 kcal/mol
4-Fe--NH-NH2
+200 kcal/mol
-NH3
H
H
4-Fe--N
-NH3
4-Fe--NH
+230 kcal/mol
4-Fe--NH-NH3
unstable
4-Fe--NH2-NH2
H
Mo--NH2-NH2
?
H
-NH3
4-Fe--NH2
-NH3
4-Fe-NH2-NH3
H
H
Mo--NH2
4-Fe--NH3
4-Fe--NH3-NH3
-NH3
H
-NH3
-2NH3
Mo/Fe/S

FIGURE 7. Calculated energy differences between the substrate isomers as intermediates and the favored reaction path (in bold) suggesting the nif reaction going through hydrazido intermediates.

TABLE II

Calculated energy differences, $\Delta E_{HNNH-NNH_2}$ (kcal/mol), between the HN—NH and N—NH_2 fragments using various methodologies.[a]

ZINDO	MOPAC	DFT	ACM	HF	MP2
-39.7	−33.2	−36.2	−35.5	−23.3	−48.0

[a] ACM stands for the adiabatic connection model (here B3LYP), HF are all-electron ab initio calculations. The nonempirical calculations utilize DZVP basis set. MOPAC calculations were done using the AM1 Hamiltonian. The BLYP functional is used in the DFT calculations.

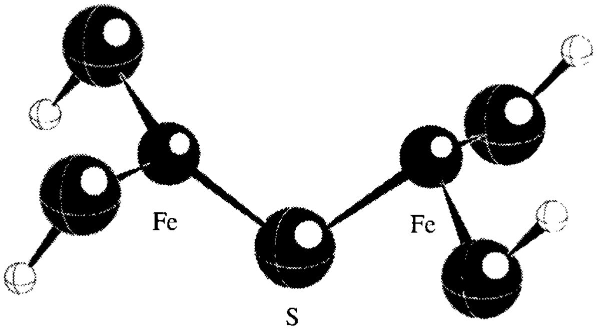

FIGURE 8. The model 3-coordinated bimetallic Fe site used to compare the DFT and INDO calculations.

predict more stable hydrazido over nitrido intermediates, which is the main target of the present study.

Even if we assume that hydrazine is formed as a reaction intermediate, several difficult questions remain unanswered at this stage of our study: Does the substrate stay and get further reduced to ammonia at this particular 4-Fe site? How mobile is the N_2H_x system and can it leave and reattach to a different metal site? How, indeed, can one break even a single N—N bond under these conditions given the relative stability of the calculated N—N bonding parameters with respect to hydrogenation? Are charged species, such as NH_4^+, involved in the dissociation and to what extent can they contribute to it? What is the role of the protein environment in the dissociation process?

We would like to speculate on this process.

Table III gives the sum of the calculated bond indices for the four intermediates and the FeMo cofactor. It includes also the hydrogen bonding between the H atoms and the sulfurs present at the 4-Fe face where the intermediate stabilization occurs. We observe that the binding between the substrate and the FeMo cofactor decreases sharply with the hydrogenation process; this could lead to desorption of the hydrazido intermediates from the surface of the cofactor, as recently suggested by Coucouvanis and co-workers [15] examining the reduction of hydrazine on similar (monocubane) Mo/Fe/S compounds. This idea is illustrated in Figure 9 and finds support through the

TABLE III

Sums of the calculated Wiberg bond indices between the N_2H_2 intermediates and the FeMo cofactor.[a]

System	2N—FeMo	*x*H...S	Total
FeMo + N_2H_0	4.471	0.000	4.471
FeMo + N_2H_1	4.018	0.012	4.030
FeMo + N_2H_2	3.207	0.033	3.240
FeMo + N_2H_3	1.203	0.109	1.312
FeMo + N_2H_4	0.655	0.134	0.789

[a] The hydrogen bonding indices between the H atoms of the intermediates and the S-atoms of the cofactor are also added to form the total bond index. The later is used as a measure the holding force between the FeMo cluster and the reaction intermediates, see also text.

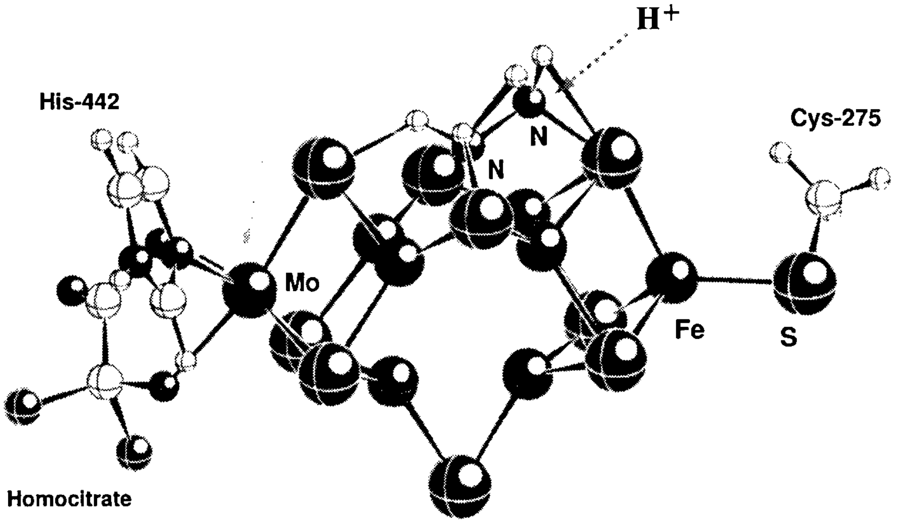

FIGURE 9. Speculated migration of the hydrazine substrate, alone or upon protonation, suggested by Coucouvanis and co-authors; see Ref. [15].

decrease of the Fe—N bond orders we observe and the relatively small H-bonding effects that contribute to it. To date, we are unable to find a more favorable site for the hydrazine, either at the Mo atom or elsewhere. As shown in a previous study [9], the Mo atom could open its environment with the addition of electrons to the FeMo cofactor. If this happens, structural rearrangement of the Mo coordination could be favored, either through a temporary detachment of the His-442 end or the carboxyl O atom bonded to the Mo, both prone to bond weakening upon reduction [9]. It is also possible that the two carboxyl groups present in the homocitrate group are protonated, detaching from Mo coordination, and thus play a central role in the reduction [15]. Further addition of electrons could then evolve hydrogen and regenerate the original Mo environment. In addition to these considerations, environmental effects may play a crucial role. The latter can be modeled, to a certain extent, using a reaction field as a substitute for the rest of the protein system. We have seen in a previous study [8] that the reaction field has no significant effect on the reaction profile of the N_2 attachment to to FeMo cofactor, and this is easy to believe given the fact that the reaction takes place mostly in the interior of the cofactor and there are no changes in net charge species involved in it. The formation and release of ammonia, however, especially externally to the cofactor, could be greatly affected by the protein surroundings. Also, N—N bond breakage either may result in neutral species, with ammonia as a product of the reaction, or NH_4^+ might be released instead. Small charged species are especially stabilized in the protein (dielectric) environments. The flow of protons to the FeMo cofactor can greatly contribute to the latter release. The net media effect of the reaction leading to the formation of ammonium ion can be estimated (Scheme 1) from our reaction field calculations to be as much as 36 kcal/mol, quite enough to promote the breakage of the already weakened ...N—N... bond. The last difference originates from the magnitude of the two leading electrostatic terms in the reaction field expressions, the charge, or Born term, and the dipole moment, or Onsager term [21]. The dielectric constant ϵ (set equal to 4 in this case, closer to similar estimates for proteins [24]) has a much smaller effect on the energetics of neutral species, as can be seen from the two expressions in Scheme 1. We thus point out that dielectric stabilization due to the presence of the protein surrounding the cofactor may contribute measurably to the N—N cleavage needed for the release of ammonia, in this case as an ion. We are presently examining in much greater detail the final stages of the process.

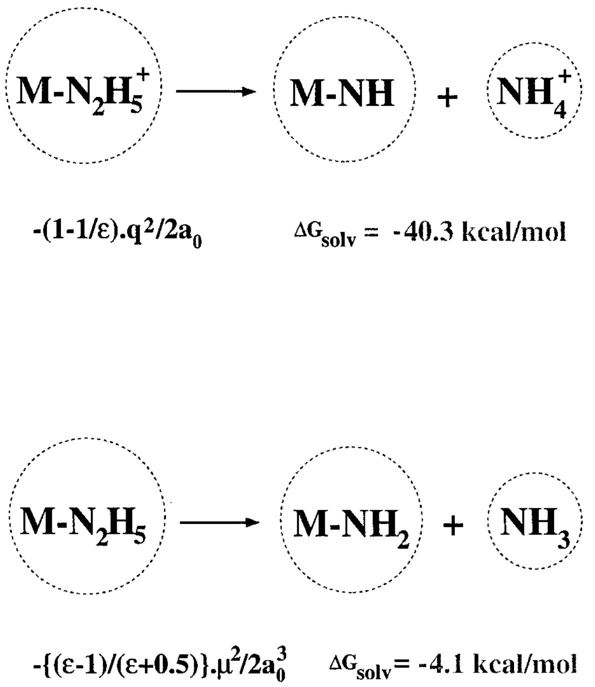
$M\text{-}N_2H_5^+ \longrightarrow M\text{-}NH + NH_4^+$
$-(1-1/\varepsilon).q^2/2a_0$
$\Delta G_{solv} = -40.3$ kcal/mol
$M\text{-}N_2H_5 \longrightarrow M\text{-}NH_2 + NH_3$
$-\{(\varepsilon-1)/(\varepsilon+0.5)\}.\mu^2/2a_0^3$
$\Delta G_{solv} = -4.1$ kcal/mol

SCHEME 1. The effect of dielectric relaxation on the reaction energetics with charged and neutral species as reactants and products. A spherical cavity self-consistent reaction field model [21] was used to model the solvent ($\epsilon = 4$ for the protein). The formulas indicate the leading term in the electrostatics; q is the Coulomb charge and μ is the dipole moment.

Conclusions

On the basis of the present theoretical model, we suggest that the biological nitrogen fixation, believed to take place at the M cluster of nitrogenase, should preferentially lead to the formation on hydrazido intermediates along the NN → NNH → NHNH → $NHNH_2$ → NH_2NH_2 path. We further speculate upon the release of NH_4^+. The formation of the ammonium ion is suggested as an aid to the final N–N cleavage due to dielectric stabilization of the small ion in the protein environment.

ACKNOWLEDGMENT

This work was supported in part through a grant from the Office of Naval Research, a National Science Foundation grant CHE-9312651, and a SUR 1996 grant from IBM.

References

1. H. Hellriegel, *Z. Ver. Rübenzuckerind. D. Reiches* **36**, 863 (1886); H. Hellriegel and H. Willfarth, *Beilageheft Z. Ver. Rübenzuckerind. D. Reiches* (1888).
2. M. K. Chan, J. Kim, and D. C. Rees, *Science* **260**, 792 (1993); see also, J. B. Howard and D. C. Rees, *Chem. Rev.* **96**, 2965 (1996); J. T. Bolin, N. Campobasso, S. T. Muchmore, T. V. Morgan, and L. E. Mortenson, in *Molybdenum Enzymes, Cofactors, and Model Systems*, E. I. Stiefel, D. Coucouvanis, and W. E. Newton, Eds. (American Chemical Society, Washington DC, 1993), p. 186, and references therein.
3. R. R. Eady and G. J. Leigh *J. Chem. Soc. Dalton Trans.*, 2379 (1994); R. R. Eady, *Chem. Rev.* **96**, 3013 (1996).
4. D. Sellmann, *Angew. Chem. Int. Ed. Engl.* **32**, 64 (1993); B. K. Burgess and J. L. Lowe, *Chem. Rev.* **96**, 2983 (1996); B. K. Burgess, *Chem. Rev.* **90**, 1377 (1990); for overviews, see E. I. Stiefel and G. N. George, in *Bioinorganic Chemistry*, I. Bertini, H. B. Gray, S. J. Lippard, and J. S. Valentine, Eds. (University Science, Mill Valley, CA, 1994), and G. J. Leigh, *Science* **268**, 827 (1995); *Ibid.*, **275**, 1442 (1997).
5. H. Deng and R. Hoffmann, *Angew. Chem. Int. Ed. Engl.* **32**, 1062 (1993).
6. I. G. Dance, *Aust. J. Chem.* **47**, 979 (1994).
7. F. B. C. Machado and E. R. Davidson, *Theor. Chim. Acta* **92**, 315 (1995).
8. K. K. Stavrev and M. C. Zerner, *Chem. Eur. J.* **2**, 83 (1996).
9. K. K. Stavrev and M. C. Zerner, *Theor. Chim. Acta* **96**(3), 141 (1997).
10. J. Christiansen, R. C. Tittsworth, B. J. Hales, and S. P. Cramer, *J. Am. Chem. Soc.* **117**, 10017 (1995).
11. M. Zerner, ZINDO program package, Quantum Theory Project, University of Florida, Gainesville, Florida; see also, M. C. Zerner, G. H. Loew, R. Kirchner, and U. Müller-Westerhoff, *J. Am. Chem. Soc.* **102**, 589 (1980); J. E. Ridley and M. C. Zerner, *Theor. Chim. Acta* **32**, 118 (1973); A. D. Bacon and M. C. Zerner, *Theor. Chim. Acta* **53**, 21 (1979).
12. A. D. Becke, in *The Challenge of d- and f- Electrons*, D. Salahub and M. Zerner, Eds., ACS Series 394, 1989; C. Lee, W. Yang, R. G. Parr, *Phys. Rev.* **37**, 785 (1988); for a comparison of different functionals, see P. J. Stephen, F. J. Devlin, C. S. Ashvar, K. L. Bak, P. R. Taylor, and M. Frisch, in *Chemical Applications of Density Functional Theory*, B. Laird, R. B. Ross, T. Ziegler, Eds., ACS Series 629, 1996.
13. Turbomole 95.0/3.0.0, InsightII, MSI/Biosym, San Diego, CA, 1997.
14. A comprehensive review on the Thorneley–Lowe scheme is given in *Molybdenum Enzymes*, T. Sprio, Ed. (Wiley, New York, 1985); see also R. N. F. Thorneley, G. A. Ashby, K. Fisher, and D. J. Lowe, in *Molybdenum Enzymes, Cofactors, and Model Systems*, E. I. Stiefel, D. Coucouvanis, and W. E. Newton, Eds. (American Chemical Society, Washington DC, 1993), p. 290, and references therein.
15. M. D. Demadis, S. M. Malinak, and D. Coucouvanis, *Inorg. Chem.* **35**, 4038 (1996); S. M. Malinak, A. M. Simeonov, P. E. Mosier, C. E. McKenna, and D. Coucouvanis, *J. Am. Chem. Soc.* **119**, 1662 (1997).
16. W. H. Orme-Johnson, in *Molybdenum Enzymes, Cofactors, and Model Systems*, E. I. Stiefel, D. Coucouvanis, and W. E. Newton, Eds. (American Chemical Society, Washington DC, 1993), p. 257.
17. D. Sellmann and J. Sutter, *J. Biol. Inorg. Chem.* **1**, 587 (1996).
18. B. Shen, L. L. Martin, J. N. Butt, F. A. Armstrong, C. D. Stout, G. M. Jensen, P. L. Stephens, G. N. LaMar, C. M. Gorst, and B. K. Burgess, *J. Biol. Chem.* **268**, 25928 (1993).
19. See W. D. Edwards and M. C. Zerner, *Theor. Chim. Acta* **72** 347 (1987); M. C. Zerner, *Int. J. Quant. Chem.* **35**, 567 (1989).
20. K. K. Stavrev and M. C. Zerner, *Chem. Phys. Lett.* **233**, 179 (1995); K. K. Stavrev and M. C. Zerner, *J. Chem. Phys.* **102**, 34 (1995); K. K. Stavrev, M. C. Zerner, and T. J. Meyer, *J. Am. Chem. Soc.* **117**, 8684 (1995); K. K. Stavrev and M. C. Zerner, *Int. J. Quant. Chem.: Quant. Biol. Symp.* **22**, 155 (1995); K. K. Stavrev and M. C. Zerner, *Chem. Phys. Lett.* **263**, 667 (1996); M. G. Cory, K. K. Stavrev, and M. C. Zerner, *Int. J. Quant. Chem.* **63**, 781 (1997).
21. M. M. Karelson and M. C. Zerner, *J. Phys. Chem.* **96**, 6949 (1992); for comparisons between models of solvation, see also K. K. Stavrev, T. Tamm, and M. C. Zerner, *Int. J. Quant. Chem.* **60**, 1585 (1996).
22. T. Yamabe, K. Hori, and K. Fukui, *Inorg. Chem.* **21**, 2816 (1982). P. S. Wagenknecht and J. R. Norton, *J. Am. Chem. Soc.* **117**, 1841 (1995); M. Hidai and Y. Mizobe, *Coord. Chem. Rev.* **95**, 1115 (1995).
23. I. G. Dance, *Chem. Commun.* **165** (1997); Y. G. Abashkin, S. K. Burt, J. R. Collins, R. E. Cachau, N. Russo, and J. W. Erickson, in *Metal-Ligand Interactions*, N. Russo and D. Salahub, Eds. (Kluwer Academic, 1996), p. 1; see also, *Chemical Applications of Density Functional Theory*, B. Laird, R. B. Ross, T. Ziegler, Eds., ACS Series 629, American Chemical Society, Washington, D.C., 1996; for limitations of density functional theory in hydrogenation reactions, see also M. T. Nguen, S. Creve, and L. G. Vanquickenborne, *J. Phys. Chem.* **100**, 18422 (1996).
24. L. Banci, I. Bertini, G. G. Svellini, and C. Luchinat, *Inorg. Chem.* **35**, 4248 (1996); see also T. Simonson and C. L. Brooks III, *J. Am. Chem. Soc.* **118**, 8452 (1996).

RHF Conformational Analysis of the Auxin Phytohormones n-Ethyl–Indole-3-Acetic Acid ($n = 4, 5, 6$)

MICHAEL RAMEK[1], SANJA TOMIĆ[2,*]
[1] *Institut für Physikalische und Theoretische Chemie, Technische Universität Graz, A-8010 Graz, Austria*
[2] *European Molecular Biology Laboratory, D-69012 Heidelberg, Germany,*

Received 21 February 1998; revised 15 May 1998; accepted 29 May 1998

ABSTRACT: RHF/6-31G* investigations of 4-, 5-, and 6-ethyl(Et)–indole-3-acetic acid (IAA) yielded 11 symmetry-unique local minima with *syn*-periplanar orientation of the —COOH group for each of these compounds. The global minima are of C_1 symmetry in all cases. Comparison with earlier results shows that ethylation or chlorination in position 5 or 6 introduces only minor changes on the orientation of the acetic acid side group, with no effect on the reaction paths related to this group. For 4-Et–IAA, the deviations from unsubstituted IAA are larger but preserve the pattern of reaction paths that is present in unsubstituted IAA, which is in contrast to 4-Cl–IAA, where local minima and reaction paths are completely different. © 1998 John Wiley & Sons, Inc. Int J Quant Chem 70: 1169–1175, 1998

Introduction

Auxin plant hormones govern many biological processes in higher plants such as cell divisions and enlargement, developmental differentiation, and the syntheses of specific proteins. Among this class of compounds, we are specifically interested in indole auxins, the parent compound of which is indole-3-acetic acid (IAA). IAA and its 4- and 6-chlorinated derivatives are naturally occurring auxins [1–5]. In addition, a large number of indole auxins have been synthesized and tested on various plant cultures [1–16]. Several auxin-binding proteins (ABP) have been distinguished, and, among them, ABP1 is considered to be the main candidate for an auxin receptor [17–26]. The effectiveness of auxins as growth promoters depends

---

Correspondence to: M. Ramek.

* *Permanent address*: Instut Ruđer Bošković, HR-10000 Zagreb, Croatia.

International Journal of Quantum Chemistry, Vol. 70, 1169–1175 (1998)
© 1998 John Wiley & Sons, Inc.
CCC 0020-7608 / 98 / 061169-07

not only on their binding affinity, but also on several other factors, for example, lipophilicity or correlation with other compounds in plants, like cytokinines, another type of plant hormone [27–29]. However, Rescher et al. [16] determined the correlation between the binding affinity and the maximum growth rate of meize coleoptil section at the optimum concentration of 10^{-6} mol/L for the following compounds: naphthalene-1-acetic acid (NAA1) > 4-Cl–IAA > 4-methyl (Me)–IAA > IAA > 4-ethyl(Et)–IAA > 2-Me–IAA. Regarding this, and the other available biological tests performed on IAA derivatives, it seems that the binding affinity is very sensitive to the type and size of the indole ring substituent in position 4.

Ab initio RHF structure investigations have been performed for IAA [30] and several mono- and dichlorinated derivatives [31, 32]. These studies yielded an interesting result, namely, that a chloro substituent at position 4 changes the potential energy surface (PES) completely, whereas chlorination at positions 5, 6, and 7 has only a marginal effect upon reaction paths and potential barriers. Although the properties of isolated molecules can be compared only to a limited extent with experimental binding data, these RHF results indicate possible binding conformations of indole auxins. The knowledge about the complex influence of weak nonbonded intramolecular interactions on the PES of these compounds makes us aware of similar influences of intermolecular interactions on the ligand conformation upon binding. The present study is an extension of these earlier RHF investigations, scrutinizing the influence of an ethyl substituent at positions 4, 5, and 6.

Computational Details and Results

Local minima and transition states were determined via RHF optimizations. Only conformers with the —COOH group in *syn*-periplanar orientation (i.e., values for the torsion angle H—O—C=O ≈ 0°) were considered, since the corresponding *anti*-periplanar conformers (H—O—C=O ≈ 180°) were 30–40 kJ/mol less stable in previous studies. The standard 6-31G* basis set was employed, which was proven to be adequate in the case of IAA [30]. The calculations were performed with the program GAMESS [33] on a variety of machines. All structures were fully optimized to a remaining root mean-square (rms) gradient less than 0.33×10^{-4} Hartree/bohr; the nature of all stationary points was verified via computation of the eigenvalues of the Hessian matrix: Local minima had no negative eigenvalues and transition states had exactly one negative eigenvalue.

The position of the carboxyl group relative to the indole ring depends on two torsion angles called T1 and T2 in the following. Using the atom numbering shown in Figure 1, T1 is the torsion angle C2—C3—C8—C9 and T2 is the torsion angle C3—C8—C9=O2. The orientation of the ethyl group is described by T3, which is the torsion angle C11—C10—C*n*—C*n* + 1 for *n*-Et–IAA. The values of T1, T2, and T3 as well as the energy of all symmetry-unique local minima (i.e., those with T1 ≥ 0°) are collected in Tables I–III.

Discussion

The energies of the various local minima of 5- and 6-Et–IAA follow a rather simple pattern: Those conformers, in which the ethyl group is in-plane with the indole ring, are approximately 5 kJ/mol higher in energy than those with a tilted ethyl group. This energy difference can clearly be related to repulsive H ⋯ H interactions. For an in-plane orientation of the ethyl group, there are two such interactions (C11—H ⋯ H—C4 in 5-Et–IAA, C11-H ⋯ H—C7 in 6-Et–IAA) with H ⋯ H distances around 2.4 Å and two (C10—H ⋯ H—C6 in 5-Et–IAA, C10—H ⋯ H—C5 in 6-Et–IAA) with H ⋯ H distances around 2.65 Å; if the ethyl group is approximately perpendicular to the plane of the indole ring, there is a total of only two such interactions (C10—H ⋯ H—C4 and C10—H ⋯ H—C6 in 5-Et–IAA, C10—H ⋯ H—C7 and C10—H ⋯ H—C5 in 6-Et–IAA), the distances of which are around 2.42 and 2.52 Å, respectively.

It is interesting to compare the data of 5- and 6-Et–IAA to those of the parent compound IAA.

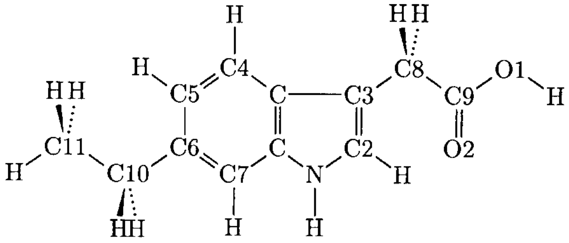

FIGURE 1. Definition of atom labels, shown for 6-Et–IAA.

TABLE I
Energy (kJ / mol) and torsion angles (degree) of all symmetry-unique local minima in the PES of 4-Et–IAA.

Energy	5.395	5.893	6.906	4.219
T1 (C9—C8—C3—C2)	0.00	103.21	78.95	92.21
T2 (O2=C9—C8—C3)	0.00	2.07	−96.47	107.17
T3 (C11—C10—C4—C5)	0.00	−2.24	−4.43	−6.95
Energy	1.476	4.540	10.292	4.886
T1 (C9—C8—C3—C2)	8.50	107.98	87.14	109.79
T2 (O2=C9—C8—C3)	−2.90	−20.77	−92.25	133.72
T3 (C11—C10—C4—C5)	−90.31	−78.11	−70.13	−79.60
Energy		2.876	2.987	0.000
T1 (C9—C8—C3—C2)		102.46	81.41	94.87
T2 (O2=C9—C8—C3)		0.19	−96.68	110.83
T3 (C11—C10—C4—C5)		91.50	94.26	92.03

Zero energy corresponds to an absolute value of −666.1894024 Hartrees.

The 6-31G*-PES of IAA contains four symmetry-unique local minima [30], with the following values of T1 and T2: 0°/0° ($E_{\mathrm{rel}} = 0$), 112.51°/103.57° ($E_{\mathrm{rel}} = 0.50$ kJ/mol), 99.06°/− 96.41° ($E_{\mathrm{rel}} = 2.00$ kJ/mol), and 111.85°/1.60° ($E_{\mathrm{rel}} = 4.36$ kJ/mol). The T1/T2 values of 5- and 6-Et–IAA therefore deviate less than 3° from those of unsubstituted IAA. A similar correspondence can be observed for the energies: For conformers with a tilted ethyl group, the maximum deviation from the IAA energy pattern is 0.31 kJ/mol (for 6-Et–IAA with T1/T2 = 112.95°/102.49°), and for those with the in-plane ethyl group, the maximum difference is 0.55 kJ/mol. The latter deviation occurs for the 5-Et–IAA conformer with T1/T2/T3 = 112.50°/101.42°/179.58° and is remarkable because only in this case is the energy lower than that of the conformer with the same orientation of the ethyl group and T1 = T2 = 0°. This deviation can be explained by the weak electrostatic C9=O2 ··· H—C4 interaction, which occurs in all 5- and 6-Et–IAA conformers with T1 ≈ T2 ≈ 100°. The O ··· H distances of this interaction are around 2.9 Å. In the specific 5-Et–IAA case, it reduces the net charge of the hydrogen atom on C4 just enough to weaken the repulsive H ··· H interactions, which were discussed above. As a result, the increase in energy for this specific conformer is less than that of all others with an in-plane ethyl group, which results in the interchange in energy. For the corre-

TABLE II
Energy (kJ / mol) and torsion angles (degree) of all symmetry-unique local minima in the PES of 5-Et–IAA.

Energy	5.426	9.461	7.141	5.376
T1 (C9—C8—C3—C2)	0.00	112.13	98.34	112.50
T2 (O2=C9—C8—C3)	0.00	2.67	−98.94	101.42
T3 (C11—C10—C5—C6)	180.00	−179.70	−179.79	179.58
Energy	0.000	4.104	1.902	0.207
T1 (C9—C8—C3—C2)	0.01	112.02	98.36	112.46
T2 (O2=C9—C8—C3)	0.04	2.54	−99.06	101.62
T3 (C11—C10—C5—C6)	−81.34	−81.09	−81.05	−81.47
Energy		4.274	1.918	0.247
T1 (C9—C8—C3—C2)		111.66	98.42	112.58
T2 (O2=C9—C8—C3)		1.40	−98.85	102.04
T3 (C11—C10—C5—C6)		81.31	81.20	81.51

Zero energy corresponds to an absolute value of −666.1926655 Hartrees.

TABLE III
Energy (kJ / mol) and torsion angles (degree) of all symmetry-unique local minima in the PES of 6-Et–IAA.

Energy	5.148	9.175	6.691	5.216
T1 (C9—C8—C3—C2)	0.00	113.18	99.53	113.02
T2 (O2=C9—C8—C3)	0.00	4.26	−99.19	101.02
T3 (C11—C10—C6—C7)	0.00	0.20	0.14	0.01
Energy	0.000	4.129	1.701	0.194
T1 (C9—C8—C3—C2)	0.20	112.63	98.89	112.95
T2 (O2=C9—C8—C3)	−0.07	3.35	−99.75	102.49
T3 (C11—C10—C6—C7)	−97.22	−97.94	−98.20	−98.14
Energy		4.161	1.708	0.190
T1 (C9—C8—C3—C2)		112.97	98.83	112.56
T2 (O2=C9—C8—C3)		3.98	−98.91	101.76
T3 (C11—C10—C6—C7)		98.11	98.62	98.33

Zero energy corresponds to an absolute value of −666.1932497 Hartrees.

sponding 6-Et–IAA conformers, in which the orientation of the ethyl group is toward C7 instead of C4, the sequence of relative energies is identical to that of IAA.

A notable difference between 5- and 6-Et–IAA, on the one hand, and unsubstituted IAA, on the other hand, is that the global minima in the former are not mirror-symmetrical, which also is a consequence of the increased H ⋯ H repulsion in the C_s orientation. The acetic acid side chain, however, is coplanar with the indole ring in the global minima of 5- and 6-Et–IAA, as it is in IAA. This arrangement results in a weak C9=O2 ⋯ H—C2 hydrogen bond with a bond order [34] of 0.016 and O ⋯ H distances of 2.391 Å (5-Et–IAA), 2.394 Å (6-Et–IAA), and 2.391 Å (IAA). This hydrogen bond also occurs in the mirror-symmetrical conformer of 5-Et–IAA and 6-Et–IAA, with the same bond order of 0.016 and O ⋯ H distances of 2.392 and 2.396 Å, respectively.

The similarity between the PES of IAA and those of 5- and 6-Et–IAA is not limited to the position of the local minima: It also extends to the T1/T2 reaction paths. Figure 2 compares the positions of all local minima and saddle points of IAA and 5-Et–IAA, and Figure 3 does the same for IAA and 6-Et–IAA. Despite the energy shift of approximately 5 kJ/mol for the conformers with an in-plane orientation of the ethyl group, the energy barriers for the internal rotations (with constant orientation of the ethyl group) are almost identical in all cases. Figure 4 shows this for the internal rotations of T2 (with T1 ≈ 100°) in IAA and 5-Et–IAA.

For 4-Et–IAA, the situation is significantly different, because of a variety of intramolecular interactions. One is the C9=O2 ⋯ H—C2 hydrogen bond, which is also present in 5- and 6-Et–IAA. It occurs for the conformers with T1 ≈ T2 ≈ 0° and is slightly stronger in 4-Et–IAA, with a bond order of 0.018 (both forms) and O ⋯ H distances of 2.314 Å (C_s form) and 2.323 Å (C_1 form). Another slightly

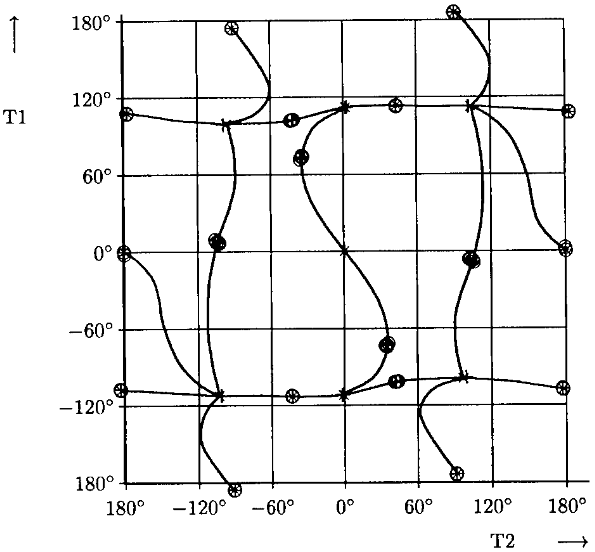

FIGURE 2. Positions of all symmetry-unique stationary points in the PES of IAA and 5-Et–IAA that relate to internal rotations of the acetic acid side chain. The solid lines indicate the reaction paths in the PES of unsubstituted IAA: (×) IAA, local minima; (⊗) IAA, saddle points; (+) 5-Et-MA, local minima; (⊕) 5-Et-MA, saddle points.

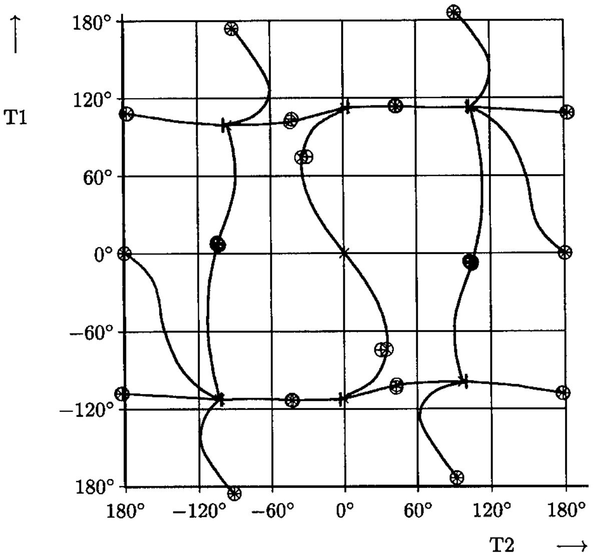

FIGURE 3. Positions of all symmetry-unique stationary points in the PES of IAA and 6-Et-IAA that relate to internal rotations of the acetic acid side chain. The solid lines indicate the reaction paths in the PES of unsubstituted IAA: (×) IAA, local minima; (⊗) IAA, saddle points; (+) 6-Et-IA, local minima; (⊕) 6-Et-IAA, saddle points.

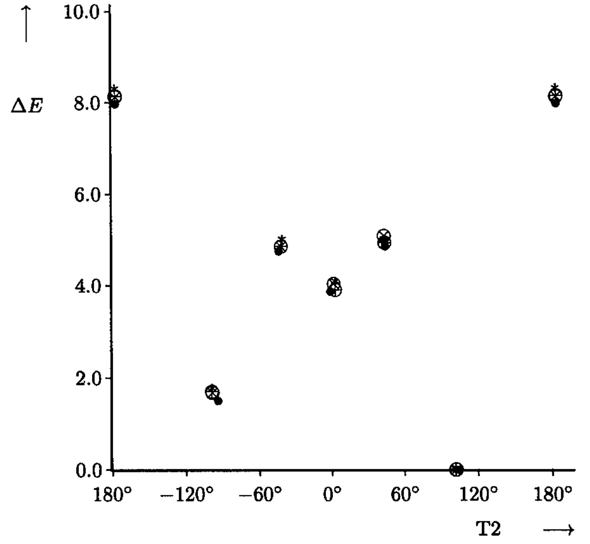

FIGURE 4. Energy of the stationary points of IAA and 5-Et-IAA with T1 ≈ 100° along the internal rotation of T2; zero energy corresponds to the conformer with T2 ≈ 100° in all cases. (●) IAA; (∗) 5-Et-IAA, T3 ≈ 180°; (⊕) 5-Et-IAA, T3 ≈ −80°; (⊗) 5-Et-IAA, T3 ≈ 80°.

stronger hydrogen bond, C10—H ⋯ O2=C9, occurs in the conformers with T1/T2/T3 = 92.21°/107.17°/ − 6.95° (H ⋯ O distance: 2.560 Å, bond order: 0.019) and T1/T2/T3 = 94.87°/110.83°/92.03° (2.552 Å, 0.021). Because of the stabilizing effect of this hydrogen bond, the latter conformation, characterized by both side chains more or less perpendicular to the indole ring plane and pointing toward opposite sides of this plane, is the global minimum in the PES. Other distances of interest in this structure are those between O1 and the hydrogen atom at position 2, which is 3.358 Å, and C10—H ⋯ H—C8, which is 2.323 Å. A weaker form of the C10—H ⋯ O2=C9 hydrogen bond is also present in the conformer with T1/T2/T3 = 102.46°/0.19°/91.50°; the H ⋯ O distance in this case is 2.750 Å and the bond order 0.011. Yet another weak hydrogen bond, C10—H ⋯ O1—C9, occurs in the conformers with T1/T2/T3 = 78.95°/ − 96.47°/ − 4.43° (H ⋯ O distance: 2.607 Å, bond order: 0.011) and T1/T2/T3 = 98.42°/ − 98.85°/81.20° (2.585 Å, 0.012).

Similar to 5- and 6-Et-IAA, repulsive H ⋯ H interactions are present in all 4-Et-IAA conformers. In contrast, however, not all of them are between aromatic and aliphatic hydrogen atoms. Instead, some H ⋯ H interactions occur between the two side chains; in the mirror-symmetrical conformer of 4-Et-IAA, for example, the hydrogen atoms of both methylene groups are pointing directly toward each other (with two H ⋯ H distances of 2.320 Å). In the local minimum of highest relative energy (E_{rel} = 10.292 kJ/mol), the C10—H ⋯ H—C8 distance is as low as 2.015 Å. (For this specific local minimum, an increase of T2 immediately leads to a saddle point at T1/T2 = 87.96°/ − 84.90°, which is only 0.003 kJ/mol higher in energy. The harmonic, unscaled vibration frequencies, which correspond to that reaction path, are 13.83 *i* and 19.19 cm^{-1} for the saddle point and the minimum, respectively. The latter value is equivalent to a zero-point energy of 0.115 kJ/mol, which means that this local minimum is just a mathematical feature of the PES, but does not produce a stable conformer.)

The considerable steric strain, which is caused by these short H ⋯ H distances, is reflected by the absolute energies of the global minima: 5-Et-IAA is about 8.6 kJ/mol and 6-Et-IAA about 10.1 kJ/mol lower in energy than is 4-Et-IAA. It also affects the positions of the local minima and the saddle points in the T1/T2 space. In contrast to 5- and 6-Et-IAA, these positions vary significantly

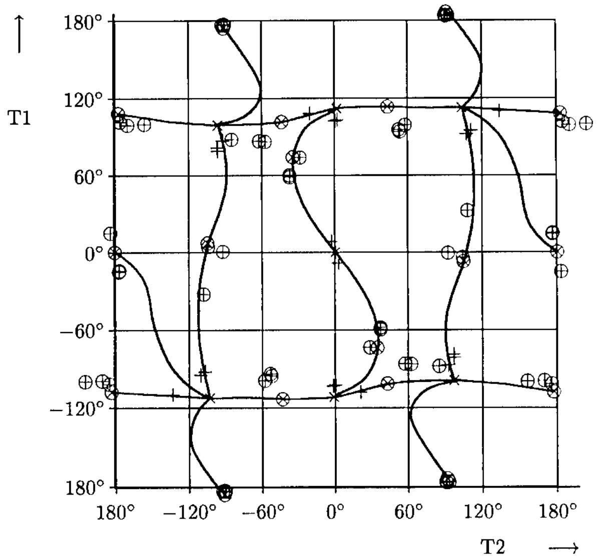

FIGURE 5. Positions of all symmetry-unique stationary points in the PES of IAA and 4-Et–IAA that relate to internal rotations of the acetic acid side chain. The solid lines indicate the reaction paths in the PES of unsubstituted IAA: (×) IAA, local minima; (⊗) IAA, saddle points; (+) 4-Et–IAA, local minima; (⊕) 4-Et–IAA, saddle points.

with the orientation of the ethyl group and deviate up to 30° from those of the parent compound IAA. Figure 5 shows the T1/T2 positions of all local minima and saddle points of 4-Et–IAA in comparison to those of IAA. Despite these deviations, the pattern of T1/T2 reaction paths in the PES of unsubstituted IAA is still recognizable in that of 4-Et–IAA. This is a remarkable result in view of the data for 4-Cl–IAA [31], where the symmetry-unique local minima are at T1/T2 positions of 0°/0°, 105.45°/− 14.01°, 110.92°/162.94°, and 6.25°/114.29° and the pattern of reaction paths is completely different (e.g., there is no internal rotation of T2 with T1 ≈ 100°).

Summary and Conclusion

The PES of 4-, 5-, and 6-Et–IAA were investigated via ab initio RHF/6-31G* calculations. For each compound, 11 symmetry-unique local minima with *syn*-periplanar orientation of the —COOH group are present in the PES. In contrast to IAA and its chlorinated derivatives, the global minima of 5- and 6-Et–IAA are not mirror-symmetrical but characterized by the acetic acid side chain coplanar with the indole ring and the ethyl group almost perpendicular to this plane. In 4-Et–IAA, a weak hydrogen bond between the two side chains yields a geometry for the global minimum, in which both side chains point toward opposite sides of the indole ring plane. In all three cases, the PES, therefore, has two global minima, which are "degenerate" in the terminology of quantum mechanics.

Comparison with the results obtained earlier for unsubstituted IAA [30] shows that ethylation in position 5 or 6 introduces only minor changes of the PES, which do not affect the reaction paths related to the acetic acid side chain. The same has been found for 5- and 6-Cl–IAA [32]. In the case of 4-Et–IAA, the deviations from unsubstituted IAA are much larger, but despite these deviations, the pattern of T1/T2 reaction paths of the IAA PES is also present in that of 4-Et–IAA. This is a remarkable contrast to the situation in 4-Cl–IAA [31], where some local minima appear at significantly different positions in T1/T2 space, and the reaction paths are completely different. This comparison shows that the different PES of 4-Cl–IAA is an effect that is specifically related to the chloro substituent at position 4. Interestingly, the qualitative picture, which one obtains from the PES of 4-Cl–IAA, IAA, and 4-Et–IAA, is well in accord with the measured biological data.

The results of this study also show that relatively weak intramolecular interactions can significantly influence the orientation of the acetic acid side chain in IAA derivatives. The same can be expected from the intermolecular interactions that enable the binding to any auxin receptor. Hence, the combined results of the current work and the previous studies of indole auxins present a basis for the investigation of the actual binding process. The acetic acid side chain, as well as any nonrigid substituent, can be expected to show a significant amount of flexibility, that is, it can easily adopt different orientations. Therefore, in the auxin-receptor complex, considerable deviations from the structures of the isolated compound or the respective solid-state structures can be anticipated.

ACKNOWLEDGMENTS

The authors want to thank Dr. Rebecca Wade for reading and commenting on the manuscript. Continued support by the Computing and Information Services Center of the Technical University Graz is also gratefully acknowledged.

References

1. P. J. Davies, *Plant Hormones and Their Role in Plant Growth and Development* (Martinus Nijhoft, Dordrecht, 1987).
2. K. V. Thimann, *Hormone Action in the Whole Life of Plants* (The University of Massachusetts Press, Amherst, 1977).
3. T. Hatano, M. Katayama, and S. Marumo, Experientia **43**, 1237 (1987).
4. G. F. Katekar and A. E. Geissler, Phytochemistry **21**, 257 (1982).
5. D. M. Reinecke, J. A. Ozga, and V. Magnus, Phytochemistry **40**, 1361 (1995).
6. W. L. Porter and K. V. Thimann, Phytochemistry **4**, 229 (1965).
7. V. Pattabhi, Curr. Sci. **59**, 1228 (1990).
8. B. Kojić-Prodić, B. Nigovć, S. Tomić, N. Ilić, V. Magnus, R. Konjević, Z. Giba, and W. L. Duax, Acta Crystallogr. B **47**, 1010 (1991).
9. B. Nigović, B. Kojić-Prodić, S. Antolić, S. Tomić, V. Puntarec, and J. D. Cohen, Acta Crystallogr. B **52**, 332 (1996).
10. S. Antolić, B. Kojić-Prodić, S. Tomić, B. Nigović, V. Magnus, and J. D. Cohen, Acta Crystallogr. B **52**, 651 (1996).
11. B. T. G. Lutz, E. van der Windt, J. Kanters, D. Klämbt, B.Kojić-Prodić, and M. Ramek, J. Mol. Struct. **382**, 177 (1996).
12. P. M. Ray, U. Dohrmann, and R. Hartel, Plant Physiol. **60**, 585 (1977).
13. T. Hatano, Y. Kato, M. Katayama, and S. Marumo, Experientia **45**, 400 (1989).
14. M. Katayama, Y. Kato, H. Kimoto, and S. Fuji, Experientia **51**, 721 (1995).
15. G. F. Katekar and A. E. Geissler, Phytochemistry **22**, 27 (1983).
16. U. Rescher, A. Walther, C. Schiebl, and D. Klämbt, J. Plant Growth Reg. **15**, 1 (1996).
17. K. Palme, J. Plant Growth Reg. **12**, 171 (1993).
18. D. Klämbt, Plant Mol. Biol. **14**, 1045 (1990).
19. A. M. Jones, Physiol. Plantarum **80**, 154 (1990).
20. A. M. Jones and P. V. Prasad, Bioassays **14**, 43 (1992).
21. M. A. Venis and M. Napier, Crit. Rev. Plant Sci. **14**, 27 (1995).
22. H. Tian, D. Klämbt, and A. M. Jones, J. Biol. Chem. **270**, 26962 (1995).
23. M. Löbler and D. Klämbt, J. Biol. Chem. **260**, 9848 (1985).
24. S. Shimomura, S. Sotobayashi, M. Futai, and T. Fukui, J. Biochem. **99**, 1513 (1986).
25. N. Inohara, S. Shimomura, T. Fukui, and M. Futai, Proc. Natl. Acad. Sci. U.S.A **86**, 3564 (1989).
26. R. M. Napier, M. A. Venis, M. A. Bolton, L. I. Richardson, and G. W. Butcher, Planta **176**, 519 (1988).
27. H. Tian, D. Klämbt, and A. Jones, J. Biol. Chem. **270**, 26962 (1995).
28. A. T. Trewaves, Nature **390**, 657 (1997).
29. T. Ichikawa, Y. Suzuki, I. Czaja, C. Schommer, A. Lessnick, J. Schell, and R. Walden, Nature **390**, 698 (1997).
30. M. Ramek, S. Tomić, and B. Kojić-Prodić, Int. J. Quantum Chem., Quantum Biol. Symp. **22**, 75 (1995).
31. M. Ramek, S. Tomić, and B. Kojić-Prodić, Int. J. Quantum Chem. **60**, 1727 (1996).
32. M. Ramek and S. Tomić, J. Mol. Struct. (Theochem), accepted.
33. M. W. Schmidt, K. K. Baldridge, J. A. Boatz, S. T. Elbert, M. S. Gordon, J. H. Jensen, S. Koseki, N. Matsunaga, K. A. Nguyen, S. Su, T. L. Windus, M. Dupuis, and J. A. Montgomery, Jr., J. Comp. Chem. **14**, 1347 (1993).
34. I. Mayer, Chem. Phys. Lett. **97**, 270 (1983).

pK_a of Cytosine on the Third Strand of Triplex DNA: Preliminary Poisson–Boltzmann Calculations

GEORGE R. PACK, LINDA WONG,* GENE LAMM
University of Illinois College of Medicine, Rockford, Illinois 61107

Received 13 March 1998; accepted 20 April 1998

ABSTRACT: The energetics of formation of a triple-helical structure in homopurine–homopyrimidine mixtures has been modeled using Poisson–Boltzmann calculations. Oligomers with the sequence $d(\mathrm{TC})_n$ and $d(\mathrm{AG})_n$ form hydrogen-bonded triple-helical structures of the form $d(\mathrm{TC})_n \cdot d(\mathrm{AG})_n \cdot d(\mathrm{TC}^+)_n$. The third base, a pyrimidine in this case, forms Hoogsteen-type hydrogen bonds with the purine, requiring that the cytosine residues of the third strand protonate at N3. The pK_a of cytosine, 4.3 in the isolated solvated molecule, is raised by the strong electrostatic field in the triple helix. We have done calculations of the effective pK_a of this cytosine and compared the results with experimental studies of triple-helix formation as a function of pH. This provides a test of various models of the dielectric constant for triplex DNA and its local environment. © 1998 John Wiley & Sons, Inc. Int J Quant Chem 70: 1177–1184, 1998

Key words: pK_a shift; acid dissociation constant; triple helix; dielectric constant

Introduction

Oligonucleotide hybridization is sufficiently robust to include formation of triple-helical constructs besides the more familiar double helices. Hybridization to form duplex structures is highly sequence specific. The high degree of complementarity of G with C and of A with T is essential for gene function. In triplex formation the third strand associates with an existing duplex through hydrogen bonding of the third-strand bases with the Watson–Crick duplex base pairs with significant specificity. The most prevalent type of triple helix is formed by binding of a homopurine or homopyrimidine single strand in the major groove of a homopurine–homopyrimidine duplex with the two pyrimidine strands antiparallel [1]. When a G–C base pair is recognized by a C on the third strand, the interaction is pH dependent, increasing with greater acidity. Arnott et al. [2] showed that protonation of the cytosine N3 allows the formation of Hoogsteen hydrogen

---

* Present address: Myriad Genetics, Salt Lake City, Utah.

Correspondence to: G. R. Pack

Contract grant sponsor: National Institute of General Medical Sciences, NIH.

Contract grant number: GM29079.

© 1998 John Wiley & Sons, Inc.
CCC 0020-7608 / 98 / 061177-08

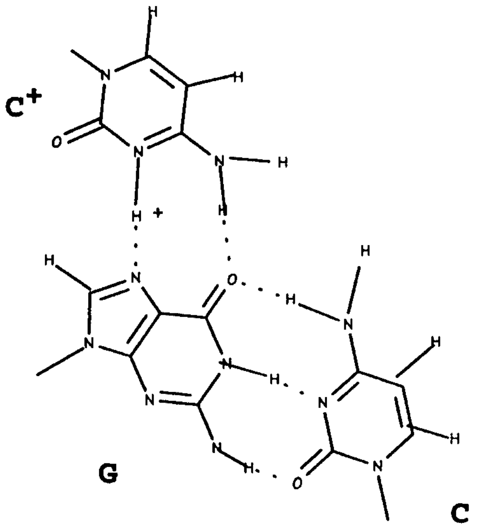

FIGURE 1. C^+–G–C triad triad of triple-helical DNA.

bonding to G as shown in Figure 1, providing a rationale for the pH dependence.

The pK_a of deoxycytidine is 4.3 in aqueous solution and varies by about 0.1 as the ionic strength goes from 0 to 1 *M* [3]. Measurements of the pH dependence of the formation of triplexes in which the third strand is *d*(CTTCCTCCTCT) show the midpoint of the association to occur at pH 5.8 [4]. A similar analysis of triple-helix formation in hairpin regions with the third strand being *d*(TTCTTCTTC) or *d*(CCTCCTCCT) yielded midpoints at 6.15 and 6.19, respectively [5]. Callahan and co-workers [6] found a triplex-formation midpoint at pH 5.6 for $d(\mathrm{CT})_8$–$d(\mathrm{AG})_8$–$d(\mathrm{CT})_8$, while Singleton and Dervan [7] found a midpoint in the association constant curve for a $d(\mathrm{CT})_5$-containing oligonucleotide to occur at pH 5.5. Lavelle and Fresco [8] provided evidence that the midpoint of the triplex-association constant versus pH curve was a measure of the cytosine pK_a by showing that on dissociation of the triplex at pH 7, one H^+ per cytosine residue is released into solution. The experimental evidence seems to indicate that the third-strand cytosine pK_a is increased by about 1.5 units when it is bound in the major groove as part of triplex DNA.

Calculations of the pK_a of titratable groups in proteins using numerical solutions to the Poisson–Boltzmann equation have met with varying degrees of success. Tanford and Kirkwood [9] developed a theory of protein titration curves based on a model of a low-dielectric spherical protein with discrete unit charges at fixed locations all embedded in a high-dielectric (aqueous) continuum. When numerical methods for solving electrostatic equations based on higher resolution protein structures became available, more accurate calculations of the pK_a's of buried groups soon followed. Using Poisson's equation, Rogers et al. [10] relied on the method of Warwicker and Watson [11] to calculate the change in potential at one site due to protonation at another. Sternberg et al. [12] used this same procedure to predict pK_a shifts in subtilisin caused by mutation of charged residues. Coupling Poisson's equation with the Boltzmann equation leads to a Poisson–Boltzmann (PB) description of the electrolyte environment of DNA. Using a dielectric constant of 2 or 4 for the protein interior and 80 for the environment, the pK_a's of several proteins have been calculated (see, e.g., [13–16]).

Representing the anisotropic atomic environment by a single dielectric constant can be a serious approximation. Warshel [17] and Warshel and Aqvist [18] have pointed out that its value depends on the property under consideration and can vary from 4 to greater than 40. Nevertheless, the computational convenience of the PB approach has prompted several groups to seek optimal representations of a single dielectric constant for the protein interior. Demchuk and Wade [19] identified two location-dependent classes of ionizable sites. To get the best agreement with experimentally determined pK_a's, solvent exposed sites were assigned a dielectric constant close to that of the aqueous solvent while buried sites had lower values between 10 and 20. In a study of 60 sites within 7 proteins, Antosiewicz [20] found that the best accuracy could be obtained with a interior protein dielectric constant of 20. This rather high value has recently been used by Schaefer et al. [21] in an application of the PB approach to the calculation of free energy differences between protein conformations. Antosiewicz et al. [20] compared computed and experimental pK_a shifts at 63 sites using a parametrized set of atomic charges and radii, PARSE, which was specifically optimized to reproduce measured solvation energies of small molecules. They found that PB-calculated pK_a shifts averaged over a set of nuclear magnetic resonance (NMR) determined protein conformations could be more accurate than the null model, in which all pK_a shifts of a titratable group are the same for all members of that group whatever their location within the protein. On the other hand, Antosiewicz et al. [20] concluded that even when the extra computational effort was made "the pK_a's calculated using a protein dielectric constant of 4 are less accurate than those computed with a less plausible protein dielectric constant of 20." Relatively little effort has been devoted to determining internal dielectric constants for nucleic acids. Yang et al. [22] analyzed a long molecular dynamics simulation of triplex DNA and found the general dielectric constant of DNA to be about 15 with the subgroups of bases, sugar atoms, and phosphates to be 4.2, 2.3, and 48.5, respectively. Lamm and Pack [23] calculated the dielectric constant of the ionic environment near the surface of the B-DNA and found it to be about 30 in the minor groove and 50 in the major groove, agreeing well with available experiments.

In the presence of the strong electrostatic potential at the DNA surface, the intrinsic pK_a of cytosine would be expected to increase due to the higher local H^+ concentration [24]. In fact, a simple PB cell model calculation [25] predicts an increase in pK_a of about 2.2 units for duplex DNA. This agrees well with measurements of the apparent pK_a's of amino acids that were covalently bound to the minor groove of duplex DNA, which show an increase of 1.5 to 2.4 units over the pK_a's in aqueous solution [26]. For triplex DNA, a similar PB cell model calculation yields a somewhat larger intrinsic pK_a change of almost 3 units due to the increased surface charge density in the model. PB calculations on a more detailed, all-atom model of triplex-helical DNA predict a pK_a change of over 5 units. These relatively simple calculations are qualitatively correct but exaggerate the experimentally determined pK_a change. This study describes initial attempts to apply the more detailed protein-based methods described above to calculate the pK_a of the cytosine of the third strand of triplex DNA. Results and conclusions follow a brief discussion of the methods used.

Methods

The system chosen was an infinite repeat of the homopyrimidine–homopurine–homopyrimidine triplex in which the third strand is protonated. The sequence for the parent duplex was poly *d*(A–G)–poly *d*(T–C); the third strand was poly *d*(T–C). Numerical Poisson–Boltzmann calculations were performed using methods previously described [25]. Briefly, the space occupied by the DNA and its environment was divided into many finite volume cells in planar cross sections perpendicular to the DNA helical axis. The finite difference version of the Poisson equation for the electrostatic potential ϕ_i at cell location i on a curvilinear grid is

$$\phi_i = \frac{4\pi v_i \rho_i/\epsilon_i + \sum_j(\phi_j \epsilon_{ij} S_{ij}/r_{ij})}{\sum_j(\epsilon_{ij} S_{ij}/r_{ij})},$$

where v_i is the volume of cell i, ρ_i is the total charge density, $\epsilon_{ij} = (\epsilon_i + \epsilon_j)/2$ is the arithmetic average of the dielectric constants of cells i and j, S_{ij} is the shared surface area of these cells, and r_{ij} is the distance between cell centers. Summations are taken over all cells j sharing a surface with a given cell i. Inside the DNA the charge within each cell was fixed as calculated from the overlap with the atomic van der Waals spheres and provided a charge density $\rho_i = q_i/v_i$. The total charge density in each cell in the environment was obtained from the individual ionic charge densities by summation: $\rho_i = \sum_k \rho_i^k$. The Boltzmann equation for each ion type can be written as

$$\rho_i^k = \frac{N_k \exp(-\beta z_k \phi_i)}{\sum_i v_i \exp(-\beta z_k \phi_i)},$$

in which z_k is the ion valence and N_k is the total number of ions of type k within the system. A finite stretch of DNA was chosen as a repeat unit and the intercell links and shared surface areas between the cells in the planar cross sections at either end of the repeat were calculated, effectively wrapping the finite element grid around to achieve an infinite repeat of linear DNA.

The thermodynamic cycle illustrated in Figure 2 was used to define the free energy of protonation

$$\begin{tikzcd}
\text{model} & \text{Cyt H}^+\text{(sol)} \arrow[r] \arrow[d] & \text{Cyt(sol)} \arrow[d] & + & \text{H}^+\text{(sol)} \\
\text{DNA} & \text{Cyt H}^+\text{(DNA)} \arrow[r] & \text{Cyt(DNA)} & + & \text{H}^+\text{(sol)}
\end{tikzcd}$$

FIGURE 2. The thermodynamic cycle used in the definition of the pK_a difference between the model compound, deoxycytidine, in water (top arrow) and deoxycytidine on the third strand of triple-helical DNA (bottom horizontal arrow). The top horizontal process is an experimental quantity that—combined with the two processes represented by the vertical arrows—defines the pK_a of the bottom horizontal process, the protonation of deoxycytidine on the third strand of triple-helical DNA.

of a cytosine residue in triplex DNA (bottom arrow) in terms of the known pK_a of cytosine in solution (top line) and the energies required to transport the charged (left vertical arrow) and uncharged (right vertical arrow) cytosine from solution into the DNA triplex. Following Bashford and Karplus [14], the expression for the fraction θ_i of cytosine i protonated is

$$\theta_i = \frac{\Sigma_{\{X\}} x_i \exp\Big[\Sigma_\mu x_\mu\big(2.303(\mathrm{pK}_{\mathrm{intr},\,\mu} - \mathrm{pH})\big) - \tfrac{1}{2}\Sigma_{\mu,\,\nu}\big(x_\mu x_\nu W_{\mu,\,\nu}(\{X\})\big)\Big]}{\Sigma_{\{X\}} \exp\Big[\Sigma_\mu x_\mu\big(2.303(\mathrm{pK}_{\mathrm{intr},\,\mu} - \mathrm{pH})\big) - \tfrac{1}{2}\Sigma_{\mu,\,\nu}\big(x_\mu x_\nu W_{\mu,\,\nu}(\{X\})\big)\Big]} \qquad (1)$$

in which $\{X\}$ is a set of "protonation state" vectors, each of which has n elements x_μ that are either 1 or 0, depending whether site μ is protonated or not. There are 2^n members of $\{X\}$ corresponding to each possible protonation state shown above. As discussed below, the fact that we are using an infinitely long model for DNA introduces some difficulties into the definition of all possible protonation states.

The intrinsic pK_a, determined by neglecting interactions between protonated sites, is given by Eq. (2),

$$\mathrm{p}K_{\mathrm{intr}} = \mathrm{p}K_{\mathrm{model}} - [\Delta\Delta \mathrm{G}_{\mathrm{Born}} - \Delta\Delta G_{\mathrm{back}}]/(2.303\ \mathrm{kT}), \qquad (2)$$

in which the following quantities are calculated from the PB-determined potentials and charges:

$$\Delta\Delta G_{\mathrm{Born}} = \tfrac{1}{2}\sum_i Q_i^p[\phi^p_{\mathrm{DNA},\,i} - \phi^p_{\mathrm{model},\,i}] - \tfrac{1}{2}\sum_i Q_i^u[\phi^u_{\mathrm{DNA},\,i} - \phi^u_{\mathrm{model},\,i}] \qquad (3)$$

and

$$\delta\Delta G_{\mathrm{back}} = \sum_j q_j[\phi^p_{\mathrm{DNA},\,j} - \phi^p_{\mathrm{model},\,j}] - \sum_j q_j[\phi^u_{\mathrm{DNA},\,j} - \phi^u_{\mathrm{model},\,j}]. \qquad (4)$$

$\Delta\Delta G_{\mathrm{Born}}$ is the difference in the Born free energy between charging site i in the model (solvated cytosine) and in DNA. Q_i^p and Q_i^u are the charges at the titrating sites when protonated and unprotonated, respectively, $\phi^p_{\mathrm{DNA},\,i}$ and $\phi^u_{\mathrm{DNA},\,i}$ similarly represent the calculated electrostatic potentials at site i when the site is protonated and unprotonated, and $\phi^p_{\mathrm{model},\,j}$ and $\phi^u_{\mathrm{model},\,j}$ are the corresponding potentials calculated in the model compound. $\Delta\Delta G_{\mathrm{back}}$ is the interaction of the titrating sites with the nontitrating charges q_j. The electrostatic repulsion between simultaneously protonated sites is given by Eq. (5):

$$\Omega_{\mu,\,\nu} = \sum_i [Q^p_{\mu,\,i} - Q^u_{\nu,\,i}][\phi^p_{\mathrm{DNA},\,j,\,\nu} - \phi^p_{\mathrm{DNA},\,j,\,\nu}]. \qquad (5)$$

$\Omega_{\mu,\,\nu}$ is the interaction of the titrating sites of DNA with each other and represents the fact that site μ is more difficult to protonate if site ν is already protonated. The pH at which $\theta_i = 0.5$ is defined as the pK_a of the site.

The finite repeat unit chosen for these calculations was the d(A-G)$_6$-d(T-C)$_6$-d(T-C)$_6$ dodecamer. The geometry of the triplex was generated from the x-ray diffraction structure of poly(dT)–poly(dA)–poly(dT) [27] by replacing alternate T–A–T triads with C–G–C$^+$ triads. Six equivalent sites of protonation, the N3 of the cytosines of the third strand, are available within this repeat unit so that 64 (2^6) protonation states are possible for the six sites. The fact that these are exactly repeated along the helical axis results in the approximation that the infinite number of protonation states possible is represented by the repeating of each of the 64 states. The calculation of the intrinsic pK_a, reflecting the tendency of a site to accept a proton when all other sites are neutral, cannot be exactly determined with this approach because protonating a single site in the repeat results in that site being protonated in each of its images. However, the repeat unit extends 39.36 Å making this image-site–central-site interaction energy small. We present a value for the intrinsic pK_a but note its approximate nature.

The 64 states include 6 singly protonated, 15 doubly protonated, 20 triply protonated, 15 with four of the six sites protonated, and 6 with five of the six sites protonated. In addition there is one state that is not protonated and one that is fully protonated. The summations in Eq. (1) are over these 64 states. Because the sites are equivalent, the extent of protonation of a single site is all that needs to be considered.

The site–site interaction term $W_{\mu,\nu}$ for an infinitely repeating polymer was determined using the nearest-neighbor (1, 2) and next-nearest (1, 3) interactions calculated using Eq. (5) based on the PB-determined electrostatic potentials. Recognizing that the PB calculation includes the effect of images of the central repeat, the PB-calculated effect of charging site 2 in the presence of a charge on site 1 (and its images) can be written as:

$$\Omega_{i,i+1} = \Omega_{1,2} = W_{1,2} = W_{1,2} + 2\sum_j W_{1,6j+1}. \quad (6)$$

Similarly, the next-nearest site–site interactions

$$\Omega_{i,i+2} = \Omega_{1,3} = W_{1,3} + 2\sum_j W_{1,6j+2}. \quad (7)$$

The indices on $\Omega_{\mu,\nu}$ range from 1 to 6 while the j subscript on $W_{1,j}$ can increase without bound. To calculate the remaining $\Omega_{\mu,\nu}$, we calculated the coulombic sums

$$\begin{aligned} W_{i,i+1}(n) &= 1/r_{i,i+1} + 2\sum_j^n 1/r_{1,6j+i+1} \\ W_{i,i+2}(n) &= 1/r_{i,i+2} + 2\sum_j^n 1/r_{1,6j+i+2} \\ &\vdots \\ W_{i,i+5}(n) &= 1/r_{i,i+5} + 2\sum_j^n 1/r_{i,6j+i+5}. \end{aligned} \quad (8)$$

The PB calculations were performed for a variety of conditions, leading to different calculated values of $\Omega_{1,2}$ and $\Omega_{1,3}$. For each PB calculation the ratio $\Omega_{1,2}/\Omega_{1,3} = x_{23}$ was determined. The coulomb sums were then truncated at n such that $W_{1,2}(n)/W_{1,3}(n) = x_{23}$. This value of n was then used to determine the ratios $x_{34} = W_{1,3}(n)/W_{1,4}(n)$, x_{45}, and x_{56}. Finally, we invoked the approximation $\Omega_{1,4} = \Omega_{1,3}/x_{34}$, $\Omega_{1,5} = \Omega_{1,4}/x_{45}$, and $\Omega_{1,6} = \Omega_{1,5}/x_{56}$.

Results and Conclusions

Poisson–Boltzmann calculations were performed using methods previously described [25]. The DNA and counterions were confined to a cylindrical cell of radius 100 Å corresponding to a nucleotide concentration of 40 mM. A concentration of 100 mM 1:1 monovalent salt was added to the DNA–counterion mixture resulting in 140 mM monovalent cations and 100 mM monovalent anions surrounding the central DNA molecule. Following Bashford and Karplus [14], PB calculations were done on the model compound (neutral and protonated) deoxycytidine, with the same grid used for the full DNA calculations. Several PB calculations were required for the central DNA. The fully unprotonated (i.e., the triplex had a charge of −36) calculation was done along with cytosine 1 protonated, cytosines 1 and 2 protonated, and cytosines 1 and 3 protonated. The doubly protonated calculations were required for the evaluation of $\Omega_{\mu,\nu}$ [Eq. (5)].

Calculations were performed assuming that the internal dielectric constant of DNA had a uniform value of 4 and that of the environment was 78.4. This gave a pK_a of 4.1 for the third-strand cytosine. Based on a pK_a of 4.3 for the model compound, incorporation of cytosine into the negative electrostatic potential environment of DNA would be expected to raise its pK_a by perhaps 2 units, as discussed earlier. The intrinsic pK_a [Eq. (2)] of 6.7 calculated for these conditions is not unreasonable, but this value is lowered to 4.1 by the site–site interactions. This result suggests that the internal DNA dielectric constant to be used in the calculation of $\Omega_{\mu,\nu}$ should be larger than the value of 4 used in the intrinsic-pK_a determination [17, 18].

A second set of calculations using an internal DNA dielectric constant of 10 yielded a pK_a of 8.7, a value high compared to experiment. The titration curves for protonation of the third-strand cytosine, calculated using Eq. (1) are shown in Figure 3. The intrinsic pK_a curve, assuming no site–site interactions, is shown along with the full titration curve to emphasize the role of those interactions, which shift the midpoint of the curve from 10.2 to 8.7. A third set of calculations with a DNA dielectric constant of 4 and a variable dielectric constant for the environment [23] was also done. The results of all these calculations are summarized in Table I.

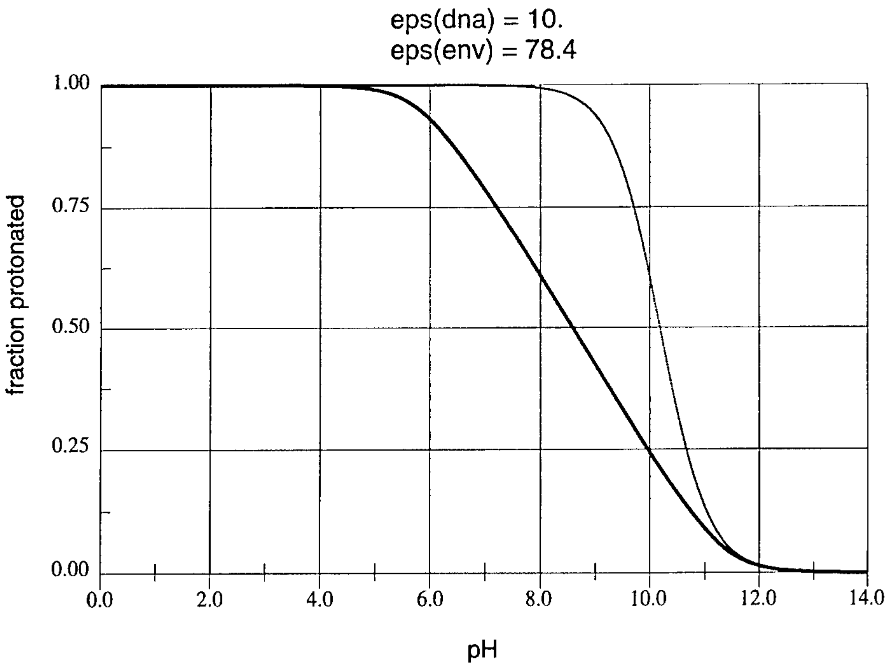

FIGURE 3. Proton titration curve for the N3 of cytosine on the third stand of triple-helical DNA. The internal dielectric constant for DNA was 10 and for the environment it was 78.4. The curve to the right represents the curve calculated assuming no site–site interaction.

Further insight into the free energy differences accompanying protonation of the third-strand cytosine can be gained by molecular orbital calculations. Using a geometry determined from an unconstrained optimization, we calculated the wave function for the C^+–G–C base triad within the PM3 approximation. Figure 4 shows the electrostatic potential in the regions surrounding each base. When the proton is removed and the electrostatic potential recalculated (without further optimization) a highly negative region appears at the position vacated by the proton, as indicated in Figure 5. (Additional optimization leads to a structure in which the exocyclic amine of the third-stand cytosine forms hydrogen bonds with both the guanine N7 and carbonyl oxygen.) This supports the suggestion of Lavelle and Fresco [8] that the presence of the proton is not primarily to stabilize the triplex by forming another hydrogen bond but rather to negate the strong electrostatic repulsion caused by overlapping of the lone-pair electrons on the guanine N7 and cytosine N3 atoms.

TABLE I
pK_a and intrinsic pK_a for the three dielectric constant combinations described in the text.

ϵ(DNA) / ϵ(env)	pK_a^{intrin}	pK_a
4./variable	14.23	10.00
10/78.4	10.18	8.70
4./78.4	6.73	4.05

Conclusions

The calculation of the pK_a shift of an ionizable site at the DNA surface can be accomplished with a fair degree of accuracy by calculating the electrostatic potential in the environment adjacent to the site of protonation [26]. The calculation of this potential is affected little by assumptions regarding the dielectric constant of the DNA interior. Sites such as the N3 of the third-strand cytosine, however, present a greater challenge. Buried within the DNA, the dielectric constant chosen for the polyion interior has a great influence on the calculated pK_a shift. The assumption that the dielectric constant of the interior of DNA can be represented by a single, isotropic, scalar quantity presents a further difficulty. At this stage it seems that the

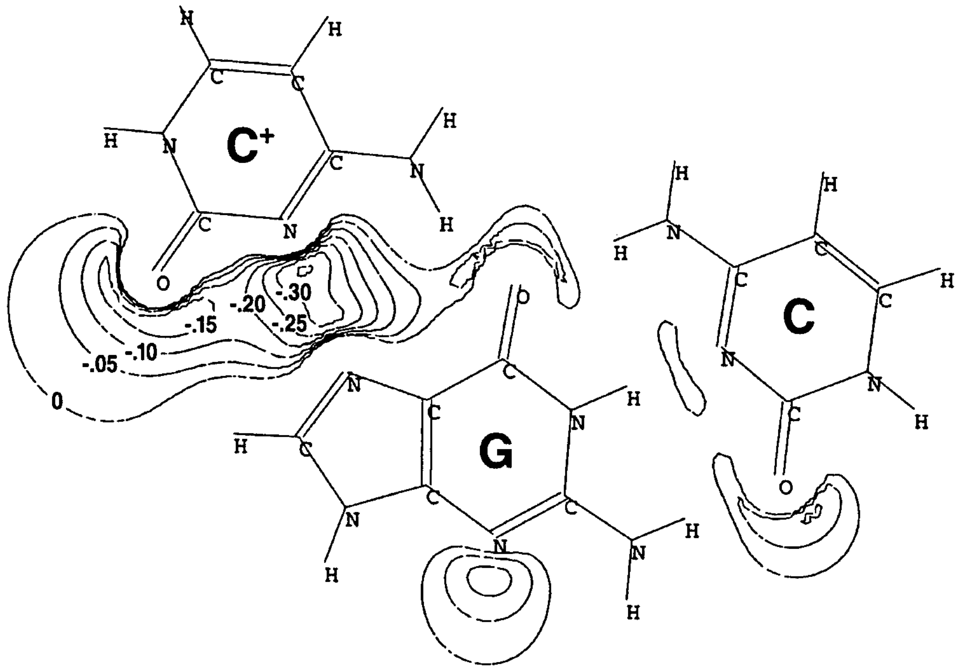
C+
G
C
-.30
-.25
-.20
-.15
-.10
-.05
0

FIGURE 4. Electrostatic potential map for the C$^+$–G–C triad calculated using the semiempirical molecular orbital PM3 method.

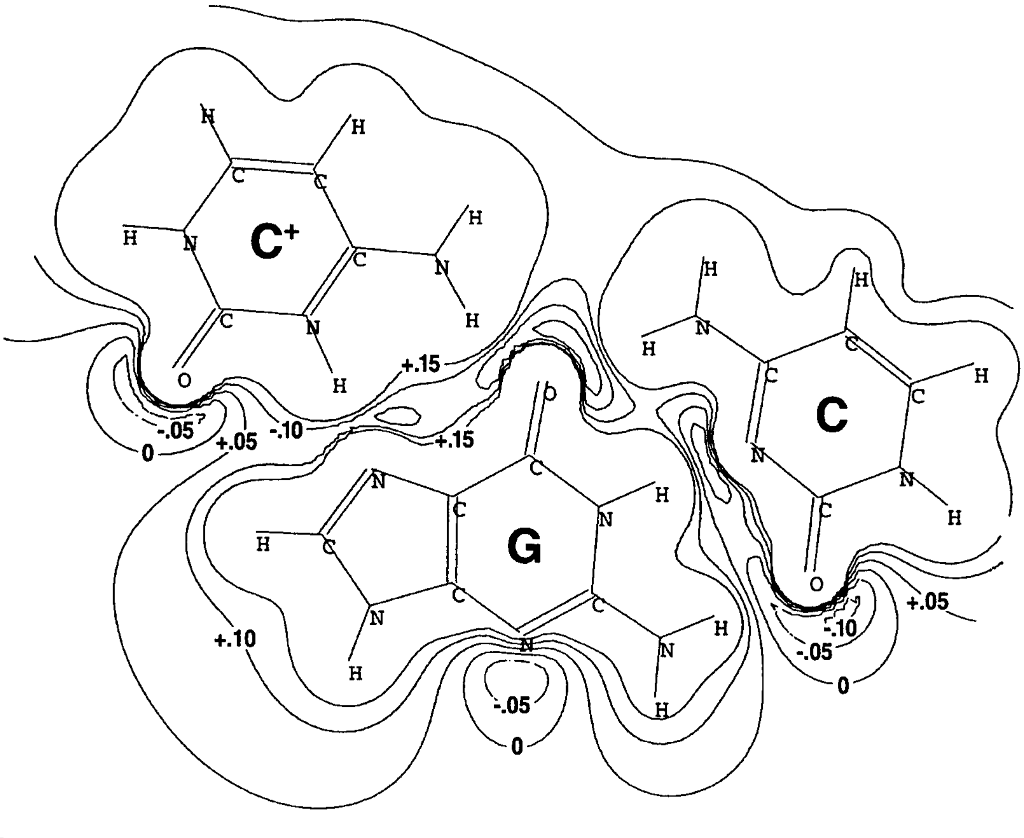
C+
G
C
+.15
+.15
+.05
-.10
-.05
0
+.10
-.05
0
+.05
-.10
-.05
0

FIGURE 5. Electrostatic potential map for the C–G–C neutral triad calculated using the semiempirical molecular orbital PM3 method. The geometry is that calculated for C$^+$–G–C.

accurate prediction of pK_a shifts within the interior of DNA awaits further developments.

ACKNOWLEDGMENTS

This work was supported in part by grant GM29079 from the National Institute of General Medical Sciences, NIH.

References

1. G. E. Plum, D. S. Pilch, S. F. Singleton, and K. J. Breslauer, Annu. Rev. Biphys. Biomol. Struct. **24**, 319 (1995).
2. S. Arnott and E. Selsing, J. Mol. Biol. **88**, 500 (1974).
3. P. O. P. T'so, *Basic Principles in Nucleic Acid Chemistry* (Academic, New York, 1974).
4. L. E. Xodo, G. Manzini, f. Quadrifoglio, G. A. van der Marel, and J. H. van Boom, *Nucl. Acids Res.* **19**, 5625 (1991).
5. P. L. Husler and H. H. Klump, *Arch. Biochem. Biophys.* **317**, 46 (1995).
6. D. E. Callahan, T. L. Trapane, P. S. Miller, P. O. P. T'so, and L.-S. Kan, *Biochemistry*, **30**, 1650 (1991).
7. S. F. Singleton and P. B. Dervan, *Biochemistry* **31**, 10995 (1992).
8. L. Lavelle and J. R. Fesco, Nucl. Acids. Res. **23**, 2692 (1995).
9. C. Tanford and J. G. Kirkwood, J. Am. Chem. Soc. **79**, 5333 (1957).
10. N. K. Rogers, G. R. Moore, and M. J. E. Sternberg, J. Mol. Biol. **182**, 613 (1985).
11. J. Warwicker and H. C. Watson, J. Mol. Biol. **157**, 671 (1982).
12. M. J. E. Sternberg, F. R. F. Hayes, A. J. Russell, P. G. Thomas, and A. R. Fersht, *Nature* **330**, 86 (1987).
13. M. K. Gilson and B. H. Honig, Proteins **3**, 32 (1988).
14. D. Bashford and M. Karplus, Biochemistry **29**, 10219 (1990).
15. H. Oberoi and N. M. Allewell, Biophys. J. **65**, 48 (1993).
16. R. V. Sampogna and B. Honig, Biophys. J. **66**, 1341 (1994).
17. A. Warshel, *Computer Modeling of Chemistry Reactions in Enzymes and Solutions* (Wiley-Interscience, New York, 1991).
18. A. Warshel and J. Aqvist, Annu. Rev. Biophys. Biophys. Chem. **20**, 267 (1991).
19. E. Demchuk and R. C. Wade, J. Phys. Chem. **100**, 17373 (1996).
20. J. Antosiewicz, J. A. McCammon, and M. K. Gilson, J. Mol. Biol. **238**, 415 (1994).
21. M. Schaefer, M. Sommer, and M. Karplus, J. Phys. Chem. B **101**, 1663 (1997).
22. L. Yang, S. Weerasinghe, P. E. Smith, and B. M. Pettitt, Biophys. J. **69**, 1519 (1995).
23. G. Lamm and G. R. Pack, J. Phys. Chem. B. **101**, 959 (1997).
24. G. Lamm and G. R. Pack, Proc. Natl. Acad. Sci. USA **87**, 9033 (1990).
25. G. R. Pack, G. A. Garrett, L. Wong, and G. Lamm, Biophys. J. **65**, 1363 (1993).
26. S. Hanlon, L. Wong, and G. R. Pack, Biophys. J. **72**, 291 (1997).
27. S. Arnott, P. J. Bond, E. Selsing, and P. J. Smith, Nucl. Acids Res. **3**, 2459 (1976).

Parametric Transform and Moment Indices in the Molecular Dynamics of *n*-Alkanes

STEPHEN P. MOLNAR,[1] JAMES W. KING[2]
[1]*Foundation for Chemistry, 1945 Elmwood Avenue, Upper Arlington, Ohio 43212*
[2]*Foundation for Chemistry, P. O. Box 116, Balsam, North Carolina 28707*

Received 20 February 1998; accepted 16 March 1998

ABSTRACT: The integrated molecular transform (FT_m) is a unitary numerical index of structure that is capable of uniquely representing different molecular structure conformations with the exception of enantiomers. Other molecular indices have been derived from FT_m as well as from the normalized molecular moment (M_n), for example, the analogous electronic and charge transforms (FT_e and FT_c) and moments (M_e and M_c). In this study, each of these indices was calculated for up to 10 sampled conformations of each of the C_1–C_{10} normal alkanes as they were subjected to a standard annealing process. Statistical analyses of the resulting data in the individual series and subsequent box plots, permitting facile examination of those results, indicated that the respective transform indices (FT_m, FT_e, FT_c) are unique, that is, with no statistically significantly overlap across the series. For the M_n and M_e indices, the numerical values for methane overlapped those of ethane in the first instance and both ethane and propane in the second. The M_c index values overlapped in several instances in the series. Inasmuch as the noted molecular indices are based only on parameters of structural origin, these results have profound implications for the correlation and estimation of properties derived not only from a general structure representation, but also for those properties which may be dependent on specific molecular conformations. This includes the potential for indices of molecular flexibility and conformationally dependent atomic electron densities. © 1998 John Wiley & Sons, Inc. Int J Quant Chem 70: 1185–1194, 1998

Introduction

The integrated molecular transform (FT_m) and normalized molecular moment (M_n) indices and their analogous electronic and charge indices are unitary numerical surrogates of either optimized (at any level) or nonoptimized structures. The indices are derived from considerations based solely on structure parameters, that is, bond distances, interatomic distances, atomic number, atomic weight, and/or quantum mechanical calculations. In the most literal sense, the indices are the result of mapping down processes that convert a

Correspondence to: J. W. King.

International Journal of Quantum Chemistry, Vol. 70, 1185–1194 (1998)
© 1998 John Wiley & Sons, Inc.
CCC 0020-7608 / 98 / 061185-10

descriptorially multivariate entity, the molecule, into a single number, and with each index, a specific feature of the molecule may be emphasized. Inasmuch as the indices have been precisely defined in a recent publication [1], their origins will not be further reviewed herein.

In general, the application of the various indices has been to correlate the structure with the chemical, physical, and pharmacological properties with a view toward extrapolation or interpolation capabilities [1–12]. However, their versatility permits an emphasis on specific molecular aspects as well, for example, only the structure (FT_m and M_n), or, if desired, the electronic (FT_e and M_e) or charge nature (FT_c and M_c) of molecules or a combination of the indices in a multivariate correlation equation. Thus, any molecular attribute may be incorporated by mathematical representation in one of the indices.

One of the concepts resulting from the existence of the unitary indices is that a measure of molecular similarity is permitted by a comparison of ratios or, perhaps, other mathematical formulations of the respective indices [5, 12]. But also of importance is the fact that, with the exception of enantiomers, the indices have been shown to uniquely represent conformers [9]. In that study, different conformations of ethane, toluene, and biphenyl were shown to be uniquely represented by the integrated molecular transform (FT_m). With such a result in hand, it seemed prudent to attempt a more general demonstration of this index capability and extend it to the corollary indices noted above. That, then, was the objective of the work reported herein. In this context, each of the C_1–C_{10} alkanes was subjected to an annealing process and up to 10 conformations sampled. The structure indices were then calculated for each conformer and a statistical comparison of the results depicted by box plots of the data.

Methodology and Results

The initial alkane structures were entered into the Chem3D Pro molecular mechanics program [13]. The molecular dynamics subset of this program provided the annealing process for each of the 10 alkanes to give conformational continuums. Each continuum was then randomly sampled to give nine or ten conformations which yielded the interatomic distances needed for calculation of the FT_m and M_n indices. The single-point energies were then calculated for each conformer by the GAMESS program (operating in the MOPAC mode with the AM1 Hamiltonian [14]) to give the necessary electron densities for calculation of FT_e and M_e and charge distributions for calculation of FT_c and M_c. The transform and moment indices were then calculated by previously described methods*; these are shown in Table I. The resulting indices for each conformer series were then statistically examined with the SCAN program [15] to give the summary data shown in Table II. The box plots shown in Figures 1–6 were generated with Sigma Plot [16].

CHARACTERISTICS OF BOX PLOTS

For ease of interpretation of the box plots, it should be noted that the width of the box is arbitrary and has no meaning in respect to the plotted data. The top and bottom limits of the box are the 75th and 25th percentiles of the data, respectively, while the data median is noted by the horizontal line across the center of the box. The line crossing the "T" on the top of the box shows the 95% confidence limit of the data; the inverted "T" on the bottom of the box represents the 5% confidence limit.

Discussion

The previous study of numerical conformer representation proved that conformers may be uniquely represented by their integrated molecular transform (FT_m) [1]. However, the question can be posed as to whether there might be some numerical overlap in a more regular compound series, such as alkanes, differing by only a methylene group. Further, the application of the integrated electronic (FT_e) and charge (FT_c) indices, the normalized molecular moment (M_n), and its analogous electronic (M_e) and charge moments (M_c) to conformational representation, had not been demonstrated.

The results of this study are best seen by a perusal of the figures. In Figure 1, the most unusual aspect is the slightly lower displacement of the methane conformer group as compared to the other groups. It is not difficult to account for this inasmuch as there appears to be a linear relation-

---

*See [1] and citations therein.

TABLE I

Calculated indices for C_1–C_{10} normal alkanes (see text for an explanation of column headings).

Carbons	FT_m	FT_e	FT_c	M_n	M_e	M_c
C1	6.987576	4.579256	0.024590	0.810334	1.124986	0.428260
C1	6.712426	4.390923	0.023975	0.935001	1.125000	0.392177
C1	6.578948	4.297664	0.024565	0.935001	1.125000	0.399510
C1	6.458280	4.222586	0.023499	0.748001	0.874989	0.465629
C1	6.210833	4.050942	0.022874	0.872668	0.999988	0.415565
C1	6.421484	4.197506	0.023717	0.623334	1.000013	0.498238
C1	6.173242	4.023162	0.022598	0.498667	0.750000	0.530247
C1	6.513076	4.255519	0.024212	0.872668	1.125000	0.411798
C1	6.147553	4.011489	0.023019	0.685668	0.750000	0.495021
C1	6.290279	4.104471	0.022979	0.748001	0.999988	0.424484
C2	41.179925	24.746405	0.057962	0.798147	0.857143	0.336114
C2	41.047766	24.656884	0.057628	0.798147	0.857143	0.337408
C2	41.096322	24.707458	0.057960	0.798147	0.857143	0.334909
C2	41.196547	24.758945	0.057378	0.798147	0.857137	0.334263
C2	41.291619	24.768512	0.057351	0.798147	0.857143	0.340662
C2	40.614203	24.365527	0.056042	0.764891	0.857143	0.339907
C2	40.465850	24.285497	0.056734	0.798147	0.857137	0.340457
C2	41.404900	24.811028	0.056462	0.764891	0.857137	0.341087
C2	40.239286	24.168651	0.057318	0.798147	0.857143	0.339892
C2	41.119917	24.718319	0.058000	0.764891	0.857143	0.335669
C3	61.730045	35.366721	0.073667	1.065844	1.050000	0.439550
C3	61.583751	35.281740	0.074173	1.065844	1.050000	0.441290
C3	61.509062	35.254482	0.073042	1.043166	1.049995	0.439138
C3	61.942748	35.432699	0.073217	1.020489	1.050000	0.434095
C3	60.412583	34.717018	0.074872	1.065844	1.049990	0.449778
C3	62.748389	35.919357	0.073979	1.020489	1.049995	0.437397
C3	62.052411	35.487362	0.070601	1.088521	1.050000	0.438612
C3	62.015678	35.468971	0.074696	1.020489	1.000000	0.443057
C3	61.930000	35.284296	0.070664	1.043166	1.000005	0.432263
C3	59.822879	34.274096	0.073421	1.065844	1.050005	0.454840
C4	79.241786	44.492780	0.092804	1.376382	1.461561	0.498671
C4	78.494188	44.057310	0.091857	1.376382	1.461533	0.499229
C4	79.409604	44.548020	0.093429	1.359177	1.461550	0.498600
C4	77.188174	43.300959	0.091158	1.376382	1.461533	0.496246
C4	78.901902	44.267885	0.094077	1.359177	1.423071	0.502933
C4	78.251678	43.921354	0.090537	1.359177	1.461533	0.504800
C4	77.297306	43.358956	0.088922	1.359177	1.461533	0.503471
C4	76.735552	43.077931	0.088287	1.393587	1.461527	0.494185
C4	77.007562	43.161377	0.086065	1.376382	1.461527	0.486074
C4	77.637438	43.435717	0.092562	1.359177	1.423077	0.506593
C5	92.856293	51.446007	0.109185	1.593895	1.625010	0.558995
C5	92.930752	51.405263	0.106200	1.607755	1.625000	0.560091
C5	93.120414	51.538966	0.106176	1.607755	1.593740	0.568756
C5	92.914801	51.512217	0.110178	1.593895	1.656250	0.545212
C5	93.569230	51.788255	0.107119	1.593895	1.593750	0.566034
C5	91.997341	50.835562	0.102806	1.621615	1.656255	0.556445
C5	93.675362	51.862599	0.105841	1.593895	1.593745	0.556779
C5	90.718127	50.260480	0.108838	1.635475	1.656250	0.573272
C5	92.203865	51.060317	0.104319	1.607755	1.624995	0.547331
C5	90.992395	50.251630	0.099873	1.663195	1.625000	0.585893

(Continued)

TABLE I
(Continued).

Carbons	FT_m	FT_e	FT_c	M_n	M_e	M_c
C6	111.808612	61.709386	0.128761	1.879848	1.894727	0.593127
C6	110.495134	60.809936	0.122568	1.891452	1.921053	0.606570
C6	109.231913	60.246225	0.126034	1.914660	1.894732	0.598337
C6	108.588437	60.239320	0.127193	1.984284	1.947368	0.598246
C6	111.569415	61.740502	0.118918	1.903056	1.868426	0.609694
C6	109.237809	60.094957	0.119726	1.926264	1.894732	0.552992
C6	112.687464	61.918144	0.117628	1.845036	1.789474	0.628347
C6	111.881502	61.679248	0.117797	1.891452	1.842110	0.630124
C6	109.855346	60.412243	0.118532	1.879848	1.842105	0.583331
C7	127.835993	70.024476	0.145468	2.215480	2.090909	0.612861
C7	127.201751	69.660087	0.142529	2.185541	2.136349	0.625831
C7	127.993452	70.097949	0.143057	2.155602	2.091384	0.641087
C7	129.428918	70.853597	0.141977	2.135642	2.136364	0.646357
C7	127.633380	69.857448	0.138810	2.165581	2.068182	0.622345
C7	125.677923	68.741534	0.137854	2.155602	2.090919	0.610405
C7	122.874897	67.052826	0.142038	2.155602	2.136359	0.618217
C7	46.974974	24.615089	0.086652	4.141550	4.227273	1.208002
C7	127.022915	69.493979	0.137449	2.145622	2.181808	0.650266
C7	127.061895	69.649755	0.138369	2.175561	2.113636	0.646219
C8	149.080229	81.497520	0.165194	2.363633	2.439995	0.651653
C8	149.613119	81.806698	0.164695	2.407404	2.420000	0.662258
C8	149.735516	81.845108	0.163517	2.389896	2.439995	0.660822
C8	148.852683	81.309880	0.162809	2.398650	2.440000	0.674522
C8	148.508235	81.056824	0.159152	2.389896	2.440005	0.673042
C8	147.340604	80.509246	0.160919	2.407404	2.440005	0.649816
C8	146.021563	79.811669	0.161177	2.424913	2.420005	0.636731
C8	143.321614	78.244635	0.158898	2.389896	2.419995	0.615587
C8	142.850651	77.994129	0.161490	2.381142	2.359995	0.631566
C8	145.980078	79.584763	0.156405	2.424913	2.419981	0.627274
C9	171.063920	93.322880	0.184141	2.736676	2.625000	0.644124
C9	171.351757	93.438945	0.183369	2.728879	2.660710	0.650103
C9	169.148191	92.130596	0.181065	2.760066	2.785714	0.655126
C9	170.326638	92.865610	0.181896	2.697692	2.678581	0.675747
C9	170.302665	92.800450	0.177425	2.721082	2.714291	0.686287
C9	170.352554	92.947907	0.181377	2.697692	2.696424	0.701479
C9	170.100057	92.730363	0.180439	2.752269	2.696424	0.672828
C9	170.100057	92.730363	0.180439	2.752269	2.696424	0.672828
C9	165.154138	89.781148	0.171287	2.619724	2.607138	0.624933
C9	164.730054	89.728341	0.177340	2.565146	2.535719	0.651846
C10	192.191653	104.606044	0.203915	3.001026	2.967747	0.670474
C10	192.191653	104.606044	0.203915	3.001026	2.967747	0.670474
C10	192.261743	104.551337	0.200315	3.022110	3.032243	0.686215
C10	189.540819	103.000049	0.198518	3.029138	2.983866	0.705895
C10	189.303787	102.864455	0.196671	3.029138	2.983866	0.711553
C10	191.010092	103.860264	0.197011	2.979941	2.935489	0.705731
C10	192.270043	104.492034	0.199814	3.015082	2.967742	0.666907
C10	187.802697	101.936861	0.194529	3.029138	3.032258	0.646869
C10	188.894104	102.551026	0.195955	3.008054	2.983876	0.633660
C10	186.937441	101.260288	0.189922	2.902632	2.854830	0.672898

TABLE II

Statistical aspects of the calculated molecular indices of the C_1–C_{10} normal alkanes.

	C1	C2	C3	C4	C5	C6	C7	C8	C9	C10
FT_m										
Mean	6.449370	40.965634	61.574755	78.016519	92.497858	110.595070	126.970125	147.130429	169.263003	190.240403
StDev	0.264600	0.386862	0.850479	0.972701	1.010085	1.446511	1.829892	2.517430	2.353495	2.012284
StError	0.083674	0.122337	0.268945	0.307595	0.319417	0.482170	0.609964	0.796081	0.744240	0.636340
95% Conf	0.189288	0.276751	0.608409	0.695844	0.722588	1.111912	1.406611	1.800901	1.683626	1.439533
99% Conf	0.271951	0.397610	0.874107	0.999725	1.038147	1.618017	2.046852	2.587369	2.418879	2.068189
n	10	10	10	10	10	9	10	10	10	10
Min	6.147553	40.239286	59.822879	76.735552	90.718127	108.588437	122.874897	142.850651	164.730054	186.937441
Max	6.987576	41.404900	62.748389	79.409604	93.675362	112.687464	129.428918	149.735516	171.351757	192.270043
FT_e										
Mean	4.213352	24.598723	35.248674	43.762229	51.196130	60.983329	69.492406	80.366047	92.247660	103.372840
StDev	0.179441	0.232939	0.451906	0.560808	0.580650	0.766562	1.072620	1.413269	1.360694	1.225576
StError	0.056744	0.073662	0.142905	0.177343	0.183618	0.255521	0.357540	0.446915	0.430289	0.387561
95% Conf	0.128368	0.166638	0.323282	0.401187	0.415381	0.589245	0.824507	1.011014	0.973404	0.876744
99% Conf	0.184427	0.239410	0.464461	0.576388	0.596782	0.857449	1.199795	1.452532	1.398497	1.259625
n	10	10	10	10	10	9	9	10	10	10
Min	4.011489	24.168651	34.274096	43.077931	50.251630	60.094957	67.052826	77.994129	89.728341	101.260288
Max	4.579256	24.811028	35.919357	44.548020	51.862599	61.918144	70.853597	81.845108	93.438945	104.606044
FT_c										
Mean	0.023603	0.057284	0.073233	0.090970	0.106054	0.121906	0.140839	0.161426	0.179878	0.198057
StDev	0.000723	0.000674	0.001493	0.002540	0.003119	0.004369	0.002796	0.002754	0.003727	0.004257
StError	0.000229	0.000213	0.000472	0.000803	0.000986	0.001456	0.000932	0.000871	0.001178	0.001346
95% Conf	0.000517	0.000482	0.001068	0.001817	0.002231	0.003358	0.002150	0.001970	0.002666	0.003045
99% Conf	0.000743	0.000692	0.001534	0.002610	0.003205	0.004886	0.003128	0.002831	0.003830	0.004375
n	10	10	10	10	10	9	9	10	10	10
Min	0.022598	0.056042	0.070601	0.086065	0.099873	0.117628	0.137449	0.156405	0.171287	0.189922
Max	0.024590	0.058000	0.074872	0.094077	0.110178	0.128761	0.145468	0.165194	0.184141	0.203915
M_n										
Mean	0.772934	0.788170	1.049970	1.369500	1.611913	1.901767	2.165581	2.397775	2.703150	3.001729
StDev	0.141533	0.016064	0.024023	0.012030	0.022680	0.038680	0.023931	0.019113	0.063453	0.038273
StError	0.044757	0.005080	0.007597	0.003804	0.007172	0.012893	0.007977	0.006044	0.020066	0.012103
95% Conf	0.101249	0.011492	0.017186	0.008606	0.016225	0.029733	0.018395	0.013673	0.045393	0.027379
99% Conf	0.145465	0.016510	0.024691	0.012364	0.023310	0.043266	0.026768	0.019644	0.065216	0.039336
n	10	10	10	10	10	9	9	10	10	10

(Continued)

TABLE II
(Continued).

	C1	C2	C3	C4	C5	C6	C7	C8	C9	C10
Min	0.498667	0.764891	1.020489	1.359177	1.593895	1.845036	2.135642	2.363633	2.565146	2.902632
Max	0.935001	0.798147	1.088521	1.393587	1.663195	1.984284	2.215480	2.424913	2.760066	3.029138
M_e										
Mean	0.987496	0.857141	1.039999	1.453845	1.625000	1.877192	2.116212	2.423998	2.669643	2.970966
StDev	0.149652	0.000003	0.021080	0.016217	0.025518	0.047440	0.034875	0.024587	0.067997	0.050319
StError	0.047324	0.000001	0.006666	0.005128	0.008070	0.015813	0.011625	0.007775	0.021503	0.015912
95% Conf	0.107057	0.000002	0.015080	0.011602	0.018255	0.036466	0.026808	0.017589	0.048643	0.035997
99% Conf	0.153809	0.000003	0.021666	0.016668	0.026227	0.053065	0.039010	0.025270	0.069886	0.051717
n	10	10	10	10	10	9	9	10	10	10
Min	0.750000	0.857137	1.000000	1.423071	1.593740	1.789474	2.068182	2.359995	2.535719	2.854830
Max	1.125000	0.857143	1.050005	1.461561	1.656255	1.947368	2.181808	2.440005	2.785714	3.032258
M_c										
Mean	0.446087	0.338037	0.441002	0.499080	0.561881	0.600085	0.630399	0.648327	0.663530	0.677068
StDev	0.047788	0.002640	0.006841	0.006008	0.012145	0.023422	0.015634	0.019975	0.022445	0.025667
StError	0.015112	0.000835	0.002163	0.001900	0.003841	0.007807	0.005211	0.006317	0.007098	0.008117
95% Conf	0.034186	0.001888	0.004894	0.004298	0.008688	0.018004	0.012018	0.014290	0.016056	0.018362
99% Conf	0.049115	0.002713	0.007031	0.006175	0.012482	0.026199	0.017487	0.020530	0.023068	0.026380
n	10	10	10	10	10	9	9	10	10	10
Min	0.392117	0.334263	0.432263	0.486074	0.545212	0.552992	0.610405	0.615587	0.624933	0.633660
Max	0.530247	0.341087	0.454840	0.506593	0.585893	0.630124	0.650266	0.674522	0.701479	0.711553

StDev, standard deviation; StError, standard error; 95% Conf and 99% Conf, 95% confidence level and 99% confidence level, respectively.

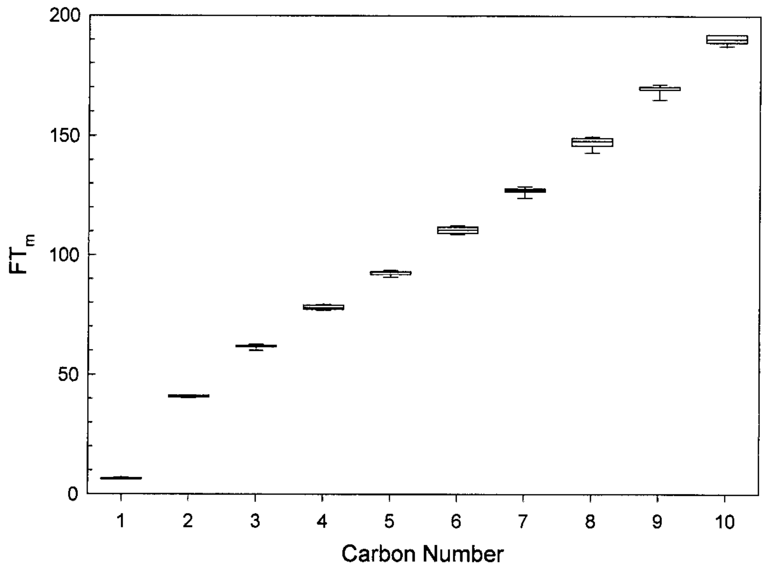

FIGURE 1. FT_m versus carbon number.

ship between the other groups consistent with the general characteristic of larger FT_m values as molecular weight increases. For methane, it may be that there is not enough structural variation in its conformers in respect to those of the C_2–C_{10} alkanes. But, more importantly, there is no overlap of index values in the series. The same comments may be noted for the FT_e indices plotted in Figure 2. In Figure 3, the displacement from strict linearity of the FT_c index of the methane conformers with respect to the remainder of the series appears to be less than for the previously noted indices; this may be due in part to the somewhat artificial consideration of the alkanes as charged species. Again, there are no overlaps of index values.

Figure 4 is a plot of M_n for the series. In this case, the behavior of methane in respect to the other hydrocarbons is unusual. Inasmuch as there

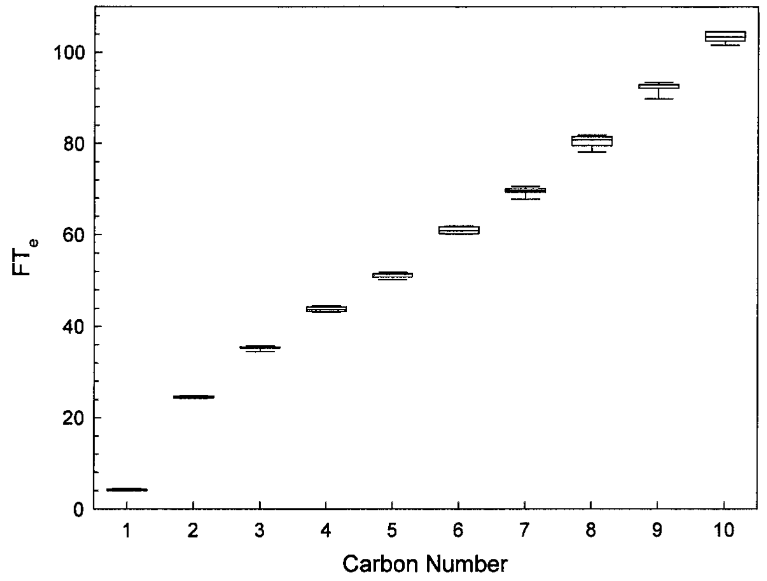

FIGURE 2. FT_e versus carbon number.

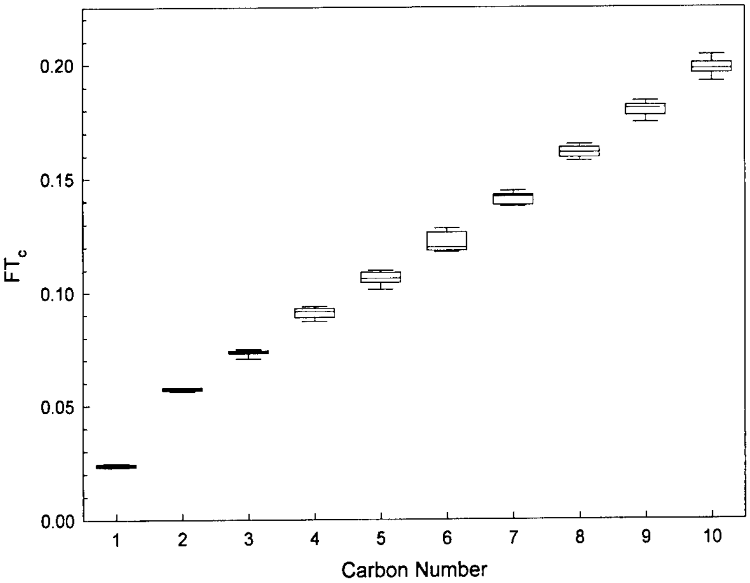

FIGURE 3. FT_c versus carbon number.

can be only limited structural variation in this molecule as it is subjected to an annealing process, an explanation of the wide index range, as reflected by the vertical dimensions of the box, remains obscure. This is true also for the M_c index plotted in Figure 5. Figure 6 is the plot of M_c for the series and is the most unusual of all, with methane again having the most variant behavior. But the appearance of the plots for the C_5–C_{10} alkanes also defies explanation other than, as noted for the FT_c data, to consider that a general representation of the alkanes as charged species is not appropriate.

Perhaps the most interesting aspect of the box plots are that, for each alkane, they give a visual indication of the variation in the index range. For instance, in Figure 1, one could surmise that the C_4, C_6, C_8, and C_{10} alkanes, by virtue of their greater index ranges as compared to the rest of the series, are more flexible than are the compounds

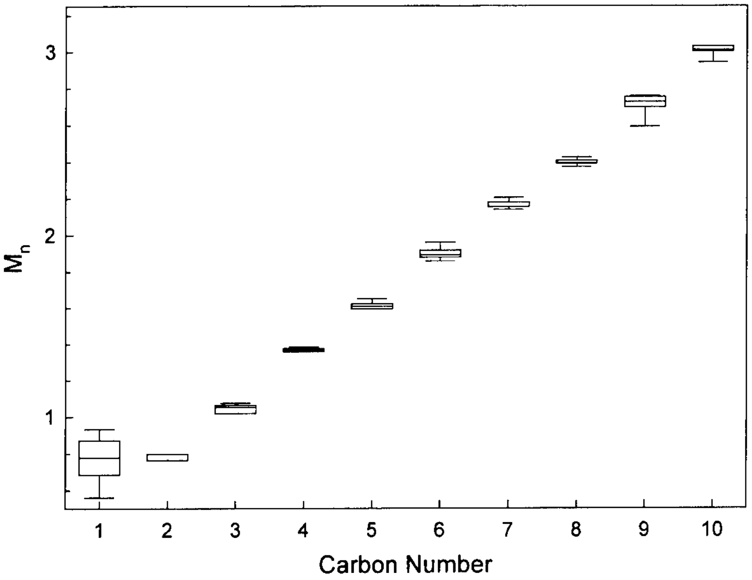

FIGURE 4. M_n versus carbon number.

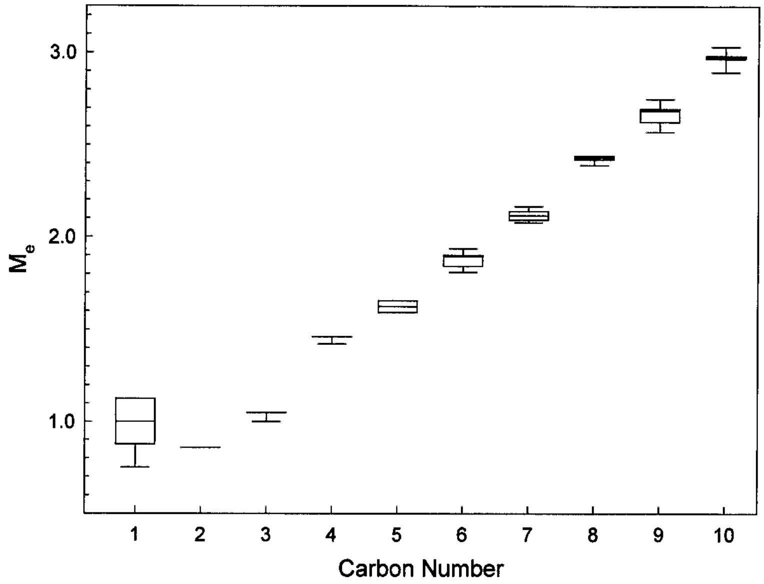

FIGURE 5. M_e versus carbon number.

with an odd number of carbon atoms. In Figure 4, the reverse appears to be the case, that is, compounds with an odd number of carbon atoms generally appear to have the wider index range. While this introduces a degree of dichotomy, inasmuch as these two indices (FT_m and M_n, respectively) are really structure indices in a strict sense, such generalizations may really be indicative of experimental behavior, with the FT_m index, because of the nature of its derivation, being the most reliable. The FT_e index of Figure 2 appears to follow the pattern of Figure 1 and thus would be confirmatory. The M_e index of Figure 5 is less consistent in its pattern than its M_n counterpart, and as it reflects the electronic nature of the molecules, probably no pattern should be presumed. For the respective charge indices shown in Figures 3 (FT_c) and 6 (M_c), no clear pattern emerges except for a tendency toward a nonlinear relationship between the compounds and this again

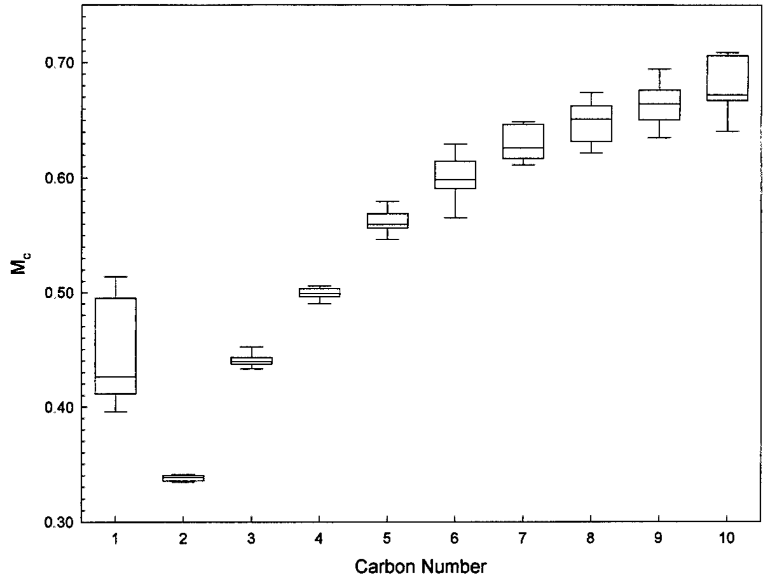

FIGURE 6. M_c versus cargon number.

suggests that these alkanes may not be well represented as charged species or that the energy relationships in the series may not be adequately reflected in the present calculations. One must also consider that the transform indices distance parameters are interatomic while the moment distances are from each atom to the geometric center of the molecule. The molecular representational quality of this difference in conformer depiction remains to be established.

Conclusions

This study has shown that conformers of each normal alkane in the C_1–C_{10} series may be uniquely numerically represented by the integrated molecular transform (FT_m). Similarly, the integrated electronic and charge transforms (FT_e and FT_c, respectively) uniquely interpret those aspects across the series, that is, there are no numerical overlaps of index values, although the specific methane conformer values in each case prevent a strict linear relationship in the series. For the normalized molecular moment (M_n) and the normalized electronic moment (M_e), methane is an outlier whose numerical values overlap those of ethane in the first instance and both ethane and propane in the second. In the case of the normalized charge moment (M_c), the extreme range of values for each alkane results in several overlaps between the respective compounds, suggesting that this particular index is not suitable for this series.

The box plots of the data in this study visually articulate the respective index values for the compounds. The variation in the range of such data for each alkane may be an indicator of conformational flexibility in the case of the FT_m and M_n indices. Similar considerations for the electronic indices (FT_e and M_e) may give an indication of the dependence of atomic electron density on structural variation. Work continues to effect a numerical definition of these considerations.

ACKNOWLEDGMENTS

The authors gratefully acknowledge the unqualified support and continuous encouragement of Mrs. Susan Molnar and Mrs. Mary Frances King and of the Master, who made the concepts, insight, and support possible.

References

1. S. P. Molnar and J. W. King, Int. J. Quantum Chem. **65,** 1047–1056 (1997).
2. J. W. King, R. J. Kassel, and B. B. King, Int. J. Quantum Chem., Quant. Biol. Symp. **17,** 27 (1990).
3. G. R. Famini, R. J. Kassel, J. W. King, and L. Y. Wilson, Quantitative Struct.-Act. Relat. **10,** 344 (1991).
4. J. W. King and R. J. Kassel, Int. J. Quantum Chem., Quantum Biol. Symp. **18,** 289 (1991).
5. J. W. King, Int. J. Quantum Chem., Quantum Biol. Symp. **20,** 139 (1993).
6. J. W. King, Int. J. Quantum Chem., Quantum Biol. Symp. **21,** 209 (1994).
7. S. P. Molnar and J. W. King, Int. J. Quantum Chem., Quantum Biol. Symp. **22,** 201 (1995).
8. S. P. Molnar and J. W. King, Int. J. Quantum Chem., Quantum Biol. Symp. **23,** 1845 (1996).
9. J. W. King and S. P. Molnar, J. Mol. Struct. (Theochem) 181 (1996).
10. J. W. King and S. P. Molnar, Int. J. Quantum Chem. **64,** 635 (1997).
11. S. P. Molnar and J. W. King, Int. J. Quantum Chem. **69,** 49 (1998).
12. J. W. King and S. P. Molnar, Paper presented at the *2nd National Chemical Information Symposium,* Charleston, SC, July 14–18, 1996.
13. *ChemDraw Pro* and *Chem3D Pro* are copyrighted (1995) products (CambridgeSoft Corp., 875 Massachusetts Ave., Cambridge, MA 02139).
14. M. W. Schmidt, K. K. Baldridge, J. A. Boatz, S. T. Elbert, M. S. Gordon, J. H. Jensen, S. Koseki, N. Matsunaga, K. A. Nguyen, S. Su, T. L. Windus, M. Dupuis, and J. A. Montgomery, Jr., J. Comp. Chem. **14,** 1347 (1993).
15. *SCAN Software for Chemometric Analysis, Reference Manual, Release 1* (Minitab, Inc., 3081 Enterprise Drive, State College, PA 16801-3008, 1995).
16. *SigmaPlot, v. 4.01* (SPSS, Inc., 444 N. Michigan Avenue, Chicago, IL 60611, 1997).

Theoretical Approach to the Pharmacophoric Pattern of $GABA_B$ Analogs

M. L. LORENZINI,[1] L. BRUNO-BLANCH,[1] G. L. ESTIÚ[2]

[1] *Química Medicinal, División Farmacia, Facultad de Ciencias Exactas, Universidad Nacional de La Plata, Casilla de Correo 243-1900—La Plata, Argentina*

[2] *Cequinor, Departamento de Química, Facultad de Ciencias Exactas, Universidad Nacional de La Plata, Casilla de Correo 962-1900—La Plata, Argentina*

Received 26 February; revised 6 May 1998; accepted 11 May 1998

ABSTRACT: In order to determine the structural requirements that are important for $GABA_B$ binding affinity, a quantum-chemical-based conformational study has been performed, followed by a similarity analysis which includes 12 $GABA_B$ analogs. Due to the flexibility of the structures, a semigrid $GABA_B$ analog [2RS-(5,5-dimethyl) morpholinyl-acetic acid] has been used as a template for the amonium moiety in order to help to identify the active conformation. Both *in vacuo*, and solvent-simulated calculations, for the physiological media modeled as water molecules, have been compared, for this analog, at ab initio (G94, 6-31 + G(d,p)) and semiempirical (PM3) levels, respectively. On the basis of this comparison, the results of *in vacuo* PM3 calculations have been chosen for the similarity analysis. We have included, in the calculations, a group of molecules heterogeneous enough to become representative of the different families that can bind to the $GABA_B$ receptor site. Following their comparison we report the leading characteristics that can be related to their binding capability and define a pharmacophoric pattern for $GABA_B$ analogs. The latter is compared with the one previously found for the binding affinity at the $GABA_A$ receptor site. © 1998 John Wiley & Sons, Inc. Int J Quant Chem 70: 1195–1208, 1998

Key words: $GABA_B$ analogs; pharmacophoric pattern; molecular similarity; quantum chemical calculations.

Correspondence to: G. L. Estiú.

Contract grant sponsors: CONICET; COFARQUIL; Colegio de Farmaceúticos de la Provincia de Buenos Aires.

International Journal of Quantum Chemistry, Vol. 70, 1195–1208 (1998)

© 1998 John Wiley & Sons, Inc.

CCC 0020-7608 / 98 / 061195-14

Introduction

Inhibition and excitation in the central nervous system (CNS) are mainly controlled by either γ-aminobutyric acid (GABA) or L-glutamate neurotransmitters. GABA, like other neurotransmitters, including L-glutamate, serotonin, and acetylcholine, activates both ionotropic ($GABA_A$) and metabotropic ($GABA_B$) receptors [1–4]. Whereas the $GABA_A$ receptor was cloned a decade ago, success in cloning the $GABA_B$ receptor is more recent (1997) [1, 5]. The ionotropic $GABA_A$ receptors are ligand-gated ion channels that produce fast synaptic transmission. Metabotropic $GABA_B$ receptors, on the other hand, couple to G proteins (guanine-nucleotide-binding proteins) and produce several divergent effects through intracellular effector systems: opening of adjacent potassium channels, closure of voltage-gated calcium channels, and inhibition of the enzyme adenylyl cyclase [2, 5]. The effects of stimulating $GABA_B$ receptors are, thus, slower and lead to a more prolonged postsynaptic inhibition, associated with some types of learning and memory.

Baclofen, a $GABA_B$ agonist, was introduced in the market in 1972 and mainly used for its therapeutic potential in several respiratory diseases, such as asthma [2, 3]. Since then, analogs of baclofen, saturated and unsaturated, have been synthesized and tested for $GABA_B$ receptor affinity [6–9]. The phosphonic and sulfonic analogs (phaclofen and saclofen, respectively), as well as the 2-hydroxy derivative of the latter [10, 11], have been shown to be antagonists at the $GABA_B$ receptor and used as neuroprotective drugs [2] to treat spasticity, absence epilepsy, anxiety, depression, and cognition deficits, as well as the respiratory depression caused by excessive doses of $GABA_B$ agonists [1]. Antidepressant properties have also became apparent for $GABA_B$ agonists [1, 3, 4]. In this framework, the conformational analysis of several baclofen analogs has demonstrated the importance of lipophilic substitutions in the heteroaromatic ring to increase the binding affinity [6, 12].

The clinical importance of $GABA_B$ analogs has stimulated the research in this field. A new class of potent phosphinic $GABA_B$ antagonists has been recently described by Froestl and co-workers [3, 13]. Lipophilic groups bound to both the phosphorous and nitrogen atoms also appear as necessary for the $GABA_B$ binding affinity to become significant. Even later; morpholine-2-acetic acid derivatives have been reported as $GABA_B$ antagonists [14]. Their affinity also increases after lipophilic substitution in position 5 of the morpholine ring.

Several conformational analyses have succeeded in identifying structural requirements for $GABA_B$ binding affinity [6, 12, 15]. They have been based, however, on the comparison of analogs of the same class, and the conclusions derived from them are only valid for the congeneric family to which they belong. With the aim of elucidating, in a less restrictive manner, the structural requirements involved in accessing the $GABA_B$ receptor, we have performed a conformational study, followed by a similarity analysis that is mainly based on the comparison of structural descriptors, including, in our research, analogs that belong to different families. Due to the consideration of dissimilar structures in the comparative analysis, the number of requirements for binding affinity derived from it is smaller, but of more general applicability for the evaluation of the binding capability.

Although cloning has given some information on the primary structure of the protein receptor, more detailed information about the $GABA_B$ binding site is lacking. Among the relevant missing information, mainly relating to the secondary, tertiary, and quaternary protein structures, it should be noted that the nature of the environment at the receptor site is not known. However, the binding of a molecule to a proteic extracellular domain of the $GABA_B$ receptor [1, 5], together with the evidence that lipophilic substitutions improve the binding capability [6, 12, 14, 15], discourages the assumption that a polar extracellular domain is involved. From a theoretical standpoint this consideration is relevant, mainly when dealing with zwitterionic structures as GABA analogs. Extracellular hydrophilic interactions imply an environment defined by the physiological media, of large dielectric constant, which is accurately modeled by water as a solvent. Intracellular, as well as extracellular interactions involving a proteic media, imply a nonpolar environment that can be approached by calculations *in vacuo*. In this framework, the comparison of the results of theoretical calculations obtained in both conditions can help in discerning the characteristics of the environment in which the interaction occurs. The computational scheme for the treatment of $GABA_B$ analogs is further complicated by the flexibility of the structures, that define several minima, very close in energy, in the potential hypersurface, and also by the fact that the active conformations, associated with the conformations at the binding site, are not necessarily those of lower energy, although, in general, close to them. These complications are generally overcome by means of the consideration of rigid analogs [16], whose structural characteristics help in discerning the requirements for the molecules to be active. However, in contrast to the case of GABA$_A$ [17], no rigid analog has been found for the GABA$_B$ receptor site. We have chosen, therefore, the partially rigid 2RS-(5,5-dimethyl)morpholinyl-acetic acid as our template, and have mainly centered our research on a conformational study that considers, for the other structures, the requirements imposed by it. Moreover, on the basis of the previous discussion, we have decided to model our system *in vacuo*, although polar and proteic environments have been compared for the semirigid analog.

The research presented in this article, which explores the conformational space of the GABA$_B$ analogs when interacting at the receptor site, gives insight, after the similarity analysis, into the conformational preferences of the structures. We are presently searching for more detailed information as part of a more ambitious project, but this achievement relies, for the moment, on the synthesis of analogs with a higher degree of rigidity or the further knowledge of the receptor site, which would allow the application of other modeling resources.

TABLE I
Binding affinity of the GABA$_B$ analogs.[a]

		GABA$_B$ Binding affinity (brain membrane)
Agonists		
b0	GABA	60 nM
b1	beta-R-hydroxy-GABA	1.3 μM
b2	R(−)-Baclofen	60 nM
b3	3-aminopropylphosphinic acid	1 -5 nM
b4	3-aminopropyl (methyl)-phosphinic acid	0.3 nM
Antagonists		
b5	3-aminopropanesulphonic acid	10 μM
b6	R-Phacofen	100 μM
b7	R-Saclofen	100 μM
b8	4-amino-3-(5-methoxy-benzo-[*b*] furan-2-yl)butiric acid	5.5 μM (ileum)
b9	CGP35348	
b10	CGP36742	100 μM (vas deferens)
b11	CGP55845	35 μM
b12	2RS-[(5,5-dimethyl)morpholinyl]-acetic acid	7 nM
b13	γ-Amino-(7-methyl-benzofuran)-butiric acid	3 ± 1 μM
		5.4 μM

[a] bn = short symbols used to refer to them.

Details of the Calculation Procedure

We have included in our analysis the set of compounds listed in Table I and shown in Figure 1, whose elements are not restricted to a unique congeneric family. As the first step of the research a thorough conformational study was performed, which was followed by a similarity analysis where stable conformations were compared. These conformations are partially defined by the structure of the morpholine acetic acid derivative, chosen as a template.

Because there is no strong evidence that supports the modeling of a polar environment surrounding the interaction site, we have based our study on the results derived from calculations *in vacuo*. However, as the influence of a polar media has not been completely rejected, solvent-simulated calculations are presently being done, for the solvent modeled as a continuum within an Onsager approach [18], in the framework of ab initio G94/6-31 + G(d,p) calculations [19]. The results of both approaches are presented in this article, in a comparative manner, for the case of the morpholine acetic acid derivative, as a way of showing that solvent simulation does not become relevant when the conformations are partially defined by the requirements imposed by our template.

In the present research, the first step of the calculation is associated with the conformational search of the fully relaxed isolated molecules. Dealing with very flexible zwitterionic molecules, *in vacuo* geometry optimization leads to severely curved structures, stabilized by proton transfer from the positive to the negative end. In order to

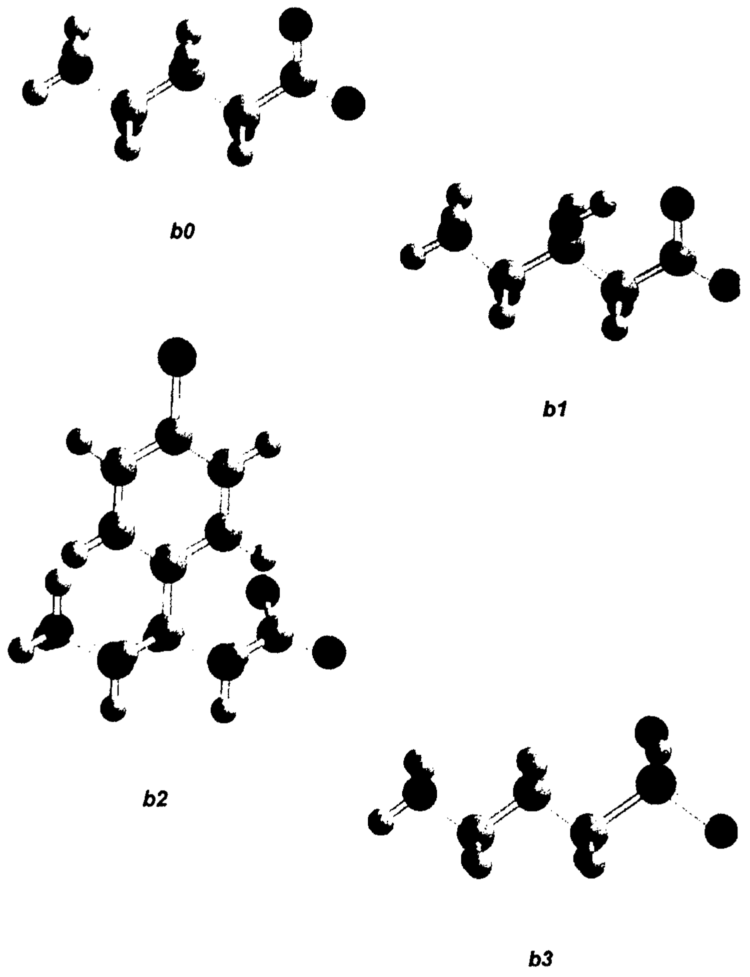

FIGURE 1. $GABA_B$ analogs included in the comparative analysis: b12, rigid analog; b13, benzofuran derivative of baclofen whose X-ray structural data have been considered in the text. Torsional angles are shown for b12: $\tau_1 = NC_1C_2C_3$, $\tau_2 = C_1C_2C_3C_4$, $\tau_3 = C_2C_3C_4O_5$, $\tau_4 = C_2C_3C_4O_6$, $\tau_5 = C_1C_2C_3Y$ (Y = third substituent of C_4, not shown), $\tau_6 = NC_1C_2O_7$, $\tau_7 = C_1C_2O_7C_8$. Red, O; blue, N; light blue, C; green, P; yellow, S.

avoid this effect, which is known to be unreal from the consideration of the requirements imposed by the morpholine acetic acid derivative, the structures have been partially frozen to the torsional angles defined by the rigid moiety of the semirigid analog. Thus, in order to perform a complete search for the accessible conformational space in the interaction site, the unfrozen torsional angles have been varied in 10° steps, from 0° to 360°, with complete relaxation of the other variables at each fixed geometry. In this way, starting with the morpholine acetic acid derivative (Fig. 1), for which the τ_1 value is well defined, the values of τ_2 associated with minimum energy were determined. For these τ_1, τ_2 values imposed on the other structures, the other torsional angles have been calculated by means of a complete search over the conformational space. On the basis of our previous experience, derived from the comparison of semiempirical (PM3, AM1, MNDO) [20] and ab initio (G94/6-31 + G(d,p)) [19] calculations for the conformational analysis of $GABA_A$ derivatives, which has shown that both the semiempirical and ab initio methodologies lead to similar results when performed *in vacuo* [17], we have chosen PM3 for the conformational analysis. The lower computational requirements associated with this methodology allow a more detailed analysis of the conformational

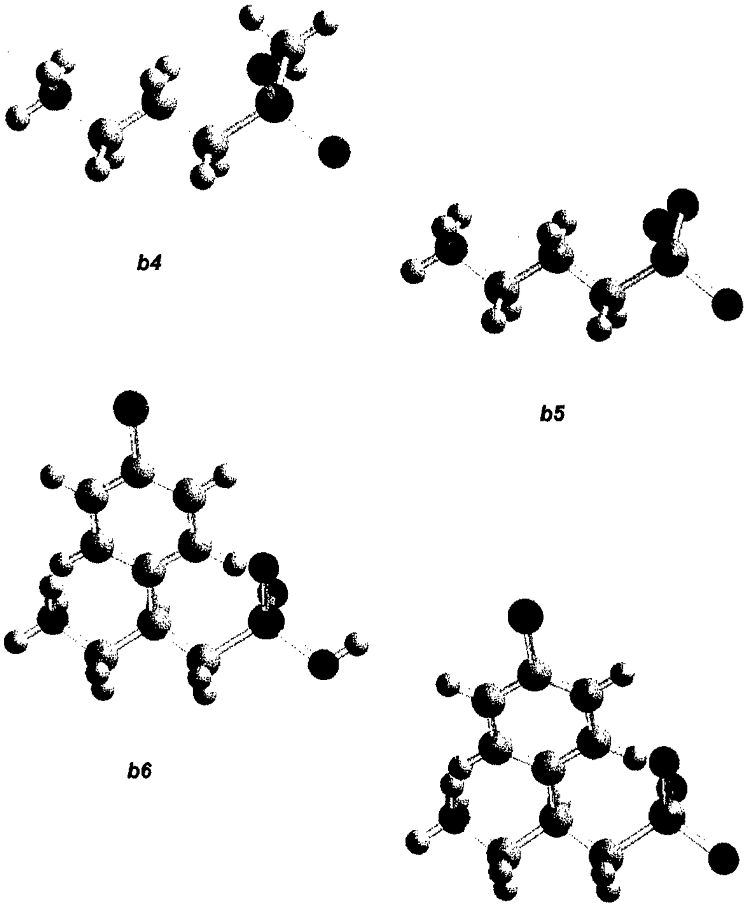

b4

b5

b6

b7

FIGURE 1. (Continued)

space. Ab initio calculations are characterized, for these flexible systems, by a slow convergence to the structure of minimum energy, which is located in a very flat region of the potential hypersurface.

Different environmental conditions have been modeled for the conformational analysis of the morpholine acetic acid derivative. The physiological media, which is the surrounding environment for hydrophilic interactions, has been simulated by water (through its dielectric constant) in the framework of an Onsager approach [18]. The active conformation for lipophilic interactions has been approached, on the other hand, by calculations *in vacuo*. Whereas ab initio (G94/6-31 + G(d,p)) calculations [18] have been performed in the first case, semiempirical PM3 calculations [20] have been done in the second. Far from being arbitrary, this decision is twofold. On one side, we have found that solvent-simulated PM3 calculations [21] do not lead to reliable results (in comparison with those derived from solvent-simulated ab initio ones). On the other side, we are interested in analyzing the confidence of the semiempirical PM3 calculations that will be used throughout this research. They have been chosen on the basis of the knowledge of the computational cost that would demand G94/6-31 + G(d,p) calculations for the evaluation of the torsional barriers around the flexible bonds, and on the similarity of the results from both approaches when used for the analysis of GABA$_A$ analogs [17].

The similarity analysis that followed the conformational search has been mainly based on the comparison of the structural parameters and on

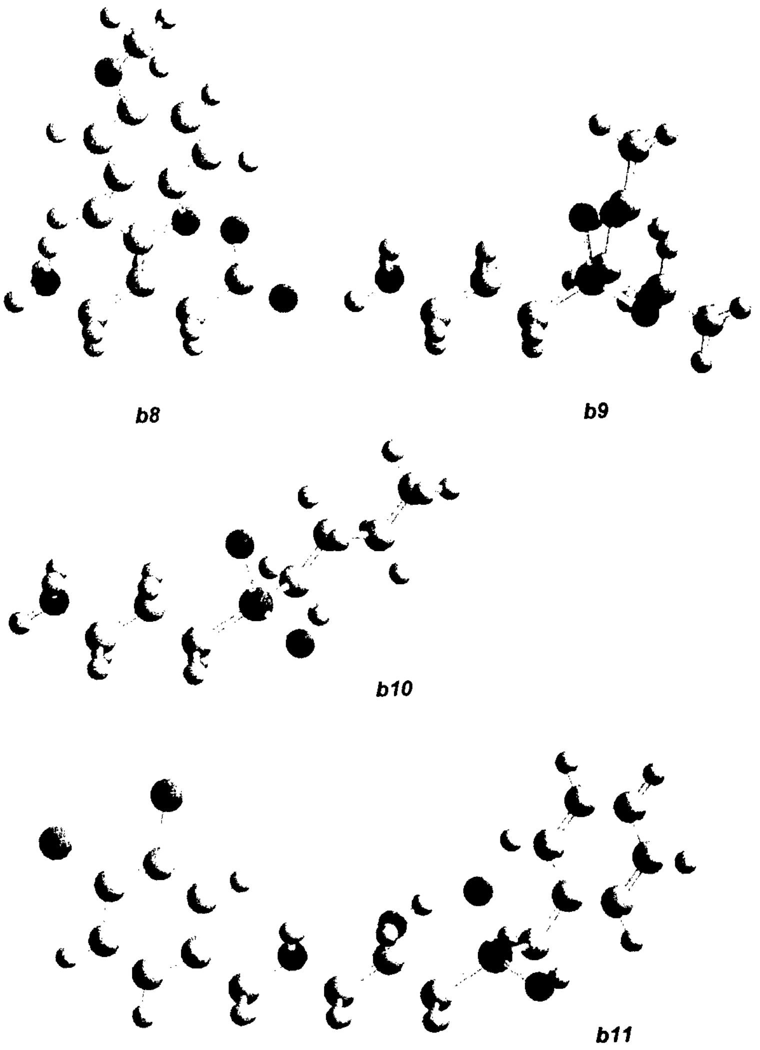

FIGURE 1. (Continued)

the use of computer graphic molecular superimposition in order to compare the structures as a whole.

Results and Discussion

STRUCTURAL CHARACTERISTICS OF THE MORPHOLINE ACETIC ACID DERIVATIVE, B12

Regardless the calculation methodology and the simulated environment, the conformational analysis of the semirigid analog indicates the stabilization of two minima, mainly defined by the value of the $C_1C_2C_3C_4$ (τ_2) torsional angle.

The calculated torsional angles derived from both methodologies (Fig. 1, b12) are given in Table II. As previously mentioned, the value of τ_2 becomes the most relevant calculated data to discern the conformation of the GABA chain in the binding site, as τ_1, τ_6, and τ_7, are defined by rigidization. τ_3 and τ_4, on the other hand, correspond to very flexible angles. Interatomic distances and planar angles are comparatively shown in Figure 2.

From the conformational analysis of the morpholin acetic acid derivative two results can be inferred:

- The conformation of the GABA chain in the $GABA_B$ analogs is defined by values of the torsional angles close to τ_1 = 170° and τ_2 = 60°/ − 60°. The energy involved in the conversion between the most stable conformers

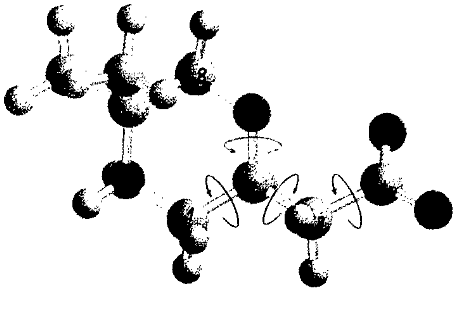

b12

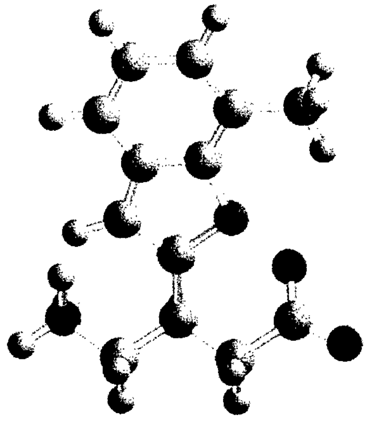

b13

FIGURE 1. (Continued)

ΔH_1 (Table III) is not large enough to disregard intermediate values of τ_2 for the definition of the active conformation.

- The close agreement between the structural parameters calculated by both methodologies demonstrate that solvent simulation does not become relevant for the analysis of the conformational space of the other derivatives of Figure 1 when, according to our interest in the active conformation, the structures are frozen to the requirements imposed by the semirigid analog. For this conformation, which is straight in the amonium side, the interaction between the charges in opposite ends followed by proton migration is precluded. The straight conformation of the semirigid analog reopens the question of whether a polar environment might be surrounding the interaction site and shows how the results of the calculations can help to

TABLE II
PM3 calculated torsional angles of the GABA$_B$ analogs.[a]

	τ_1	τ_2	τ_3	τ_4	τ_5	τ_6	τ_7
b12	178	60	158	−22		53	−60
	171	*74*	*167*	*−14*		*52*	*−62*
	159	−59	−144	36		51	59
	−177	*−54*	*−160*	*24*		*57*	*−66*
B0	170	60	150	−30			
	170	−60	−146	35			
B1	170	60	152	−28			
	170	−60	−129	49			
B2	170	60	157	−23		48	54
	170	−60	−158	23		45	58
B3	170	60	−30	96	−143*		
	170	60	−142	−16	100*		
	170	−60	20	146	−93*		
	170	−60	−80	45	160*		
B4	170	60	−151	−22	90**		
	170	60	−36	91	−150**		
	170	−60	−92	37	150**		
	170	−60	22	151	−90**		
B5	170	60	−135	−18	100		
	170	−60	170	−65	50		
B6	170	60	0.0	−30	80 +	47	58
	170	−60	−116	19	130 +	44	54
	170	−60	−175	47	−60 +	36	52
B7	170	60	−160	−42	75	56	60
	170	−60	157	−79	37	46	95
b8	170	60	156	−25		46	97
	170	−60	−150	30		43	98
B9	170	60	−168	−34	−80 + +		
	170	60	165	−57	50 + +		
	170	−60	−124	11	120 + +		
	170	−60	40	175	−70 + +		
b10	170	60	−151	−20	90 + +		
	170	60	102	−27	−140 + +		
	170	−60	−92	37	150 + +		
	170	−60	21	151	−90 + +		
b11	170	60	−30	−99	−143 + +		
	170	−60	31	153	−89 + +		
	170	−60	97	24	143 + +		

[a] In all the cases but b12, τ_1 and τ_2 are kept fixed to 170° and 60° / − 60°, the latter being close to the one that result from the optimization. Ab initio results for b_{12} are given in italics. Atoms considered in the definition of τ_5: (*); H; (**); primary C; (+); OH; (++); secondary C. Results for more than one minimum are given.

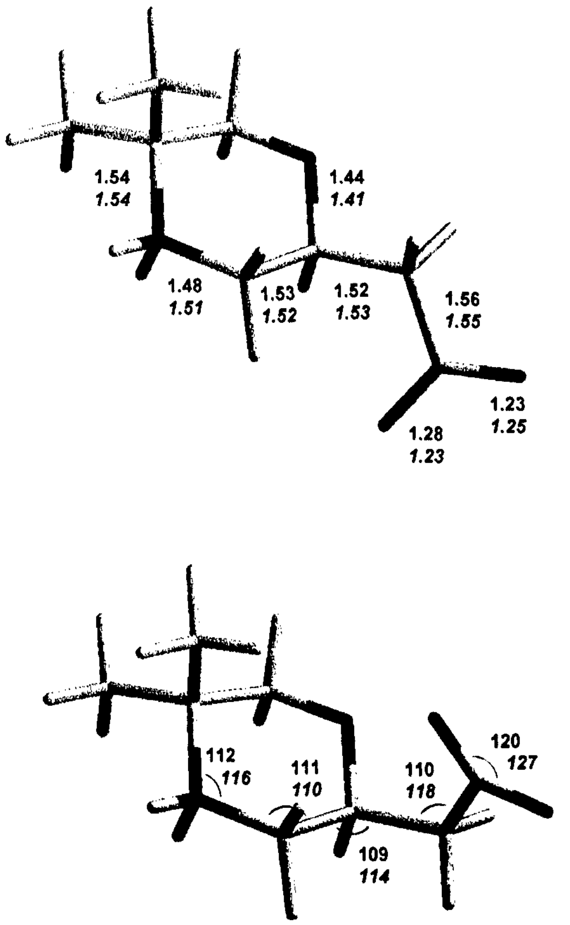

FIGURE 2. Comparison of the structural descriptors (bond distances and planar angles) that result from PM3 and solvent-simulated ab initio calculations (italics) for b12. Bond distances are indicated in the conformation associated with $\tau_2 = 60°$, planar angles in the conformation defined by $\tau_2 = -60°$. Torsional angles are compared in Table II.

understand the characteristics of the interaction in the binding site.

ANALYSIS OF THE "SEMIRIGID" BACLOFEN ANALOGS

As we are interested in the active conformation of the GABA$_B$ analogs, which is partially defined by b12, we have frozen the value of τ_1 to 170°, which is an intermediate value between those associated with the two minima calculated for b12. In order to perform the conformational analysis of the baclofen analogs, including saclofen and phaclofen, we have worked on the other structural parameters scanning the conformational space by means of a 360° rotation of τ_2, in 10° steps, with complete relaxation of the other parameters.

In agreement with the results derived from the study of b12 two minima were found, defined by values of τ_2 close to $+60/-60$. The energy involved in the mutual interconversion between both conformers is smaller than the one calculated for b12.

It should be mentioned that, when b12 is analyzed by means of a complete scanning of the active space through the rotation of τ_2 in 360°, a third minimum develops at $-120°$. However, this minimum implies a significant distortion of the morpholine ring. This fact supports the conclusion that values close to either 60° or $-60°$ in τ_2, together with 170° in τ_1, will define the conformation of the GABA chain in the binding site.

For the analysis of the other torsional angles a similar procedure has been followed. Keeping τ_1 fixed to 170°, τ_2 has been kept to either 60° or $-60°$, a value that is close enough to the one that results from the previous optimization. For the semirigid geometries thus defined, the conformational space has been again scanned by means of a 360° rotation of τ_3 in 10° steps with complete relaxation of the other parameters. This rotation implies the simultaneous modification of τ_3 and τ_4. The resulting conformations, described by the torsional angles, are given in Table II. The optimized values of τ_3, τ_4, and τ_5 (Table II) are difficult to compare, as they involve different groups, with either two or three atoms bonded to carbon, phosphorus, or sulfur atoms. It gives, however, good agreement for the carboxylate containing molecules. In relation to the baclofen analogs, τ_6 and τ_7 have been also considered. The most stable conformation corresponds to $\tau_7 = 60°$. The energy difference between this conformation and the one imposed by the semirigid analog, defined by $\tau_7 = -60°$ (Table II) amounts to 4 kcal/mol, with an associated rotational barrier of 6.0 kcal/mol. The latter is in close agreement with the -65.3 value determined by X-ray diffraction analysis for the 7-methyl benzofuran analog of baclofen (b13, Fig. 1) [12].

COMPARATIVE ANALYSIS INCLUDING ALL THE COMPOUNDS OF THE SET

The previously described conformational analysis, based on the partial rigidization of the molecules to the parameters imposed by b12, has been extended to the other molecules of the series (b0, b1, b3, b4, b5, b9, b10, b11). Data reported in Table II demonstrate that the previous discussion is not restricted to the baclofen analogs, but also applies to the other elements of the set.

The first step of the optimization, for τ_1 fixed to 170°, results in two minima, defined by τ_2 values close to 60 and -60, respectively. The energy difference between them (ΔE, Table III) does not allow discernment among both possibilities for the definition of the characteristics of the active conformation. In relation to the torsional barriers, the largest value among the flexible derivatives corresponds to b0, where the height is associated to the simultaneous rotation about the CC bond that

TABLE III

Distance [Å] from the positive center to each of the atoms that define the negative center.[a]

	τ_2	d(N—O)	d(N—O)	d(N—O)	d(N—X)	d	ΔE (kcal / mol)	ΔH_1 (kcal / mol)	ΔH_2 (kcal / mol)
b12	60	5.58	3.83		4.35	4.70	0.29	8	
	−60	5.48	3.75		4.27	4.61	0.00		
b0	60	5.55	3.81		4.32	4.68	1.83	12	9
	−60	5.51	3.77		4.28	4.64	0.00		9
b1	60	5.59	3.92		4.36	4.75	0.00	12	3
	−60	5.35	3.76		4.21	4.55	3.71		3
b2	60	5.56	3.80		4.36	4.68	1.67	8	9
	−60	5.48	3.78		4.31	4.63	0.00		9
b3	60	5.61	3.83		4.61	4.72	3.85	4	8
	60	5.51	3.80		4.59	4.65	3.58		
	−60	5.50	3.60		4.49	4.55	0.77		8
	−60	5.41	3.74		4.46	4.57	0.00		
b4	60	5.68	3.74		4.56	4.71	0.00	8	8
	60	5.54	3.79		4.55	4.66	0.03		
	−60	5.34	3.80		4.55	4.57	0.03		8
	−60	5.35	3.74		4.56	4.54	0.01		
b5	60	5.65	3.90	5.47	4.67	4.77	2.43	6	9
	−60	5.26	3.86	4.82	4.53	4.56	0.00		9
b6	60	5.56	3.80		4.62	4.68	0.00	7	11
	−60	5.32	3.79		4.56	4.55	2.26		10
	−60	5.24	3.80		4.59	4.52	4.37		
b7	60	5.63	3.90	5.45	4.63	4.76	0.00	7	8
	−60	5.40	3.77	5.62	4.62	4.58	1.75		9
b8	60	5.67	3.96		4.44	4.81	0.59	9	14
	−60	5.27	3.97		4.32	4.60	0.00		13
b9	60	5.61	3.77		4.43	4.69	1.72	8	10
	60	5.63	3.70		4.42	4.66	0.00		
	−60	5.24	3.80		4.58	4.52	3.50		10
	−60	5.28	3.73		4.60	4.51	3.64		
b10	60	5.68	3.81		4.60	4.74	2.79	7	9
	60	5.67	3.82		4.60	4.74	3.94		
	−60	5.35	3.72		4.50	4.53	0.65		8
	−60	5.31	3.70		4.51	4.51	0.00		
b11	60	5.58	3.79		4.61	4.68	3.57	7	8
	−60	5.29	3.71		4.41	4.50	0.00		8
	−60	5.38	3.68		4.43	4.53	1.06		

[a] d = distance from the N to the mean point of the overlapping negative charges. ΔE = relative PM3 calculated energy differences between the conformations defined by τ_2. $\Delta H_1, \Delta H_2$ = energy barriers around τ_1, τ_2, respectively.

defines the τ_3 value. Rotational barriers around the CC bond associated with τ_3 are also given in Table III.

In order to learn about the structural requirements associated with the binding affinity, we have superimposed the structures that result from the optimization, constrained in the τ_1, τ_2 values, with our template, defined by b12. The graphical superposition was preceded by the analytical comparison of the distance between the positive and negative centers of charge, for the conformations defined by $\tau_2 = 60°/-60°$ (Table III). The distance between the positive nitrogen and two of the negative oxygen atoms is the same, within 0.25 Å, for the molecules under consideration, which is indicative of the fact that the centers of charge will be easily overlapped. If the mean position between the two centers of negative charge is considered, the calculated distance is in agreement with the one observed by X-ray crystallography for the furan, thienyl, benzofuran, and benzothiophene analogs of baclofen (4.6 Å) [12, 22–24] (b13, Fig. 1) and with the one calculated by molecular dynamics for the phosphinic antagonist CGP55845 [15].

Figure 3 shows the results of the graphical superposition, exemplified by the superposition of b12 with b0, b7, b8, and b9. The conformations defined by $\tau_2 = 60°/-60°$ have been comparatively considered. Graphic superpositions for the other GABA$_B$ analogs are available upon request.

In agreement with the previous analytical comparison, the positive and negative centers of charge

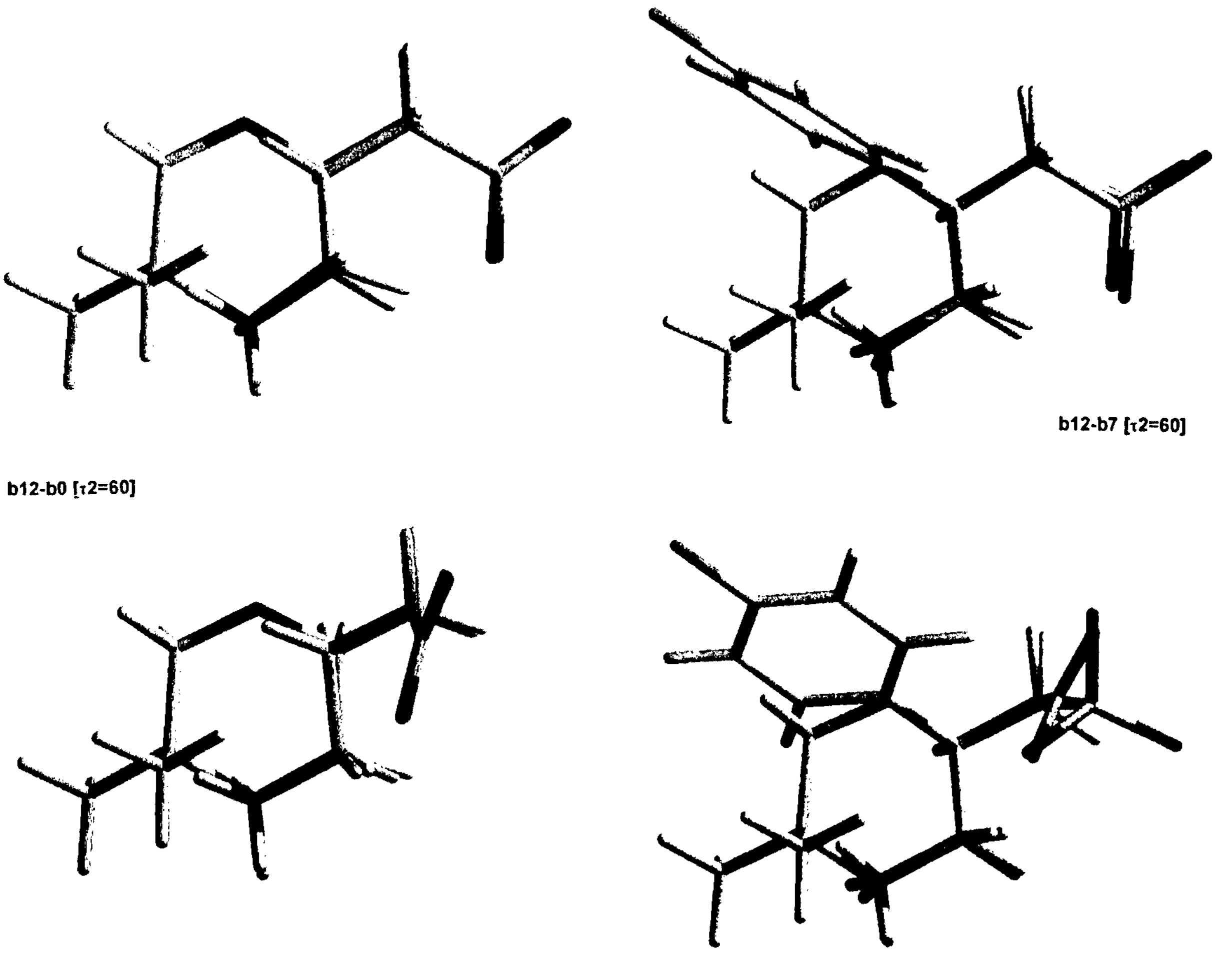

b12-b0 [τ2=60]

b12-b7 [τ2=60]

b12-b0 [τ2=-60]

b12-b7 [τ2=-60]

FIGURE 3. Superposition of GABA$_B$ analogs with the template, b12. Although the superposition has been analyzed for all the molecules, 4 out of 11 are given as example. Superposition has been analyzed for both stable conformations defined by $\tau_2 = 60°/-60°$.

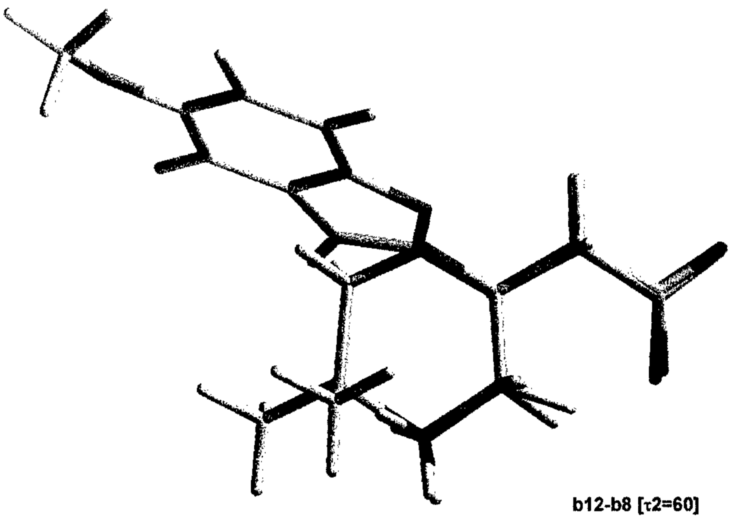

b12-b8 [τ2=60]

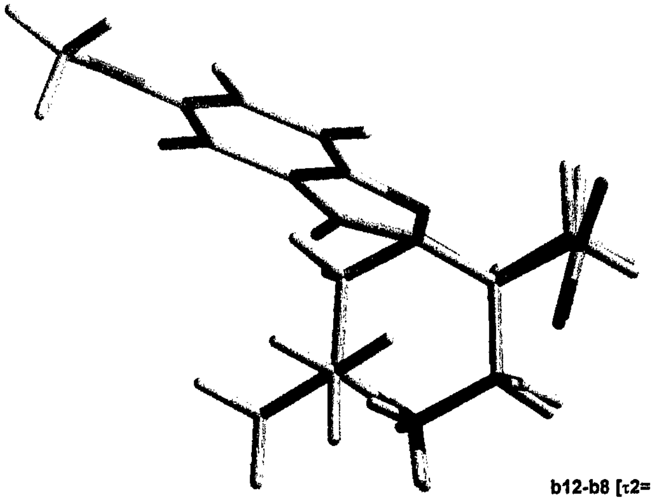

b12-b8 [τ2=-60]

FIGURE 3. (Continued)

overlap for all the molecules of the series. For the case of the baclofen analogs, the aromatic substituent in β position overlaps with the oxygen atom of the morpholine ring. This superposition involves the R-configuration of the baclofen derivatives, which are known to be the active species for receptor binding. For the morpholine acetic acid derivatives, on the other hand, the active configuration is S on C_2 of the morpholine ring. Estereoisomeric requirements should also be considered, thence, in the definition of the pharmacophoric pattern of $\mathrm{GABA_B}$ analogs. Lipophilic substitutions in β position have been extensively investigated. It has became evident that, in addition to the estereoisomerism, requirements related to the size of the substituent have to be met. It has been found [15] that a size over a limit, defined by two methyl groups bonded to C_5 of the morpholine ring decrease the activity in the series of the morpholine acetic acid derivatives.

On the basis of the previous analysis we are able to suggest a pharmacophoric pattern for $\mathrm{GABA_B}$ analogs which is not restricted to a unique congeneric family. It is defined by: (1) a positive center associated with an ammonium group; (2) a negative center defined by two oxygen atoms; (3) a distance between them of $4.6\ (-^{+}0.1)$ Å, measured from the nitrogen atom to the mean point of the two overlapping oxygens; (4) a straight conformation in the positive end; (5) a torsional angle τ_2 restricted to values between 60° and $-60°$; and (6) a configuration in the β position of the GABA chain superimposable on the R-enantiomer of the baclofen analogs. The characteristics of this pattern

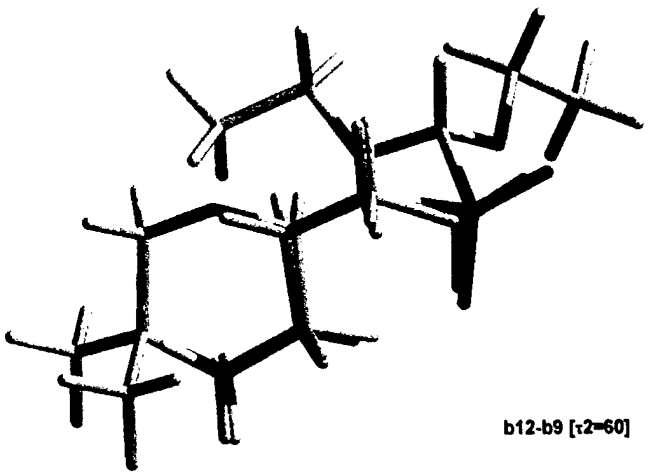

b12-b9 [$\tau 2$=60]

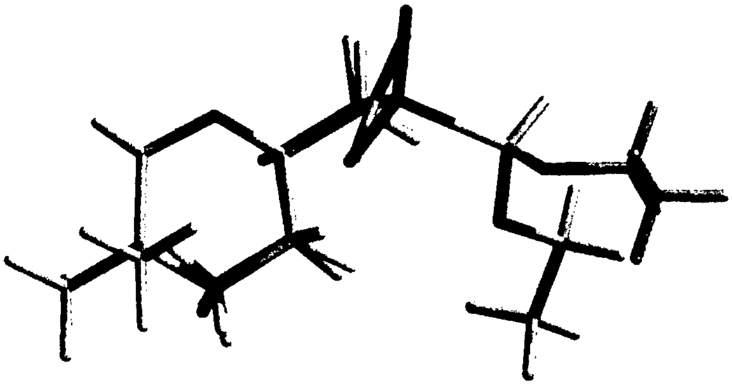

b12-b9 [$\tau 2$=-60]

FIGURE 3. (Continued)

indicate that τ_2 becomes relevant for its definition. Although 60° and $-60°$ appear, at first glance, as equivalent, they do not define equivalent conformations but mirror images, and only one, defined by a value of τ_2 between these limits, will be capable of accessing the receptor site. The question remains pen and would probably need the design, synthesis, and biological evaluation of, at least, a new compound, rigidified in the negative end.

TABLE IV
Torsional angles for the GABA molecule at the $GABA_A$ and $GABA_B$ receptor sites.[a]

	τ_1	τ_2	τ_3	τ_4	d (Å)
GABA-A	15	180	180	0	> 5.30
GABA-B	170	60	150	−30	4.60
	170	−60	−150	30	

[a] d = distance from the positive to the negative end that defines the pharmacophore.

CONFORMATIONS OF THE GABA MOLECULE IN THE $GABA_A$ AND $GABA_B$ RECEPTOR SITES

Table IV and Figure 4 show the differences in the conformations of the GABA molecule when interacting with either $GABA_A$ or $GABA_B$ receptor sites. τ_1 and τ_2 define important differences between both conformations. Whereas the value of τ_1 implies opposite orientations of the positive end, it should be remarked that the value $\tau_2 = 180°$, which corresponds to minimum energy for the $GABA_A$ agonists, belongs to a point of maximum energy in the conformational space of the $GABA_B$ analogs.

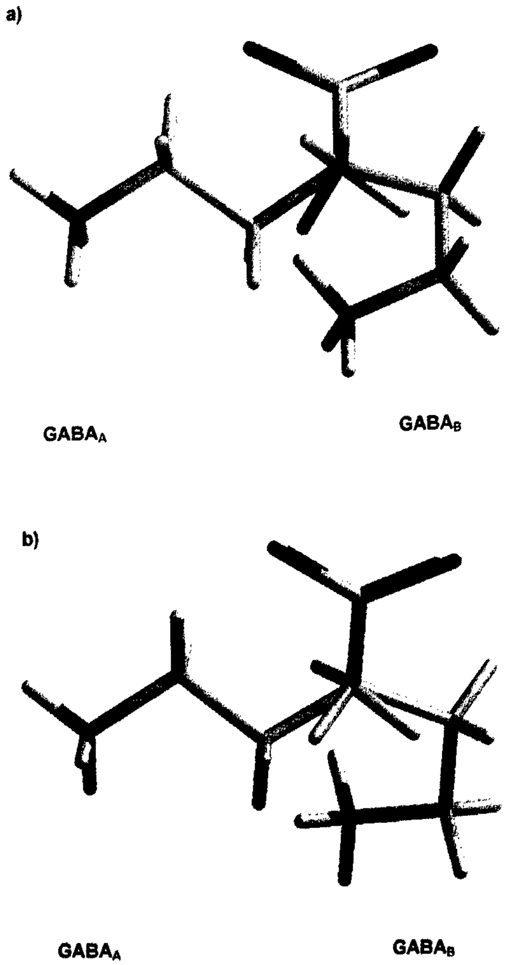

FIGURE 4. Superposition of the GABA molecule in the conformations associated with the GABA$_A$ and GABA$_B$ receptor sites. (a) GABA$_B$ conformation for $\tau_2 = 60°$. (b) GABA$_B$ conformation for $\tau_2 = -60°$.

Conclusions

A conformational study, followed by the identification of similar fragments taking into account the flexibility of the molecules, has led us to suggest a pharmacophoric pattern for GABA$_B$ binding affinity, revealing the following features: (1) a positive center associated with an ammonium group; (2) a negative center defined by two oxygen atoms; (3) a distance between them of 4.6 Å, measured from the nitrogen atom to the mean point of the overlapping negative oxygens; (4) a straight conformation in the positive end; (5) a torsional angle τ_2 restricted to values between 60° and $-60°$; and (6) a configuration in the β position of the GABA chain superimposable on the R-enantiomer of the baclofen analogs.

The main difficulty of this research was associated with the flexibility of the structures and the lack of fully rigid GABA$_B$ analogs. This fact leaves a question open about the accuracy of the definition of the conformational characteristics of the negative end. However, we have approached the pharmcophore closely enough to be able to discern the differences in the conformation of the GABA molecule at the GABA$_A$ and GABA$_B$ receptor sites.

Present research is oriented to the design and synthesis of completely rigid analogs and to the homology modeling of the receptor on the basis of the comparison of the amino acid sequences of GABA and glutamate metabotropic receptors.

ACKNOWLEDGMENT

This work was supported in part through grants from Consejo Nacional de Investigaciones Científicas y Técnicas de la República Argentina (CONICET), Universidad Nacional de La Plata, Cooperativa Farmacéutica de Quilmes (COFARQUIL), and Colegio de Farmacéuticos de la Provincia de Buenos Aires, Argentina. The authors gratefully acknowledge the Cátedra de Química Cuántica, Facultad de Química, Universidad de la República Oriental del Uruguay for the use of the computer facilities. One of us (M.L.L.) would like to acknowledge Colegio de Farmacéuticos de la Provincia de Buenos Aires for a research fellowship.

References

1. K. Kaupmann, K. Huggel, J. Heid, P. J. Flor, S. Bischoff, S. J. Mickel, G. McMaster, C. Angst, H. Bittiger, W. Froestl, and B. Bettler, Nature **386**, 239 (1997).
2. N. G. Bowry, Annu. Rev. Pharmacol. Toxicol. **33**, 109 (1993).
3. H. Bittiger, W. Froestl, S. J. Mickel, and H. R. Olpe, Trends Pharmacol. Sci. **16**, 391 (1993).
4. D. I. Kerr and J. Ong, Drug Discovery Today **1**, 371 (1996).
5. N. G. Bowery and D. A. Brown, Nature **386**, 223 (1997).
6. M. Ansar, S. Al Alkoum Ebrik, R. Mouhoub, P. Berthelot, C. Vaccher, M. P. Vaccher, N. Flouquet, D. H. Caignard, P. Renard, B. Pirard, M. C. Rettori, G. Evrard, F. Durant, and M. Debaert, Eur. J. Med. Chem. **31**, 449 (1996).
7. C. Muller-Uri, E. A. Singer, and W. Fleischnacker, J. Med. Chem. **29**, 125 (1986).
8. D. I. B. Kerr, J. Ong, R. H. Prager, B. D. Gynther, and D. R. Curtis, Brain Res. **405**, 150 (1987).

9. P. Berthelot, C. Vaccher, A. Musadad, N. Flouquet, M. Debaert, M. Luyckx, and C. Brunet, J. Med. Chem. **34**, 2557 (1991).
10. D. I. B. Kerr, J. Ong, G. A. R. Johnston, J. Abbenante, and R. H. Prager, Neurosci. Lett. **92**, 92 (1988).
11. P. Berthelot, C. Vaccher, A. Musadad, N. Flouquet, M. Debaert, and M. Luyckx, J. Med. Chem. **30**, 743 (1987).
12. B. Pirard, B. Paquet, G. Evrard, P. Berthelot, C. Vaccher, M. H. Ansard, M. Debaert, and F. Durant, Eur. J. Med. Chem. **30**, 851 (1995).
13. W. Froestl, S. J. Mickel, G. Von Sprecher, H. Bittiger, and H. R. Olpe, Pharmacol. Commun. **2**, 52 (1992).
14. D. J. Blythin, S-Ch. Kuo, H-J. Shue, A. T. McPhail, R. W. Chapman, W. Kreutner, C. Rizzo, H. S. She, and R. West, Biorg. Med. Chem. Lett. **6**, 1529 (1996).
15. B. Pirard and F. Durant, J. Comput.-Aided Mol. Design **10**, 31 (1996).
16. B. Macchia, A. Balasamo, M. C. Breschi, G. Chiellini, A. Lapucci, M. Macchia, C. Manera, A. Marinelli, C. Martini, R. Scatizzi, and U. Barreta, J. Med. Chem. **36**, 3077 (1993).
17. M. L. Lorenzini, L. E. Bruno-Blanch, and G. L. Estiú, submitted.
18. L. Onsager, Electric Moments Molecules Liquids, **58**, 1486 (1936).
19. M. J. Frisch, G. W. Trucks, H. B. Schlegel, P. M. Gill, B. G. Johnson, M. A. Robb, J. R. Cheeseman, T. Keith, G. A. Petersson, J. A. Montgomery, K. Raghavachari, M. A. Al-Laham, V. G. Zakrzewski, J. V. Ortiz, J. B. Foresman, C. Y. Peng, P. Y. Ayala, W. Chen, M. W. Wong, J. L. Andres, E. S. Replogle, R. Gomperts, R. L. Martin, D. J. Fox, J. S. Binkley, D. J. Defrees, J. Baker, J. P. Stewart, M. Head-Gordon, C. Gonzalez, and J. A. Pople, Gaussian 94, Revision B.3, Gaussian, Inc., Pittsburgh, 1995.
20. J. P. Stewart, Mopac, version 7.0, F. J. Seiler Research Laboratory, United States Air Force Academy, CO 80840.
21. G. D. Hawkins, G. C. Lynch, D. J. Giesen, Y. Rossi, J. W. Storer, D. A. Liotard, C. J. Cramer, and D. G. Truhlar, Amsol, version 5.4, Univ. Minnesota, Minneapolis, Minnesota.
22. P. Berthelot, C. Vaccher, and N. Flouquet, Eur. J. Med. Chem. **26**, 395 (1991).
23. B. Pirard, G. Evrard, and B. Norberg, J. Cryst. Spec. Res. **23**, 843 (1993).
24. B. Pirard, G. Evrard, and B. Norberg, Bull. Soc. Chim. Belg. **102**, 639 (1993).

Optimal Molecular Connectivity Descriptors for Nitrogen-Containing Molecules

MILAN RANDIĆ, JAN CZ. DOBROWOLSKI*

Department of Mathematics & Computer Science, Drake University, Des Moines, Iowa 50311

Received 23 February 1998; revised 26 May 1998; accepted 1 June 1998

ABSTRACT: We report on optimal molecular connectivity descriptors for nitrogen atoms in amines for use in structure–property correlations. The descriptors represent generalized molecular connectivity indices with adjusted diagonal entries in the adjacency matrices of the corresponding molecular graphs, such that the standard error in a regression for boiling points in a set of amines is minimized. Advantages of the so-optimized descriptors for multivariate regression analysis in structure–property–activity studies are discussed. © 1998 John Wiley & Sons, Inc. Int J Quant Chem 70: 1209–1215, 1998

Introduction

One of the critical initial steps in modeling structure–property and structure–activity relationships is the selection of molecular descriptors to be used in such models. In the earlier development of QSAR, the quantitative structure–activity relationship studies [1], the selected molecular properties have been often used as molecular descriptors. While this is quite legitimate, such an approach has been characterized as structure-cryptic [2], because it expresses biological activities in terms of molecular properties, simpler and presumably better understood; nevertheless, such an approach does not offer direct insight on the structure–property relationship. The success of such approach reflects the situation that the, although yet unknown, same structural factors may play the critical role in different molecular properties [3].

Chemical graph theory [4] advocates an alternative approach to QSAR and to the structure–property–activity relationship studies based on mathematically derived molecular descriptors. Such descriptors, often referred to as topological indices, include the well-known Wiener index W [5], the Hosoya index Z [6], and the connectivity index χ [7], the latter one being the most widely used [8]. The Wiener index counts the number of carbon atoms on each side of bond in a molecule, the Z

Correspondence to: M. Randić.

* Fulbright Visiting Scholar on leave from Industrial Chemistry Research Institute and Drug Institute, Lab. Theor. Meth. and Calc., 30/34 Chelmska St., Warsaw, Poland.

© 1998 John Wiley & Sons, Inc.

CCC 0020-7608 / 98 / 061209-07

index counts nonadjacent bonds in the carbon skeleton of a molecule, while χ is a bond additive quantity in which bonds of different types (involving primary, secondary, tertiary carbons) are given different weights. As initially introduced, all three indices (and the same is true for many, but by no means all, topological indices) were defined for carbon molecular skeletons. This leaves the problem of their generalization to heteroatomic molecules open. Kier and Hall [9] recognized the importance of extending the definition of the connectivity index to heteroatoms and proposed the so-called valence connectivity indices for which the rules are given as to how to represent heteroatoms. The concept of the valence connectivity indices also extends to "higher" connectivity indices [10]. Kupchik considered an alternative route to generalized connectivity indices by modifying empirically the difference in bond length between the heteroatom–carbon bond and the carbon–carbon bond [11]. The modifications were based on the differences in the covalent radius between the heteroatom and the carbon atoms. The corresponding extensions of W and Z for heteroatoms have not been yet considered, but, recently, weighted paths for heteroatoms were considered [12].

Representation of Heteroatoms

It is apparent that in order to cover the increased variation in the structural features that the heteroatom introduces molecules involving heteroatoms require additional descriptors. The approach of Kier and Hall [8] implies that heteroatoms differently weigh bonds of different kinds. The characterization of heteroatoms by graph-theoretical rather than physicochemical schemes has advantages, as it is independent of whether selected experimental data are available and, if available, whether they are reliable.

An alternative approach of modifying the connectivity indices so that they can better characterize the presence of heteroatoms to that of Kier and Hall was recently outlined for chlorine atoms in clonidine compounds [13]. The approach may be viewed as analogous to the early modifications of the Hückel molecular orbitals method for heteroatoms [14], while the approach of Kier and Hall would be analogous to the approach of Slater for modification of simple atomic orbitals used in the early quantum chemical calculations. A way to differentiate heteroatoms in a Hückel matrix, or the adjacency matrix of a molecular graph, is to modify the diagonal and the off-diagonal elements. An earlier study showed that modification of off-diagonal elements has produced a small effect [15].

Changes in the diagonal elements of adjacency matrices, as has already been seen on chlorine atoms in clonidine-type compounds, influences the magnitudes of computed weighted paths more strongly [13]. In Table I, we show how the paths of length one, paths of length two, and paths of length three vary as we change the diagonal entry corresponding to nitrogen in a graph of 1-aminohexane. The same table applies to other heteroatoms placed at the end of the chain of six carbon atoms, for example, it equally applies to 1-hexanol. The difference between 1-hexanol and a-aminohexane will be in different corresponding values for the parameter y.

The weighted paths for n-heptylamine were obtained from the ALL PATH program [16] by replacing the zero diagonal entries in the input adjacency matrix with the value of y selected. The weight of bonds in the calculation of the connectivity index are defined as $1/\sqrt{m \cdot n}$, where m and n are the valences of the incident atoms (vertices). By introducing parameters x and y to be associated with atoms of different kinds, here, carbon and nitrogen atoms, respectively, the weight of bond (m, n) changes from $1/\sqrt{(m \cdot n)}$ to $1/\sqrt{[(m + x) \cdot (n + y)]}$.

TABLE I
Variation of path numbers $^1\pi$, $^2\pi$, and $^3\pi$ for 1-aminohexane as a function of the diagonal entry for the nitrogen atoms (diagonal entries for carbon atoms are assumed zero).

y	$^1\pi$	$^2\pi$	$^3\pi$
0.5	3.2845	1.3922	0.5711
0	3.4142	1.4571	0.6036
−0.25	3.5236	1.5118	0.6309
−0.50	3.7071	1.6036	0.6768
−0.75	4.1213	1.8107	0.7803
−0.80	4.2883	1.8941	0.8221
−0.85	4.5326	2.0164	0.8832
−0.90	4.9432	2.2216	0.9858
−0.95	5.8694	2.6847	1.2175

In Table I, we show how the count of the paths changes as y decreases from small positive values and approaches the limiting value of -1 (assuming $x = 0$). In general, both x and y will change. For example, as we will see in the next section, the values $x = 1.25$ and $y = -0.65$ are found as optimal for carbon and nitrogen atoms, respectively, when considering the boiling points in amines. The optimal value of $x = 1.25$ corresponds to a change of the valence for carbon atoms in a molecular graph from their values of 1 and 2 to the values 2.25 and 3.25 for the terminal and the bridge carbon atoms, respectively. Similarly, the formal valence of the terminal nitrogen atom becomes 0.35 instead of remaining equal to 1. These changes in the x and y values alter the relative role that the carbon and nitrogen atoms play. The negative values of y result in a more pronounced role of the heteroatom. However, the relative role of the shorter and longer paths for the carbon atom or the nitrogen atom have not changed.

In Figure 1, we plotted $^2\pi$ against $^1\pi$ and $^3\pi$ against $^1\pi$ for the weighted path numbers given in Table I. Although as the diagonal entry of the adjacency matrix decreases and the magnitudes of the path numbers $^1\pi$, $^2\pi$, and $^3\pi$ increase, their relative importance remains unchanged as is reflected by the linear correlation (shown in Fig. 2) between them.

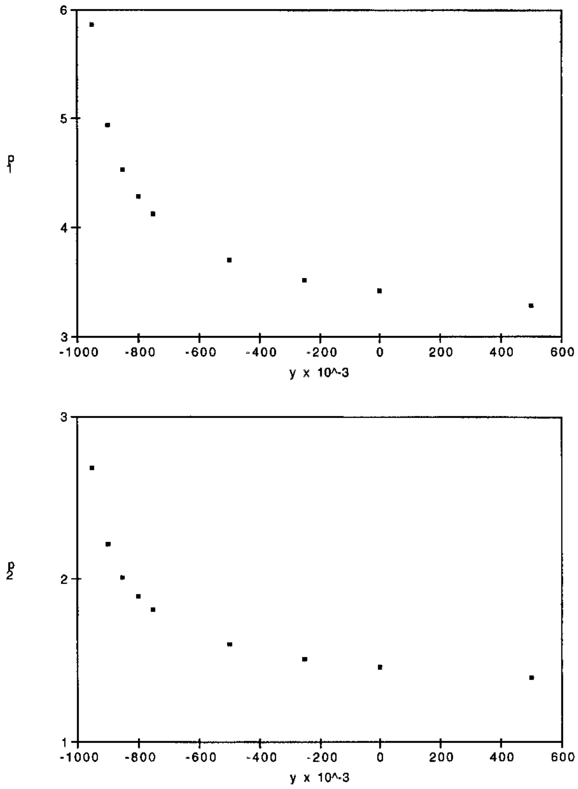

FIGURE 1. Variation of the $^1\pi$ as a function of the diagonal entry for the nitrogen atom in the adjacency matrix of the molecular graph of 1-aminohexane.

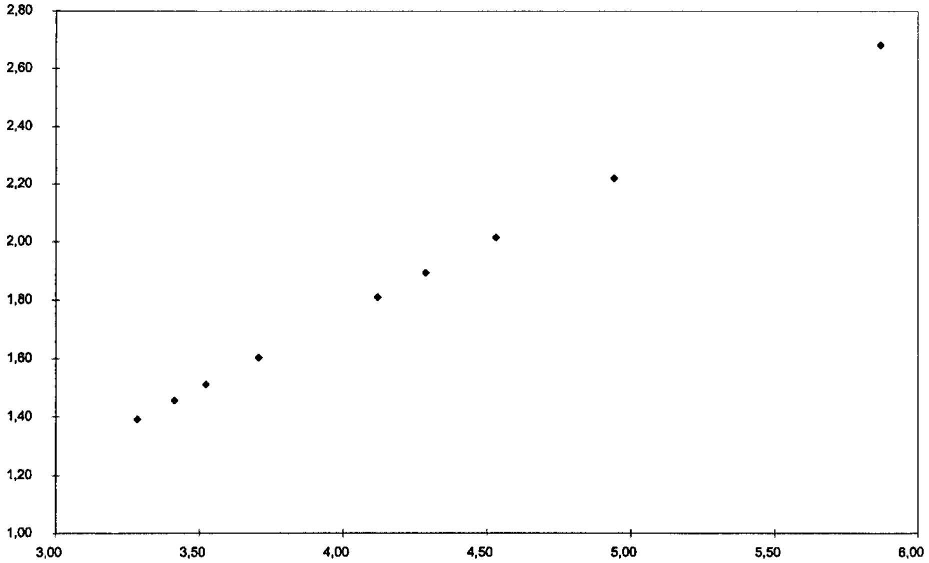

FIGURE 2. Plot of the magnitudes of $^2\pi$ against $^1\pi$ for different values of y (assuming $x = 0$), showing a linear relationship.

Search for the Optimal Descriptors

The outlined approach illustrates the potential of the modified descriptors to discriminate atoms of different kinds. The problem is to find the optimal values for x and y to be used in structure–activity studies. One way to select the best values of x and y is to minimize the standard error s in the multiple-regression analyses (MRA). Having thus defined the procedure for discrimination among heteroatoms by having the diagonal entries in the adjacency matrices as variables, we have to search for the best parameters to describe different atoms in different situations. Several factors will influence such a search:

1. The selection of the compounds.
2. The selection of the property.
3. The selection of the descriptors to be used.

All these factors (and possibly other) have to be examined. Of particular interest is to find how sensitive are the so-derived parameters on the choice of compounds, on the choice of properties, and on the choice of the descriptors used and how they depend on the number of descriptors used. The early results on alcohols and their boiling points [17] are encouraging. In the case of alcohols and their boiling points, $x = 1.5$ and $y = -0.85$ gave the best single-variable regression. Here, x and y stand for the carbon and oxygen atoms' diagonal entries, respectively. The use of the above values for x and y reduced the standard error s by more than one-half when a comparison was made with the similar regression in which the carbon and oxygen atoms were not discriminated.

In this article, we report the corresponding analysis for the regression of the boiling points in nitrogen-containing amines. The result is of interest possibly in the future search for optimal descriptors for nitrogen atoms when considering other molecular properties and when considering other nitrogen-containing compounds.

Regression of Boiling Points for Amines

In Table II, we list 16 primary amines, their experimental boiling points (as reported in [8]), the generalized connectivity indices based on the values of $x = 1.25$ and $y = -0.65$, the calculated boiling points, and the difference between the observed and the calculated values. If we do not differentiate between the carbons and the nitrogens (i.e., when $x = y = 0$), the regression of the boiling points against the connectivity indices has

TABLE II

The weighted paths numbers ($^1\pi$), experimental boiling points (Bp_{exp}), calculated boiling points (Bp calcd), and the difference between the experimental and calculated values (Diff.) for a number of primary amines, with the values assumed for x and y corresponding to the optimal values $x = 1.25$ and $y = -0.65$.

Molecule	$^1\pi$	Bp_{exp}	Bp_{calcd}	Diff.
1-Aminononane	3.46126	201	204.9	−3.9
1-Aminooctane	3.15357	180	179.2	+0.8
1-Aminoheptane	2.84588	155	153.5	+1.5
1-Aminohexane	2.53818	130	127.8	+2.2
1-Amino-4-methylpentane	2.46883	125	122.0	+2.9
2-Aminohexane	2.39755	114.5	116.1	−1.6
1-Aminopentane	2.23049	104	102.2	+1.8
1-Amino-2-methylbutane	2.16893	96	97.0	−1.0
1-Amino-3-methylbutane	2.16114	96	96.4	−0.4
2-Aminopentane	2.08986	92	90.4	+1.6
3-Aminopentane	2.09766	91	91.1	−0.1
2-Amino-2-methylbutane	1.93152	78	77.2	+0.8
1-Aminobutane	1.92280	77	76.5	+0.5
1-Amino-2-methylpropane	1.85344	69	70.7	−1.7
2-Aminobutane	1.78217	63	64.7	−1.7
1-Aminopropane	1.61511	49	50.8	−1.8

for the standard error $s = 3.49$°C. It is desirable from a practitions' point of view to aim at the standard errors in the boiling points below 1°C, if possible. The standard error of almost 3.5°C is clearly unsatisfactory. It is not surprising that the simple connectivity index ($x = 0$, $y = 0$) cannot offer good results for alcohol boiling points. For example, the boiling points for 2-methylpentamine (114.5°C) and 4-methylpentamine (125°C) differ by more than 10°C, yet the two molecules have the same molecular graph (when the carbon atom and the nitrogens are not discriminated).

If we vary x, the variable describing the carbon atoms, we can reduce the standard error s somewhat. When $x = 1.25$ (see Table III), s is reduced to 3.01°C. However, by changing the diagonal parameter for nitrogen, we achieve a dramatic improvement in the reduction of the standard error. When $y = -0.65$°C (while $x = 0$), the standard error s becomes 2.08°C. To find the optimal values for these parameters and to locate the minimum in s by changing both, x and y, we screened some 20 points in the x, y space. As we see from Table III, the minimal standard error, close to 1.90°C, is obtained when $x = 1.25$ and $y = -0.65$. The regression equation corresponding to the *so* optimal parameters of x and y is

$$\mathrm{Bp}_{\mathrm{calc}} = 83.456\,{}^{1}\pi - 83.992$$

$$s = 1.91 \qquad r = 0.9990 \qquad F = 7298$$

Here, r is the regression coefficient, F is Fisher ratio, and ${}^{1}\pi$ stands for the weighted path of length 1 (i.e., the modified connectivity index using $x = 1.25$ and $y = -0.65$). Figure 3 shows a plot of calculated boiling points against the experimental values.

Discussion

The first thing to observe is that the variable graph descriptors (with optimal values of x and y) have reduced the standard error s in the regression of the boiling points in primary alkylamines by almost one-half when compared with the regression based on simple molecular graphs. Typically, in multivariate regression analysis, a reduction of s by half is not easy to achieve, and when reported, often it is achieved by introducing one or more additional molecular descriptors. In contrast, we obtained improved regression still using a single molecular descriptor. The disadvantage of using two or more descriptors over a single descriptor is in the difficulties in the interpretation of the results. Generally, molecular descriptors (topological indices) are interrelated, often strongly interrelated. Due to the interrelatedness of the descriptors, it is not possible to identify the separate roles that individual descriptors play. Even though, recently, the question of interrelatedness of descriptors has finally been successfully resolved [18], nevertheless, it is easier to interpret correlations based on a single descriptor.

Introduction of orthogonal descriptors [18] requires that one order the descriptors, that is, priorities the variables. This can sometimes be accomplished naturally (like in the case of ordering paths according to their length), but sometimes the ordering of the descriptors is not apparent. Hence,

TABLE III

Variation of the standard error s as a function of x and y when weighted paths ${}^{1}\pi$ are used as single descriptor in the regression analysis. x and y represent parameters for carbon and nitrogen atoms, respectively.

	y					
	−0.80	−0.70	−0.65	−0.60	−0.50	0
$x = 0$			2.0812			3.4876
$x = 1.00$	2.6031	1.9632	1.9131	1.9471	2.1213	
$x = 1.25$	2.5366	1.9463	1.9069	1.9506	2.1336	3.0082
$x = 1.50$	2.4697	1.9293	1.9137	1.9674	2.1615	
$x = 1.75$		1.9249	1.9270			
$x = 2.00$			1.9511			

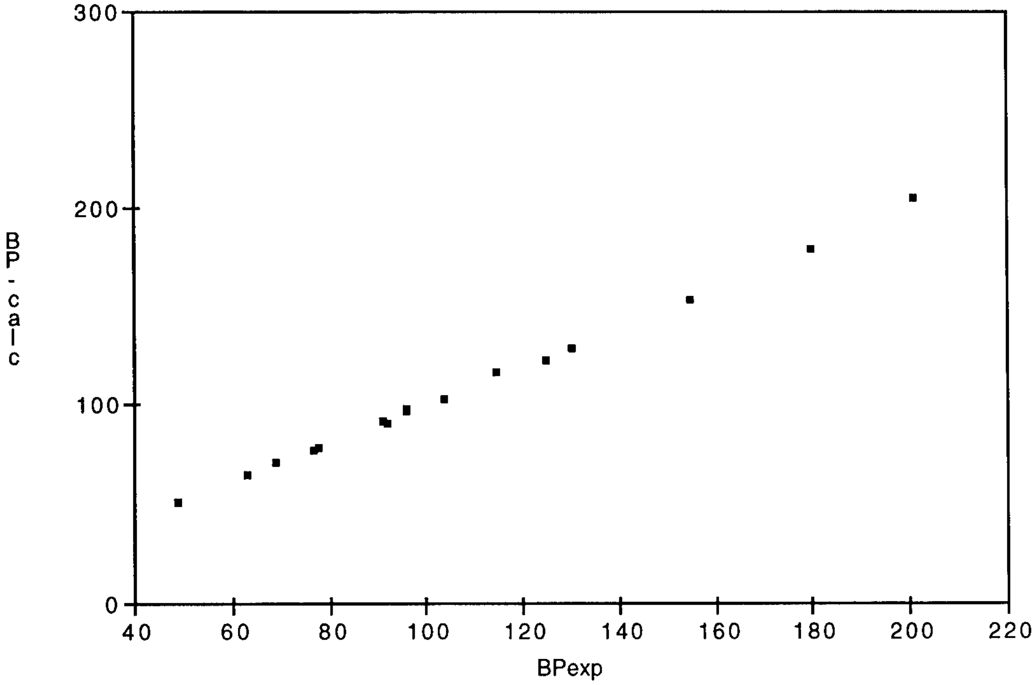

FIGURE 3. Calculated boiling points against the experimental boiling points for the amines examined.

use of a single descriptor clearly has advantages in this respect. An optimal descriptor offers a direct structural interpretation for the property in terms of the dominant variable. In addition, single descriptors, or a set of structurally related descriptors [19], facilitates comparative studies. Recently, in an extensive comparative study of the properties of octanes [20], it was found that only a few molecular descriptors emerge as the best when compared to alternatives. The molecular connectivity indices have been found often among those that give the best regressions. With the outlined procedure, we have initiated an important direction in the search for best molecular descriptors for structure–property studies. We may expect not only improved regression analyses but, hopefully, better insights into the dependence of molecular properties on the shape, the size, and the functionality of molecule forms.

ACKNOWLEDGMENTS

J. Cz. D. would like to thank the Fulbright Foundation for the scholarship award to visit Drake University and the faculty of the Mathematics and Computer Science at Drake University for their hospitality. We thank Professor Gustavo A. Arteca from the Laurentian University (Sudbury, Canada) for helpful comments.

References

1. C. Hansch, Acc. Res., **2**, 232 (1969).
2. N. Trinajstić, M. Randić, and D. J. Klein, Acta Pharm. Jugosl. **36**, 267 (1986).
3. M. Randić and P. Seybold, SAR QSAR Environ. **1**, 77 (1993).
4. N. Trinajstić, *Chemical Graph Theory*, 2nd ed. (CRC Press, Boca Raton, FL, 1992).
5. H. Wiener, J. Am. Chem. Soc. **69**, 2636 (1947).
6. H. Hosoya, Bull. Chem. Soc. Jpn. **44**, 2332 (1971).
7. M. Randić, J. Am. Chem. Soc. **97**, 6609 (1975).
8. L. B. Kier and L. H. Hall, *Molecular Connectivity in Chemistry and Drug Design* (Academic Press, New York, 1976). L. B. Kier and L. H. Hall, *Molecular Connectivity in Structure–Activity Analysis* (Research Studies Press, Letchworth, England, 1986).
9. L. B. Kier and L. H. Hall, J. Pharm. Chem. **65**, 806 (1976).
10. L. B. Kier, W. J. Murray, M. Randić, and L. H. Hall, J. Pharm. Sci. **65**, 1226 (1976).
11. E. J. Kupchik, Quantum Stuct.-Act. Relat. **8**, 98 (1989).
12. M. Randić and S. Basak, J. Chem. Inf. Comput. Sci., in press. M. Randić, New J. Chem. **21**, 945 (1997).
13. M. Randić, Chemometr. Intel. Lab. Syst. **10**, 213 (1991).
14. A. Streitwieser, Jr., *Molecular Orbital Theory for Organic Chemists* (Wiley, New York, 1961).

15. S. C. Grossman, B. Jerman-Blažič Džonova, and M. Randić, Intl. J. Quantum Chem. Quantum Biol. Symp. **12**, 123 (1986).
16. M. Randić, G. M. Brissey, R. B. Spencer, and C. L. Wilkins, Comput. Chem. **3**, 5 (1979). A. J. Stuper, W. E. Brugger, and P. C. Jurs, *Computer Assisted Studies of Chemical Structure and Biological Function* (Wiley-Interscience, New York, 1979).
17. M. Randić, J. Comput. Chem. **12**, 970 (1991).
18. M. Randić, New J. Chem. **15**, 517 (1991). M. Randić, J. Chem. Inf. Comput. Sci. **31**, 311 (1991). M. Randić, Croat. Chem. Acta **64**, 43 (1991). M. Randić, J. Mol. Struct. (Theochem) **233**, 45 (1991).
19. M. Randić and N. Trinajstic, J. Mol. Struct. (Theochem) **284**, 209 (1993).
20. M. Randić, Croat. Chem. Acta **66**, 289 (1993).

International Journal of

Quantum Chemistry

Volume 70
1998

Editor-in-Chief

Per-Olov Löwdin
University of Florida at Gainesville, USA
Uppsala University, Sweden

Editors

Erkki Brändas
Uppsala University, Sweden
Yngve Öhrn
University of Florida at Gainesville, USA

Associate Editors

Osvaldo Goscinski
Uppsala University, Sweden
Sten Lunell
Uppsala University, Sweden
John R. Sabin
University of Florida at Gainesville, USA
Michael C. Zerner
University of Florida at Gainesville, USA

Assistant Editor

Leif Eriksson
Uppsala University, Sweden

Honorary Editors

Gerhard Herzberg
National Research Council,
Ottawa, Ontario, Canada
Jerome Karle
Naval Research Laboratory at
Washington, DC, USA
Rudy Marcus
California Institute of Technology at
Pasadena, USA

Editorial Board

Jiri Čížek
University of Waterloo, Ontario, Canada
Enrico Clementi
Université Louis Pasteur, Strasbourg, France
Raymond Daudel
Académie Européene de Arts, des Sciences
et des Lettres, Paris, France
Ernest Davidson
Indiana University at Bloomington, USA
George G. Hall
University of Nottingham, UK
Laurens Jansen
Kusnacht, Switzerland
Norman H. March
University of Oxford, UK
Roy McWeeny
Università di Pisa, Italy
Saburo Nagakura
Graduate University for Advanced Studies,
Yokohama, Japan
Kimio Ohno
Hokkaido Information University, Japan
Josef Paldus
University of Waterloo, Ontario, Canada
Robert G. Parr
University of North Carolina at Chapel Hill, USA
Ruben Pauncz
Technion, Haifa, Israel
John A. Pople
Northwestern University at Evanston, Illinois, USA
Alberte Pullman
Institut de Biologie Physico-Chimique,
Paris, France
Paul von Ragué Schleyer
Universität Erlangen-Nürnberg,
Erlangen, Germany
Harrison Shull
Naval Postgraduate School,
Monterey, California, USA
Tang Au-Chin
Jilin University, Changchun, China
Rudolf Zahradník
Czech Academy of Sciences,
Prague, Czech Republic

Advisory Editorial Board

Teijo Åberg
Helsinki University of Technology, Espoo,
Finland
Axel D. Becke
Queen's University, Kingston, Ontario, Canada
Gian Luigi Bendazzoli
Università di Bologna, Italy
Jerzy Cioslowski
The Florida State University at Tallahassee, USA
Timothy Clark
Universität Erlangen-Nürnberg, Germany
Mireille Defranceschi
DPEL/SERGD/LMVT,
Fontenay Aux Roses, France
Karl F. Freed
The University of Chicago, Illinois, USA
Odd Gropen
University of Tromsø, Norway
Trygve Helgaker
University of Oslo, Norway
Ming-Bao Huang
Academia Sinica,
Beijing, People's Republic of China
Hiroshi Kashiwagi
Kyushu Institute of Technology, Fukuoka, Japan
Eugene S. Kryachko
Academy of Sciences of Ukraine, Kiev, Ukraine
Sven Larsson
Chalmers University of Technology,
Gothenburg, Sweden
Lucas Lathouwers
Universitair Centrum (RUCA), Antwerp, Belgium
Shyi-Long Lee
National Chung Chang University,
Taiwan, Republic of China
Josef Michl
University of Colorado at Boulder, USA
Nimrod Moiseyev
Israel Institute of Technology, Israel
John D. Morgan III
University of Delaware at Newark, USA
Cleanthes A. Nicolaides
National Hellenic Research Foundation, Greece
J. Vincent Ortiz
Kansas State University at Manhattan, USA
Lars Pettersson
University of Stockholm, Sweden
Leon Phillips
University of Canterbury,
Christchurch, New Zealand
Martin Quack
ETH Zürich, Switzerland
Leo Radom
Australian National University, Australia
William Reinhardt
University of Washington at Seattle, USA
Sten Rettrup
H. C. Ørsted Institut, Copenhagen, Denmark
C. Magnus L. Rittby
Texas Christian University at Fort Worth, USA
Michael Robb
King's College, London, UK
Mary Beth Ruskai
University of Massachusetts at Lowell, USA
Harold Scheraga
Cornell University at Ithaca, New York, USA
Vipin Srivastava
University of Hyderabad, India
Nicolai F. Stepanov
Moscow State University, Russia
Jiazong Sun
Jilin University, Changchun,
People's Republic of China
Donald G. Truhlar
University of Minnesota at Minneapolis, USA
Peter Wolynes
University of Illinois at Urbana, USA
Robert E. Wyatt
The University of Texas at Austin, USA

Editorial Production, John Wiley & Sons: Sheila Kaminsky

The *International Journal of Quantum Chemistry* (ISSN 0020-7608) is published semimonthly with one extra issue in January, March, May, July, August, and November by John Wiley & Sons, Inc., 605 Third Avenue, New York, New York 10158.

Copyright © 1998 John Wiley & Sons, Inc. All rights reserved. No part of this publication may be reproduced in any form or by any means, except as permitted under section 107 or 108 of the 1976 United States Copyright Act, without either the prior written permission of the publisher, or authorization through the Copyright Clearance Center, 222 Rosewood Drive, Danvers, MA 01923, (508) 750-8400, fax (508) 750-4470. Periodicals postage paid at New York, NY, and at additional mailing offices.

The code and the copyright notice appearing at the bottom of the first page of an article in this journal indicate the copyright owner's consent that copies of the article may be made for personal or internal use, or for the personal or internal use of specific clients, on the condition that the copier pay for copying beyond that permitted by Sections 107 or 108 of the US Copyright Law.

This consent does not extend to the other kinds of copying, such as copying for general distribution, for advertising or promotional purposes, for creating new collective work, or for resale. Such permission requests and other permission inquiries should be addressed to the Permissions Dept.

Subscription price (Volumes 66–70, 1998): $4,439.00 in the US, $4,739.00 in Canada and Mexico, $4,964.00 outside North America. All subscriptions outside US will be sent by air. Personal rate (available only if there is an institutional subscription): $195.00 in North America, $375.00 outside North America. Subscriptions at the personal rate are available only to individuals. Payment must be made in US dollars drawn on a US bank. Claims for undelivered copies will be accepted only after the following issue has been received. Please enclose a copy of the mailing label. Missing copies will be supplied when losses have been sustained in transit and where reserve stock permits.

Please allow four weeks for processing a change of address. For subscription inquiries, please call (212) 850-6645; e-mail: SUBINFO@Wiley.com.

Postmaster: Send address changes to *International Journal of Quantum Chemistry*, Caroline Rothaug, Director, Subscription Fulfillment and Distribution, Subscription Department, John Wiley & Sons, Inc., 605 Third Avenue, New York, NY 10158.

Advertising Sales: Inquiries concerning advertising should be forwarded to Advertising Sales Manager, Advertising Sales, John Wiley & Sons, Inc., 605 Third Avenue, New York, NY 10158; (212) 850-8832. Advertising Sales, European Contacts: Bob Kern or Nicky Douglas, John Wiley & Sons, Ltd., Baffins Lane, Chichester, West Sussex PO19 1UD, England. Tel.: 44 1243 770 350/367; Fax: 44 1243 770 432; e-mail: adsales@wiley.co.uk.

Reprints: Reprint sales and Inquiries should be directed to the customer service department, John Wiley & Sons, Inc. 605 Third Ave., New York, NY 10158. Tel: 212-850-8776.

Manuscripts should be submitted in triplicate and accompanied by an executed Copyright Transfer Form to the Editorial Office, *International Journal of Quantum Chemistry*, Quantum Chemistry Group, Uppsala University, Box 518, S-75120, Uppsala, Sweden. Authors may also submit manuscripts to the Editorial Office, *International Journal of Quantum Chemistry*, Quantum Theory Project, 2301 NP Building #92, P.O. Box 118435, Museum Road and North South Drive, University of Florida, Gainesville, Florida 32611-8435. **Information for Contributors** appears in the first and last issue of each volume. **All other correspondence** should be addressed to the *International Journal of Quantum Chemistry*, Publisher, Interscience Division, Professional, Reference, and Trade Group, John Wiley & Sons, Inc., 605 Third Avenue, New York, NewYork 10158, U.S.A. The contents of this journal are indexed or abstracted in *Chemical Abstracts, Chemical Titles, Chemical Database, Current Contents/Physical, Chemical, and Earth Sciences, Research Alert (ISI), Science Citation Index (ISI)*, and *SCISEARCH Database (ISI)*.

This paper meets the requirements of ANSI/NISO
Z39. 48–1992 (Permanence of Paper). ∞

International Journal of Quantum Chemistry Author Index—Volume 70

Abu-Awwad, F. See Murray, J. S., 1137
Ågren, H. See Luo, Y., 219
Agresti, A. See Alagona, G., 395
Alagona, G.
—; Ghio, C.; Agresti, A.; Pratesi, R.: Ab Initio Relative Stability of a Few Conformers of Bilirubin *in Vacuo* and in Aqueous Solution (PCM), 395
André, J.-M. See Champagne, B., 751
Anusooya, Y.
—; Chakrabarti, A.; Pati, S. K.; Ramasesha, S.: Ring Currents in Condensed Ring Systems, 503
Arteca, G. A.
Analysis of Three-Dimensional Molecular Shape Using Surface Area and Molecular Volume Scaling Descriptors, 981
Atabek, O. See Pérez Del Valle, C., 199

Bartlett, R. J. See Del Bene, J. E., 1003
Belmiloud, D.
—; Jacon, M.: DVR Study of the $\tilde{A}^2B_2 \leftarrow \tilde{X}^2A_1$ Absorption Spectrum of NO_2, 475
Benaissa, A. See Vigneron, J.-P., 1093
Benco, Ľ. See Turi Nagy, L., 341
Bergström, R. See Persson, P., 1055
Bertin, V. See Castillo, S., 1029
Bhattacharyya, S. P. See Medhi, C., 415
Bicca de Alencastro, R. See Guimarães, C. R. W., 1145
Boettger, J. C.
Relativistic Effects on the Structural Phase Stability of Molybdenum, 825
Boone, A. J.
—; Magers, D. H.; Leszczyński, J.: Searches on the Potential Energy Hypersurfaces of $GeCH_2$, $GeSiH_2$, and Ge_2H_2, 925
Bouferguene, A.
—; Etemadi, B.; Jones, H. W.: Calculations on Diatomic Molecules with Slater-Type Orbital Basis Sets, 89
Brändas, E. J. See Levitina, T., 1017
Bruno-Blanch, L. See Tasso, S. M., 1127
—; See Lorenzini, L., 1195
Bunge, C. F.
—; Jáuregui, R.; Ley-Koo, E.: Optimal Decoupling of Positive- and Negative-Energy Orbitals in Relativistic Electronic Structure Calculations Beyond Hartree–Fock, 805
Burke, K.
—; Cruz, F. G.; Lam, K.-C.: Unambiguous Exchange–Correlation Energy Density for Hooke's Atom, 583
Butler, L. G.
—; Maverick, A. W.; Gallegos, C. H.; Goettee, J. D.; Marshall, B. R.; Fowler, C. M.; Rickel, D. G.; Gonzales, J. M.; Tabaka, L. J.: Some Aspects of Data Processing for an Optical Absorption Experiment in a Pulsed 1000-Tesla Magnet, 797
Bytautas, L.
—; Klein, D. J.: Symmetry Aspects of Nonrigid Molecules and Transition Structures in Chemical Reactions, 205

Calderone, A.
—; Vigneron, J.-P.: Computation of the Electromagnetic Harmonics Generation by Stratified Systems Containing Nonlinear Layers, 763
Calzado, C. J. See San Miguel, M. A., 351
—; See Fernádez Sanz, J., 359
Canuto, S. See Serrano, A., 745
Cao, Z.
—; Wu, W.; Zhang, Q.: Spectroscopic Constants and Bonding Features of the Low-Lying States of LiB and LiB^+: Comparative Study of VBSCF and MO Theory, 283
Casida, M. E.
—; Casida, K. C.; Salahub, D. R.: Excited-State Potential Energy Curves from Time-Dependent Density-Functional Theory: A Cross Section of Formaldehyde's $^1A_1$ Manifold, 933
Casida, K. C. See Casida, M. E., 933
Castellano, O. See Soscún, H., 951
Castillo, S.
—; Bertin, V.; Solano-Reyes, E.; Luna-García, H.; Cruz, A.; Poulain, E.: Theoretical Studies on the Hydrogen Activation by Iridium Dimers, 1029
Chakrabarti, A. See Anusooya, Y., 503
Champagne, B.
—; Perpète, É. A.; André, J.-M.: Nonresonant Frequency Dispersion of the Electronic Second Hyperpolarizability of *All-Trans* Polysilane Chains: An Ab Initio TDHF Oligomeric Approach, 751
Chen, J. See Wang, Q., 515
Chen, K. See Wang, Q., 515
Chen, T.-L. See Xiao, S.-X., 375
Chernyak, V. See Tretiak, S., 711
Chu, S.-Y. See Su, M.-D., 961
Chuang, Y.-Y.
—; Cramer, C. J.; Truhlar, D. G.: The Interface of Electronic

International Journal of Quantum Chemistry, Vol. 70, pp. 1219–1224 (1998)

Structure and Dynamics for Reactions in Solution, 887
Contreras, R. H. See Peralta, J. E., 105
Cooper, D. L. See Thorsteinsson, T., 637
Cramer, C. J. See Chuang, Y.-Y., 887
Crawford, T. D.
—; Stanton, J. F.: Investigation of an Asymmetric Triple-Excitation Correction for Coupled-Cluster Energies, 601
Cruz, A. See Castillo, S., 1029
Cruz, F. G. See Burke, K., 583

Deb, B. M. See Dey, B. K., 441
De Brito Mota, F.
—; Justo, J. F.; Fazzio, A.: Structural and Electronic Properties of Silicon Nitride Materials, 973
Del Bene, J. E.
—; Watts, J. D.; Bartlett, R. J.: Structure and Poperties of NH_5^{2+}: A Dication with Two 2-electron 3-center Bonds, 1003
Delhalle, J. See Flammant, I., 1045
Delphino da Motta Neto, J. See Guimarães, C. R. W., 1145
Derycke, I. See Vigneron, J.-P., 1093
Dey, B. K.
—; Deb, B. M.: Femtosecond Quantum Fluid Dynamics of Helium Atom Under an Intense Laser Field, 441
Díaz, G. See Soscún, H., 951
Dobrowolski, J. Cz.
—; Mazurek, A. P.: C_{60} Carbyne Knots (from 0_1 to 6_3): Theoretical NMR Spectra, 1009
—; See Randić, M., 1209
Dolgounitcheva, O.
—; Zakrzewski, V. G.; Ortiz, J. V.; Ratovski, G. V.: Electron Propagator Theory of Conformational Effects of Anisole and Thioanisole Photoelectron Spectra, 1037
Dorfman, S.
—; Fuks, D.; Liubich, V.: Sign of the Interaction Parameter in Disordered Fe–Al Alloys, 1067
Dorman, S. See Ellis, D. E., 1085
Dudev, T. See Galabov, B., 331
Durig, J. R. See Galabov, B., 331

Ebner, C.
—; Sansone, R.; Probst, M.: Quantum Chemical Study of the Interaction of Nitrate Anion with Water, 877
Ellis, D. E.
—; Dorfman, S.; Fuks, D.; Evenhaim, R.; Mundim, K. C.: Embedded Cluster and Supercell Study of the Structure of the Interstitial Cu—C Solid Solutions, 1085
Estiú, G. L. See Tasso, S. M., 1127
—; See Lorenzini, L., 1195
Etemadi, B. See Bouferguene, A., 89
Evenhaim, R. See Ellis, D. E., 1085

Fang, D.-C. See Xu, Z.-F., 321
Fazzio, A. See De Brito Mota, F., 973
Fernández Sanz, J.
—; Rabaâ, H.; Poveda, F. M.; Márquez, A. M.; Calzado, C. J.: Theoretical Models for γ-Al_2O_3 (110) Surface Hydroxylation: An Ab Initio Embedded Cluster Study, 359
—; See San Miguel, M. A., 351
Flammant, I.
—; Fripiat, J. G.; Delhalle, J.: Advantages of the Fourier Space RHF Band Structure Approach: Application to Polyoxymethylene Using a Distributed Basis Set of *s*-Type Gaussian Functions, 1045
Fowler, C. M. See Butler, L. G., 797
Freund, L.
—; Klessinger, M.: Photochemical Reaction Pathways of Ethylene, 1023
Friedemann, R.
—; Von Fircks, A.; Naumann, S.: GROMOS-MD Simulations on the Coenzyme Thiamin Diphosphate in Apoenzyme Environment, 407
Fripiat, J. G. See Flammant, I., 1045
Fu, X.-Y. See Xu, Z.-F., 321
Fuks, D. See Dorfman, S., 1067
—; See Ellis, D. E., 1085

Galabov, B.
—; Dudev, T.; Ilieva, S.; Durig, J. R.: Creation of Intensity Theory in Vibrational Spectroscopy: Key Role of Ab Initio Quantum Mechanical Calculations, 331
Galasso, V.
Theoretical Study of Structure and NMR Properties of the μ-Hydrido-Bridged Cyclodecyl Cation and Related Systems, 313
Gallegos, C. H. See Butler, L. G., 797
Ghio, C. See Alagona, G., 395
Goettee, J. D. See Butler, L. G., 797
Gonzales, J. M. See Butler, L. G., 797
Gorb, L.
—; Leszczynski, J.: Intramolecular Proton Transfer in Monohydrated Tautomers of Cytosine: An Ab Initio Post-Hartree–Fock Study, 855
Guimarães, C. R. W.
—; Delphino da Motta Neto, J.; Bicca de Alencastro, R.: Phytochrome Structure: A New Methodological Approach, 1145

Hagmann, M. J.
Stable and Efficient Numerical Method for Solving the Schrödinger Equation to Determine the Response of Tunneling Electrons to a Laser Pulse, 703
Harris, F. E.
More About the Leaky Aquifer Function, 623
Herman, M. F.
The Development of Semiclassical Dynamical Methods and Their Application to Vibrational Relaxation in Condensed-Phase Systems, 897
Hernández, J. See Soscún, H., 951

Heryadi, D. See McKellar, A. J., 729
Hinchliffe, A. See Soscún, H., 951
Hoggan, P. E. See Safouhi, H., 181

Iguchi, K. See Tachikawa, M., 491
Ilieva, S. See Galabov, B., 331
Ishikawa, Y. See Vilkas, M. J., 813

Jacon, M. See Belmiloud, D., 475
Jáuregui, R. See Bunge, C. F., 805
Ji, R. See Wang, Q., 515
Jiang, H. See Wang, Q., 515
Jones, H. W. See Bouferguene, A., 89
Jonsson, D. See Luo, Y., 219
Jubert, A. H. See Michelini, M. C., 693
Justo, J. F. See De Brito Mota, F., 973

Kállay, M. See Surján, P. R., 571
Kamada, K.
—; Ueda, M.; Nagao, H.; Tawa, K.; Sugino, T.; Shimizu, Y.; Ohta, K.: Effect of Heavy Atom on the Second Hyperpolarizability of Tetrahydrofuran Homologs Investigated by Ab Initio Molecular Orbital Method, 737
Karasiev, V.
—; Ludeña, E. V.; López-Boada, R.: SCF Calculations with Density-Dependent Local-Exchange Potential, 591
Karna, S. P.
Theory and Calculations of Electric Field Effects on Hyperfine Interactions, 771
Katriel, J.
Products of Arbitrary Class-Sums in the Symmetric Group, 429
Kieninger, M.
—; Ventura, O. N.; Suhai, S.: Density Functional Investigations of Carboxyl Free Radicals: Formyloxyl, Acetyloxyl, and Benzoyloxyl Radicals, 253
King, J. W. See Molnar, S. P., 1185
Kiribayashi, S. See Nakano, M., 269
Klein, D. J.
—; Bytautas, L., 205
Klessinger, M. See Freund, L., 1023
Koc, K. See Vilkas, M. J., 813
Kryachko, E. S.
Water Cluster Approach to Study Hydrogen-Bonded Pattern in Liquid Water: Ab Initio Orientational Defects in Water Hexamers and Octamers, 831
Kumar, A.
—; Saha, B. C.; Weatherford, C. A.: Single-Electron-Capture Cross Sections by Alpha-Particles from Ground State $K(4s)$ and Rb(5s): A Molecular-State Approach, 909

Lam, K.-C. See Burke, K., 583
Lamm, G. See Pack, G. R., 1177
Larin, A. V.
—; Vercauteren, D. P.: Approximations of the Mulliken Charges for the Oxygen and Silicon Atoms of Zeolite Frameworks Calculated with a Periodic Hartree–Fock Scheme, 993
Lefebvre, R. See Pérez Del Valle, C., 199
Leszczynski, J. See Gorb, L., 855
—; See Boone, A. J., 925
Levitina, T.
—; Brändas, E. J.: Perturbed Ellipsoidal Wave Functions for Quantum Scattering, 1017
Ley-Koo, E. See Bunge, C. F., 805
Li, X.
—; Paldus, J.: Unitary-Group-Based Open-Shell Coupled-Cluster Method with Corrections for Connected Triexcited Clusters. I. Theory, 65
Liška, M. See Turi Nagy, L., 341
Liubich, V. See Dorfman, S., 1067
Longo, E. See Martins, J. B. L., 367
Longstreet, A. See Paikeday, J. M., 943
López-Boada, R. See Karasiev, V., 591
Lorenzini, L.
—; Bruno-Blanch, L.; Estiú, G. L.: Theoretical Approach to the Pharmacophoric Pattern of GABA$_B$ Analogs, 1195
Ludeña, E. V. See Karasiev, V., 591
Luna-García, H. See Castillo, S., 1029
Lunell, S. See Persson, P., 1055
Luo, Y.
—; Jonsson, D.; Norman, P.; Ruud, K.; Vahtras, O.; Minaev, B.; Ågren, H.; Rizzo, A.; Mikkelsen, K. V.: Some Recent Developments of High-Order Response Theory, 219

Mach, P. See Turi Nagy, L., 341
Machado, E. See Sierraalta, A., 113
Magers, D. H. See Boone, A. J., 925
Malrieu, J.-P. See Reinhardt, P., 167
March, N. H.
Differential Equations of Ground-State Electron Density and Slater Sum in Atoms and Moleculars With and Without External Fields, 779
Márquez, A. M. See Fernádez Sanz, J., 359
Marshall, B. R. See Butler, L. G., 797
Martins, J. B. L.
—; Longo, E.; Taft, C. A.: Co$_2$ and NH$_3$ Interactions with ZnO Surface: An AM1 Study, 367
Masuda, K. See Takahashi, J., 379
Maverick, A. W. See Butler, L. G., 797
Mayer, I.
The Chemical Hamiltonian Approach for Treating the BSSE Problem of Intermolecular Interactions, 41
Mazurek, A. P. See Dobrowolski, J. Cz., 1009
Mazziotti, D. A.
3,5-Contracted Schrödinger Equation: Determining Quantum Energies and Reduced Density Matrices without Wave Functions, 557
McKellar, A. J.
—; Heryadi, D.; Yeager, D. L.: Balanced Complete Active Space Choices with the Multi-

configurational Spin Tensor Electron Propagator Method: The Vertical Ionization Potentials of NH$_2$, 729
Medhi, C.
—; Bhattacharyya, S. P.: Macroscopic Solvent Polarization-Induced Reorganization of the Electron Density in Different Excited States: A Study on Formaldehyde Molecule by a Multiconfiguration Self-Consistent Reaction-Field Method, 415
Michelini, M. C.
—; Pis Diez, R.; Jubert, A. H.: A Density Functional Study of Small Nickel Clusters, 693
Micov, M. See Turi Nagy, L., 341
Mikkelsen, K. V. See Luo, Y., 219
Minaev, B. See Luo, Y., 219
Mitani, M. See Shigeta, Y., 659
—; See Nagao, H., 1075
Molnar, S. P.
—; King, J. W.: Parametric Transform and Moment Indices in the Molecular Dynamics of n-Alkanes, 1185
Mori, K. See Tachikawa, M., 491
Morokuma, K.
Introduction to Special Issue: The Ninth International Congress of Quantum Chemistry, 1
Mosley, D. H.
Perspectives for Java-Based Computational Quantum Chemistry, 159
Mukamel, S. See Tretiak, S., 711
Mundim, K. C. See Ellis, D. E., 1085
Murray, J. S.
—; Abu-Awwad, F.; Politzer, P.; Wilson, L. C.; Troupin, A. S.; Wall, R. E.: Molecular Surface Electrostatic Potentials of Anticonvulsant Drugs, 1137

Nagao, H.
—; Mitani, M.; Nishino, M.; Shigeta, Y.; Yoshioka, Y.; Yamaguchi, K.: Possibility of Charge-Mediated Superconductors in the Intermediate Region of Metal–Insulator Transitions, 1075
—; See Shigeta, Y., 659
—; See Kamada, K., 737
Nagaoka, M.
—; Okuno, Y.; Yamabe, T.: "Statistical–Mechanical" Understanding of Chemical Reaction Mechanism in Solution: Energy Fluctuations and Heat Capacities for Isomerization of Formamidine in Aqueous Solution, 133
—; See Okuyama-Yoshida, N., 95
—; See Takahashi, J., 379
Nagy, Á.
Excited States in the Density Functional Theory, 681
Nakano, M.
—; Yamada, S.; Kiribayashi, S.; Yamaguchi, K.: Hyperpolarizabilities of One-Dimensional H$_n$ Systems: Second Hyperpolarizability Density Analyses for Regular and Charged Solitonlike Linear Chains, 269
—; Yamaguchi, K.: Numerical Coupled Liouville Approach: Quantum Dynamics of Linear Molecular Aggregates Under Intense Electric Fields, 77
Naumann, S. See Friedemann, R., 407
Nishino, M. See Nagao, H., 1075
Norman, P. See Luo, Y., 219

Öhrn, N. Y.
—; Sabin, J. R.; Zerner, M. C.: Introduction to Proceedings of the 38th Annual Sanibel Symposium (Chemistry), 529
—; Sabin, J. R.; Zerner, M. C.: Introduction to the Proceedings of the 38th Annual Sanibel Symposium (Biology), 1099
Ohta, K. See Kamada, K., 737
Okuno, Y. See Nagaoka, M., 133
Okuyama-Yoshida, N.
—; Nagaoka, M.; Yamabe, T.: Transition-State Optimization on Free Energy Surface: Toward Solution Chemical Reaction Ergodography, 95
Ortiz, E. See Viruela, P. M., 303
Ortiz, J. V.
Approximate Brueckner Orbitals and Shakeup Operators in Electron Propagator Calculations: Applications to F$^-$ and OH$^-$, 651
—; See Dolgounitcheva, O., 1037

Pack, G. R.
—; Wong, L.; Lamm, G.: pK_a of Cytosine on the Third Strand of Triplex DNA: Preliminary Poisson–Boltzmann Calculations, 1177
Pahl, Felix A.
Atomic Calculations with an Augmented Fourier Basis, 189
Paikeday, J. M.
—; Longstreet, A.: Effective Potential for e-Neon and e-Argon Scattering by DCS Minimization at Intermediate Energies, 943
Paldus, J. See Li, X., 65
Parrinello, M. See Rovira, C., 387
Pati, S. K. See Anusooya, Y., 503
Payne, J. O. See Schmiedekamp, L. A., 863
Peralta, J. E.
—; Ruiz de Azúa, M. C.; Contreras, R. H.: Electrostatic Effect of the Polar Bond–Polarizable Bond Interaction on ^{13}C Chemical Shifts, 105
Pérez Del Valle, C.
—; Lefebvre, R.; Atabek, O.: Dressed Potential Energy Surface of the Hydrogen Molecule in High-Frequency Floquet Theory, 199
Perpète, É. A. See Champagne, B., 751
Persson, P.
—; Stashans, A.; Bergström, R.; Lunell, S.: Periodic INDO Calculations of Organic Adsorbates on a TiO$_2$ Surface, 1055
Pinchon, D. See Safouhi, H., 181
Pipek, J.
—; Varga, I.: Scaling Behavior of Energy Functionals of Highly Complex Electronic Distributions, 125
Pis Diez, R. See Michelini, M. C., 693
Politzer, P. See Murray, J. S., 1137

Porter, L. E.
Bethe–Bloch Stopping-Power Parameters for GaAs and ZnSe, 919
Poulain, E. See Castillo, S., 1029
Poveda, F. M. See Fernádez Sanz, J., 359
Povill, À. See Reinhardt, P., 167
Pratesi, R. See Alagona, G., 395
Probst, M. See Ebner, C., 877

Qian, Z.
—; Sahni, V.: Analytical Asymptotic Structure of the Pauli, Coulomb, and Correlation–Kinetic Components of the Kohn–Sham Theory Exchange–Correlation Potential in Atoms, 671

Rabaâ, H. See Fernádez Sanz, J., 359
Ramasesha, S. See Anusooya, Y., 503
Ramek, M.
—; Tomić, S.: RHF Conformational Analysis of the Auxin Phytohormones *n*-Ethyl–Indole-3-Acetic Acid ($n = 4, 5, 6$), 1169
Randić, M.
—; Dobrowolski, J. Cz.: Optimal Molecular Connectivity Descriptors for Nitrogen-Containing Molecules, 1209
Ratovski, G. V. See Dolgounitcheva, O., 1037
Reinhardt, P.
—; Malrieu, J.-P.; Povill, À.; Rubio, J.: Localized Orbitals in Nonmetallic Ring Systems, 167
Rickel, D. G. See Butler, L. G., 797
Ritchie, B.
—; Weatherford, C. A.: Use of a Fast Fourier Transform (FFT) 3D Time-Dependent Schrödinger Equation Solver in Molecular Electronic Structure, 627
Rizzo, A. See Luo, Y., 219
Rovira, C.
—; Parrinello, M.: Oxygen Binding to Iron–Porphyrin: A Density Functional Study Using Both LSD and LSD + GC Schemes, 387
Rubio, J. See Reinhardt, P., 167
Ruette, F. See Sierraalta, A., 113
Ruiz de Azúa, M. C. See Peralta, J. E., 105
Ruud, K. See Luo, Y., 219

Sabin, J. R. See Öhrn, N. Y., 529, 1099
Safouhi, H.
—; Pinchon, D.; Hoggan, P. E.: Efficient Evaluation of Integrals for Density Functional Theory: Nonlinear *D* Transformations to Evaluate Three-Center Nuclear Attraction Integrals over *B* Functions, 181
Saha, B. C. See Kumar, A., 909
Sahni, V. See Qian, Z., 671
Sakai, S.
Theoretical Model for the Reaction Mechanisms of Singlet Carbene Analogs into Unsaturated Hydrocarbon and the Origin of the Activation Barrier, 291
Salahub, D. R. See Casida, M. E., 933
San Miguel, M. A.
—; Calzado, C. J.; Fernández Sanz, J.: First Principles Study of Na Adsorption on TiO_2 (110) Surface, 351
Sansone, R. See Ebner, C., 877
Schmelcher, P.
Ground States of Atoms and Molecules in Strong Magnetic Fields, 789
Schmiedekamp, L. A.
—; Payne, J. O.: Intramolecular Hydrogen Bonding in Resonance-Stabilized Systems, 863
Serrano, A.
—; Canuto, S.: Structure Dependence of the Low-Lying Excited States and the First Dipole Hyperpolarizability of Phenol Blue, 745
Shigeta, Y.
—; Takahashi, H.; Yamanaka, S.; Mitani, M.; Nagao, H.; Yamaguchi, K.: Density Functional Theory Without the Born–Oppenheimer Approximation and Its Application, 659
—; See Nagao, H., 1075
Shimizu, Y. See Kamada, K., 737
Sierraalta, A.
—; Ruette, F.; Machado, E.: Topology of Electronic Densities Taken from Parametric Methods: A Predictive Tool?, 113
Solano-Reyes, E. See Castillo, S., 1029
Soscún, H.
—; Hernández, J.; Castellano, O.; Díaz, G.; Hinchliffe, A.: Ab Initio SCF–MO Study of the Topology of the Charge Distribution of Acid Sites of Zeolites, 951
Sporken, R. See Vigneron, J.-P., 1093
Stanton, J. F. Crawford, T. D., 601
Stashans, A. See Persson, P., 1055
Stavrev, K. K.
—; Zerner, M. C.: Studies on the Hydrogenation Steps of the Nitrogen Molecule at the *Azotobacter vinelandii* Nitrogenase Site, 1159
Steiner, M. M. See Wenzel, W., 147
Su, M.-D.
—; Chu, S.-Y.: Singlet–Triplet Splitting and the Activation of C—H Bond for (η^5-C_5H_5)M(CO) Isoelectronic Fragments: A Theoretical Study, 961
Sugino, T. See Kamada, K., 737
Suhai, S. See Kieninger, M., 253
Surján, P. R.
—; Kállay, M.; Szabados, Á.: Nonconventional Partitioning of the Many-Body Hamiltonian for Studying Correlation Effects, 571
Suzuki, K. See Tachikawa, M., 491
Szabados, Á. See Surján, P. R., 571

Tabaka, L. J. See Butler, L. G., 797

Tachikawa, M.
—; Mori, K.; Suzuki, K.; Iguchi, K.: Full Variational Molecular Orbital Method: Application to the Positron-Molecule Complexes, 491
Taft, C. A. See Martins, J. B. L., 367
Takahashi, H. See Shigeta, Y., 659
Takahashi, J.
—; Nagaoka, M.; Masuda, K.: Quantum Mechanical Treatment for the Diffusion Process of a Hydrogen Atom on the Amorphous Water Ice Surface, 379
Tasso, S. M.
—; Bruno-Blanch, L.; Estiu, G. L.: On the Origin of the Lack of Anticonvulsant Activity of Some Valpromide Derivatives, 1127
Tasumi, M. See Torii, H., 241
Tawa, K. See Kamada, K., 737
Thorsteinsson, T.
—; Cooper, D. L.: Modern Valence Bond Descriptions of Molecular Excited States: An Application of CASVB, 637
Tomić, S. See Ramek, M., 1169
Torii, H.
—; Tasumi, M.: Intermolecular Hydrogen Bonding and Low-Wave-Number Vibrational Spectra of Formamide, *N*-Methylformamide, and *N*-Methylacetamide in the Liquid State, 241
Tretiak, S.
—; Chernyak, V.; Mukamel, S.: Excited Electronic States of Carotenoids: Time-Dependent Density-Matrix-Response Algorithm, 711
Troupin, A. S. See Murray, J. S., 1137
Truhlar, D. G. See Chuang, Y.-Y., 887
Tunega, D. See Turi Nagy, L., 341
Turi Nagy, L.
—; Micov, M.; Benco, Ľ; Liška, M.; Mach, P.; Tunega, D.: Electronic Structure of Alumina Surface, 341

Ueda, M. See Kamada, K., 737

Vahtras, O. See Luo, Y., 219
Varga, I. See Pipek, J., 125
Ventura, O. N. See Kieninger, M., 253
Vercauteren, D. P. See Larin, A. V., 993
Vigneron, J.-P.
—; Benaissa, A.; Derycke, I.; Wiame, A.; Sporken, R.: Atomic Motion at Germanium Surfaces: Scanning Tunneling Microscopy and Monte Carlo Simulations, 1093
—; See Calderone, A., 763
Vilkas, M. J.
—; Ishikawa, Y.; Koc, K.: Second-Order Multiconfigurational Dirac–Fock Calculations on Boronlike Ions, 813
Viruela, P. M.
—; Viruela, R.; Orti, E.: Difficulties of Density Functional Theory in Predicting the Torsional Potential of 2,2′-Bithiophene, 303
Viruela, R. See Viruela, P. M., 303
Von Fircks, A. See Friedemann, R., 407

Wall, R. E. See Murray, J. S., 1137
Wang, Q.
—; Jiang, H.; Chen, J.; Chen, K.; Ji, R.: On the Possible Reaction Pathway for the Acylation of AChE-Catalyzed Hydrolysis of ACh: Semiempirical Quantum Chemical Study, 515
Watts, J. D. See Del Bene, J. E., 1003
Weatherford, C. A. See Ritchie, B., 627
—; See Kumar, A., 909
Wenzel, W.
—; Steiner, M. M.; Wilson, K. G.: Scaling Behavior of Dynamic Correlation Effects, 147
Excitation Energies in Brillouin–Wigner-Based Multireference Perturbation Theory, 613
Wiame, A. See Vigneron, J.-P., 1093
Wilson, K. G. See Wenzel, W., 147
Wilson, L. C. See Murray, J. S., 1137
Wong, L. See Pack, G. R., 1177
Wu, W. See Cao, Z., 283

Xiao, S.-X.
—; Yang, S.-Y.; Chen, T.-L.: Electronic Structure and Catalytic Properties of Waugh-Type Anion (NiMo$_9$O$_{32}$)$^{6-}$, 375
Xu, Z.-F.
—; Fang, D.-C.; Fu, X.-Y.: Ab Initio Study on the Reaction 2NH$_2$ → NH + NH$_3$, 321

Yamabe, T. See Okuyama-Yoshida, N., 95
—; See Nagaoka, M., 133
Yamada, S. See Nakano, M., 269
Yamaguchi, K. See Nakano, M., 77
—; See Nakano, M., 269
—; See Shigeta, Y., 659
—; See Nagao, H., 1075
Yamanaka, S. See Shigeta, Y., 659
Yang, S.-Y. See Xiao, S.-X., 375
Yeager, D. L. See McKellar, A. J., 729
Yoshioka, Y. See Nagao, H., 1075

Zakrzewski, V. G. See Dolgounitcheva, O., 1037
Zerner, M. C. See Öhrn, N. Y., 529, 1099
—; See Stavrev, K. K., 1159
Zhang, Q. See Cao, Z., 283

International Journal of Quantum Chemistry Subject Index—Volume 70

Ab initio, 269, 1009
Ab initio calculations, 313, 331
Ab initio embedded cluster calculations, 351
Ab initio Hartree–Fock embedded cluster calculations, 359
Ab initio HF methods, 113
Ab initio HF/6-311(*d*, *p*) calculation, 831
Ab initio molecular orbital methods, 291, 737
Ab initio molecular orbital theory, 951
Ab initio multiconfigurational self-consistent-field calculations (MC SCF), 1029
Ab initio post-Hartree–Fock, 855
Absorption spectra, 1145
Absorption spectrum, 475
Acetylcholinesterase, 515
Acid sites, 951
Activation barrier, 291
Acylation process, 515
Adatom–surface interaction models, 1093
Adiabatic connection, 681
Adsorption, 367, 1055
Alignment, 199
Alkali atoms, 909
Alkali metal atoms, 351
Alkanes, 1185
Alumina, 341
α-particles, 909
Amide compounds, 241
AM1, 367
Amorphous water ice suface, 379
Analytic energy gradient theory, 601
Anticonvulsant activity, 1127
Anticonvulsants, 1137
Approximate Brueckner orbitals, 651
Argon atoms, 943
Atom–laser interaction, 441
Atomic Hartree–Fock, 189
Atomic motion, 1093
Atoms, 789
Augmented Fourier basis, 189
Avoided crossings, 933

Band structure, 1045
Barkas-effect parameter, 919
Basis set, 113
Basis-set reduction (BSR), 613
Bcc–fcc structural energy difference, 825
Bessel function, 623
Bethe–Bloch theory, 919
Bi-isonicotinic acid, 1055
Bithiophene, 303
Bond alternation, 269
Born-Oppenheimer approximation (BOA), 659
Boronlike ions, 813
Bosonization, 711
Brillouin–Wigner multireference perturbation theory, 613
BSSE problem of intermolecular interactions, 41

Canonical molecular orbitals, 1037
Carbon allotrope, 1009
Carbonyloxyl radicals, 253
Carbyne, 1009
Carotenoids, 711
Car–Parrinello molecular dynamics, 387
CASPT2, 253
CASVB, 637
Catalytic mechanism, 515
Catalytic properties, 375
Charge-mediated superconductor, 1075
Charge transfer, 909
Chemical Hamiltonian approach (CHA), 41
Chemical reactions, 253
Chemical shifts, 313
cis–trans isomerization, 1023
Classical molecular dynamics (MD) simulation, 379
Class-sums, 429
Close coupling, 909
^{13}C magnetic shieldings, 105
^{13}C-NMR, 1009
Composites, 1085
Condensed phases, 897
Configuration interaction, 813
Conformational studies, 407
Conical intersections, 1023
Conjugated molecules, 503
Connected triexcited clusters, 65
Continuum solvent, 395
Correction vector technique, 503
Correlation effects, 571, 1037
Correlation–kinetic effects, 671
Coulomb repulsion, 671
Coupled-cluster calculations, 1003
Coupled-cluster doubles calculation, 651
Coupled-cluster theory, 601
Coupled Liouville equation, 77
Cytosine complexes, 855

"Dangling" bond, 831
Density functional BLYP calculations, 951
Density functional calculations, 387
Density functional theory, 441, 583, 591, 659, 681, 779, 1159
Density matrix response functions, 711
DFT, 253
DFT calculations, 303
Diatomic molecules, 89
Dication, 1003
Differential scattering cross-section (DCS), 943
Diffusion process, 379
Dimer, 693
Discrete variable representation (DVR), 475
Double zeta basis sets, 321
Dressed molecular states, 199
DV-Xα method, 375
Dynamic correlation effects, 147

Electric field effects, 771
Electromagnetism, 763
Electron correlation, 269, 571
Electron densities, 125
Electron density contours, 981
Electron–electron interaction, 1075
Electronic charge density, 415
Electronic density Laplacian, 113
Electronic structure, 375
Electronic-structure calculations, 623, 1067, 1085
Electron propagator, 729
Electron propagator calculations, 1037
Electron propagator methods, 651
Electrons, 703, 943
Ellipsoidal coordinate system, 1017
Energy functionals, 125
Energy-gradient method, 321
Energy transfer, 134
Equation-of-motion coupled-cluster theory, 601
Equilibrium solvation path (ESP) approximation, 887
Equilibrium structure, 313
Exchange–correlation energy, 583
Exchange-energy, 591
Exchange potential, 591
Excited states, 283, 637
Excited state surfaces, 933
External magnetic field, 789

Fast Fourier transform (FFT), 627
Fe–Al alloys, 1067
Femtosecond dynamics, 441
First dipole hyperpolarizability, 745
Floquet theory, 199
Formamidine, 134
Fourier-fitted torsional potentials, 303
Fourier space, 1045
Free energy surface, 95
Frequency-dependent electronic second hyperpolarizability, 751
Full-potential linear muffin-tin orbital (FP–LMTO) method, 825
Full variational molecular orbital method, 491
Fused-sphere surfaces, 981

$GABA_B$ analogs, 1195
γ-Al_2O_3(110) surface hydroxylation, 359
Gas-phase stability, 395
Gaussian-type functions, 89, 1045
Germanium surfaces, 1093
Green's function, 729
Ground-state density amplitude, 779
Ground states, 789

Hamiltonian, 41
Hartree–Fock, 737, 951
Hartree–Fock (HF) reference state, 571
Hartree–Fock orbitals, 651
H-bond pattern, 831
Heat capacity, 134
Heme models, 387
Heteropoly compounds, 375
HF/STO-3G*-optimized geometries, 1137
High harmonic generation, 441
High-order response theory, 219
Homopurine–homopyrimidine mixtures, 1177
Hooke's atom, 583
Hydrocarbons, 981
Hydrogen activation, 1029
Hydrogenation of N_2, 1159
Hydrogen atom, 379
Hydrogen bonding, 241, 407
Hydrogen chain, 269
Hydrogen molecule, 199
[1,2]hydrogen shift, 1023
Hydrology, 623
Hydroxylation, 359
Hyperfine interactions, 771
Hyperpolarizability, 77, 269, 745

Indole auxins, 1169
Infrared (IR) spectroscopy, 863
Integrated molecular transform (FT_m), 1185
Intense fields, 199
Intensities, 241
Intensity theory, 331
Intermolecular proton transfer, 855
Internal rotation, 303
Intramolecular H bonds, 395
Intramolecular hydrogen bonding, 863
Intrinsic reaction coordinate (IRC), 95, 321

Ionization potenitals, 729
Iridium clusters, 1029
Iron–porphyrin, 387
Isomerizations, 253
Isotopes, 659

Jahn–Teller deformations, 693
Java, 159

Kato's theorem, 681
Knot, 1009
Kohn–Sham (KS) theory exchange–correlation potential, 671
Krieger, Li, and Iafrate (KLI) approximation, 681

Leaky aquifer function, 623
LiB, 283
Linear molecular aggregate, 77
Liquid structure, 241
Liquid water, 831
Localized orbitals, 167
Local spin density functional theory, 693
Low-lying absorption transition, 745
Low-wave-number vibrational spectra, 241

Macroscopic solvation, 415
Magnetic shielding constants, 105
Many-Body Hamiltonian, 571
Maxwell's equations, 763
MBPT, 147
MCSTEP, 729
Mean excitation energy, 919
Metal–insulator transitions, 1075
Microstructure, 1085
Mixed quantum-classical calculational procedure, 897
Modern valence bond theory, 637
MO expansion, 909
Molecular connectivity indices, 1209
Molecular dynamics simulations, 351
Molecular dynamics, 134, 407, 1185
Molecular electronic structure, 627
Molecular similarity, 981, 1195
Molecular surface electrostatic potentials, 1137
Molecules, 789

Møller–Plesset (MP) partition, 571
Molybdenum, 825
Monte Carlo simulations, 973, 1093
MP2 calculations, 303
μ-hydrido-bridging, 313
Mulliken charges, 993
Multicenter integrals, 89
Multiconfiguration self-consistent reaction-field model, 415
Multifractal structures, 125
Multireference perturbation theory, 147

Na adsorption, 351
Negative-energy orbitals, 805
Neon atoms, 943
NH_2, 729
Nitrate anion, 877
Nitrate–water cluster geometries, 877
Nitrate–water interaction, 877
Nitrogenase, 1159
Nitrogen atoms, 1209
Nitrogen molecule, 1159
Nonadiabatic transitions, 897
Nondiabatic singlet photoreactions, 1023
Nonlinear *D* transformations, 181
Nonlinear optical (NLO) processes, 751
Nonlinear optics, 763
Nonlinear properties, 219
Nonlinear response, 711
Nonrigid molecule, 205
N-representability conditions, 557
N-scaling, 711
Nuclear attraction integral, 181
Nuclear magnetic resonance (NMR), 863
Nuclear spin–spin coupling constants, 313
Nuclear wave function, 491

Object-oriented programming, 159
Octachlorodirhenate, 797
One-electron systems, 789
Open-shell systems, 65
Optical bistability, 77
Optical retarded field, 77
Optimal decoupling, 805
Optimum geometries, 925
Orbital relaxation, 491
Orbitals, 805
Ordering, 1067
Orientational defect, 831
Outer valence Green's function, 1037
Oxidative addition reaction, 961
Oxyheme, 387

Pariser–Parr–Pople model, 503
Partial third-order calculations, 1037
Pauli exclusion principle, 671
Pauli potential, 779
Pentacoordinate nitrogen, 1003
Periodic Hartree–Fock, 993
Periodic INDO, 1055
Periodic SCF, 341
Periodic structures, 167
Perturbation theory, 147, 167, 601
Perturbation-theory calculations, 863
Perturbative corrections, 65
Perturbed Lamé wave functions, 1017
Pharmacophoric pattern, 1195
Phase transitions, 1067
Phenol Blue, 745
Photoelectron spectra, 1037
Phytochrome, 1145
Point charge model, 395
Point charges, 359
Poisson–Boltzmann calculations, 1177
Polar bond, 105
Polar media, 855
Polarizable bond, 105
Polarization, 415
Polarization functions, 321
Polarization potential, 943
Polymers, 1045
Polysilane chains, 751
Positive-energy orbitals, 805
Positron affinity, 491
Positron-molecule complex, 491
Potential energy hypersurfaces, 925
Potential energy surface (PES), 205, 475, 961, 1029
Potential functions, 877
Primary-space wave function, 613
Projectile–target combination, 919
Proton transfer, 134
Pulsed magnetic field, 797
Quadruple metal bonds, 797
Quantum chemical calculations, 1195
Quantum chemistry software, 159
Quantum energies, 557
Quantum fluid dynamics, 441

Rapid evaluation, 181
Reaction path, 205
Reduced density matrices, 557
Relativistic configuration interaction (CI) calculations, 805
Relativistic pseudopotentials, 1029
Relativity, 813, 825
Resonance-stabilized systems, 863
Restricted Hartree–Fock, 1045
RHF/6-31G* investigations, 1169
Ring currents, 503
Rutile, 1055

Scaling theory, 147
Scanning tunneling microscopy (STM), 1093
Scattering data, 1017
Schrödinger equation, 703, 779, 1017
Schrödinger wave function, 671
Second hyperpolarizabilities, 737
Second-order Møller–Plesset (MP2), 951
Second-order multiconfigurational Dirac–Fock self-consistent-field calculations, 813
Second-order perturbation theory, 925
Self-consistent-field calculation, 591
Semiclassical surface-hopping propagator, 897
Semiempirical, 367, 1145
Separable equilibrium solvation (SES) approximation, 887
Silicon nitride systems, 973
Single excited state, 681
Singlet carbene analogs, 291
Singlet–triplet splitting, 961
Slater sum, 779
Slater-type functions, 89
Small nickel clusters, 693
Solid solutions, 1085
Solution chemical reaction ergodography, 95

Solutions, 887
Solvation free energy, 395
Solvation Model 5, 887
Solvents, 745
Spectroscopic constants, 283
Spin-coupled wave function, 637
Stopping power, 919
Stratified system, 763
Structural phase stability, 825
Structure–property correlations, 1209
Surface potential, 341
Symmetric group, 429
Symmetry group, 205

Tersoff functional form, 973
Tetrahydrofuran homologs, 737
Three-electron systems, 789
3,5-contracted Schrödinger equation, 557
TiO_2 rutile surface, 351
TiO_2 surface, 1055
Time-dependent density-functional theory, 933
Time-dependent Hartree–Fock, 711, 751
Time-dependent Schrödinger equation, 627
Topological isomerism, 1009
Transfer matrix, 763
Transition-metal cluster geometries, 693
Transition state, 515
Transition-state optimization, 95
Transition structure, 205
Triple-excitation corrections, 601
Triple-helical structure, 1177
Triple zeta basis sets, 321
Tunneling transit time, 703
Two-electron systems, 789
Unambiguous exchange–correlation energy density, 583
Unitary-group-based perturbation theory, 65
Unsaturated hydrocarbon, 291

Valence bond method, 503
Valpromide derivatives, 1127
van der Waals radii, 981
VBSCF, 283
Vibrational frequencies, 877
Vibrational spectroscopy, 331
Vibrational transitions, 897

Water cluster, 831
Waugh-type anion, 375
Wave functions, 557
World Wide Web, 159

Zeeman effect, 797
Zeolite, 993, 951
ZnO, 367

International Journal of

Quantum Chemistry

Contents for Volume 70, 1998

Issue No. 1, 1998

Special Issue: The Ninth International Congress of Quantum Chemistry (Part I of II)

Guest Editors: Keiji Morokuma, Ernest R. Davidson, and Henry F. Schaefer, III

Introduction
K. Morokuma **1**

List of Participants **3**

The Chemical Hamiltonian Approach for Treating the BSSE Problem of Intermolecular Interactions
I. Mayer **41**

Unitary-Group-Based Open-Shell Coupled-Cluster Method with Corrections for Connected Triexcited Clusters. I. Theory
X. Li and J. Paldus **65**

Numerical Coupled Liouville Approach: Quantum Dynamics of Linear Molecular Aggregates Under Intense Electric Fields
M. Nakano and K. Yamaguchi **77**

Calculations on Diatomic Molecules with Slater-Type Orbital Basis Sets
A. Bouferguene, B. Etemadi, and H. W. Jones **89**

Transition-State Optimization on Free Energy Surface: Toward Solution Chemical Reaction Ergodography
N. Okuyama-Yoshida, M. Nagaoka, and T. Yamabe **95**

Electrostatic Effect of the Polar Bond–Polarizable Bond Interaction on ^{13}C Chemical Shifts
J. E. Peralta, M. C. Ruiz de Azúa, and R. H. Contreras **105**

Topology of Electronic Densities Taken from Parametric Methods: A Predictive Tool?
A. Sierraalta, F. Ruette, and E. Machado **113**

Scaling Behavior of Energy Functionals of Highly Complex Electron Distributions
J. Pipek and I. Varga **125**

"Statistical-Mechanical" Understanding of Chemical Reaction Mechanism in Solution: Energy Fluctuations and Heat Capacities for Isomerization of Formamidine in Aqueous Solution
M. Nagaoka, Y. Okuno, and T. Yamabe **133**

Scaling Behavior of Dynamic Correlation Effects
W. Wenzel, M. M. Steiner, and K. G. Wilson **147**

Perspectives for Java-Based Computational Quantum Chemistry
D. H. Mosley **159**

Localized Orbitals in Nonmetallic Ring Systems
P. Reinhardt, J.-P, Malrieu, À. Povill, and J. Rubio **167**

Efficient Evaluation of Integrals for Density Functional Theory: Nonlinear *D* Transformations to Evaluate Three-Center Nuclear Attraction Integrals over *B* Functions
H. Safouhi, D. Pinchon, and P. E. Hoggan **181**

Atomic Calculations with an Augmented Fourier Basis
F. A. Pahl **189**

Dressed Potential Energy Surface of the Hydrogen Molecule in High-Frequency Floquet Theory
C. Pérez del Valle, R. Lefebvre, and O. Atabek **199**

Symmetry Aspects of Nonrigid Molecules and Transition Structures in Chemical Reactions
L. Bytautas and D. J. Klein **205**

Some Recent Developments of High-Order Response Theory
Y. Luo, D. Jonsson, P. Norman, K. Ruud, O. Vahtras, B. Minaev, H. Ågren, A. Rizzo, and K. V. Mikkelsen **219**

Issue No. 2, 1998

Special Issue: The Ninth International Congress of Quantum Chemistry (Part II of II)

Guest Editors: Keiji Morokuma, Ernest R. Davidson, and Henry F. Schaefer, III

Intermolecular Hydrogen Bonding and Low-Wave-Number Vibrational Spectra of Formamide, *N*-Methylformamide, and *N*-Methylacetamide in the Liquid State
H. Torii and M. Tasumi **241**

Density Functional Investigations of Carboxyl Free Radicals: Formyloxyl, Acetyloxyl, and Benzoyloxyl Radicals
M. Kieninger, O. N. Ventura, and S. Suhai **253**

Hyperpolarizabilities of One-Dimensional H_n Systems: Second Hyperpolarizability Density Analyses for Regular and Charged Solitonlike Linear Chains
M. Nakano, S. Yamada, S. Kiribayashi, and K. Yamaguchi **269**

Spectroscopic Constants and Bonding Features of the Low-Lying States of LiB and LiB^+: Comparative Study of VBSCF and MO Theory
Z. Cao, W. Wu, and Q. Zhang **283**

Theoretical Model for the Reaction Mechanisms of Singlet Carbene Analogs into Unsaturated Hydrocarbon and the Origin of the Activation Barrier
S. Sakai **291**

Difficulties of Density Functional Theory in Predicting the Torsional Potential of 2,2′-Bithiophene
P. M. Viruela, R. Viruela, and E. Orti **303**

Theoretical Study of Structure and NMR Properties of the μ-Hydrido-Bridged Cyclodecyl Cation and Related Systems
V. Galasso **313**

Ab Initio Study on the Reaction $2NH_2 \rightarrow NH + NH_3$
Z.-F. Xu, D.-C. Fang, and X.-Y. Fu **321**

Creation of Intensity Theory in Vibrational Spectroscopy: Key Role of Ab Initio Quantum Mechanical Calculations
B. Galabov, T. Dudev, S. Ilieva, and J. R. Durig **331**

Electronic Structure of Alumina Surface
L. Turi Nagy, M. Micov, Ľ. Benco, M. Liška, P. Mach, and D. Tunega **341**

First Principles Study of Na Adsorption on TiO_2 (110) Surface
M. A. San Miguel, C. J. Calzado, and J. Fernández Sanz **351**

Theoretical Models for γ-Al_2O_3 (110) Surface Hydroxylation: An Ab Initio Embedded Cluster Study
J. Fernández Sanz, H. Rabaâ, F. M. Poveda, A. M. Márquez, and C. J. Calzado **359**

CO_2 and NH_3 Interaction with ZnO Surface: An AM1 Study
J. B. L. Martins, E. Longo, and C. A. Taft **367**

Electronic Structure and Catalytic Properties of Waugh-Type Anion $(NiMo_9O_{32})^{6-}$
S.-X. Xiao, S.-Y. Yang, and T.-L. Chen **375**

Quantum Mechanical Treatment for the Diffusion Process of a Hydrogen Atom on the Amorphous Water Ice Surface
J. Takahashi, M. Nagaoka, and K. Masuda **379**

Oxygen Binding to Iron–Porphyrin: A Density Functional Study Using Both LSD and LSD + GC Schemes
C. Rovira and M. Parrinello **387**

Ab Initio Relative Stability of a Few Conformers of Bilirubin *in Vacuo* and in Aqueous Solution (PCM)
G. Alagona, C. Ghio, A. Agresti, and R. Pratesi **395**

GROMOS-MD Simulations on the Coenzyme Thiamin Diphosphate in Apoenzyme Environment
R. Friedemann, A. Von Fircks, and S. Naumann **407**

Issue No. 3, 1998

Theoretical and Computational Developments

Macroscopic Solvent Polarization-Induced Reorganization of the Electron Density in Different Excited States: A Study on Formaldehyde Molecule by a Multiconfiguration Self-Consistent Reaction-Field Method
C. Medhi and S. P. Bhattacharyya **415**

Products of Arbitrary Class-Sums in the Symmetric Group
J. Katriel **429**

Femtosecond Quantum Fluid Dynamics of Helium Atom Under an Intense Laser Field
B. Kr. Dey and B. M. Deb **441**

Properties, Dynamics, and Electronic Structure of Atoms and Molecules

DVR Study of the $\tilde{A}^2B_2 \leftarrow \tilde{X}^2A_1$ Absorption Spectrum of NO_2
D. Belmiloud and M. Jacon **475**

Full Variational Molecular Orbital Method: Application to the Positron–Molecule Complexes
M. Tachikawa, K. Mori, K. Suzuki, and K. Iguchi **491**

Properties, Dynamics, and Electronic Structure of Condensed Systems and Clusters

Ring Currents in Condensed Ring Systems
Y. Anusooya, A. Chakrabarti, S. K. Pati, and S. Ramasesha **503**

Molecular Structure, Dynamics, and Function of Biological Systems

On the Possible Reaction Pathway for the Acylation of AChE-Catalyzed Hydrolysis of ACh: Semiempirical Quantum Chemical Study
Q. Wang, H. Jiang, J. Chen, K. Chen, and R. Ji **515**

Books Received **527**

Issue No. 4/5, 1998

Introduction
N. Y. Öhrn, J. R. Sabin, and M. C. Zerner **529**

List of Participants **531**

3,5-Contracted Schrödinger Equation: Determining Quantum Energies and Reduced Density Matrices Without Wave Functions
D. A. Mazziotti **557**

Nonconventional Partitioning of the Many-Body Hamiltonian for Studying Correlation Effects
P. R. Surján, M. Kállay, and Á. Szabados **571**

Unambiguous Exchange–Correlation Energy Density for Hooke's Atom
K. Burke, F. G. Cruz, and K.-C. Lam **583**

SCF Calculations with Density-Dependent Local-Exchange Potential
V. Karasiev, E. V. Ludeña, and R. López-Boada **591**

Investigation of an Asymmetric Triple-Excitation Correction for Coupled-Cluster Energies
T. D. Crawford and J. F. Stanton **601**

Excitation Energies in Brillouin–Wigner-Based Multireference Perturbation Theory
W. Wenzel **613**

More About the Leaky Aquifer Function
F. E. Harris **623**

Use of a Fast Fourier Transform (FFT) 3D Time-Dependent Schrödinger Equation Solver in Molecular Electronic Structure
B. Ritchie and C. A. Weatherford **627**

Modern Valence Bond Descriptions of Molecular Excited States: An Application of CASVB
T. Thorsteinsson and D. L. Cooper **637**

Approximate Brueckner Orbitals and Shakeup Operators in Electron Propagator Calculations: Applications to F^- and OH^-
J. V. Ortiz **651**

Density Functional Theory Without the Born–Oppenheimer Approximation and Its Application
Y. Shigeta, H. Takahashi, S. Yamanaka, M. Mitani,
H. Nagao, and K. Yamaguchi **659**

Analytical Asymptotic Structure of the Pauli, Coulomb, and Correlation–Kinetic Components of the Kohn–Sham Theory Exchange–Correlation Potential in Atoms
Z. Qian and V. Sahni **671**

Excited States in Density Functional Theory
Á. Nagy **681**

A Density Functional Study of Small Nickel Clusters
M. C. Michelini, R. Pis Diez, and A. H. Jubert **693**

Stable and Efficient Numerical Method for Solving the Schrödinger Equation To Determine the Response of Tunneling Electrons to a Laser Pulse
M. J. Hagmann **703**

Excited Electronic States of Carotenoids: Time-Dependent Density-Matrix-Response Algorithm
S. Tretiak, V. Chernyak, and S. Mukamel **711**

Balanced Complete Active Space Choices with the Multiconfigurational Spin Tensor Electron Propagator Method: The Vertical Ionization Potentials of NH_2
A. J. McKellar, D. Heryadi, and D. L. Yeager **729**

Effect of Heavy Atom on the Second Hyperpolarizability of Tetrahydrofuran Homologs Investigated by Ab Initio Molecular Orbital Method
K. Kamada, M. Ueda, H. Nagao, K. Tawa, T. Sugino, Y. Shimizu, and K. Ohta **737**

Structure Dependence of the Low-Lying Excited States and the First Dipole Hyperpolarizability of Phenol Blue
A. Serrano and S. Canuto **745**

Nonresonant Frequency Dispersion of the Electronic Second Hyperpolarizability of *All-Trans* Polysilane Chains: An Ab Initio TDHF Oligomeric Approach
B. Champagne, É. A. Perpète, and J.-M. André **751**

Computation of the Electromagnetic Harmonics Generation by Stratified Systems Containing Nonlinear Layers
A. Calderone and J.-P. Vigneron **763**

Theory and Calculations of Electric Field Effects on Hyperfine Interactions
S. P. Karna **771**

Differential Equations for Ground-State Electron Density and Slater Sum in Atoms and Molecules With and Without External Fields
N. H. March **779**

Ground States of Atoms and Molecules in Strong Magnetic Fields
P. Schmelcher **789**

Some Aspects of Data Processing for an Optical Absorption Experiment in a Pulsed 1000-Tesla Magnet
L. G. Butler, A. W. Maverick, C. H. Gallegos, J. D. Goettee, B. R. Marshall, C. M. Fowler, D. G. Rickel, J. M. Gonzales, and L. J. Tabaka **797**

Optimal Decoupling of Positive- and Negative-Energy Orbitals in Relativistic Electronic Structure Calculations Beyond Hartree–Fock
C. F. Bunge, R. Jáuregui, and E. Ley-Koo **805**

Second-Order Multiconfigurational Dirac–Fock Calculations on Boronlike Ions
M. J. Vilkas, Y. Ishikawa, and K. Koc **813**

Relativistic Effects on the Structural Phase Stability of Molybdenum
J. C. Boettger **825**

Water Cluster Approach To Study Hydrogen-Bonded Pattern in Liquid Water: Ab Initio Orientational Defects in Water Hexamers and Octamers
E. S. Kryachko **831**

Intramolecular Proton Transfer in Monohydrated Tautomers of Cytosine: An Ab Initio Post-Hartree–Fock Study
L. Gorb and J. Leszczynski **855**

Intramolecular Hydrogen Bonding in Resonance-Stabilized Systems
L. A. Schmiedekamp-Schneeweis, and J. O. Payne **863**

Quantum Chemical Study of the Interaction of Nitrate Anion with Water
C. Ebner, R. Sansone, and M. Probst **877**

The Interface of Electronic Structure and Dynamics for Reactions in Solution
Y.-Y. Chuang, C. J. Cramer, and D. G. Truhlar **887**

The Development of Semiclassical Dynamical Methods and Their Application to Vibrational Relaxation in Condensed-Phase Systems
M. F. Herman **897**

Single-Electron-Capture Cross Sections by Alpha-Particles from Ground State *K*(4*s*) and Rb(5*s*): A Molecular-State Approach
A. Kumar, B. C. Saha, and C. A. Weatherford **909**

Bethe–Bloch Stopping-Power Parameters for GaAs and ZnSe
L. E. Porter **919**

Searches on the Potential Energy Hypersurfaces of $GeCH_2$, $GeSiH_2$, and Ge_2H_2
A. J. Boone, D. H. Magers, and J. Leszczyński **925**

Excited-State Potential Energy Curves from Time-Dependent Density-Functional Theory: A Cross Section of Formaldehyde's $^1A_1$ Manifold
M. E. Casida, K. C. Casida, and D. R. Salahub **933**

Effective Potential for e-Neon and e-Argon Scattering by DCS Minimization at Intermediate Energies
J. M. Paikeday and A. Longstreet **943**

Ab Initio SCF–MO Study of the Topology of the Charge Distribution of Acid Sites of Zeolites
H. Soscún, J. Hernández, O. Castellano, G. Díaz, and A. Hinchliffe **951**

Singlet–Triplet Splitting and the Activation of C—H Bond for (η^5-C_5H_5)M(CO) Isoelectronic Fragments: A Theoretical Study
M.-D. Su and S.-Y. Chu **961**

Structural and Electronic Properties of Silicon Nitride Materials
F. De Brito Mota, J. F. Justo, and A. Fazzio **973**

Analysis of Three-Dimensional Molecular Shape Using Surface Area and Molecular Volume Scaling Descriptors
G. A. Arteca **981**

Approximations of the Mulliken Charges for the Oxygen and Silicon Atoms of Zeolite Frameworks Calculated with a Periodic Hartree–Fock Scheme
A. V. Larin and D. P. Vercauteren **993**

Structure and Properties of NH_5^{2+}: A Dication with Two 2-Electron 3-Center Bonds
J. E. Del Bene, J. D. Watts, and R. J. Bartlett **1003**

C_{60} Carbyne Knots (from 0_1 to 6_3): Theoretical NMR Spectra
J. Cz. Dobrowolski and A. P. Mazurek **1009**

Perturbed Ellipsoidal Wave Functions for Quantum Scattering
T. Levitina and E. J. Brändas **1017**

Photochemical Reaction Pathways of Ethylene
L. Freund and M. Klessinger **1023**

Theoretical Studies on Hydrogen Activation by Iridium Dimers
S. Castillo, V. Bertin, E. Solano-Reyes, H. Luna-García, A. Cruz, and E. Poulain **1029**

Electron Propagator Theory of Conformational Effects on Anisole and Thioanisole Photoelectron Spectra
O. Dolgounitcheva, V. G. Zakrzewski, J. V. Ortiz, and G. V. Ratovski **1037**

Advantages of the Fourier Space RHF Band Structure Approach: Application to Polyoxymethylene Using a Distributed Basis Set of *s*-Type Gaussian Functions
I. Flamant, J. G. Fripiat, and J. Delhalle **1045**

Periodic INDO Calculations of Organic Adsorbates on a TiO_2 Surface
P. Persson, A. Stashans, R. Bergström, and S. Lunell **1055**

Sign of the Interaction Parameter in Disordered Fe–Al Alloys
S. Dorfman, D. Fuks, and V. Liubich **1067**

Possibility of Charge-Mediated Superconductors in the Intermediate Region of Metal–Insulator Transitions
H. Nagao, M. Mitani, M. Nishino, Y. Shigeta, Y. Yoshioka, and K. Yamaguchi **1075**

Embedded Cluster and Supercell Study of the Structurre of the Interstitial Cu–C Solid Solutions
D. E. Ellis, S. Dorfman, D, Fuks, R. Evenhaim, and K. Mundim **1085**

Atomic Motion at Germanium Surfaces: Scanning Tunneling Microscopy and Monte Carlo Simulations
J.-P. Vigneron, A. Benaissa, I. Derycke, A. Wiame, and R. Sporken **1093**

Issue No. 6, 1998

Introduction
N. Y. Öhrn, J. R. Sabin, and M. C. Zerner **1099**

List of Participants **1101**

On the Origin of the Lack of Anticonvulsant Activity of Some Valpromide Derivatives
S. M. Tasso, L. Bruno-Blanch, and G. L. Estiú **1127**

Molecular Surface Electrostatic Potentials of Anticonvulsant Drugs
J. S. Murray, F. Abu-Awwad, P. Politzer, L. C. Wilson, A. S. Troupin, and R. E. Wall **1137**

Phytochrome Structure: A New Methodological Approach
C. R. W. Guimarães, J. Delphino da Motta Neto, and R. Bicca de Alencastro **1145**

Studies on the Hydrogenation Steps of the Nitrogen Molecule at the *Azotobacter vinelandii* Nitrogenase Site
K. K. Stavrev and M. C. Zerner **1159**

RHF Conformational Analysis of the Auxin Phytohormones n-Ethyl–Indole-3-Acetic Acid ($n = 4, 5, 6$)
M. Ramek and S. Tomić **1169**

pK_a of Cytosine on the Third Strand of Triplex DNA: Preliminary Poisson–Boltzmann Calculations
G. R. Pack, L. Wong, and G. Lamm **1177**

Parametric Transform and Moment Indices in the Molecular Dynamics of n-Alkanes
S. P. Molnar and J. W. King **1185**

Theoretical Approach to the Pharmacophoric Pattern of GABA$_B$ Analogs
M. L. Lorenzini, L. Bruno-Blanch, and G. L. Estiú **1195**

Optimal Molecular Connectivity Descriptors for Nitrogen-Containing Molecules
M. Randić, and J. Cz. Dobrowolski **1209**

Volume Title Page **1217**

Author Index **1219**

Subject Index **1225**

Volume Table of Contents .... **I**

Published Symposia .... **XII**

Published Symposia of the *International Journal of Quantum Chemistry*

1967	QUANTUM CHEMISTRY SYMPOSIUM NO. 1 (Proceedings of the International Symposium on Atomic, Molecular, and Solid-State Theory)
1968	QUANTUM CHEMISTRY SYMPOSIUM NO. 2 (Proceedings of the International Symposium on Atomic, Molecular, and Solid-State Theory and Quantum Biology)
1969	QUANTUM CHEMISTRY SYMPOSIUM NO. 3 PART 1 (Proceedings of the International Symposium on Atomic, Molecular, and Solid-State Theory and Quantum Biology)
1970	QUANTUM CHEMISTRY SYMPOSIUM NO. 3 PART 2 (Proceedings of the International Symposium on Atomic, Molecular, and Solid-State Theory and Quantum Biology)
1971	QUANTUM CHEMISTRY SYMPOSIUM NO. 4 (Proceedings of the International Symposium on Atomic, Molecular, and Solid-State Theory and Quantum Biology)
1971	QUANTUM CHEMISTRY SYMPOSIUM NO. 5 (Proceedings of the International Symposium on Atomic, Molecular, and Solid-State Theory and Quantum Biology)
1972	QUANTUM CHEMISTRY SYMPOSIUM NO. 6 (Proceedings of the International Symposium on Atomic, Molecular, and Solid-State Theory and Quantum Biology)
1973	QUANTUM CHEMISTRY SYMPOSIUM NO. 7 (Proceedings of the International Symposium on Atomic, Molecular, and Solid-State Theory and Quantum Biology)
1974	QUANTUM CHEMISTRY SYMPOSIUM NO. 8 (Proceedings of the International Symposium on Atomic, Molecular, and Solid-State Theory and Quantum Statistics) QUANTUM BIOLOGY SYMPOSIUM NO. 1 (Proceedings of the International Symposium on Quantum Biology and Quantum Pharmacology)

1975 QUANTUM CHEMISTRY SYMPOSIUM NO. 9
(Proceedings of the International Symposium on Atomic, Molecular, and Solid-State Theory and Quantum Statistics)
QUANTUM BIOLOGY SYMPOSIUM NO. 2
(Proceedings of the International Symposium on Quantum Biology and Quantum Pharmacology)

1976 QUANTUM CHEMISTRY SYMPOSIUM NO. 10
(Proceedings of the International Symposium on Atomic, Molecular, and Solid-State Theory and Quantum Statistics)
QUANTUM BIOLOGY SYMPOSIUM NO. 3
(Proceedings of the International Symposium on Quantum Biology and Quantum Pharmacology)

1977 QUANTUM CHEMISTRY SYMPOSIUM NO. 11
(Proceedings of the International Symposium on Atomic, Molecular, and Solid-State Theory, Collision Phenomena, and Computational Methods)
QUANTUM BIOLOGY SYMPOSIUM NO. 4
(Proceedings of the International Symposium on Quantum Biology and Quantum Pharmacology)

1978 QUANTUM CHEMISTRY SYMPOSIUM NO. 12
(Proceedings of the International Symposium on Atomic, Molecular, and Solid-State Theory, Collision Phenomena and Computational Methods)
QUANTUM BIOLOGY SYMPOSIUM NO. 5
(Proceedings of the International Symposium on Quantum Biology and Quantum Pharmacology)

1979 QUANTUM CHEMISTRY SYMPOSIUM NO. 13
(Proceedings of the International Symposium on Atomic, Molecular, and Solid-State Theory, Collision Phenomena, Quantum Statistics, and Computational Methods)
QUANTUM BIOLOGY SYMPOSIUM NO. 6
(Proceedings of the International Symposium on Quantum Biology and Quantum Pharmacology)

1980 QUANTUM CHEMISTRY SYMPOSIUM NO. 14
(Proceedings of the International Symposium on Atomic, Molecular, and Solid-State Theory, Collision Phenomena, Quantum Statistics, and Computational Methods)
QUANTUM BIOLOGY SYMPOSIUM NO. 7
(Proceedings of the International Symposium on Quantum Biology and Quantum Pharmacology)

1981 QUANTUM CHEMISTRY SYMPOSIUM NO. 15
(Proceedings of the International Symposium on Atomic, Molecular, and Solid-State Theory, Collision Phenomena, and Computational Quantum Chemistry)
QUANTUM BIOLOGY SYMPOSIUM NO. 8
(Proceedings of the International Symposium on Quantum Biology and Quantum Pharmacology)

1982 QUANTUM CHEMISTRY SYMPOSIUM NO. 16
(Proceedings of the International Symposium on Quantum Chemistry, Theory of Condensed Matter, and Propagator Methods in the Quantum Theory of Matter)
QUANTUM BIOLOGY SYMPOSIUM NO. 9
(Proceedings of the International Symposium on Quantum Biology and Quantum Pharmacology)

1983 QUANTUM CHEMISTRY SYMPOSIUM NO. 17
(Proceedings of the International Symposium on Atomic, Molecular, and Solid-State Theory, Collision Phenomena and Computational Quantum Chemistry)
QUANTUM BIOLOGY SYMPOSIUM NO. 10
(Proceedings of the International Symposium on Quantum Biology and Quantum Pharmacology)

1984 QUANTUM CHEMISTRY SYMPOSIUM NO. 18
(Proceedings of the International Symposium on Atomic, Molecular, and Solid-State Theory, and Computational Quantum Chemistry)
QUANTUM BIOLOGY SYMPOSIUM NO. 11
(Proceedings of the International Symposium on Quantum Biology and Quantum Pharmacology)

1985 QUANTUM CHEMISTRY SYMPOSIUM NO. 19
(Proceedings of the International Symposium on Atomic, Molecular, and Solid-State Theory, Scattering Problems, Many Body Phenomena, and Computational Quantum Chemistry)
QUANTUM BIOLOGY SYMPOSIUM NO. 12
(Proceedings of the International Symposium on Quantum Biology and Quantum Pharmacology)

1986 QUANTUM CHEMISTRY SYMPOSIUM NO. 20
(Proceedings of the International Symposium on Atomic, Molecular, and Solid-State Theory, Scattering Problems, Many Body Phenomena, and Computational Quantum Chemistry)

1986 QUANTUM BIOLOGY SYMPOSIUM NO. 13
(Proceedings of the International Symposium on Quantum Biology and Quantum Pharmacology)

1987 QUANTUM CHEMISTRY SYMPOSIUM NO. 21
(Proceedings of the International Symposium on Quantum Chemistry, Solid-State Theory, and Computational Methods)
QUANTUM BIOLOGY SYMPOSIUM NO. 14
(Proceedings of the International Symposium on Quantum Biology and Quantum Pharmacology)

1988 QUANTUM CHEMISTRY SYMPOSIUM NO. 22
(Proceedings of the International Symposium on Quantum Chemistry, Solid-State Theory, and Computational Methods)
QUANTUM BIOLOGY SYMPOSIUM NO. 15
(Proceedings of the International Symposium on Quantum Biology and Quantum Pharmacology)

1989 QUANTUM CHEMISTRY SYMPOSIUM NO. 23
(Proceedings of the International Symposium on Quantum Chemistry, Solid-State Theory, and Molecular Dynamics)
QUANTUM BIOLOGY SYMPOSIUM NO. 16
(Proceedings of the International Symposium on Quantum Biology and Quantum Pharmacology)

1990 QUANTUM CHEMISTRY SYMPOSIUM NO. 24
(Proceedings of the International Symposium on Quantum Chemistry, Solid State Physics, and Computational Methods)
QUANTUM BIOLOGY SYMPOSIUM NO. 17
(Proceedings of the International Symposium on Quantum Biology and Quantum Pharmacology)

1991 QUANTUM CHEMISTRY SYMPOSIUM NO. 25
(Proceedings of the International Symposium on Quantum Chemistry, Solid State Physics, and Computational Methods)
QUANTUM BIOLOGY SYMPOSIUM NO. 18
(Proceedings of the International Symposium on Quantum Biology and Quantum Pharmacology)

1992 QUANTUM CHEMISTRY SYMPOSIUM NO. 26
(Proceedings of the International Symposium on Atomic, Molecular, and Condensed Matter Theory and Computational Methods)
QUANTUM BIOLOGY SYMPOSIUM NO. 19
(Proceedings of the International Symposium on the Application of Fundamental Theory to Problems of Biology and Pharmacology)

1993 QUANTUM CHEMISTRY SYMPOSIUM NO. 27
(Proceedings of the International Symposium on Atomic, Molecular, and Condensed Matter Theory and Computational Methods)
QUANTUM BIOLOGY SYMPOSIUM NO. 20
(Proceedings of the International Symposium on the Application of Fundamental Theory to Problems of Biology and Pharmacology)

1994 QUANTUM CHEMISTRY SYMPOSIUM NO. 28
(Proceedings of the International Symposium on Atomic, Molecular, and Condensed Matter Theory and Computational Methods)
QUANTUM BIOLOGY SYMPOSIUM NO. 21
(Proceedings of the International Symposium on the Application of Fundamental Theory to Problems of Biology and Pharmacology)

1995 QUANTUM CHEMISTRY SYMPOSIUM NO. 29
(Proceedings of the International Symposium on Atomic, Molecular, and Condensed Matter Theory and Computational Methods)
QUANTUM BIOLOGY SYMPOSIUM NO. 22
(Proceedings of the International Symposium on the Application of Fundamental Theory to Problems of Biology and Pharmacology)

1996 QUANTUM CHEMISTRY SYMPOSIUM NO. 30
(Proceedings of the International Symposium on Atomic, Molecular, and Condensed Matter Theory and Computational Methods)
QUANTUM BIOLOGY SYMPOSIUM NO. 23
(Proceedings of the International Symposium on the Application of Fundamental Theory to Problems of Biology and Pharmacology)

1997 QUANTUM CHEMISTRY SYMPOSIUM NO. 31
(Proceedings of the International Symposium on Atomic, Molecular, and Condensed Matter Theory and Computational Methods)
QUANTUM BIOLOGY SYMPOSIUM NO. 24
(Proceedings of the International Symposium on the Application of Fundamental Theory to Problems of Biology and Pharmacology)

1998 QUANTUM CHEMISTRY SYMPOSIUM NO. 32
(Proceedings of the International Symposium on Atomic, Molecular, and Condensed Matter Theory)
QUANTUM BIOLOGY SYMPOSIUM NO. 25
(Proceedings of the International Symposium on the Application of Fundamental Theory to Problems of Biology and Pharmacology

All of the above symposia can be individually purchased from the Subscription Department, John Wiley & Sons.

DISK SUBMISSION INSTRUCTIONS

Please return your final, revised manuscript on disk as well as hard copy. The hard copy must match the disk.

The Journal strongly encourages authors to deliver the final, revised version of their accepted manuscripts (text, tables, and, if possible, illustrations) on disk. Given the near-universal use of computer word-processing for manuscript preparation, we anticipate that providing a disk will be convenient for you, and it carries the added advantages of maintaining the integrity of your keystrokes and expediting typesetting. Please return the disk submission slip below with your manuscript and labeled disk(s).

Guidelines for Electronic Submission (also available at http://www.interscience.wiley.com)

Text

Storage medium. 3-1/2" high-density disk in IBM MS-DOS, Windows, or Macintosh format.

Software and format. Microsoft Word 6.0 is preferred, although manuscripts prepared with any other microcomputer word processor are acceptable. Refrain from complex formatting; the Publisher will style your manuscript according to the Journal design specifications. Do not use desktop publishing software such as Aldus PageMaker or Quark XPress. If you prepared your manuscript with one of these programs, export the text to a word processing format. Please make sure your word processing program's "fast save" feature is turned off. Please do not deliver files that contain hidden text: for example, do not use your word processor's automated features to create footnotes or reference lists.

File names. Submit the text and tables of each manuscript as a single file. Name each file with your last name (up to eight letters). Text files should be given the three-letter extension that identifies the file format. Macintosh users should maintain the MS-DOS "eight dot three" file-naming convention.

Labels. Label all disks with your name, the file name, and the word processing program and version used.

Illustrations

All print reproduction requires files for full color images to be in a CMYK color space. If possible, ICC or ColorSync profiles of your output device should accompany all digital image submissions.

Storage medium. Submit as separate files from text files, on separate disks or cartridges. If feasible, full color files should be submitted on separate disks from other image files. 3-1/2" high-density disks, CD, Iomega Zip, and 5 1/4" 44- or 88-MB SyQuest cartridges can be submitted. At authors' request, cartridges and disks will be returned after publication.

Software and format. All illustration files should be in TIFF or EPS (with preview) formats. Do not submit native application formats.

Resolution. Journal quality reproduction will require greyscale and color files at resolutions yielding approximately 300 ppi. Bitmapped line art should be submitted at resolutions yielding 600–1200 ppi. These resolutions refer to the output size of the file; if you anticipate that your images will be enlarged or reduced, resolutions should be adjusted accordingly.

File names. Illustration files should be given the 2- or 3-letter extension that identifies the file format used (i.e., .tif, .eps).

Labels. Label all disks and cartridges with your name, the file names, formats, and compression schemes (if any) used. Hard copy output must accompany all files.

Detach and return with labeled disk(s)

- -

Corresponding author's name ______________________ E-mail address: ____________ Telephone: ____________

Manuscript number: ____________ Type of computer: ____________ Program(s) & version(s) used: ____________

Miscellaneous: ____

I certify that the material on the enclosed disk(s) is identical in both word and content to the printed copy herewith enclosed.

Signature: ______________________________ **Date:** ____________

COPYRIGHT TRANSFER AGREEMENT

Date:

To:

Production/Contribution ID#____________ Publisher/Editorial office use only

Re: Manuscript entitled ____

____ (the "Contribution")

for publication in ______________________________________ (the "Journal")

published by John Wiley & Sons, Inc. ("Wiley").

Dear Contributor(s):

Thank you for submitting your Contribution for publication. In order to expedite the publishing process and enable Wiley to disseminate your work to the fullest extent, we need to have this Copyright Transfer Agreement signed and returned to us as soon as possible. If the Contribution is not accepted for publication this Agreement shall be null and void.

A. COPYRIGHT

1. The Contributor assigns to Wiley, during the full term of copyright and any extensions or renewals of that term, all copyright in and to the Contribution, including but not limited to the right to publish, republish, transmit, sell, distribute and otherwise use the Contribution and the material contained therein in electronic and print editions of the Journal and in derivative works throughout the world, in all languages and in all media of expression now known or later developed, and to license or permit others to do so.

2. Reproduction, posting, transmission or other distribution or use of the Contribution or any material contained therein, in any medium as permitted hereunder, requires a citation to the Journal and an appropriate credit to Wiley as Publisher, suitable in form and content as follows: (Title of Article, Author, Journal Title and Volume/Issue Copyright © [year] John Wiley & Sons, Inc. or copyright owner as specified in the Journal.)

B. RETAINED RIGHTS

Notwithstanding the above, the Contributor or, if applicable, the Contributor's Employer, retains all proprietary rights other than copyright, such as patent rights, in any process, procedure or article of manufacture described in the Contribution, and the right to make oral presentations of material from the Contribution.

C. OTHER RIGHTS OF CONTRIBUTOR

Wiley grants back to the Contributor the following:

1. The right to share with colleagues print or electronic "preprints" of the unpublished Contribution, in form and content as accepted by Wiley for publication in the Journal. Such preprints may be posted as electronic files on the Contributor's own website for personal or professional use, or on the Contributor's internal university or corporate networks/intranet, or secure external website at the Contributor's institution, but not for commercial sale or for any systematic external distribution by a third party (e.g., a listserve or database connected to a public access server). Prior to publication, the Contributor must include the following notice on the preprint: "This is a preprint of an article accepted for publication in [Journal title] © copyright (year) (copyright owner as specified in the Journal)". After publication of the Contribution by Wiley, the preprint notice should be amended to read as follows: "This is a preprint of an article published in [include the complete citation information for the final version of the Contribution as published in the print edition of the Journal]", and should provide an electronic link to the Journal's WWW site, located at the following Wiley URL: http://www.interscience.Wiley.com/. The Contributor agrees not to update the preprint or replace it with the published version of the Contribution.

2. The right, without charge, to photocopy or to transmit online or to download, print out and distribute to a colleague a copy of the published Contribution in whole or in part, for the Contributor's personal or professional use, for the advancement of scholarly or scientific research or study, or for corporate informational purposes in accordance with Paragraph D.2 below.

3. The right to republish, without charge, in print format, all or part of the material from the published Contribution in a book written or edited by the Contributor.

4. The right to use selected figures and tables, and selected text (up to 250 words, exclusive of the abstract) from the Contribution, for the Contributor's own teaching purposes, or for incorporation within another work by the Contributor that is made part of an edited work published (in print or electronic format) by a third party, or for presentation in electronic format on an internal computer network or external website of the Contributor or the Contributor's employer.

5. The right to include the Contribution in a compilation for classroom use (course packs) to be distributed to students at the Contributor's institution free of charge or to be stored in electronic format in datarooms for access by students at the Contributor's institution as part of their course work (sometimes called "electronic reserve rooms") and for in-house training programs at the Contributor's employer.

D. CONTRIBUTIONS OWNED BY EMPLOYER

1. If the Contribution was written by the Contributor in the course of the Contributor's employment (as a "work-made-for-hire" in the course of employment), the Contribution is owned by the company/employer which must sign this Agreement (in addition to the Contributor's signature), in the space provided below. In such case, the company/employer hereby assigns to Wiley, during the full term of copyright, all copyright in and to the Contribution for the full term of copyright throughout the world as specified in paragraph A above.

2. In addition to the rights specified as retained in paragraph B above and the rights granted back to the Contributor pursuant to paragraph C above, Wiley hereby grants back, without charge, to such company/employer, its subsidiaries and divisions, the right to make copies of and distribute the published Contribution internally in print format or electronically on the Company's internal network. Upon payment of the Publisher's reprint fee, the institution may distribute (but not resell) print copies of the published Contribution externally. Although copies so made shall not be available for individual re-sale, they may be included by the company/employer as part of an information package included with software or other products offered for sale or license. Posting of the published Contribution by the institution on a public access website may only be done with Wiley's written permission, and payment of any applicable fee(s).

E. GOVERNMENT CONTRACTS

In the case of a Contribution prepared under U.S. Government contract or grant, the U.S. Government may reproduce, without charge, all or portions of the Contribution and may authorize others to do so, for official U.S. Government purposes only, if the U.S. Government contract or grant so requires. (U.S. Government Employees: see note at end).

F. COPYRIGHT NOTICE

The Contributor and the company/employer agree that any and all copies of the Contribution or any part thereof distributed or posted by them in print or electronic format as permitted herein will include the notice of copyright as stipulated in the Journal and a full citation to the Journal as published by Wiley.

G. CONTRIBUTOR'S REPRESENTATIONS

The Contributor represents that the Contribution is the Contributor's original work. If the Contribution was prepared jointly, the Contributor agrees to inform the co-Contributors of the terms of this Agreement and to obtain their signature to this Agreement or their written permission to sign on their behalf. The Contribution is submitted only to this Journal and has not been published before, except for "preprints" as permitted above. (If excerpts from copyrighted works owned by third parties are included, the Contributor will obtain written permission from the copyright owners for all uses as set forth in Wiley's permissions form or in the Journal's Instructions for Contributors, and show credit to the sources in the Contribution.) The Contributor also warrants that the Contribution contains no libelous or unlawful statements, does not infringe on the rights or privacy of others, or contain material or instructions that might cause harm or injury.

CHECK ONE:

[____]Contributor-owned work

Contributor's signature ____________________ Date ____________

Type or print name and title ____________________

Co-contributor's signature ____________________ Date ____________

Type or print name and title ____________________

ATTACHED ADDITIONAL SIGNATURE PAGE AS NECESSARY

[____]Company/Institution-owned work
(made-for-hire in the
course of employment)

Company or Institution (Employer-for-Hire) ____________________ Date ____________

Authorized signature of Employer ____________________ Date ____________

[____]U.S. Government work

Note to U.S. Government Employees

A Contribution prepared by a U.S. federal government employee as part of the employee's official duties, or which is an official U.S. Government publication is called a "U.S. Government work," and is in the public domain in the United States. In such case, the employee may cross out Paragraph A.1 but must sign and return this Agreement. If the Contribution was not prepared as part of the employee's duties or is not an official U.S. Government publication, it is not a U.S. Government work.

[____]U.K. Government work (Crown Copyright)

Note to U.K. Government Employees

The rights in a Contribution prepared by an employee of a U.K. government department, agency or other Crown body as part of his/her official duties, or which is an official government publication, belong to the Crown. In such case, the Publisher will forward the relevant form to the Employee for signature.

International Journal of Quantum Chemistry Information for Contributors

1. Manuscripts should be submitted in triplicate and accompanied by an executed Copyright Transfer Form to the Editorial Office, International Journal of Quantum Chemistry, Quantum Chemistry Group, University of Uppsala, Box 518, S-75120 Uppsala, Sweden. Authors may also submit manuscripts to the Editorial Office, International Journal of Quantum Chemistry, Quantum Theory Project, 2301 NP Building #92, P.O. Box 118435, Museum Road and North South Drive, University of Florida, Gainesville, Florida 32611-8435.

   All other correspondence should be addressed to the Publisher, Professional, Reference, & Trade Group, John Wiley & Sons, Inc., 605 Third Ave., New York, NY 10158.

2. It is the preference of the Editors that papers be published in the English language. However, if the author desires that his paper be published in French or German, it is necessary that a particularly complete and comprehensive synopsis be furnished in English.

3. Manuscripts should be submitted in triplicate (one *original*, two carbon copies) typed *doubled spaced* throughout and on one side of each sheet only, on a *heavy* grade paper with margins of at least 2.5 cm on all sides. Copyright: No article can be published unless accompanied by a signed publication agreement, which serves as a transfer of copyright from author to publisher. A publication agreement may be obtained from the editor or the publisher. A copy of the publication agreement appears in most issues of the journal. Only original papers will be accepted and copyright in published papers will be vested in the publisher. It is the author's responsibility to obtain written permission to reproduce material that has appeared in another publication. A copy of that agreement, executed and signed by the author, is now required with each manuscript submission. (If the article is a "work made for hire," the agreement must be signed by the employer.)

4. A short synopsis (maximum length 200 words) is required. The synopsis should be a summary of the entire paper, not the conclusions alone. If the paper is written in French or German, a synopsis in English should also be prepared. The paper should be reasonably subdivided into sections and, if necessary, subsections.

5. A list of five key words or phrases for indexing must accompany each submission.

6. Authors are cautioned to type—wherever possible—all mathematical and chemical symbols, equations, and formulas. If these must be handwritten, please print clearly and leave ample space above and below for printer's marks; please use only ink. All Greek or unusual symbols should be identified in the margin the first time they are used. Please distinguish in the margins of the manuscript between capital and small letters of the alphabet wherever confusion may arise (e.g., k, K, k). Please underline with a wavy line all vector quantities. Use fractional exponents to avoid root signs.

   The nomenclature sponsored by the International Union of Pure and Applied Chemistry is requested for chemical compounds. Unit abbreviations should follow the practices of the American Institute of Physics. Chemical bonds should be correctly placed, and double bonds clearly indicated. Valence is to be indicated by superscript plus and minus signs.

7. The references should be numbered consecutively in the order of their appearance and should be complete, including authors' initials and—for unpublished lectures or symposia—the title of the paper, the date, and the name of the sponsoring society. Please compile references on a separate sheet at the end of the manuscript. Abbreviations of journal titles should conform to the *Bibliographic Guide for Editors & Authors* published by the American Chemical Society.

   References should be limited to literature citations. Explanatory or supplementary material should be treated either as footnotes to text or appendices. Examples:

   [1] D. N. Zubarev, *Nonequilibrium Statistical Thermodynamics* (Consultants Bureau, Plenum, New York, 1974).

   [2] H. Adachi, M. Tsukada, and C. Satoko, J. Phys. Soc. Jpn. **45**, 875 (1978).

   [3] K. Fukui, T. Yonezawa, C. Nagata, H. Katou, A. Imamura, and K. Morokuma, in *Introduction to Quantum Chemistry* (Kagakudojin, Kyoto, 1963), Vol. **1**, p. 197.

8. A limited number of color figures that are of critical importance and that significantly enhance the presentation will be considered for publication at the publisher's expense. Color separations or

transparencies (negatives or positives) are optimal. Color slides are preferable to color prints. Any cropping of the color figure should be clearly indicated. Final decision on publication of color figures will be at the discretion of the Editor.

9. Each table should be supplied on a separate sheet (not interspersed with text). Please supply numbers and titles for all tables. All table columns should have an explanatory heading.

10. Please supply legends for all figures and compile these on a separate sheet.

11. Figures should be professionally prepared and submitted in a form suitable for reproduction (camera-ready copy). Computer-generated graphs are acceptable only if they have been printed with a good quality laser printer. Artwork is generally reduced so that the type in the figures is about 2.5 mm high. The maximum final size of figures for this journal is 16 x 21 cm after reduction. Good glossy photographs are required for halftone reproductions. If in doubt about the preparation of illustrations suitable for reproduction, please consult the publisher at the address given in paragraph 1.

12. Senior authors will receive 50 reprints of their articles without charge. Additional reprints can be ordered and purchased by filling out the form enclosed with the proof.

13. The publisher will do everything possible to ensure prompt publication. It will therefore be appreciated if manuscripts and illustrations conform from the outset to the style of the journal. Contributors should use the *Style Manual* of the American Institute of Physics; papers will otherwise have to be returned to the author for revision.

    Corrected proofs must be sent back to the publisher within two days to avoid the risk of the author's contribution having to be held over to a later issue.

Available on STN International

Look no further than your own computer terminal to find the results of worldwide polymer research with . . .

CHEMICAL JOURNALS ONLINE

WILEY POLYMER JOURNALS (CJ Wiley)

now available as part of **CHEMICAL JOURNALS ONLINE**, comprises three authoritative journals published by John Wiley & Sons, Inc.:

JOURNAL OF APPLIED POLYMER SCIENCE

JOURNAL OF POLYMER SCIENCE

BIOPOLYMERS

With CHEMICAL JOURNALS ONLINE, you will have the capability to search and display original polymer research • vital experimental data • experimental procedures • new preparation techniques • literature citations • crossover to other chemical information including CAS Online.

Easily accessible and cost-effective, CHEMICAL JOURNALS ONLINE (which also includes journals from the Royal Society of Chemistry and the American Chemical Society) will enable you to obtain immediate results without even leaving your desk!

To find out more about how CJ Wiley — and the *entire* CHEMICAL JOURNALS ONLINE database — can work for you, call toll-free 800-227-5558. An American Chemical Society sales representative will be pleased to answer any questions you might have.

You can also write to the Marketing/Communications Department, American Chemical Society, 1155 Sixteenth Street, N.W., Washington, D. C. 20036.

The Computer-Powered
Full-Text Search System
From The American
Chemical Society

CHEMICAL JOURNALS ONLINE

No

Busy? As a research chemist you are always in need of fast access to a wide spectrum of information.

time

Chem-Inform reaction abstracts are custom-made for busy chemists.
You get the „essential chemistry" of a paper at a glance. The complete research results and reaction schemes are presented as easy to read structural formulae.

to

ChemInform is edited by experts for experts. It contains approximately 17.000 abstracts per year from nearly 200 international journals.

waste !

Chem-Inform is now available on CD-ROM. With a mouse-click you have rapid access to the current progress in synthesis and preparative methods.

Free the flow of information!

Chem-Inform Abstracts are for Synthesis Chemists. You can choose between:

➔ the up-to-date content of the weekly journal (ISSN 1431-5890)
➔ the targeted speed of the CD-ROM (ISSN 1431-5890)
➔ the two together

Order your free demo version/free sample copy and detailed information at:

WILEY-VCH
P.O. Box 10 11 61
D -69451 Weinheim
Germany

Phone: +49 (0) 6201 606 458
Fax: +49 (0) 6201 606 184
e-mail: sales-journals@vchgroup.de
Internet: http://www.vchgroup.de

WILEY-VCH

FIZ CHEMIE BERLIN

ChemInform
Reaction Abstracts – Print + CD-ROM

New in ...

Quantum Physics

TEXTBOOK

Bachor, H.-A.

A Guide to Experiments in Quantum Optics

1997. Approx XVI, 400 pages, 170 figs.
Softcover. Approx $70.00
ISBN 3-527-29298-5
Publication date: November 1997

This book differs from other excellent but theoretical texts in that it focuses on actual experiments and explains the underlying physics. It addresses limitations of equipment, what is measurable and what are the future goals.

TEXTBOOK

Zubarev, D. / Morozov, V. / Röpke, G.

Statistical Mechanics of Nonequilibrium Processes

Volume 1: Basic Concepts, Kinetic Theory
1996. 375 pages, 19 figs.
Hardcover. Approx $70.00
ISBN 3-05-501708-0

Volume 2: Relaxation and Hydrodynamic Processes
1997. 375 pages, 12 figs.
Hardcover. Approx $ 98.00
ISBN 3-05-501709-9

In the first part of this two-volume textbook a unified approach to the modern statistical theory of nonequilibrium processes is given. Applications to classical and quantum kinetic theory of nonideal gases, to plasmas and solid state physics are presented. In Volume 2 applications of the general approach given in the first volume are considered. Applications in transport theory, relaxation processes, and hydrodynamics are presented.

TEXTBOOK

Dittrich, T. et al.

Quantum Transport and Dissipation

1997. X, 372 pages, approx 96 figs.
Hardcover. Approx $70.00
ISBN 3-527-29261-6
Publication date: November 1997

For those who need a compact and clear introduction at a graduate level to the theory that underlies reserach into mesoscopic systems, this book is highly recommended.

TEXTBOOK

Murayama, Y.

Mesoscopic Systems

1998. Approx XII, 325 pages, 90 figs.
Hardcover. Approx $69.95
ISBN 3-527-29376-0
Publication date: April 1998

Future high-tech applications such as nanotechnology require a deep understanding of the physics of Mesoscopic systems. This introduction discusses a variety of typical surface, optical, transport, and magnetic properties of Mesoscopic systems with reference to many experimental observations. It is written for physics, materials science and engineering students who want to catch up with current research or high-tech development.

MONOGRAPH

Gramß, T. et al.

Non-Standard Computation

Molecular Computation – Cellular Automata – Evolutionary Algorithms – Quantum Computers

1997. Approx XVI, 230 pages, 80 figs.
Softcover. Approx $70.00
ISBN 3-527-29427-9
Publication date: November 1997

This exciting book provides the first overview of and introduction to the chemical, biological and physical non-standard computation concepts which promise to solve highly computationly intensive problems by a massive parallelism and a clever use of other effects: Molecular and Quantum Computers, and Genetic Algorithms.

TEXTBOOK

Schleich, W.P. / Mayr, E. / Krähmer, D.

Quantum Optics in Phase Space

1997. Approx XII, 270 pages, 80 figs.
Softcover. Approx $70.00
ISBN 3-527-29435-X
Publication date: December 1997

Based on a two-semester graduate course given at the University of Ulm, Germany, this book provides a compact introduction to the theory. It gives a good preparation for research and can either be used alone or with other books.

Prices are subject to change without notice.

The new
global
force in
scientific
publishing

WILEY-VCH

Physical Methods in Chemistry

Now Complete

Second Edition

Series Editors:
Bryant W. Rossiter
& J.F. Hamilton
both of Eastman Kodak Company

This well-respected series provides chemists in a wide range of industries and research with an appreciation for the potential and limitations of the many techniques used in evaluating and analyzing substances and materials. The volumes include coverage of theory and apparatus.

▪▪▪▪▪▪▪▪▪▪▪▪▪▪▪▪▪▪▪▪▪▪▪▪▪▪▪

TO ORDER: You can order these and other Wiley titles through your bookseller or send your order direct to:
John Wiley & Sons, Inc. Attention: S. Schinder
605 Third Avenue New York, NY 10158-0012
or
Call toll free: 1-800-US-WILEY (1-800-879-4539)
In Canada, call 1-800 263-1590.

Prices subject to change without notice and may be higher outside the U.S.

Special Set Price $1695 • Save Over 15%

10-Volume Set
0-471-57086-9
$1695

Vol. 1 Components of Scientific Instruments and Applications to Chemical Research
0-471-08034-9 1986
834pp. $210

Vol. 2 Electrochemical Methods
0-471-08027-6 1986
904pp. $210

Vol. 3A Determination of Chemical Composition and Molecular Structure
0-471-85401-1 1987
624pp. $165

Vol. 3B Determination of Chemical Composition and Molecular Structure
0-471-85051-9 1989
971pp. $190

Vol. 4 Microscopy
0-471-08026-8 1991
560pp. $165

WILEY
Publishers Since 1807

Vol. 5 Determination of Structural Features of Crystalline and Amorphous Solids
0-471-52509-X 1990
640pp. $150

Vol. 6 Determination of Thermodynamic Properties
0-471-57087-7 1992
750pp. $245

Vol. 7 Determination of Elastic and Mechanical Properties
0-471-53438-2 1991 $110

Vol. 8 Determination of Electronic and Optical Property
0-471-54407-8 1993
400pp. $150

Vol. 9A Investigations of Surfaces and Interfaces
0-471-54406-X 1992
528pp. $140

Vol. 9B Investigations of Surfaces and Interfaces
0-471-54405-1 1993
750pp. $250

Vol. 10 Supplement and Cumulative Index
0-471-57086-9 1993
ca.450pp. $195

JOIN WILEY ONLINE

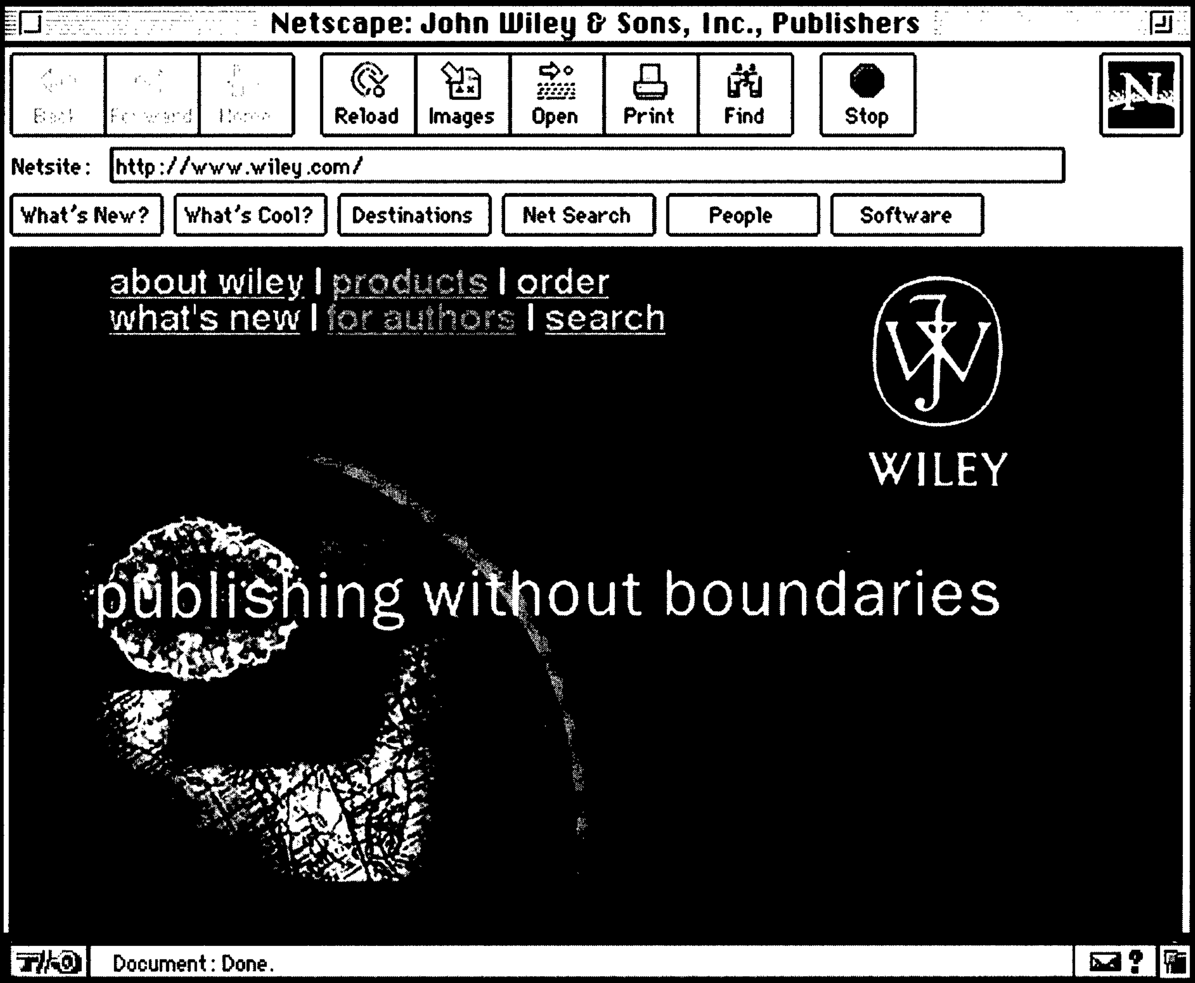
Netscape: John Wiley & Sons, Inc., Publishers
Back
Forward
Home
Reload
Images
Open
Print
Find
Stop
N
What's New?
What's Cool?
Destinations
Net Search
People
Software
about wiley | products | order
what's new | for authors | search
WILEY
publishing without boundaries

Netsite: http://www.wiley.com/

Document: Done.

Drop in and explore. Get the very latest information on new books, journals, and other publications along with special promotions and publicity. Discover a variety of online services, including online journals. Download a sample chapter or software. And much more.

STOP BY TODAY!
www.wiley.com/

WILEY
Publishers Since 1807

0020-7608(1998)70:6;1-#